AD-A043 632 HUGHES AIRCRAFT CO CULVER CITY CA DISPLAY PRODUCTS DEPT F/G 20/6
DIFFRACTION OPTICS STUDY.(U)
JUN 77 W N LEWIS, D H CLOSE, L G COOK F33615-76-C-0508
UNCLASSIFIED AMRL-TR-76-119 NL

1 OF 3
AD A043632



AD A043632

AMRL-TR-76-119



DIFFRACTION OPTICS STUDY

W. N. LEWIS
D. H. CLOSE
L. G. COOK
R. S. JACOBS

DISPLAY PRODUCTS DEPARTMENT
HUGHES AIRCRAFT COMPANY
CENTINELA & TEALE STREETS
CULVER CITY, CALIFORNIA 90230

DDC
RECEIVED
SEP 1 1977
C

JUNE 1977

Approved for public release; distribution unlimited.

AU No.
DDC FILE COPY

AEROSPACE MEDICAL RESEARCH LABORATORY
AEROSPACE MEDICAL DIVISION
AIR FORCE SYSTEMS COMMAND
WRIGHT-PATTERSON AIR FORCE BASE, OHIO 45433

NOTICES

When US Government drawings, specifications, or other data are used for any purpose other than a definitely related Government procurement operation, the Government thereby incurs no responsibility nor any obligation whatsoever, and the fact that the Government may have formulated, furnished, or in any way supplied the said drawings, specifications, or other data, is not to be regarded by implication or otherwise, as in any manner licensing the holder or any other person or corporation, or conveying any rights or permission to manufacture, use, or sell any patented invention that may in any way be related thereto.

Please do not request copies of this report from Aerospace Medical Research Laboratory. Additional copies may be purchased from:

National Technical Information Service
5285 Port Royal Road
Springfield, Virginia 22161

Federal Government agencies and their contractors registered with Defense Documentation Center should direct requests for copies of this report to:

Defense Documentation Center
Cameron Station
Alexandria, Virginia 22314

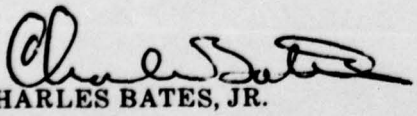
TECHNICAL REVIEW AND APPROVAL

AMRL TR 76-119

This report has been reviewed by the Information Office (OI) and is releasable to the National Technical Information Service (NTIS). At NTIS, it will be available to the general public, including foreign nations.

This technical report has been reviewed and is approved for publication.

FOR THE COMMANDER



CHARLES BATES, JR.
Chief
Human Engineering Division
Aerospace Medical Research Laboratory

AIR FORCE/56780/10 August 1977 — 150

SECURITY CLASSIFICATION OF THIS PAGE *(When Data Entered)*

REPORT DOCUMENTATION PAGE

READ INSTRUCTIONS BEFORE COMPLETING FORM

1. REPORT NUMBER: AMRL-TR-76-119
2. GOVT ACCESSION NO.
3. RECIPIENT'S CATALOG NUMBER
4. TITLE *(and Subtitle)*: DIFFRACTION OPTICS STUDY.
5. TYPE OF REPORT & PERIOD COVERED: Final report, 1 Mar-30 Sep 76,
6. PERFORMING ORG. REPORT NUMBER
7. AUTHOR(s): W. N. Lewis, L. G. Cook, D. H. Close, R. S. Jacobs
8. CONTRACT OR GRANT NUMBER(s): F33615-76-C-0508
9. PERFORMING ORGANIZATION NAME AND ADDRESS: Display Products Department, Hughes Aircraft Company, Culver City, California 90230
10. PROGRAM ELEMENT, PROJECT, TASK AREA & WORK UNIT NUMBERS: 62202F, 7184-04-48
11. CONTROLLING OFFICE NAME AND ADDRESS: Aerospace Medical Research Laboratory, Aerospace Medical Division, Air Force Systems Command, Wright-Patterson Air Force Base, Ohio 45433
12. REPORT DATE: June 1977
13. NUMBER OF PAGES: 224
14. MONITORING AGENCY NAME & ADDRESS *(if different from Controlling Office)*: 225 p.
15. SECURITY CLASS. *(of this report)*: UNCLASSIFIED
15a. DECLASSIFICATION/DOWNGRADING SCHEDULE
16. DISTRIBUTION STATEMENT *(of this Report)*: Approved for public release; distribution unlimited
17. DISTRIBUTION STATEMENT *(of the abstract entered in Block 20, if different from Report)*

DDC RELEASED SEP 1 1977 C

18. SUPPLEMENTARY NOTES: This work was supported in part by the Laboratory Director's Fund.
19. KEY WORDS *(Continue on reverse side if necessary and identify by block number)*:
Diffraction optics
Optical systems design
Canopy holographic display
Laser applications technology
Holographic visor display
20. ABSTRACT *(Continue on reverse side if necessary and identify by block number)*:
A study has been conducted to determine the feasibility of extending the information display capability in a modern fighter aircraft through the employment of diffraction optics techniques. Baseline concepts were designed using (1) reflective holographic optical elements on the aircraft canopy and (2) transmissive holographic optical elements on the operator's flight helmet visor. Evaluation of these systems' performance by computer was conducted. State-of-the-art surveys in holographic technology, image sources and materials
(continued on reverse)

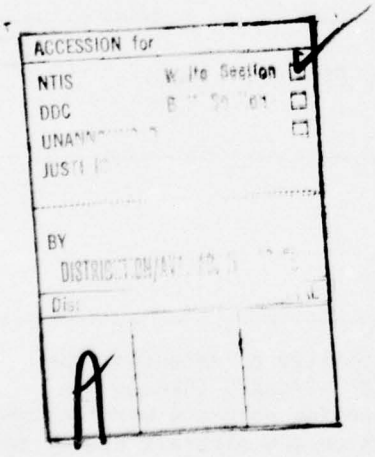
DD FORM 1 JAN 73 1473 EDITION OF 1 NOV 65 IS OBSOLETE

SECURITY CLASSIFICATION OF THIS PAGE *(When Data Entered)*

AD 410 352

Block 20. (cont'd)

technology are presented. The impact of future advances in the state of the art on the feasibility of these systems is discussed. Requirements for the extended display technology are formulated, using simulated encounter and mission analysis data.



PREFACE

The analysis of mission functions and their demands on the display capabilities of the modern fighter aircraft avionics system was analyzed by R. S. Jacobs. This task resulted in the generation of requirements for the systems proposed herein.

The task team of Messrs. Jacobs, J. J. Ferrer, L. G. Cook, H. H. Jones, W. N. Lewis and Dr. D. H. Close were the primary contributors to development of the concepts as a result of many hours of "brainstorming" the problem. Mr. Cook was responsible for mathematically describing the canopy, and generating the optical raytrace information. His major achievement in this effort has been the optical solution of the image tilt disparities such that the image holograms could be utilized as described herein.

Dr. Close, who has been a pioneer in the Diffraction optical elements technology conducted the parametric studies of the optical geometries involved and evaluated the relative merits of the many systems discussed. In addition, he has provided the answers to questions of technical feasibility in the areas of Diffraction optics fabrication, processing and materials technology.

W. R. Lichty is to be recognized for his contribution in developing and analyzing the concept of the visor mounted diffraction display. W. N. Lewis was project engineer, responsible for the image source technology section as well as the overall project effort and the compilation of the final report.

Mr. J. H. Brindle of the U.S. Air Force, Aerospace Medical Research Laboratory (AMRL/HEA) has acted as the project monitor for this effort and is the prime contact regarding this study program.

This effort was supported in part by the
Laboratory Director's Fund.

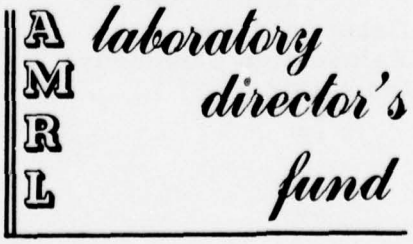


TABLE OF CONTENTS

Section			Page
	1.0	INTRODUCTION	1
	2.0	BASELINE SYSTEMS SUMMARY	3
	2.1	Review	3
	2.2	Requirements	9
	2.3	Reflective System	10
	2.3.1	Single vs Multiple HOEs	11
	2.4	Transmission System	11
	3.0	OPERATIONAL REQUIREMENTS	15
	3.1	Introduction	15
	3.2	Mission Analysis	16
	3.2.1	Assumptions	17
	3.2.2	Tactical Missions	18
	3.2.3	Information Requirements	18
	3.2.4	Canopy Display Information Requirements	21
	3.2.5	Information Analysis	25
	3.3	Display Requirements Analysis	27
	3.3.1	Field of View Requirements	27
	3.3.2	Air-to-Air Analysis	28
	3.3.3	Air-to-Ground Field of View Analysis	31
	3.3.4	Summary of *Field of View* Requirements	32
	3.4	Display Performance Requirements	35
	3.4.1	Display Refreshment Requirements	36
	3.4.2	Display Color	37
	3.5	Anthropometric Considerations	37
	4.0	DIFFRACTION OPTICS DISPLAY TECHNOLOGY	41
	4.1	HOE Technology	41
	4.1.1	Physical Description	41
	4.1.2	Technology Overview	42
	4.2	HOE Design and Analysis	44
	4.2.1	General	45
	4.3	HOE Fabrication Technology	51
	4.3.1	Exposure Apparatus	51
	4.3.2	Processing Techniques	52
	4.4	HOE Recording Materials	53
	4.4.1	Display System Requirements	53
	4.4.2	Available Materials	54
	4.5	HOE Future Developments	55
	4.5.1	Needed Improvements	55
	4.5.2	Design and Analysis	57
	4.5.3	Fabrication Techniques	57
	4.5.4	Materials	57

TABLE OF CONTENTS

Section			Page
	4.6	Image Source Technology	59
	4.6.1	Introduction	59
	4.6.2	General	60
	4.6.2	Lasers	70
	4.6.3	Light Emitting Diodes	78
	4.6.4	Liquid Crystals	84
	4.6.5	Incandescent Image Source	106
	4.6.6	Image Source Tradeoffs and Conclusio s	109
	5.0	SYSTEM FEASIBILITY AND TRADEOFFS	115
	5.1	Design Considerations	115
	5.1.1	Physical Design Considerations	115
	5.1.2	Canopy versus Separate Substrate	125
	5.2	Optical Design Considerations	128
	5.2.1	Summary of Reflection HOE	128
	5.3	Canopy Display Performance	134
	5.3.1	Optical Efficiency Across the Field of View	137
	5.3.2	Image Quality	140
	5.3.3	Chromatic Dispersion	146
	5.3.4	See-Through Characteristics	146
	5.4	Systems Based on Transmission HOEs	148
	5.4.1	Configurations	148
	5.4.2	Spectral Flare Characteristics	151
	5.4.3	Conclusions	154
	6.0	BASELINE SYSTEMS	159
	6.1	Physical Description	159
	6.1.1	Reflective Holographic Description	159
	6.1.2	Transmission Holographic Visor System	163
	6.2	Optical Design	173
	6.2.1	Introduction	173
	6.2.2	First Order Design Considerations	175
	6.2.3	Cockpit and Canopy	177
	6.2.4	Representative Design Geometries	178
	6.2.5	Conclusions	180
	6.3	Alternate System Configurations	184
	6.3.1	Projector Mounted on Head Rest	184
	6.3.2	Fiber Optics Coupler	185
	6.3.3	Single, Multistate Projector	187
	6.4	Conclusion	187
	6.5	Recommendations	189
	6.5.1	Helmet Mounted Display	189
	6.5.2	Canopy Display	190

TABLE OF CONTENTS

Appendix		Page
A	Mission Analysis Functional Flow Block Diagrams	191
B	Liquid Crystal Material Characteristics. .	207
C	Canopy Geometry Characteristics	213

LIST OF ILLUSTRATIONS

Figure		Page
1.	Baseline reflective HOE system	10
2.	Baseline transmissive HOE system	12
3.	Location of forward HOE image sources	13
4.	Air-to-air target coverage versus azimuth field of view	30
5.	Distribution of target elevation line-of-sight as a function of angle above the ADL	31
6.	First pass attach geometry	32
7.	Relative coverage of first pass ground target versus azimuth and elevation FOV and maximum G limit	33
8.	Suggested placement of diffraction optics display	34
9.	Requirements for see-through display luminance	35
10.	Critical flicker fusion threshold frequency of the human eye as a function of ambient light intensity	36
11.	Spectral sensitivity of the human eye	37
12.	Neck movement and rotation	38
13.	Angles of sight at various head position (after Brues, 1946)	39
14.	Distribution of incident light when acted on by a holographic optical element	45
15.	Two limiting types of thick phase hologram	46
16.	Spectral distribution of P43 phosphor	65
17.	Spectral distribution of P44 phosphor	66
18.	Achievable contrast ratio versus source brightness for various background brightness levels	69
19.	Components of a scanned laser display system	71
20.	Relative intensity versus wavelength – LEDs	79
21.	Spectral emission characteristics of a typical GaAsP LED	84
22.	Liquid crystal scattering lobe	86
23.	Brightness and contrast of a typical LX display	87
24.	Dynamic scattering liquid crystal cell operation and viewing geometry	88
25.	Liquid crystal alphanumeric display module mounting	89
26.	Experimental results on liquid crystal samples	91

LIST OF ILLUSTRATIONS

Figure		Page
27.	Characteristics of LX examples (experimentally determined)	92
28.	Display contrast	94
29.	Imaging schemes using liquid crystal	97
30.	On-axis schlieren system	98
31.	Off axis viewing system	99
32.	Light source brightness control	100
33.	LX-HOE image source concept	101
34.	Illumination concept for LX/Holographic HUD	102
35.	Preliminary outline of Advanced HUD	103
36.	Mercury arc-phosphor lamp	104
37.	Spectral distribution of tungsten – Halogen incandescent lamp	107
38.	Effect of filtering on incandescent lamp	108
39.	Spectral emission characteristics of reflective hologram/CRT combination	113
40.	F-16 cockpit instrumentation	116
41.	Pilot in F-16 cockpit	116
42.	View looking forward in YF-16 cockpit	117
43.	Canopy/design eye coordinate system	118
44.	F-16 canopy reflections of -10° elevation lines of sight.	118
45.	F-16 canopy reflections of 0° elevation lines of sight	119
46.	F-16 canopy reflections of 10° elvation lines of sight	119
47.	F-16 canopy reflections of 20° elevation lines of sight	120
48.	F-16 canopy reflections of 30° elevation lines of sight	120
49.	F-16 canopy reflections of 40° elevation lines of sight	121
50.	3-Hologram system in F-16 cockpit geometry	122
51.	5-Hologram system in F-16 cockpit geometry	123
52.	7-Hologram system in F-16 cockpit geometry	124
53.	8-Hologram system in F-16 cockpit geometry	124
54.	Canopy geometry consideration	126
55.	Examination of design eye/canopy geometry	127
56.	Example of alternate substrate installation	127
57.	Construction geometry for an image hologram	129

LIST OF ILLUSTRATIONS

Figure		Page
58.	Typical system configuration for an image hologram	131
59.	Illustration of a bend angle of 80° with positive asymmetry	132
60.	Illustration of a bend angle of 80° with negative asymmetry	132
61.	Illustration of a bend angle 5°, giving large negative asymmetry	133
62.	Illustration of a positive tilt of the y-fan, vertical field image surface	135
63.	Illustration of the field gap required for independent display segments	136
64.	Illustration of the source gap required to prevent multiple images	138
65.	Chief ray efficiency for a vertical cylinder hologram subtrate with $\Omega = 50°$, $2\theta = 65°$, d = 20 in., f = 25 in. and a substrate radius of 13.8 in.	139
66.	Vertical field size as a function of asymmetry angle	139
67.	Vertical field size as a function of bend angle for hologram tilt of 50°	140
68.	Image surfaces for a typical image hologram on vertical cylinder substrate	141
69.	Image surface tests for image holograms on flat substrates as functions of asymmetry angle	142
70.	Image surface tilts for image holograms on horizontal cylinder substrates as a function of asymmetry angle for substrate radius of 16 in.	142
71.	Vertical fan image surface tilt for image holograms on horizontal cylinder substrates of different radii	143
72.	Image surface tilts for image holograms on vertical cylinder substrates as a function of asymmetry angle	143
73.	Image surface tilts for the "head projector" configuration with a vertical cylinder substrate	144
74.	Image surface tilts for a constant tilt angle of 50° with a vertical cylinder substrate	145
75.	Image errors for an untilted image source	145

LIST OF ILLUSTRATIONS

Figure		Page
76.	Chromatic angular dispersion as a function of asymmetry angle	147
77.	Typical display system geometry using a transmission hologram on the pilot's visor	148
78.	Image surfaces for a typical transmission image hologram	149
79.	Chief ray diffraction efficiency across the vertical field of view for a typical transmission hologram	150
80.	Distortion for a wedge transmission hologram	150
81.	Magnified view of the hologram fringes	152
82.	Geometry of high efficiency flare calculation	153
83.	Grating geometry	153
84.	Bragg condition geometry	154
85.	Cockpit flare angle as a function of wavelength of peak efficiency	155
86.	Observed flare angle as a function of wavelength of peak efficiency	155
87.	High efficiency flare geometry, drawn to scale	156
88.	Hologram arrangement on canopy	160
89.	Location of HOE image sources	162
90.	Reflection angles off chosen HOE sites	164
91.	Transmission holographic visor optical system	165
92.	Display brightness rationale	167
93.	P-43 phosphor spectral distribution	168
94.	Transmission hologram optical geometry	169
95.	Representative display format showing effect of chromatic dispersion	170
96.	Optical geometry illustration	171
97.	Holographic lens efficiency	172
98.	CRT symbol brightness	172
99.	Construction and reconstruction of I) an image hologram and II) a pupil hologram	174
100.	First order optical schematic of relayless display using an image hologram	175
101.	First order optical schematic of relayed display using a pupil hologram	176
102.	F-16 cockpit and canopy	178
103.	A holographic lens having an 80 degree bend angle, a 20 degree asymmetry angle, and a single image tilt of 48 degrees	179

LIST OF ILLUSTRATIONS

Figure		Page
104.	Geometrical aberration curves for the hologram with 80 degree bend angle and 20 degree asymmetry angle	181
105.	A holographic lens having a 5 degree bend angle, a 50 degree asymmetry angle, and a single image tilt of 3 degrees . .	182
106.	Geometrical aberration curves for the Hologram with 5 degree bend angle and 50 degree asymmetry angle	183
107.	Headrest mounted projection technique for illuminating holograms on canopy	185
108.	Fiber optic bundle-coupled projection technique for illuminating canopy mounted holograms	186
109.	Infrared source-slaved projection technique for illuminating holograms on canopy	187
110.	Concept for multiple line of sight coverage by a single source	188

LIST OF TABLES

Table		Page
1.	See-through Display Requirements	9
2.	Missions Function Summary	19
3.	Information Requirement Coding	22
4.	Mission Segments versus Information Requirements	23
5.	Visor/Canopy Display Symbology Requirements	24
6.	Symbol Element Information Attributes	26
7.	A/A Dogfight Simulation Parameters	29
8.	Hologram Recording Material Requirements for Desired Display System Characteristics	54
9.	State-of-the-Art Performance for Available Thick Phase Hologram Recording Materials	55
10.	Characteristics of Several CRT Types	62
11.	Selected Phosphor Characteristics of Yellow-Green Phosphors	64
12.	Selected CRT Characteristics	68
13.	Laser Sources Available	72
14.	Laser Scanning Techniques	76
15.	Acousto-Optic Scanning State-of-the-Art	78
16.	Characteristics of Several LED Materials	82
17.	Monolithic GaP LED Array Performance Characteristic	83
18.	Present Display Performance	93
19.	Image Source Characteristics	109
20.	Reflective Holographic System Performance Summary	159
21.	Optical Characteristics of Hologram Having an 80 Degree Bend Angle and a 20 Degree Asymmetry Angle	179
22.	Optical Characteristics of Hologram Having a 5 Degree Bend Angle and a 50 Degree Asymmetry Angle	182

1.0 INTRODUCTION

The objective of this study program is feasibility determination concerned with the employment of holographic optical elements to enhance display capabilities in a modern fighter aircraft. Specifically addressed are the utilizations of 1) reflective holographic elements on the aircraft canopy and 2) transmissive holographic elements on the operator's helmet visor. These concepts are developed into systems which will augment existing cockpit displays by presenting important supplementary information out of the boresighted display area.

Extensive background information is provided in the areas of 1) display technology 2) materials technology and optical design technology. A look ahead in the various technology areas is also provided for identification of areas where state-of-the-art improvements will impact the feasibility of the advanced concepts. Tradeoff exercises have also been conducted where applicable.

Baseline designs for both the transmissive and reflective concepts are summarized in Section 2.0. The system requirements, both operational and psychophysical are discussed in Section 3.0. Section 4.0 contains an extensive overview of the entire holographic optics technology. Comparison and descriptions of suitable diffraction optic image sources concludes Section 4.0.

Section 5.0 is concerned with the feasibility aspects of the two system concepts. Physical and optical design consideration are discussed and evaluated. The detailed descriptions of both baseline system designs are contained in Section 6.0. The optical designs and their performance are also covered in this section which concludes with alternatives and recommendations based on study findings.

2.0 BASELINE SYSTEMS SUMMARY

2.1 REVIEW

The objective of this study program is a determination of the feasibility of applying the technology of diffraction optics to the task of enhancing presentation of information to an operator of a modern fighter aircraft. More specifically, the study has been directed to investigations of extending existing information display capabilities by employing holographic optical elements in 1) a reflective mode on the aircraft canopy and 2) a transmissive mode on the operator's helmet visor. Both display approaches are to present a see-through capability similar to a conventional Head-up display.

The current art in see-through display devices is composed of Head-up displays (HUDs) and some Helmet mounted displays (HMDs). Head-up displays are precision flight instruments which provide a see-through display whose symbology-to-outside world registration accuracy is sufficient to enable effective weapons delivery. Because of the many physical restrictions encountered in the typical fighter cockpit, the fields of view presented by typical HUDs are less than adequate for presentation of ancillary information without undesirable clutter. The field of view characteristics of a HUD are functions of the size of the collimating optical element and the size of the combining glass. The sizes of both of these constituents are restricted by the cockpit installation.

The HMD is unique because it does not demand any space on the instrument panel. Fields of view are moderate – limited by the size of the display source and the relay optics. The type of information presented on a HMD is different from that on a HUD because the displays are not registered nor necessarily associated with outside world objects. Head trackers have been developed to enable the HMD information content to be updated as a function of operator line of sight direction, thus enhancing the utility of the display. The major drawback to conventional HMDs is the weight of the display apparatus on the helmet.

Currently, wider field of view HUDs and lighter HMDs are being developed, both employing diffraction optical elements. The diffraction optics HMD incorporated a reflective, holographic, collimating element on the inside of the

PRECEDING PAGE BLANK-NOT FILMED

flight helmet visor to present a collimated image of a one-inch CRT to one of the pilot's eyes. There are wide field of view HUDs using conventional optics, however, the diffraction optics HUD represents the zenith of advanced HUD designs in terms of superior performance characteristics. The major advantages associated with the diffraction optics technology are lighter weight, better see-through characteristics and significantly higher display efficiencies.

The concepts under investigation in this study are the next logical extensions of the applications of both diffraction optics technology and operator-centered information display technology. For the transmission display on the helmet visor, the display source has been removed from the helmet. Instead, the holographic collimating element acts upon discrete sources in the cockpit, collimating them and directing them to the operator's line of sight. The reflective system concept uses one or more display sources which are acted upon by reflective holographic collimating elements located on the canopy surface and directed to the operator's line of sight. Both techniques enable presentation of information which is supplementary to the primary HUD function information and any information displayed by these extended systems does not coincide with the HUD field of view.

The primary justification for expanding the see-through display capability is the improvement of the operator capability for effective target acquisition and weapon delivery. This is accomplished by providing display of essential information for the performance of these tasks while permitting heads-up operation of the aircraft. Requirements of an expanded capability system of this type must address locations and types of information to be displayed as well as field of view coverage and psychophysical parameters. These requirements have, in part, been generated through studies of HUD effectiveness in a variety of mission simulations.

Analyses of mission segments have pointed out information needs of the pilot while his attention is focused outside the cockpit. There are a variety of symbol elements which may be presented to augment pilot capability and are not related to any specific object in the outside world. These would be suitable for display by a canopy or visor based system. The major benefit, however, of these supplementary displays is the enhancement of the head-up field of view over those of even the most advanced HUDs. In addition, certain symbology which was originally included in the HUD field may be relegated to a peripheral display area thus decluttering the armament sector.

The coverage of potential target lines of sight has been identified as an area which has need for increased attention. Air-to-air situation demands, based on simulation studies identified the need for increased coverage directly above the HUD combiners. Air-to-ground field of view analyses have pointed up the utility of increased azimuth coverages over those of a conventional HUD. Based on these studies and assumptions of mission distributions, need priorities were assigned to lines of sight such that further system design efforts might be based on the most efficient utilization of canopy and cockpit space. Anthropometric analysis was also applied to assure that the chosen system was compatible with operator needs and capabilities.

Two baseline system concepts were defined, analyzed and iterated into their most feasible form using the F-16 cockpit geometry. Limited cockpit space for display sources proved to be the major obstacle in the concept developments. Control of spectral flare and chromatic dispersion was a fundamental problem with the transmissive visor-based system. Adverse canopy geometry proved to be a difficulty with the reflective system which had to be overcome. Neither approach yielded superior results, however, the reflective system showed acceptable image quality for limited fields of view.

The baseline reflective system employs eight holographic elements (HOEs) on the aircraft canopy. Each element has a unique display source at its focus and provides a separate, collimated display to the pilot along a unique line of sight. The eight HOEs are clustered around the central HUD sector and, in conjunction with it, provide a segmented wide angle coverage of $\pm 30^{o}$ in azimuth and -15^{o} to $+30^{o}$ in elevation. Each HOE has a 10^{o} by 10^{o} field coverage and fills a 3-inch diameter exit pupil. Although individual fields of view are modest, the overall coverage encompasses the most utilized areas of the canopy. The displays may be interactive and so configured that they direct the pilot to look into the area of interest. The large number of discrete sources presents a packaging problem. They do, however, provide a backup capability should any one source malfunction. The transmissive visor-mounted system evolved into a two display/source system for two helmet visor-mounted holographic elements. Each element provides a monocular pupil and can be seen by a single eye only. The sources are CRTs and are located at either side of the instrument panel. Depending on the direction of operator observation, either one or the other eye can observe the collimated display. Both displays may not be viewed simultaneously.

Both of the baseline concepts experience problems, however, the transmissive system's spectral flare difficulty does not lend itself to ready solution with today's techniques. The reflective system concept's major problem is the packaging of the multiple sources within the cockpit confines without hampering physical motion or obscuring visual capability.

The utilization of diffraction optics elements as collimators is a relatively young concept that has evolved over the past few years from the holographic recording technology. It encompasses the design and application of lens-like components which use optical diffraction rather than refraction or reflection to steer light. The ultimate advantages are in weight (the optical action takes place in a thin gelatin layer rather than at thick air-glass surfaces) and efficiency (the holographic element is able to reflect a narrow select wavelength with 80 percent efficiency while transmitting 90 percent of incident visible energy). These two features, more than any others, make diffraction optics an important, advanced concept for airborne head-up applications.

The design and production of HOEs involves a variety of new technologies such as complex computerized optical designs, holographic recording materials and chemical processing techniques. The more traditional disciplines of display optical design also apply; hence the new technology lends itself readily to existing analysis tools and techniques. The current choice for HOE recording materials is dichromated gelatin, a chemically complex material which is relatively difficult to process. Currently, glass is the choice for the gelatin hologram substrate. It provides an environmentally stable package under temperature-humidity exposure. The next generation in HOE packaging will involve the development of plastic as a lighter, more workable, base medium, resulting in lower manufacturing costs.

The availability of suitable display sources to be used in conjunction with diffraction optical systems is rather limited. The criteria of high brightness and narrow bandwidth restricts the available choices to a select few. First round choices were; 1) the CRT; 2) the liquid crystal display; 3) scanned laser display; 4) light emitting diodes and 5) incandescent lamps. The incandescent lamp was the only broadband source considered. It was eliminated due to efficiency considerations. The remainder of the sources were all relatively narrow band, however, the light emitting diode also proved to be inefficient as well as unstable and the liquid crystal did not readily lend itself to the proposed installation for the reflective HOE system. The laser and the CRT are the final

choices for the baseline system. The tradeoff between the laser and the CRT is geometry dependent.

In order to accomplish optical raytracing of the F-16 canopy and determine its optical characteristics as a reflector, the coordinates of the canopy were programmed into a computer and a surface mapping was generated. Using this surface information, rays could be traced from the eye to a location on the canopy and the reflected ray direction computed. In this manner, an optimum source location could be determined for each HOE on the canopy. The results of this exercise indicated that all rays from the design eye to the canopy were reflected to locations along the fuselage axis, between the pilot's knees, etc. Based on this information, the sill areas on either side of the canopy were chosen as display source sites. The sill areas represent a minimum departure from a symmetrical geometry.

The geometry of the F-16 canopy presents a unique and difficult problem for the optical designer, especially for systems employing diffraction optics. The canopy shape is optimal for a supersonic, aerodynamic body, however, its geometry as the substrate for the reflective holographic elements is clearly adverse. The majority of the canopy's forward portion makes extremely large angles with the operator's line of sight and steps must be taken to avoid the exaggerated chromatic dispersion realized with either this drastically asymmetric optical geometry or the image quality degradation experienced with large bend angles. For HOEs located on either side of the HUD, positions have been found on the canopy sill which represent reasonable compromises in asymmetry but with excessive bend angle. For the HOEs located on the fuselage axis, two, over-the-shoulder sources are required. The over-the-shoulder geometry results in small bend angles and a very large asymmetry condition where dispersion would become objectionable.

Considerations of using a sub-canopy or modified surface to alleviate these optical geometry problems were given, however, the probability of creating unwanted reflections and complicating the problem deterred and, finally, terminated that line of thought.

With the HOE locations set and the optical characteristics of the canopy defined, the computerized optical design was undertaken in earnest. For holographic optical systems, two limiting cases are possible. These are the image hologram and the pupil hologram. The image hologram is characterized by good axial imagery and a large pupil, but relatively small fields of view are

achievable due to inherent aberrations and efficiency considerations. The pupil hologram, on the other hand, is characterized by high efficiency across the field and thus a large field of view, but with some axial aberrations. Image hologram systems may be constructed without relay optics, whereas pupil holograms normally require a relayed system to obtain the desired result. For this application a relayless image hologram is the most desirable in that no optics are required between the display source and the hologram.

In the image hologram systems designed for the F-16 canopy, large image surface tilt disparities exist. These tilts must be corrected if the collimated images are to have reasonable quality. By manipulating the construction optics and tilting the display planes, these problems may be overcome and acceptable imagery may be achieved.

For analysis of system performance, two representative geometries were analyzed by computer. One of the geometries consisted of a cylinder with a tilted vertical axis and the image source near the exit pupil. The other example was a tilted cylindrical surface with the source at an 80° angle to the design eye/hologram line of sight. The former example is representative of the over-the-shoulder source and the latter is the sill mounted source. The over-the-shoulder geometry produced 4 milliradians of axial coma and 4 mrad/nanometer of chromatic dispersion. The sill-mounted geometry produced 6 mrad of axial coma and 1 mrad of dispersion per nanometer. The consequences of these aberrations are as follows: 1) The high dispersion of the over-the-shoulder approach precludes using a CRT as the source because of its 2.5 nm emission spectrum. Only a laser source is sufficiently narrow banded to produce acceptable imagery with minimum image smear. 2) The sill-mounted systems will work with a CRT source as their dispersion is much less.

A more serious problem occurs with the axial coma and spherical aberration present in both systems. The coma manifests itself as image motion when the head is moved. This motion is tolerable for a non-registering system, however it is apt to be annoying. The manifestation of spherical aberration, however, is a binocular disparity between the two eyes which can be quite annoying, if not uncomfortable. Both of these representative cases have pointed out that the geometries encountered in the F-16 do not readily lend themselves to a reflective holographic system and resultant fields of view must be quite small if these disparities are to be maintained at an acceptable level.

The transmission visor system is also plagued by spectral flare and chromatic dispersion problems. Rainbow colored images of bright objects will be experienced, displaced from each other along the grating axis. This is a fundamental problem arising from the nature of the diffraction plane geometry in the transmission hologram. The psychophysical effect of these distortions is felt to be so objectionable as to render the transmission system unworkable with today's techniques.

Both system concepts require further work before they can be effectively utilized in a cockpit situation.

2.2 REQUIREMENTS

The requirements for a baseline, see-through display are presented in Table 1. They are representative of operator needs dictated by required mission and weapon delivery functions of the modern fighter aircraft. The see-through displays characterized in the table are intended as a supplement to an existing HUD, hence the registration accuracy may be somewhat reduced from that of the typical HUD. Other requirements are also relaxed for this reason; however, viewability characteristics have not been compromised in this study.

TABLE 1. SEE-THROUGH DISPLAY REQUIREMENTS

Total Field Coverage (including existing HUD)	
Horizontal	±30 degrees
Vertical	-15 to +30 degrees
Individual HOE FOV	10 degrees (circular)
Symbol Brightness to Eye	1800 fL minimum
See-Through Transmission	>80 percent
Registration Accuracy	1 degree or better
Resolution	2 mrad
Contrast Ratio	1.2 minimum
Binocular Disparity	<4 mrad
Installation	Compatible with F-16 cockpit geometry
Outside World Coloration	Negligible
Exit Pupil Size	
Reflection System	3½" H x 2½" V biocular
Transmission System	1 to 1½" dia each eye

The requirements in the table are slanted toward a reflection type system. Most of the table is also applicable to a transmissive visor system; however, the field coverage and registration accuracy requirements do not apply to the helmet display because of its dissimilar geometry. It should be noted that, in most cases, the numerical values of the characteristics represent a practical minimum based on previous experience in see-through displays. Tradeoffs which affect these numbers will no doubt be in order. Therefore, they should be regarded as tentative baseline quantities rather than solid requirements.

2.3 REFLECTIVE SYSTEM

The approach to be employed for the canopy mounted reflection hologram system is described herein and is illustrated in Figure 1. Research into operator mission requirements has yielded information on system demands which establishes priorities for the locations of Holographic Optical Elements (HOEs) on the canopy. Although an alternate substrate to the canopy was

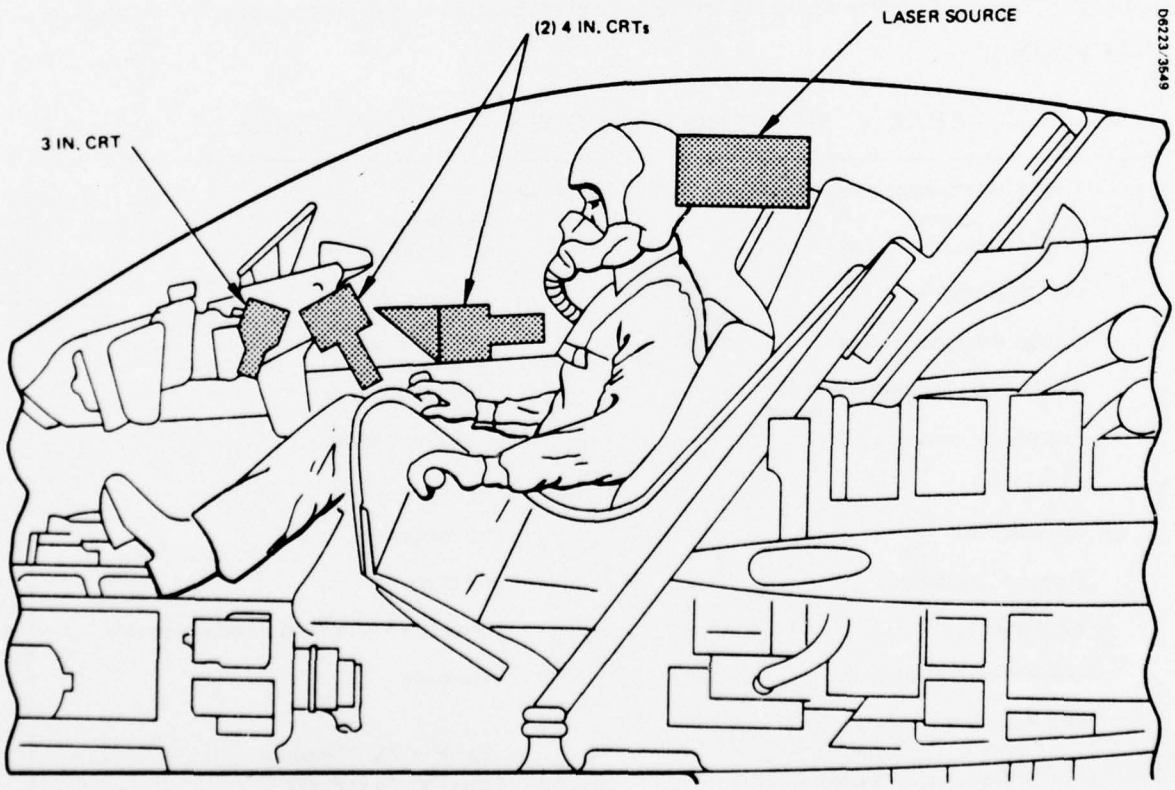


Figure 1. Baseline reflective HOE system.

considered, the baseline system places the HOEs on the F-16 inside canopy surface. The operator's field consists of eight HOEs, located adjacent to one another and clustered around the zero azimuth point. The locations of the HOEs span azimuth angles of $\pm 30^{\circ}$ and 0° to $+30^{\circ}$ in elevation. The HOEs do not overlap. The individual field coverage of each HOE is $10^{\circ} \times 10^{\circ}$ and its relation to the borders of the HOE is a variable depending on the height of the operator's eye. The mission data has indicated that these sites are the most effective locations for the HOEs.

2.3.1 Single vs Multiple HOEs

In the baseline system, each HOE is the collimating optical element for a unique image source. In spite of the additional space and cost required for separate sources, there are several reasons why it is a reasonable approach. First, the optical requirement at an object plane for two different HOEs is most likely so different that it is not reasonable to attempt adapting the same image source to both cases. Second, if the object state is switched to accommodate multiple displays – it is necessary to sense which HOE is being regarded so that the proper state is selected, i.e., a head tracker is employed. Third, duplication of displays provides backup should one display malfunction. The overall lack of complexity associated with multiple sources seems to override the additional bulk and expense. Locations of the image sources in the cockpit were determined by tracing rays from the eye to the HOE centers and noting the reflected ray's angle and strike point at the cockpit sill line. Generally, these reflected rays terminated at or near the centerline of the fuselage. The image sources were then laterally displaced the minimum distance from the symmetrical strike point towards the canopy sill, the sill being a convenient spot which has minimum obstruction of the pilot's outside world vision and is physically out of the way of controls and operations. The image sources for the side HOEs are symmetrically located at either side of the fuselage. The image sources for the two centrally located HOEs are located about shoulder height behind the operator's head on either side. These locations are optically very asymmetric, however, there is no convenient location at or near the symmetrically reflected ray.

2.4 TRANSMISSION SYSTEM

The baseline system utilizing transmission holographic elements on the operator's visor tailored for the F-16 aircraft is shown in Figure 2. Two CRT

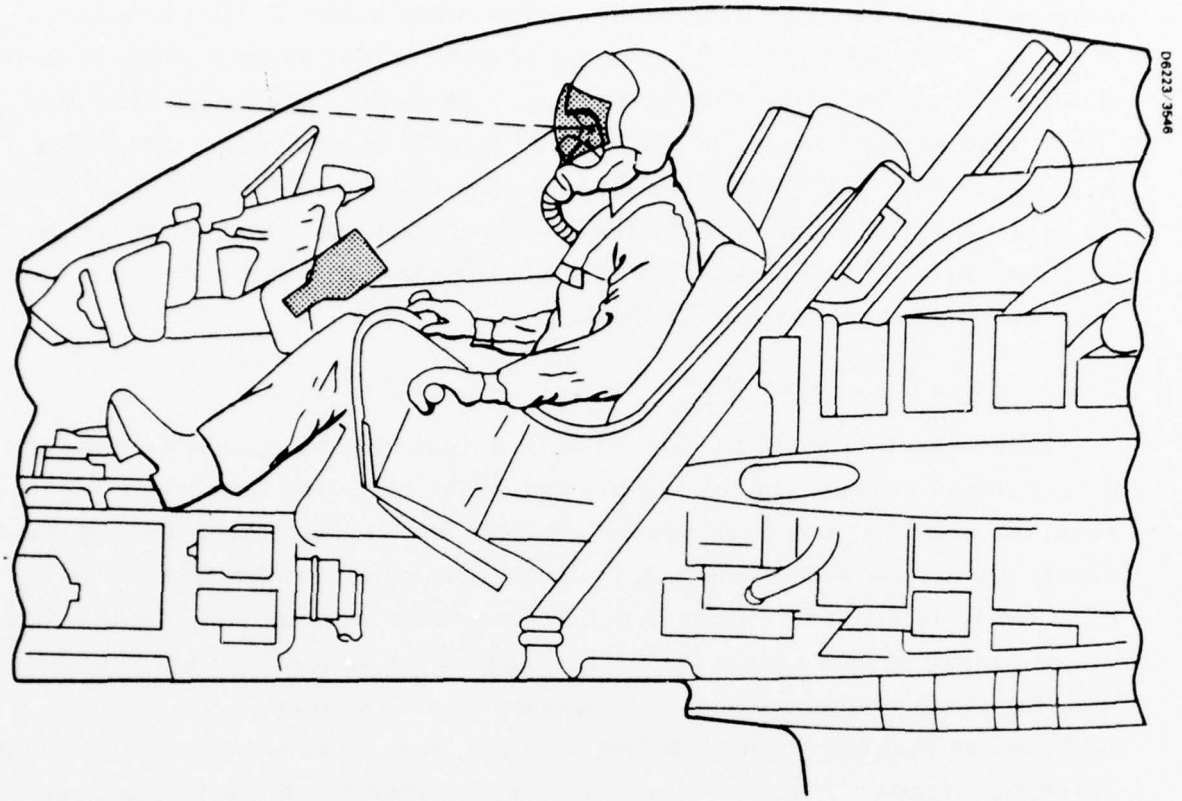


Figure 2. Baseline transmissive HOE system.

image sources are used at symmetrically located stations on either side of the F-16 instrument panel. These stations were determined to be the only reasonable locations for the required image sources. A view which better illustrates these locations is shown in Figure 3.

The visor contains two holographic elements. Each element is so constructed and aligned that with the visor pointed off towards the left, the left eye will see a collimated display fixed in space. Similarly, a right oriented visor will produce a collimated display at the right eye. The exit pupils of the system are such that the head and eye have a reasonable amount of freedom of motion – however, the efficiency falloff of the HOEs on the visor may cause some vignetting of the display as head motion exceeds certain limits. The system is such that both eyes are prevented from simultaneously viewing the two displays.

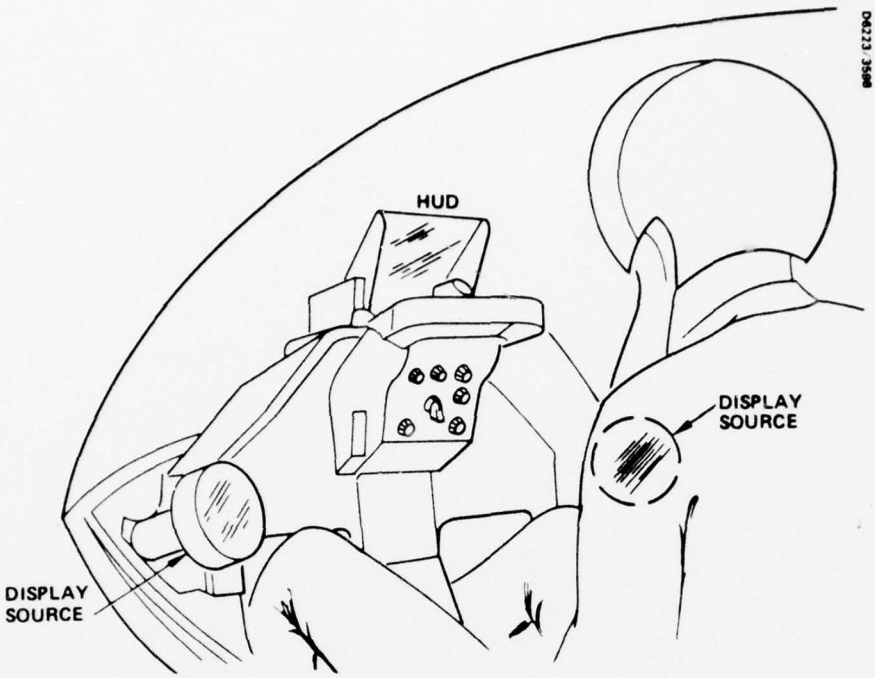


Figure 3. Location of forward HOE image sources.

The transmissive system presented herein and described in detail in the design section has many problems associated with its operation. Several are considered at this time to be insoluble. Among these problems are dispersion, spectral flare and spurious reflections, all to be described in detail. The feasibility of this system appears, in general, to be extremely limited.

3.0 OPERATIONAL REQUIREMENTS

3.1 INTRODUCTION

The modern tactical fighter aircraft is a carefully designed system intended to assist the pilot in the achievement of his mission objectives. Designing the system, and in particular that portion of the system in constant communication with the pilot, is a process that involves the determination of the functional assignments between man and machine. Specific functional assignments should be made to the pilot, or to electronic or mechanical system components in such a way as to obtain the best overall system performance or cost effectiveness. Because humans are more efficient than machines in the performance of certain kinds of tasks, and less efficient in the performance of others, optimum overall performance often results when the pilot and aircraft systems work together. Collaboration of this sort inevitably involves the continuous flow of information between man and machine. Devices used by the pilot to pass information to the aircraft are called controls. Devices used by the aircraft to communicate information to the pilot are called displays.

Displays are categorized according to the perceptual channel employed and format of information encoding. Because the information flow rate capacity of the visual system is so great relative to that of the other senses, information which changes rapidly through a broad range of alternatives is best presented to the eye. Often while performing mission related tasks, the pilot must collect visual information originating both inside and outside of the aircraft system. Because quantitative indications of airspeed, altitude, heading, etc., are difficult to extract from the visual world, these data must be presented explicitly via system internal displays. Other types of information are more directly available from the visual environment. Experience has demonstrated the importance of direct vision as a source of target presence and relative location information, even when the system includes alternate sensors of this data.

Because vision is a highly directional sense, design consideration must be given to the location of displayed information within the visual environment.

PRECEDING PAGE BLANK-NOT FILMED

When critical information is to be found in the external visual world, information presented simultaneously from within the system must be displayed in close proximity to the same externally directed line of sight. Display devices providing this capability have come to be known as "head-up" displays because the pilot may observe them without looking down into the cockpit. Head-up displays are most useful for the presentation of information which must be correlated with or viewed colinearly with information from the external scene. Since externally originating information may arrive at the pilot's eye along any sight line through the canopy, the mechanism for presentation of internally derived signals must not be opaque. Information from both sources are "combined" along a single viewing axis by a semi-transparent reflector which transmits outside light and reflects internal data from an indirectly viewed source.

The ideal head-up display should present information at any viewing location that the pilot requires. The technology required to accomplish large area information display within the constraints and confines of a fighter aircraft cockpit has not been available. The approaching development of practical diffraction-based holographic optical elements holds out the possibility that such displays might be realized in the near future. Existing avionic display mechanizations are the result of optimization of the system as described above, subject to the limitations of available technology. Wide field of view diffraction optical displays represent a major departure in display capability. They can, therefore, be expected to have significant impact not only on the ability to present information but also on the decision as to what information should be presented. The source of the information presentation requirement is the mission itself. To develop these requirements for a system with diffraction optics displays, mission of a 1980-1990 tactical aircraft have been examined.

3.2 MISSION ANALYSIS

The mission analysis was directed to the identification of pilot information requirements for each segment of a 1980-1990 tactical aircraft mission. Eight candidate missions were analyzed by means of functional flow diagrams. These diagrams provided the framework for the analysis of pilot/system functional requirements during each mission phase. Mission functions were

then analyzed to establish pilot information requirements. These requirements were then translated into specific display symbology and performance requirements.

3.2.1 Assumptions

It was assumed that the 1980-1990 tactical aircraft will be a land-based, supersonic, one-man vehicle designed to maintain air superiority and to conduct air-to-ground strike missions. In the allocation of functional responsibilities, the pilot was assumed to be responsible for the following during mission operations:

- Command Decision Making
- Tactical Situation Assessment
- Flight Control (manual or autopilot monitoring, including high and low altitude operations)
- Navigation
- Visual and Aided Visual Search for Targets, Checkpoints
- Visual and Aided Visual Acquisition
- Sensor Search and Acquisition
- TV Guided Weapon Acquisition
- Correlation of Sensor Presentations with Direct Visual Scene when Necessary
- Visual Weapon Delivery

Other functional responsibilities were assumed to be automated.

The 1980-1990 tactical aircraft was assumed to have a radar capability consisting of the following:

- Air-to-Air Modes
  - Conventional search and track
  - Moving target search and track
  - Ranging (boresight or reticle-slaved)
- Air-to-Ground Modes
  - Conventional forward sector ground map with prominent target track (PPI)
- Compatible with
  - IFF
  - Beacons
  - Missile TV

All-weather operations were assumed as a goal, including delivery of bombs, air-to-air and air-to-ground missiles, and gunfire. Visual, blind, and radar-aided weapon delivery modes are as follows: loft, roll-ahead, dive toss, glide and laydown, with continuously computed release solutions. Air-to-ground missiles include: Walleye, Maverick, Shrike and ARM. Both radar and IR air-to-air missiles were considered. They are assumed to be similar to the Sidewinder and Sparrow III. A high-rate-of-fire internally carried gun was assumed for use against airborne or ground targets.

3.2.2 Tactical Missions

Eight candidate missions were specified for the potential 1980-1990 tactical operations.

- Combat Air Patrol (CAP)
- Intercept (INTCPT)
- Fighter Escort-Close-Air Support (FE/CAS)
- Fighter Escort – Interdiction (FE/INT)
- Close Air Support – Self Escort (CAS/SE)
- Interdiction – Self Escort (INT/SE)
- Long Range Strike (LRS)
- Ferry

Each mission was analyzed to determine the major segments or functions which must be performed to complete the standard mission goals. Functional flow block diagrams have been developed for each mission. These diagrams are included as Appendix A of this report. Twenty-eight major mission functions were identified. As shown in Table 2, these functions may be pertinent to several or all of the candidate missions. However, these functions provide the primary structure for the development of specific requirements for the presentation of information to the pilot.

3.2.3 Information Requirements

Individual mission functions (segments) were further analyzed to identify the types of information which must be made available to the pilot. This information ranged from the very basic data such as attitude, which is common to all functions, to highly specialized data such as the missile video used in the

TABLE 2. MISSIONS FUNCTION SUMMARY

Mission Functions	Missions						
	CAP	INT	FE CAS	FE INT	CAS SE	INT SE	LRS
Routine Operations							
1. Takeoff	X	X	X	X	X	X	X
2. Independent Transit (etc)	X	X	X	X	X	X	X
3. Formation Transit (etc)	X	X	X	X	X	X	X
4. NAV Update, Visual	X	X	X	X	X	X	X
5. NAV Update, Sensor	X	X	X	X	X	X	X
6. Land	X	X	X	X	X	X	X
Low Altitude Operations							
7. Dash – TF				X		X	
8. Low Altitude Cruise (TA)							X
9. NAV Update, Visual				X		X	X
10. NAV Update, Sensor				X		X	X
Air-to-Air Operations							
11. Transit (etc) Air-to-Air Search	X	X	X	X	X	X	X
12. Transit (etc) Search, Track Classification/Identification	X	X	X	X	X	X	X
13. Launch (Long Range)	X	X	X	X	X	X	X
14. Intercept and Identification, Visual	X	X	X	X	X	X	X
15. Launch (Close Range	X	X	X	X	X	X	X
16. Gun Attack	X	X	X	X	X	X	X
17. Hit/Damage Evaluation	X	X	X	X	X	X	X
18. Maneuver to Counterattack	X	X	X	X	X	X	X
Air-to-Ground Operations							
19. Search/Acquisition, Visual					X	X	X
20. Search/Acquisition, Forward Sector, Sensor					X	X	X
21. Search/Acquisition per Ground Link FAC					X	X	
22. Search/Acquisition, Offset Sensor					X	X	X
23. Acquisition, Missile Sensor					X	X	
24. Launch, Air-to-Ground Missile					X	X	
25. Attack, Guns and Rockets					X	X	X
26. Deliver Bomb(s)					X	X	X
27. Guide Missile					X	X	
28. Hit/Damage Evaluation					X	X	X

target acquisition function. In all, 17 categories of information were identified as necessary in pilot performance of the tactical mission functions:

1. Basic Attitude – Own aircraft pitch and roll.
2. Steering Commands – Two dimensional steering commands, either pitch and roll or pitch and azimuth. Pullup commands are also included.
3. Basic Flight Information – Heading, air speed, altitude, and when at low altitude, ground intercept of own velocity vector.
4. Flight Commands – Heading, altitude and/or airspeed commands.
5. Landing – Glide slope and localizer deviation, angle of attack, and markers.
6. Designation Recticle Cursor – A symbol viewed against the outside world or against radar imagery representing an accurately known (to the computer) LOS to be used for checkpoint or target designation. May be fixed in A/C coordinates or moved via hand controller.
7. Aiming Indicator – A symbol viewed against the outside world or against sensor imagery, positioned by the computer, which represents the nominal impact point (instantaneous and/or predicted) for guns, rockets, or bombs.
8. Predicted Target(s) Information – A search aid, viewed against the outside world or against sensor imagery, positioned by the computer in the appropriate format and including both position and rate information, as available, based on stored position data. "Target: may apply to all air contacts (enemy, friendly, or unknown), ground targets, checkpoints, I. P. 's, etc.
9. Tracked Target(s) Information – Same as 8 except based on a target being actively tracked. May take the form of azimuth, elevation, slant range, ground range, relative velocity, relative altitude, etc.
10. Launch Limits Information – In/out of range or angle indication, time-to-go, maximum and minimum range, allowable steering error, "g" limits, speed limits, and/or optimum launch/firing/release zone.
11. Threat Information – Bearing to radar illumination source and/or type and/or range and/or air contact detection.
12. Missile Video – Video from missile requiring pilot acquisition, e. g., Walleye, Maverick.
13. Data Link Targets and Commands – Symbols representing position rate, number, and/or type of air contacts being tracked by airborne, ship-board, or ground based command center. Also, symbols associated with one or more of the data link targets indicating such things as mandatory attack, do not attack, attack priorities, etc.
14. Air to Air Radar – Radar display presented in either C-scan, B-scan, or B-scan formats.
15. Forward Sector Radar Map – Conventional, real-time radar map of the ground in the forward sector.

16. Navigation Information – Cartographic information for the purpose of navigating and assessing own position and course relative to preplanned courses, checkpoints, destinations, ground targets, restricted flight areas, known ground threats, etc.

17. Target Reference Aids – Reconnaissance photographs, sensor imagery, detailed maps, or sketches based on reconnaissance which can be compared with sensor presentations to aid in target (or checkpoint or IP) detection identification; may include intelligence annotations.

In the process of determining what information is required to perform a mission segment, it became clear that there are several levels of "requirement". Some information types are critical to the task if performance is not to be degraded and, therefore, must be continuously displayed. Other types will improve the probability of success, if available; and so on.

The symbols used to differentiate between levels of "requirement" and several examples are shown in Table 3.

During the identification of information requirements associated with performance of each mission segment, it became apparent that for some functions these requirements vary with conditions under which the operation occurs. Of particular impact in this respect are weather (e. g., VFR versus IFR, and Day versus Night) and tactical policy regarding transmission silence. Table 4 presents the results of analyses of the information requirements appropriate to various mission segments as a function of these conditions.

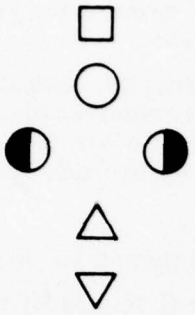
3.2.4 Canopy Display Information Requirements

The final step in the analysis process was directed to the translation of basic information requirements into specific symbols which might be presented in canopy display areas. These symbology requirements are presented in Table 5.

The display modes listed are by no means exhaustive. The modes were primarily selected to illustrate the maximum number of symbols required. There are many sub-modes (not listed) in which the symbols shown will not appear.

Specific symbology formats appropriate to each display mode are not of great concern here. What is important is to take note of symbol loading and consequent clutter associated with display in a small field of view HUD. In the worst case identified here, (Air-to-Ground Gun and Rocket delivery),

TABLE 3. INFORMATION REQUIREMENT CODING



Required continuously

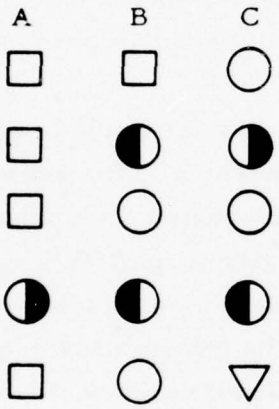
Required on demand (pilot option), additive

Required on demand (pilot option), alternatives

Displayed if available

Pilot optional when available, additive

Examples



"C" is displayed on pilot option and in addition to "A" and "B".

Either "B" or "C" can be displayed with "A".

Either "B" or "C" or both can be displayed with "A:.

At the pilot option either (1) "A" or (2) "B" and "C" is displayed.

At pilot option, either

"A" alone, or

"A" and "B", or

"A" and "B" and "C", providing "C" is available, or

"A" and "C", providing "C" is available.

some 23 separate symbols, many of which are dynamic, must be presented simultaneously.

Requirements of this magnitude clearly highlight the need for augmenting the information presentation capabilities of present day HUD's. The information presentation requirements identified by the mission analysis process provide the primary basis for the definition of the display system performance requirements.

TABLE 4. MISSION SEGMENTS VERSUS INFORMATION REQUIREMENTS

MISSION SEGMENTS	CONDITIONS						INFORMATION CATEGORY																			
	DAY	NIGHT	VFR / IFR	TRANSMIT OK	VFR / IFR	NO TRANSMIT	BASIC ATTITUDE INFORMATION	STEERING COMMANDS	BASIC FLIGHT INFORMATION	FLIGHT COMMANDS	LANDING	DESIGNATOR RETICLE/CURSOR	AIMING INDICATOR	PREDICTED TARGET(S) INFORMATION	TRACKED TARGET(S) INFORMATION	LAUNCH LIMITS INFORMATION	THREAT INFORMATION	MISSILE VIDEO	DATA LINK TARGET(S) AND COMMANDS	AIR-TO-AIR RADAR	FORWARD SECTOR RADAR MAP	NAVIGATION INFO	TARGET REFERENCE AIDS	OUTSIDE VISUAL CONTACT
ROUTINE OPERATIONS																										
1. TAKEOFF	●	●	●	●	●	●	□	△	□	△												◯		□		
2. INDEPENDENT TRANSIT (ETC)	●	●	●	●	●	●	□	◯	□	□							△					□		□		
3. FORMATION TRANSIT (ETC)	●	●	●	●	●		□	△	□	□							△					□		□		
4. NAV UPDATE, VISUAL	●	●		●	●		□	△	□	□		◯		△			△					□		□		
5. NAV UPDATE, SENSOR RADAR	●	●	●				□	△	□	□							△				◑	◑	◑	◯		
				●	●	●	□	△	□	□							△					◑	◑	◯		
6. LAND	●	●	●	●	●	●	□	△	□	△	△													□		
LOW ALTITUDE OPERATIONS																										
7. DASH – TF	●	●					□	◯	□	□							△					□		□		
8. LOW ALTITUDE CRUISE	●	●		●	●		□	◯	□	□							△					□		□		
9. NAV UPDATE, VISUAL	●	●		●	●		□	◯	□	□		◯		△			△					□		□		
10. NAV UPDATE, SENSOR	●	●	●				□	◯	□	□							△				◑	◑	◑	◯		
				●	●	●	□	◯	□	□							△					◑	◑	◯		
AIR-TO-AIR OPERATIONS																										
11. TRANSIT (ETC), AIR-TO-AIR SEARCH	●	●	●				□	◯	□	□							△			□		□		□		
				●	●	●	□	◯	□	□							△					□		□		
12. TRANSIT (ETC), SEARCH, TRACK,	●	●	●				□	◯	□	□							△			□		□		□		
CLASSIFY/IDENTIFY				●	●	●	□	◯	□	□							△					□		□		
13. LAUNCH (LONG RANGE)	●	●	●				□	◯	□	◯					◯	□	△			□				□		
14. INTERCEPT AND IDENTIFY, VISUAL	●	●					□	□	□	◯					□	□	△			□		◯		□		
				●	●		□	□	□	◯					□	△	△					◯		□		
15. LAUNCH (CLOSE RANGE)	●	●	●				□	△	□						△	□	△			◯				□		
				●	●	●	□	△	□						△	□	△							□		
16. GUN ATTACK	●	●					□		◯				□		▽	△	△			□				□		
			●			●	□		◯				□		▽		△									
				●	●		□		◯				□		▽		△									
17. HIT/DAMAGE EVALUATION	●	●	●	●	●	●																		□		
18. MANEUVER TO COUNTERATTACK	●	●		●	●												□									
AIR-TO-GROUND OPERATIONS																										
19. SEARCH/ACQUISITION, VISUAL	●	●		●	●		□		□	△		◯		△			△					□		□		
20. SEARCH/ACQUISITION, FORWARD SECTOR, SENSOR RADAR	●	●	●				□		□	△							△				□	◑	◑	◯		
				●	●	●	□		□	△							△					◑	◑	◯		
21. SEARCH/ACQUISTION PER GROUND LINK, FAC	●	●					□		□	△		◯		□			△				□	□		□		
			●				□		□	△							△				□	□		□		
				●	●		□		□	△		◯		□			△					□		□		
						●	□		□	△							△					□		□		
23. ACQUISITION, MISSILE SENSOR	●			●			□		□			◯					△	□				□		□		
24. LAUNCH AIR-TO-GROUND MISSILE	●	●	●	●	●	●	□	□	□	□					△	□	△					◯		□		
25. ATTACK, GUNS AND ROCKETS	●	●	●	●	●	●	□		□				□		▽	△	△					◯		□		
26. DELIVER BOMB(S)	●	●	●	●	●	●	□	◯	□	◯			□		▽	△	△					◯		□		
27. GUIDE MISSILE	●			●			□	◯	□	◯							△					◑	◑	□		
28. HIT/DAMAGE EVALUATION	●	●		●	●																			□		

TABLE 5. VISOR/CANOPY DISPLAY SYMBOLOGY REQUIREMENTS

| DISPLAY MODES | SYMBOLOGY REQUIREMENTS | | |

3.2.5 Information Analysis

By careful analysis of pilot information needs during each mission segment, we determined which specific items of information must be presented while the pilot's primary attention is focused outside the cockpit. We shall now consider which items can be presented by diffraction optic means to meet these needs, and try to determine the characteristics of a diffraction optics display system optimized for presentation of these data.

Table 6 summarizes the results of an examination of the important attributes of each of the identified symbol elements. The dimension of information encoding, presentation, location reference, and resolution/positioning accuracy are important determinants of display device performance requirements.

The most pronounced improvement in display capability provided by a diffraction optical display will be the enlargement of the head-up field of view over that available from even the most advanced HUD concepts presently in design. Those information elements which are presented against the frame of reference of the aircraft nose or armament datum line are unlikely to be positioned outside the field of view of contemplated HUD. Thus, they cannot be used to support a requirement for the diffraction optics system.

Those symbol elements that must be positioned over or near the target line of sight, or which must be visible when the pilot's attention is focused on the target cannot be reasonably constrained to the HUD field of view. These elements will be the most important source of requirements on the diffraction display system.

In addition, other data whose location in the visual field is not critical might be moved out of the HUD field into the visual periphery for purposes of decluttering the forward display area. Speed and altitude scales, for example, could be enlarged for easier interpretation without cluttering the HUD if they were moved outward in the visual field. An enlarged horizon line extending beyond the angular limits of the HUD might provide a more sensitive indication of bank angle and roll rate.

Based upon the data presented here and upon the presumption that the diffraction optical display will be used to augment the HUD rather than to

TABLE 6. SYMBOL ELEMENT INFORMATION ATTRIBUTES

ITEM	INFORMATION CODING DIMENSION			SYMBOL POSITION AND USE REFERENCE FRAME				SYMBOL PLACEMENT ACCURACY REQUIRED		
	SYMBOL SHAPE	SYMBOL POSITION	SYMBOL PRESENCE	AIRCRAFT NOSE	ADL	TARGET L.O.S.	ARBI-TRARY	$< 1^{\circ}$	$\sim 1^{\circ}$	ARBI-TRARY
HORIZONTAL BAR		X		X					X	
AIRCRAFT SYMBOL		X		X					X	
PITCH SCALE		X		X					X	
HEADING SCALE		X		X					X	
HEADING COMMAND		X		X					X	
ALTITUDE SCALE		X					X		X	
ALTITUDE COMMAND		X					X		X	
RANGE DIGITS	X						X			X
SPEED SCALE		X					X		X	
SPEED COMMAND		X					X		X	
STEERING DOT		X		X		△			X	
STEERING ERROR CIRCLE		X		X		△			X	
IMPACT POINT		X			X			X		
BREAKAWAY			X			△	X			X
RELEASE			X				X			X
RETICLE		X			X	△		X		
SOLUTION CUE		X			X	△		X		
FLIGHT PATH MARKER		X		X				X		
TIME TO GO	X					△	X		X	
RANGE RATE	X					△	X		X	
ZENITH/NADIR		X		X					X	
PITCH/ROLL STEERING		X		X					X	
TARGET CUE		X				X			X	
DISCRETES			X				X			X
PULL UP CUE			X			△	X			X
ENERGY MANEUVERABILITY		X				△	X		X	
ILS GLIDE PATH COMMAND		X		X					X	
OUTER WARNING			X				X			X
LAUNCH ENVELOPE		X			X	△			X	

△ DENOTES CRITICAL FOCUS OF ATTENTION
X DENOTES FRAME OF REFERENCE

replace it, the conclusion of this analysis is that the diffraction optics display will be advantageous for display of:

- Steering dot and allowable error circle
- Time to go
- Range rate
- Pitch/roll commands
- ILS Data
- Warning information
- Breakaway and pull-up cue
- Master warning

and most importantly,

- Target cueing information
- Launch envelope limits
- Energy maneuverability.

It will be useful to declutter the HUD if employed to present:

- An extended horizon
- Discrete state information.

We have determined which information should be presented on the diffraction optics display. The next section will consider how large the display must be and where it should be positioned to present this information satisfactorily.

3.3 DISPLAY REQUIREMENTS ANALYSIS

The mission analyses of the preceding pages have suggested which kinds of information can be advantageously presented by means of a diffraction optics based canopy or visor display. It remains to optimize the design of this display in order to present this information in the most effective way. Two important issues to be addressed in that regard are the display visual field size and psychophysical performance requirements.

3.3.1 Field of View Requirements

Reference to Table 6 will reveal that the informational elements identified there are required to be positioned in one of three regions of the visual environment: 1) close to the aircraft velocity vector (e.g., artificial horizon,

aircraft symbol), 2) close to the line of sight of air-to-air or air-to-ground targets (e.g., target cue, launch envelope limits), or 3) where space permits in the periphery. If the diffraction optics display design is to be responsive to the mission needs, its field of view must include: 1) a region around the aircraft's velocity vector, 2) sufficient area away from the velocity to cover the distribution of target lines of sight to the degree that is cost effective and useful, and 3) enough peripheral area for uncluttered presentation of remaining elements.

Of these requirements, the need to cover potential target lines of sight is the one with the greatest impact on the design and has been the subject of intensive analysis. The distribution of sightlines associated with air-to-air targets differs from that of air-to-ground targets and, thus, the two will be considered separately.

3.3.2 Air-to-Air Analysis

For long range air-to-air engagements, the target may or may not be visible during periods of display activity. In either case the maintenance of visual contact with the target is not of critical importance (if possible at all), and the geometry of the situation is such that the sightline may be freely manipulated by aircraft maneuvers at the pilot's option. It is the short range air-to-air engagement that demands constant visual contact between the pilot and his target, and it is also this situation which, because of short range and high maneuvering velocities, provides less immediate control of this line of sight. For these reasons, the distribution of close-quarter air-to-air target lines of sight are of greatest interest.

In order to determine this distribution, some twenty close-quarter engagements were examined using a Hughes developed TACOM-III digital air-to-air simulation. Parameters used for the participant aircraft are given in Table 7. These are representative of capabilities likely to be available for the short-range IR-guided missile equipped F-16 and threat class aircraft in the near term.

The two simulated aircraft flew identical 10^{o} lead pursuit steering after a random detection time delay from initial states. Initial conditions were picked to be representative of the range of plausible geometries which might result from: 1) friendly GCI, 2) hostile GCI, or 3) chance encounter operations.

TABLE 7. A/A DOGFIGHT SIMULATION PARAMETERS

SYMBOL	DEFINITION	VALUE
T_{MAX}	MAXIMUM COMBAT TIME	30 sec
ΔT	ITERATION TIME INCREMENT	0.3 sec
$\dot{\sigma}_{MAX_A}$	FRIENDLY MAXIMUM TARGET DESIGNATION LINE OF SIGHT RATE	30°/sec
$\dot{\sigma}_{MAX_B}$	THREAT MAXIMUM TARGET DESIGNATION LINE OF SIGHT RATE	30°/sec
$\dot{\sigma}_{MAX_{MSL\ A}}$	FRIENDLY SRM MAXIMUM TARGET LINE OF SIGHT RATE	25°/sec
$\dot{\sigma}_{MAX_{MSL\ B}}$	THREAT SRM MAXIMUM TARGET LINE OF SIGHT RATE	3°/sec
R_{MAX_L} (A)	FRIENDLY MAXIMUM MISSILE LAUNCH RANGE	24,000 ft
R_{MIN_L} (A)	FRIENDLY MINIMUM MISSILE LAUNCH RANGE	4,800 ft
R_{MAX_L} (B)	THREAT MAXIMUM LAUNCH RANGE	20,000 ft
R_{MIN_L} (B)	THREAT MINIMUM LAUNCH RANGE	2,000 ft

Aerodynamic models of a recently operational USN tactical fighter and of a representative threat aircraft were built into the TACOM-III software.

Samples of line of sight were obtained at each 0.3 second of simulated flight. The accumulated samples were then subjected to statistical analysis. Results showed that targets tend to appear close to the aircraft centerline in azimuth and 10-20° above the ADL for the largest proportion of the time when the friendly fighter is in an attacking position. Figure 4 shows the cumulative distribution of samples of azimuth angle versus probability of occurrence. It can be seen that the distribution is very steeply curved from the centerline out to a point about 20-30° off axis at which point the curve flattens out. If an azimuth field-of-view of ±30° can be provided, we can predict from the simulation that virtually all azimuth line-of-sight deviations can be accommodated.

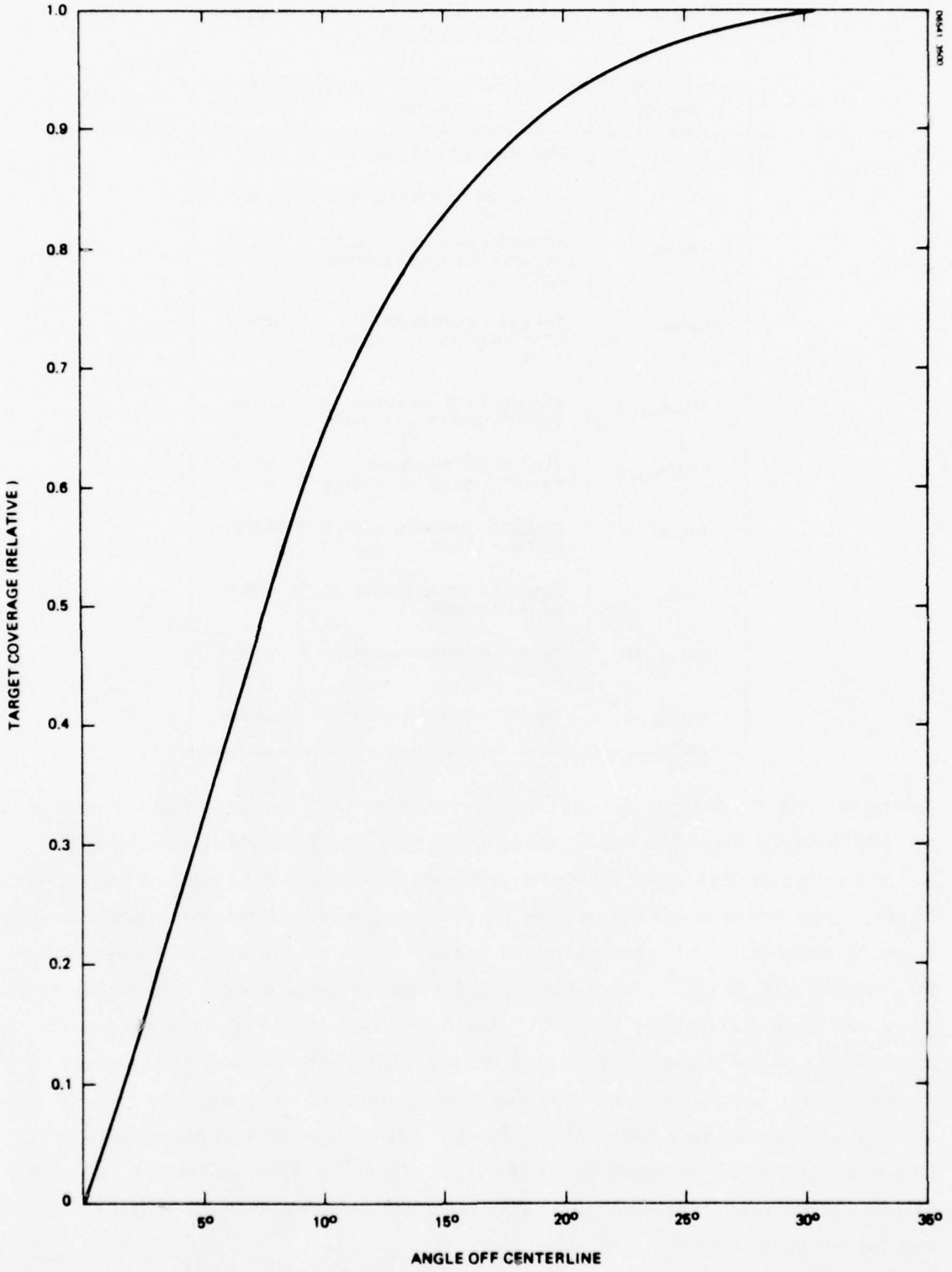


Figure 4. Air-to-air target coverage versus azimuth field of view.

Figure 5 presents a similar distribution for the elevation axis. It can be seen that there is a steeply sloped portion of the curve extending up to approximately 20° above the ADL at which point the distribution begins to flatten out. Provision of coverage up to 20° above the ADL will allow for cueing or designation functions some 70 percent of the time the target is in an attackable geometry, while to extend coverage to nearly 100 percent would require more than 40°.

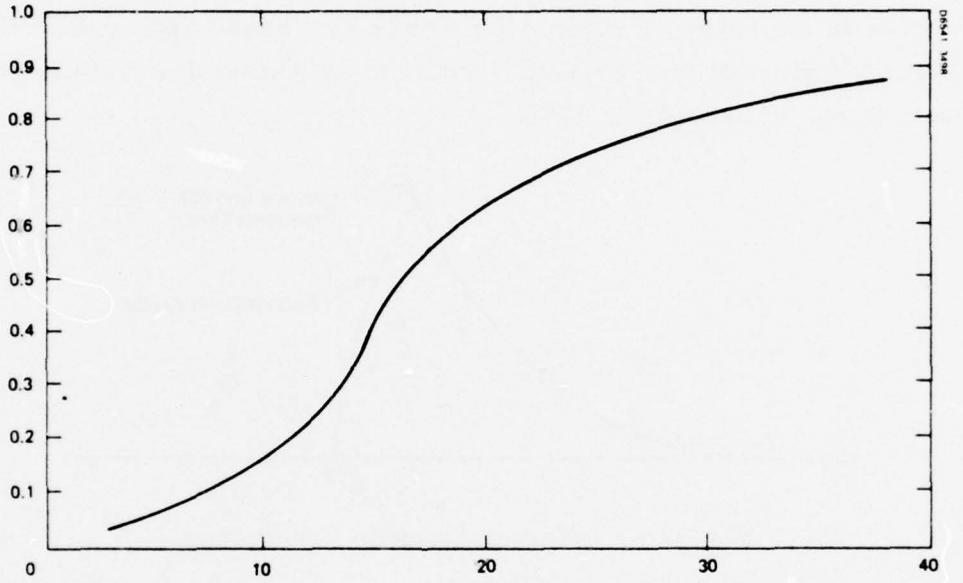


Figure 5. Distribution of target elevation line-of-sight as a function of angle above the ADL.

To meet the needs of the short range air-to-air application in the most cost effective manner, the field of view should be selected to maximize the target coverage obtained for each dollar invested. While the relationship between cost and coverage angle is not likely to be linear, it is not unreasonable to assume that the shoulders of the coverage curve which provide the greatest coverage per unit size may represent the cost effective design point as well.

3.3.3 Air-to-Ground Field of View Analysis

If the geometry of a first pass ground attack is considered simplistically, it can be demonstrated that targets must be within a region on the ground bounded by a g-limited turn path and the pilot s recognition range.

Figure 6 shows these constraints graphically. Here, Target "A" will be recognizable by the pilot, but he will be unable to overfly it directly to deliver ordnance. Target "B" is both recognizable and attackable. Target "C" is attackable but beyond recognition range. In fact, not all attacks must be made on the first pass, but if the pilot can maneuver to manipulate the target approach angle for subsequent passes, the target location no longer impacts the desired display FOV. Also, there is no one recognition range for a given target, but rather range should be related to probability of recognition along with g-level, visibility, target size, contrast, etc. In fact, in our analysis, a probabilistic approach to recognition range was based upon data from the Low Light TV Simulation Program conducted by Autonetics Division of Rockwell Corp. in September 1968.

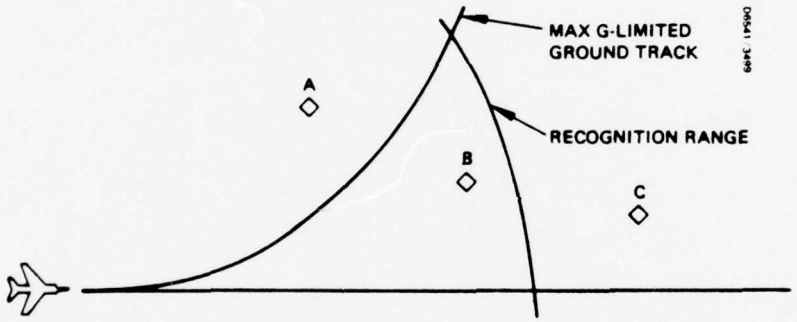


Figure 6. First pass attack geometry.

A distribution of relative area coverage within the turning path of the aircraft, weighted by the recognition probability curves from the referenced source is plotted in Figure 7 against the parameter of maximum g-limit. Since this limit varies with weapon load, three levels have been examined. Examination reveals that there is no definite breakpoint associated with either azimuth or elevation distributions and that in general, the more angular coverage available in the display, the better. This coverage should be centered about the vertical centerline in azimuth and should be below the ADL for A/G applications.

3.3.4 Summary of Field of View Requirements

One must assign priorities to the missions in order to arrive at a definitive requirement set. For the present study, we have assumed a vehicle whose primary function is air-to-air superiority with limited additional

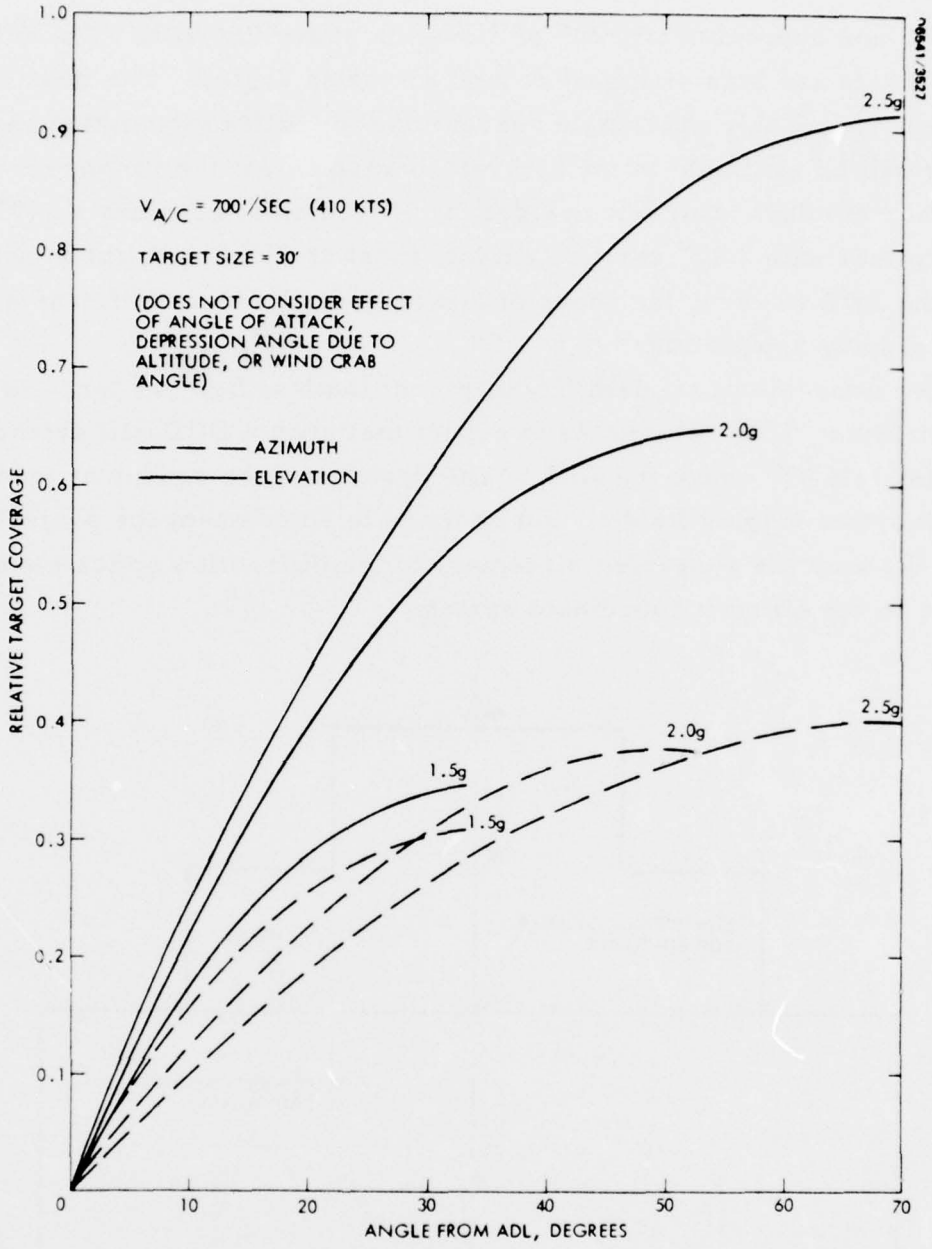


Figure 7. Relative coverage of first pass ground target versus azimuth and elevation FOV and maximum G limit.

air-to-ground capability. Accordingly, a reasonable design philosophy is to let the air-to-air requirements have greatest impact on the system design and to accept what capability to conduct air-to-ground operations naturally results.

We have determined that to be responsive to the air-to-air needs of the system, the pilot should be able to view target line of sight related data in a region extending approximately 30° either side of centerline in azimuth about

the ADL, and approximately 20° of elevation above the ADL. The azimuth requirements are less stringent at high elevation angles. The likelihood is great that reasonably wide angle conventional or diffraction optics based HUD devices will be available in the aircraft to supplement the canopy or visor diffraction display. Current designs for HUD displays feature a ±17° azimuth field together with a 22° vertical extent, most of which will likely be placed below the ADL to serve the needs of air-to-ground and takeoff/landing information display applications.

Since over-the-nose visibility in recent tactical fighters tends to be around -15° minimum, it is reasonable to expect that such a HUD will extend up to approximately +7° above the ADL. The position of the canopy or visor diffraction optics display field should be made to supplement the projected HUD. Figure 8 shows the suggested placement of the diffraction optics elements relative to the aircraft coordinate system.

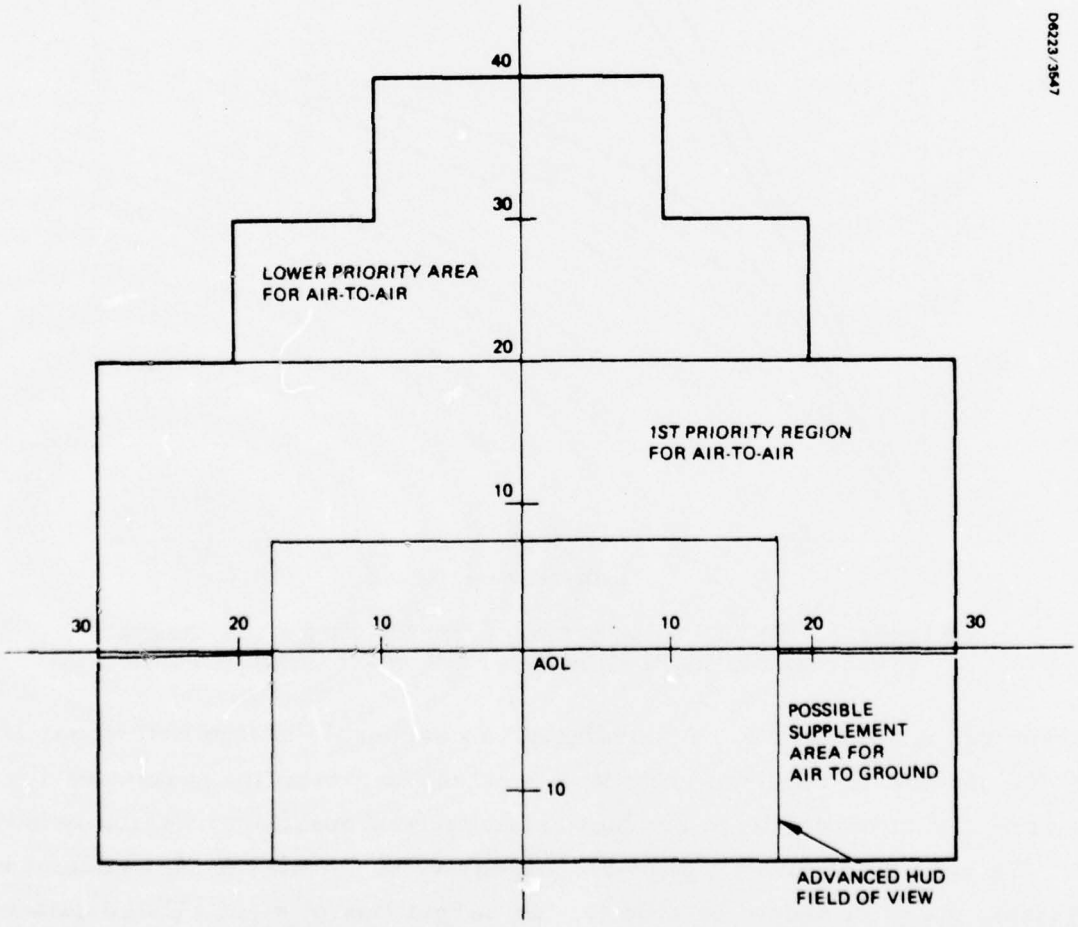


Figure 8. Suggested placement of diffraction optics display.

3.4 DISPLAY PERFORMANCE REQUIREMENTS

The performance requirements for the diffraction optics display are largely determined by the psychophysical properties of the human pilot who will use it. The most important characteristics to consider are contrast/ shades of grey capability, refresh rate, and color.

Many forms of information encoding are used to communicate data to pilots. Symbol shape and locate are commonly used on HUD devices as opposed to shades of gray because of source brightness limitations.

The difficulty of multiple shades of gray on a see-through display may be appreciated by considering the following. After attenuation by passing through the windshield and hologram, some 90 percent of the external ambient light level must be competed with to provide sufficient contract for visibility. Figure 9 illustrates just how much source brightness is required for various ambient conditions. For a 9,000 Ft-Lambert brightness at the hologram, satisfactory symbols will be viewed with a source brightness of approximately 3,300 FT-Lamberts. In order to present even marginal video (4 shades of gray), in excess of 10,000 FT-Lamberts must be available. This requirement can not be met with current technology.

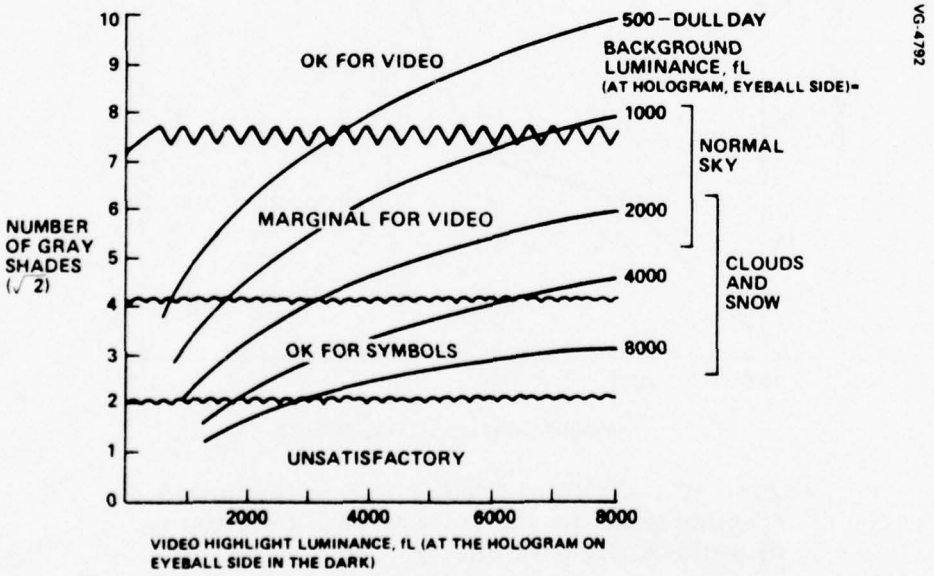


Figure 9. Requirements for see-through display luminance.

3.4.1 Display Refreshment Requirements

The display refresh rate required is determined by the properties of the observer's eye. Information updated faster than a certain threshold rate will be perceived as essentially continuous. This threshold rate is determined principally by the accommodated light level of the observer's eye. Figure 10 shows this relationship. For a 10,000 fL accommodation level, it may be seen that a display refresh rate of approximately 60 Hertz is required.

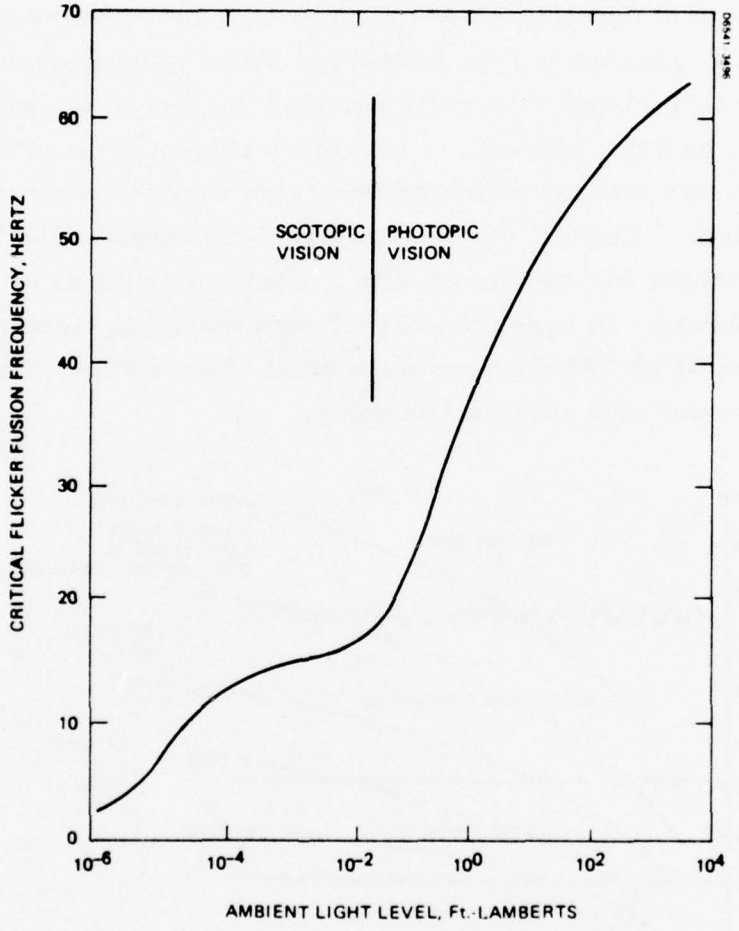


Figure 10. Critical flicker fusion threshold frequency of the human eye as a function of ambient light intensity.

3.4.2 Display Color

We have determined that a considerable source brightness is required to provide a $\sqrt{2}$ symbol contrast ratio against a 10,000 fL background. The eye is not equally responsive to all colors of light. The problem of providing useful information via a diffraction optics display is minimized by selection of a symbol color with good visual sensitivity and reasonable cromatic contrast against the background. Figure 11 shows the relative efficiency of the human eye as a function of illumination wavelength. Selection of a display color in the 550 nm region maximizes the efficiency of the energy transmission by the communication channel to the operator. At the same time, reasonably good chromatic contrast is provided by this choice.

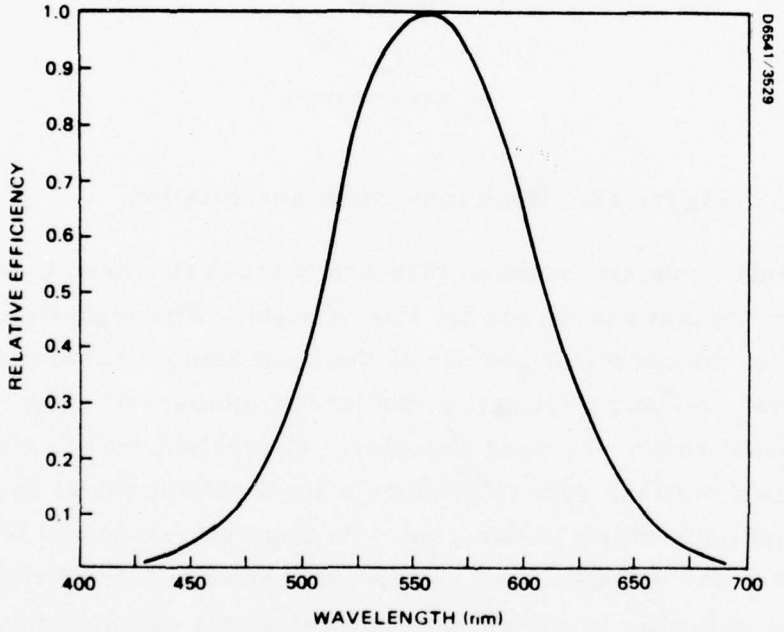


Figure 11. Spectral sensitivity of the human eye.

3.5 ANTHROPOMETRIC CONSIDERATIONS

The design of the diffraction optical system must take into account the viewing location and line of sight of the observer's eye. These are consequences of the motion of the head, and rotation of the eye relative to the head. The head itself is capable of three types of motion that result in displacement of the eye position. These movements, illustrated in Figure 12, include ventral-dorsal flexion, right-left rotation, and right-left flexion. The first two are

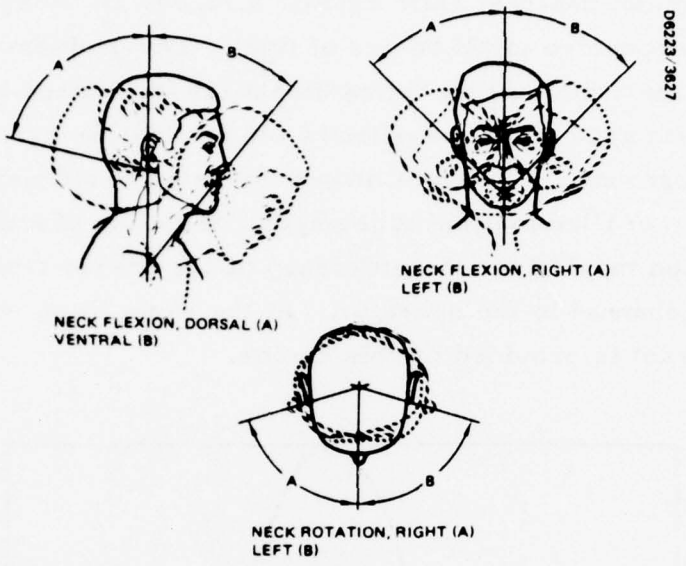


Figure 12. Neck movement and rotation.

of greatest present concern because they are most easily used by a pilot during high-g maneuvers to direct his line of sight. The right-left flexion motion results in the center of gravity of the head being displaced from the center of support creating a fatiguing unbalanced moment of sizeable magnitude acting against relatively weak muscles. Ventral-dorsal flexion and right-left rotation motions sum to produce a three-dimensional surface of possible eye locations which is complex. During ventral-dorsal flexion, the center of rotation for the left-right rotation movement is itself rotated forward about a point low in the neck, resulting in the compound curved surface relating the movement of the center of the eye and ear as illustrated in Figure 13.

At any particular head orientation, the eye can rotate with respect to its socket in any combination of vertical and horizontal angular displacements within limits. In relation to a standard straight ahead viewing reference, these limits are 35^{o} to the right, left or downward, or 25^{o} upward. The normal angle of regard is approximately straight ahead. Other viewing angles involve sustained ocular muscle tension and consequent fatigue.

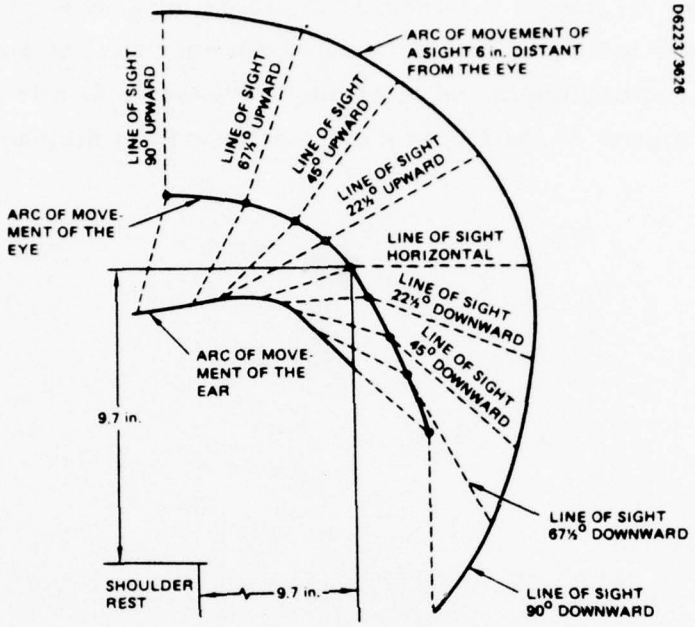


Figure 13. Angles of sight at various head position (after Brues, 1946).

Considering the total effect of head and eye rotations, it is possible to describe the range of achievable foveal orientations and, thus, define the possible areas for display placement. Alternatively, for a given display location, a surface which describes all the possible viewing locations can be found. Points in the surface represent points at which the bridge of the pilot's nose can be located so that the entire display is accessable to at least one eye. It can be seen that the design use of a simple standard eye position would lead to difficulty because there is no such position from which all possible display locations could be viewed. Further, alignment of the viewing axis for certain of the locations toward the standard design eye position would require an impossible line of vision to achieve from that position.

In the presence of high 'g' forces, the pilot's head motion will be highly constrained. The head will certainly be placed against the headrest for comfort and support. Rotations of the head out of the plane of acceleration during

such conditions are quite likely to result in rapid loss of equilibrium and thus will be avoided. When the head is reclined against the headrest, scanning is accomplished by means of eye motion alone. Then, the visual field will be restricted to a region of the cockpit which extends upwards from the bottom of the HUD and includes none of the instrument panel at all. Obviously, any information requirements the pilot may have while in this condition must be satisfied by means of the HUD or diffraction optics display.

4.0 DIFFRACTION OPTICS DISPLAY TECHNOLOGY

In this section we discuss in detail the technology required to design, analyze and fabricate display systems based on holographic optical elements (HOEs). The section begins with an introduction that gives the physical concept of a HOE and an overview of the technology. Section 4.2 then provides the details of HOE function, design and analysis. Sections 4.3 and 4.4 cover the fabrication technology and the hologram recording materials. Following the state-of-the-art discussion, Section 4.5 discusses future developments of the technology that can impact the development of display systems in the next 5 to 10 years. Finally, the requirements and state-of-the-art of image sources are discussed in Section 4.6.

4.1 HOE TECHNOLOGY

4.1.1 Physical Description

A HOE can be considered as a simple lens element, as a grating, and as a dielectric mirror (the last more for reflection holograms). In this section we discuss the similarities to each of these analogous devices, to provide a conceptual basis for the later discussions.

The similarities of a HOE to a single thin lens element are primarily that both add a relatively simple phase term to an incident wavefront. This phase term is a smooth function of the angle of incidence of the incident wave, and, based on the nature of this phase term, the element can perform various functions in an optical system. An important similarity is that neither element can provide angular magnification by itself. The elements are different in that the HOE is usually made to operate off-axis, while the lens is not. Here, off-axis means that the input and output axes of the element are not colinear. Both elements generally operate over a range of angles about the input and output axes, and desired performance can only be obtained over a limited range of such angles.

The similarity of a HOE to a grating is that both operate by diffraction from a more-or-less periodic structure that fills the aperture of the element. The analogy is closest for a transmission HOE, where the hologram structure bears a strong similarity to the grooves of a conventional grating. Both

transmission and reflection HOEs possess strong chromatic dispersion characteristic of diffraction from the periodic structure. For the holographic lens, this dispersion appears as a strong dependence of focal power on wavelength, as well as a strong angular dispersion for transmission and asymmetric reflection holograms. Another similarity with gratings is that the HOE can in general diffract light into several diffraction orders. Often, the HOE structure is designed to exhibit Bragg diffraction effects such that all but a single diffraction order are weak.

The view of a HOE as a diffraction grating is very useful in understanding HOE characteristics. The HOE is a recording of interference fringes in a light-sensitive material. These fringes form quasi-planar surfaces that have some local orientation to the surface of the recording material. We consider the grating "grooves" as being the intersections of the fringe surfaces with the substrate surface. Then the image characteristics, i.e., phase transformation, image location and size, and aberrations, are determined entirely by the locations of the fringe intersections with the surface. The amplitude of the diffracted wave (or waves) depends on the distribution and nature of the fringe recording in the volume of the recording material. This clean separation of the geometry of the diffracted wave from its amplitude benefits HOE technology tremendously.

The analogy of a HOE with a multilayer dielectric mirror holds rather well for reflection holograms, especially when the asymmetry is small. In this case the fringe surfaces are nearly parallel to the hologram substrate. The analogy mostly pertains to thick, phase holograms, where the fringes are recorded as a modulation of the refractive index of the material. In this case, which is a very important one for holographic displays, the recorded fringe structure forms a multilayer structure that typically has an index differential of 0.06 and 60 layers. This particular combination of parameters gives a peak reflectivity (diffraction efficiency) of about 80 percent and a spectral bandwidth of about 10 nm. This reflectivity and bandwidth are particularly useful in displays because they provide good see-through while maintaining relatively high reflectivity.

4.1.2 Technology Overview

In this section we briefly discuss the technology involved in developing a visual display system based on HOEs. The first step in this development

is to choose tentative design forms for each of the functional assemblies of the system. For example, a conventional relay lens might be based on a triplet design form. Similarly, the HOE or HOEs must be chosen for particular efficiency or image characteristics. The choice in both cases is based on the experience of the designer and the available literature on the subject.

The second step in the system development is to examine the geometry of the application and the desired system parameters, and to produce a first order design that can provide the desired characteristics. In this step the designer must choose the focal lengths of the elements, the basic geometrical relationships between the elements, and the apertures of the elements. These decisions are based on numerous tradeoffs that limit several of the parameters. Often the decisions in this step require changes in the design forms chosen in the previous step.

Once the designer has a viable first order design, the detailed analysis and design of the system begins. As with conventional optics, this is accomplished using computer-based raytracing. The procedure tends to be more complex with HOEs because of off-axis operation and the multilayer nature of hologram raytracing. The off-axis operation reduces the symmetry of the system, leading in general to more and larger aberrations. The multilayer nature of hologram raytracing occurs because the hologram is fabricated using two construction beams that do not appear in the final system. These two construction beams are formed by two separate optical systems that are, in general, complex sets of elements. This complexity has the advantage of introducing more flexibility into the design as well as the potential of precorrecting aberrations by changes in the construction beam optical systems. However, the analysis is much more difficult.

The design procedures for optical systems with HOEs retain most of the features of conventional optical design procedures. The designer manipulates the various parameters of the system to achieve the desired performance. He introduces new parameters when necessary. Often several parameters may be varied simultaneously to optimize a particular performance parameter. Again, the process is hindered by the complexity of the geometry and the multi-system nature of the problem. The process is highly dependent on the experience and expertise of the designer, particularly in the more complex and demanding systems.

The output of the design process consists of optical shop drawings for the elements of the final system and those of the construction beam optical systems. For all systems a set of tolerances give the limits on material characteristics, surface figure and element positions. These data are the basis for fabrication of the system.

Fabrication of the system consists of mechanical and optical tasks. The mechanical tasks are similar to those for conventional lens design, but are most complex because of the off-axis operation of the system. The optical tasks consist of conventional lens element fabrication (often more complex because of the off-axis geometry), and the hologram fabrication.

Fabrication of the hologram consists basically of the recording of a fringe pattern in a film of hologram recording material on the desired substrate. The fringe pattern is produced by the interference between the two hologram construction beams. The hologram recording apparatus is an interferometer, designed to produce the proper fringe pattern. The major requirement beyond the proper pattern is to maintain the stability of the fringe pattern during the recording time.

The hologram recording material is a crucial part of the technology. Not only must the material record the fine fringe pattern, it must be sufficiently stable in the operational environment to maintain the characteristics of the hologram. To date, only one material has been found with the desired combination of parameters. This material is dichromated gelatin (DCG). DCG operation is based on the hardening of a gelatin layer by the action of light. The gelatin is sensitized to the light by a dichromate compound. Hardening of the gelatin produces changes in physical density and therefore changes in the refractive index. The index modulation is the phase hologram recording. DCG has received much attention because of its unique properties, and it has proved to be a difficult but durable and satisfactory material.

4.2 HOE DESIGN AND ANALYSIS

In this section we discuss the details of HOE function, design and analysis.

4.2.1 General

There are three major characteristics that determine the performance of HOEs in optical systems. These are the optical efficiency of the element, the image quality provided by the element, and the see-through characteristics of the element. The optical efficiency of a HOE is of particular importance because the light does not inherently go in the desired direction. This is indicated in Figure 14, which shows how the light incident on a holographic element is distributed into a diffracted beam, which is used, an undiffracted beam, which is not used, and the losses in the element. This is in strong contrast to the situation in conventional optics, where the undiffracted beam is the desired beam in the system.

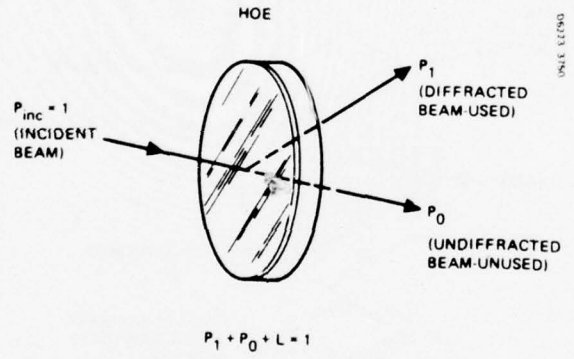


Figure 14. Distribution of incident light when acted on by a holographic optical element.

Display systems usually require high optical efficiency. There are two ways to obtain high efficiency, i.e., high diffraction efficiency, from a HOE; a blazed surface relief hologram, and a thick, phase hologram. The blazed surface relief hologram is useful if a broad range of wavelengths must be diffracted with relatively high efficiency. Display systems, however, depend on the wavelength selective properties of thick phase holograms to achieve the desired see-through characteristics. Therefore, display applications require the second technique for achieving high efficiency, i.e., the recording of the holographic fringes as a modulation of the refractive index of the material. This recording is distributed throughout the volume of the recording material.

A thick, phase hologram is characterized by a fringe spacing that is small compared to the thickness of the film of recording material. There are two basic types of thick phase holograms, called transmission and reflection types. A transmission hologram is made with two construction beams incident from the same side of the recording material. When a transmission hologram is reconstructed, the undiffracted and the diffracted beams both exit from the opposite side of the hologram from the incident beam. The reflection hologram is characterized by the two construction beams being incident from opposite sides of the hologram during construction, and the diffracted beam being reflected from the hologram as in a mirror during reconstruction. The two limiting types of thick phase holograms are indicated schematically in Figure 15. In these limiting types the construction beams are incident on the material at equal angles to the normal to the

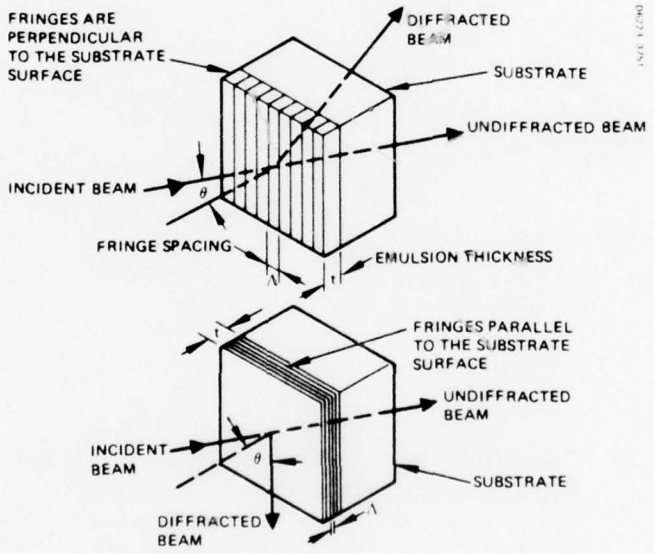


Figure 15. Two limiting types of thick phase hologram.

substrate. In the transmission hologram this results in fringes that are perpendicular to the substrate. In the reflection hologram this geometry results in fringes that lie parallel to the substrate surface. In this case the fringes are standing waves in space, separated by about 1/2 the wavelength of the recording light in the material. This results in a much closer fringe spacing for the reflection hologram than typically occurs in a transmission hologram. In the reflection holograms that typically appear in display systems, the fringe spacing corresponds to spatial frequencies in excess of 5000 cycles/mm. Therefore the hologram recording material has to be capable of responding to extremely fine detail, in order to be capable of recording these reflection hologram.

The theoretical peak diffraction efficiency of thick phase holograms is a function of the amplitude of the index modulation, the thickness of the recording film, the reconstruction wavelength and the geometry of the hologram. The functional dependence of the peak diffraction efficiency on these parameters is shown in equation 1 for the thick phase transmission hologram, and in equation 2 for the thick phase reflection hologram. In these equations $K = \cos\theta$, where θ is the angle of incidence of the reconstruction beam, measured in the material,

$$\eta_T = \sin^2\left(\frac{\pi\Delta nt}{\lambda K}\right) \tag{1}$$

$$\eta_R = \tanh^2\left(\frac{\pi\Delta nt}{\lambda K}\right) \tag{2}$$

The fact that the fringe spacing is small compared to the thickness of the film of recording material means that the thick phase holograms show relatively rapid variations of diffraction efficiency with angle and wavelength. These variations are characteristic of Bragg diffraction effects. Although there are many similarities in the behavior of efficiency with angle and wavelength for the two limiting types of holograms, the transmission hologram is characterized by a strong angular selectivity at a given wavelength, and the reflection hologram is characterized by a strong wavelength selectivity at a given angle. The characteristic bandwidths are primarily a function of the ratio of the fringe spacing in the material to the thickness of the recording material. These relationships are shown in equations 3 and 4.

$$\Delta\theta_T = \frac{\Lambda n_o}{t} \tag{3}$$

$$\frac{(\Delta\lambda)_R}{\Lambda} = \frac{\Lambda}{t} \tag{4}$$

Thick phase holograms are theoretically capable of 100 percent peak diffraction efficiency. In practice, efficiency values approaching 100 percent are observed. There is some loss due to residual absorption in the material, but most of the loss in thick phase holograms is due to scattering in the recording material. For displays this scattering must be maintained at a low level in order to allow good see-through conditions. Typically, a loss of up to 5 percent is acceptable.

The efficiency characteristics of the thick phase holograms are highly important in determining the performance of display systems based on these elements. Depending on how the HOE is used in the system, the variation of efficiency can limit the angular field of view, the pupil size, or the f/number of the system. These system effects will be discussed in detail in the following section.

The second major characteristic of HOEs is their effect on the image quality of the display system. The fact that the input and output axes of the HOE are not colinear means that the aberrations are typically larger than those that occur in a rotationally symmetric optical system. In particular such a biaxial system can show axial coma and astigmatism. These aberrations and the other aberrations of the system typically increase rapidly as the off-axis angle is increased.

There are three basic methods for correcting the aberrations of the holographic element. The first of these makes use of the fact that if a hologram is reconstructed in exactly the same geometry in which it was exposed, it has zero aberration. Unfortunately, this performance is limited to a single pair of conjugate points. Therefore, if the hologram must cover an extended field of view, this exact hologram is not suitable.

The second major approach to correcting the hologram aberrations is to use a conventional relay lens following the hologram. In this case the hologram is usually designed to provide the desired efficiency characteristics in the system, and the relay lens must be provided to remove the associated aberrations.

Finally, the third approach to correcting hologram aberrations is to fabricate the hologram with aspheric construction waves. This approach, which is a powerful technique, can be combined with either of the two above basic approaches.

The last of the major HOE features is the see-through characteristics of the element. These include scattering, coloration and spectral flare. For a cockpit display, these characteristics are extremely important. Scattering causes a cloudiness in the element that makes it difficult to see through to the outside world. As discussed above, scattering is not a problem if it is held to less than about 5 percent. Coloration, characteristic of reflection holograms, occurs because the HOE reflects part of the energy incident from the outside world. This leads to a dichroic effect, which gives a slightly discolored appearance to the outside world. It is the particular combination of high efficiency and narrow spectral bandwidth of thick phase reflection holograms that allows a useful tradeoff between this dichroic coloration and the system optical efficiency.

In the spectral flare effect, an external light source, typically the sun, is diffracted by the holographic element into the user's visual field. Because transmission holograms have a relatively broad spectral range, spectral flare effectively eliminates them from consideration for use in cockpit displays. This point is discussed in more detail below. With thick reflection holograms the spectral flare can be avoided, provided the HOE is properly fabricated. With proper fabrication techniques, the diffraction components corresponding to spectral flare cannot satisfy the Bragg condition and so remain at negligible amplitude.

Dispersion characteristics of HOEs play a relatively small role in determining the characteristics of the display. Because the optical characteristics of the HOEs vary rapidly with wavelength, the system is restricted to light sources with relatively narrow spectral bandwidths. This is consistent with the use of narrow spectral bandwidth reflection holograms to obtain desirable see-through characteristics.

In some cases, the angular dispersion of transmission and asymmetric reflection HOEs causes excessive blur of the image. In these cases the angular dispersion can be compensated by adding a second dispersive element to the system. The amount of angular dispersion is such that a second hologram is usually required for compensation.

The efficiency characteristics of HOEs lead to two limiting design forms for the holographic element in a display system. We call these limiting forms the image hologram and the pupil hologram. The image hologram is fabricated with construction beams that correspond to the on-axis conjugate points desired in the display. Therefore, the image hologram provides perfect image quality on-axis, and a large exit pupil. As the field of view and f/number of the system are increased, however, the efficiency of the image hologram drops rapidly, and the aberrations rapidly rise. Therefore the image hologram is most useful in systems that require a large exit pupil and have a small field of view and large focal length.

The pupil hologram is designed to provide perfect imaging of the system exit pupil onto the light source. It therefore provides high efficiency across the entire field of view. In this case the efficiency characteristics of the HOE tend to limit the size of the system exit pupil. Therefore the pupil hologram is most useful in systems that require a large field of view, high f/numbers, and permit a relatively small pupil. In general there is a continuous tradeoff between the characteristics of these two limiting types.

Efficiency Calculations. HOE diffraction efficiency plays a fundamental role in the performance of display optical systems. Therefore the theoretical calculation of diffraction efficiency is an extremely important part of the design and analysis process. The calculation of diffraction efficiency is based on Kogelnik's coupled wave theory.* As used in the design process, this theory pertains to thick, phase holograms with no loss. Both transmission and reflection holograms are included. The calculation assumes a single diffracted order and operation near the Bragg angle. The theory further assumes that the reconstructed ray is coplanar with the two construction rays and the surface normal. The polarization is perpendicular to the plane of incidence, and surface interactions are ignored.

In the design and analysis process, Kogelnik's equations are applied to geometries beyond those assumed in the derivation. In particular, the equations are used with residual absorption, for skew rays, and implicitly, for both polarizations. Furthermore, the analysis procedure ignores surface

*H. Kogelnik, "Coupled Wave Theory for Thick Hologram Gratings," Bell Syst. Tech. J. 48, 2909-2947 (1969)

reflections. Physically, the extended application of these equations is expected to give an upper bound for the absolute efficiencies. However, the results are valid for relative efficiency calculations, for example, in the calculation of the extent of the field of view or pupil size as limited by hologram efficiency. When important, polarization effects and surface reflections can be included. In practice, this method gives good agreement with experimentally observed efficiencies. Since it is the variation of efficiency that primarily determines performance, these techniques give a valid approach to system design.

In the system design process, these equations are used to calculate the efficiency of each ray traced, assuming values for the thickness of the film of recording material and the amplitude of the index modulation. To compare experimentally observed efficiencies with these theoretical calculations, the observed peak efficiency is corrected for surface reflections and combined with measured values of film thickness to calculate a value for the amplitude of the index modulation. These values of index modulation and thickness are then used in the raytrace program to give the variation of efficiency with the system parameters. As noted above, this procedure gives good agreement between experimentally observed efficiencies and those calculated by the raytrace programs.

4.3 HOE FABRICATION TECHNOLOGY

The fabrication of HOEs requires an exposure apparatus and the recording material and processing techniques to give the desired performance characteristics and environmental stability. Since the current state-of-the-art recording material is dichromated gelatin (DCG), the processing techniques described here are appropriate for that material. Required hologram recording material characteristics and the characteristics of available materials are discussed in the following section.

4.3.1 Exposure Apparatus

The HOE exposure apparatus must provide the design geometry to within the specified tolerances. It must also provide a high degree of stability over the period of time required to expose the hologram. The purpose of the HOE exposure apparatus is therefore to provide the desired exposure beams, to position the HOE substrate correctly in the beams, and to maintain the required degree of stability during the exposure time.

The HOE is made by exposing a layer of recording material to the superposition of two light waves. The two light beams are mutually coherent. The HOE is therefore formed as an exposure of the recording material to an interference pattern, or set of interference fringes. In order to obtain a useful recording, this interference pattern must remain stationary with respect to the layer of recording material during the exposure; otherwise the recorded pattern is smeared and the HOE is degraded or destroyed.

The exposure apparatus must provide the stability of the fringe pattern relative to the layer of recording material. This stability is achieved by stabilizing the fringes in space and stabilizing the substrate in space, thereby achieving the relative stability of the fringes and substrate. The equipment required to do this consists of a vibration isolated table and an acoustic shield to remove the disruption influences coming from the outside environment, and opto-electronic systems to achieve and monitor the interferomentric stability inside. In practice, the exposure apparatus must achieve a stability of better than 1/10 fringe, often for a period of several hours.

4.3.2 Processing Techniques

In order to be useful in the display system, a HOE must have the proper see-through characteristics, as well as the proper wavelength and efficiency of operation. In the current state-of-the-art, we use a phase hologram, recorded in dichromated gelatin (DCG). A phase hologram is recorded as a variation of the refractive index of the recording material, so that there is no absorption of light in the material. DCG is used as the recording material because it is the only recording material that can provide the required variation of refractive index, while still maintaining an excellent see-through capability.

DCG records the holographic pattern by a varying physical density, with more dense areas corresponding to brighter areas in the interference pattern. The changes in density produce changes in the refractive index to provide a thick phase holographic recording. The exposed DCG is developed to produce a larger index variation than that produced during the exposure period. This development consists basically of a swelling of the gelatin layer, followed by a rapid dehydration. The final thickness of the layer depends on the post-development processing, and several techniques are used to bring the layer to the proper final value in a stable condition.

The behavior of DCG in hologram recording is controled by numerous parameters, spread over several procedures. Careful process control is required to obtain the right combination of characteristics in DCG. Since the hologram exists in a layer of gelatin, it has a sensitivity to moisture that makes it necessary to seal the hologram with some kind of cover, after the hologram preparation is complete.

The two most important performance parameters of the HOE are the peak diffraction efficiency and the spectral wavelength at which that peak efficiency is attained in the display system geometry. The peak efficiency is determined by the amplitude of the index modulation and the thickness of the gelatin film. The amplitude of the index modulation is essentially proportional to the total exposure of the film. The final wavelength of peak optical efficiency is determined by several parameters of the fabrication process. In addition to the relative humidity, parameters like the amount of gelatin prehardening, the concentration of dichromate in the sensitizing solution, the temperature of the development solutions, and the temperature are important in fixing this peak wavelength. All of these parameters can be controled, and we can therefore control the final wavelength. The techniques used to achieve the final wavelength are designed to make the HOE arrive at the final wavelength with a high degree of environmental stability. The stabilization procedures provide useful HOE lifetimes of several years in typical environmental conditions.

Numerous methods for preparing uniform gelatin films have been devised. Principal techniques include moving a substrate through a stationary gelatin solution (dip coating), moving a solution across an open substrate (doctor blading), fabricating a film on one substrate and transferring it to another (film transfer), and casting the film directly from a solution of gelatin (fiim casting). All of these techniques have been used to provide high quality gelatin films for hologram recording.

4.4 HOE RECORDING MATERIALS

4.4.1 Display System Requirements

A viable HOE technology depends on the availability of high-quality hologram recording materials, just as conventional lens technology depends on the availability of optical glass. With HOEs, additional emphasis on the

materials results from the fact that the optical efficiency of the system is closely tied to the recording material parameters.

The characteristics usually required in the HOE recording material are: Peak diffraction efficiency of at least 80 percent of the incident beam; high contrast recording of interference fringes at spatial frequencies of from less than 1000 to over 6000 cycles/mm; good stability under extremes of temperature, relative humidity and light exposure; and less than 5 percent loss of light from scattering and residual absorption. In addition, there are usually requirements on the spectral bandwidth and/or angular bandwidth of the diffraction efficiency. Table 8 gives the requirements for desired display system characteristics.

TABLE 8. HOLOGRAM RECORDING MATERIAL REQUIREMENTS FOR DESIRED DISPLAY SYSTEM CHARACTERISTICS

Characteristic	Material Requirement
• Efficiency	$\Delta nt \geq \lambda/2$; $(\Delta n)_{max} = 0.1$
• Angular and Spectral Response	t = 5 to 20 μm
• Residual Losses	Less than 5 percent
• Aperture Size	Uniformity over >50 cm x 50 cm
• Sensitivity	$\geq$50 mJ/cm^2 desired
• Yield	>50 percent
• Lifetime	>1000 h
• Spatial Resolution	6000 cycles/mm

4.4.2 Available Materials

The available recording materials that best meet the requirements for HOE display systems are photopolymers, bleached photographic emulsions, and dichromated gelatin (DCG). All of these can provide thick phase holograms with useful index modulation, spatial resolution, stability and aperture. Each material has limitations. For photopolymers, the resolution is limited to about 2500 cycles/mm, and the index modulation is limited to about 0.01. For bleached photographic emulsions, the major limitation is the high scattering level arising from the granular distribution of silver halide crystals in the emulsion. A further limitation in many cases is the maximum index modulation of about 0.03. For DCG the major limitation is its relatively poor reproducibility when driven to high effective index modulation (up to

about 0.1). Additional limitations are the difficulty in obtaining uniformity over large apertures and the relatively low exposure sensitivity (typical exposure at 515 nm for high index modulation is 0.1 to 1 J/cm2). Table 9 summarizes the properties of these materials.

TABLE 9. STATE-OF-THE-ART PERFORMANCE FOR AVAILABLE THICK PHASE HOLOGRAM RECORDING MATERIALS

Characteristic	Photopolymers	Bleached Silver Halide	Dichromated Gelatin
Index Modulation, Δn	0.01	0.03	0.07
Thickness, μm	5-20	5-15	5-20
Scattering Loss	<0.05 to >0.2	~0.15	<0.05
Aperture Size, cm^2	10 x 10	50 x 50	40 x 40
Yield	~0.5	~0.5	~0.2
Lifetime, h	~10 to >1000	>1000	>1000
Resolution, cy/mm	~2500	>5000	>6000
Sensitivity, mJ/cm^2	1 to 10	~0.1	100 to 1000

At present, dichromated gelatin is the only acceptable material for display applications, because of its high effective index modulation, excellent spatial resolution and low scattering loss. Process control provides the needed uniformity and reproducibility, and a highly-stabilized exposure apparatus allows long exposure times to compensate for low sensitivity.

4.5 HOE FUTURE DEVELOPMENTS

In this section we summarize the state-of-the-art of HOE technology, compared to the needs for the canopy display system described below. We then discuss the probable areas of development in the next 5 to 10 years, and their effect on the feasibility of HOE display systems.

4.5.1 Needed Improvements

The canopy display system discussed in Section 6 is a sophisticated concept that requires some advancement in the state-of-the-art of HOE technology. In particular, in the design and analysis area, more development is needed in

the use of aberrated construction beams. This would provide a better understanding of the tradeoffs available between image quality and field of view/pull size adjustments. The available analysis techniques are adequate for the foreseeable future.

The state-of-the-art (SOA) in fabrication techniques is nearly adequate for the canopy display system. Reflection HOEs up to about 20 by 40 cm in aperture have been successfully fabricated on curved glass substrates, and smaller HOEs on plastic substrates have been made. The difficulty with the new system is that of accommodation of the aircraft canopy in the fabrication procedures: there is a problem of its fitting into the exposure apparatus, and there are questions of stabilizing it for the holographic exposure. While these are not fundamental problems, they do present technological difficulties. One promising approach is to fabricate the canopy HOEs on separate substrates, and to laminate these into the canopy structure.

Depending on the exact fabrication procedures employed, the SOA of DCG is probably adequate for the canopy display system. In a system of this complexity, however, it would be desirable to improve the overall uniformity and process control, in order to improve yield.

The environmental effects experienced by a hologram mounted on the canopy is a subject which requires an in-depth study. An initial look at this area suggests possible problems due to high temperatures and high stresses. Information on F-16 canopy temperatures experienced in flight has indicated that the holograms will be operating well below its thermal destruction temperature of 150°C. Temperatures experienced on the ground in a closed cockpit are liable to be more severe due to the "greenhouse effect". More important than temperature itself may be the stresses and distortion in the canopy caused by large temperature gradients or external aerodynamic pressures. In general, the entire subject of canopy flexure must be addressed from both a HOE damage and an image degradation viewpoint.

It can be safely said that moderate flexures of the canopy which do not cause sealing loss or delaminations should render no damage to the HOE medium. This requires a fairly flexible cover or seal on the inside canopy surface which will exhibit compliance for moderate distortions.

The optical effects of canopy flexure, on the other hand, is a highly sophisticated problem which does not permit ready analysis. A distorted canopy shape would have to be mathematically described and a computer ray

trace performed on the shape to determine the magnitude of image degradation, if any. Theory says that the shape of the substrate does not affect the optical characteristics of the HOE, at least in the first order. In addition, we are not dealing with perfect or even near-perfect imagery, thus the distortion threshhold which must be exceeded before a noticeable image degradation results may be quite high. Speaking in other than generalities in this area, however, is not possible without specific data on the deformations to be expected.

Finally, existing image sources, i.e., CRTs, are probably viable for the canopy display system. Considerably better packaging and easier system design would be obtained if a more ideal source were available. This ideal source would be small, efficient, and bright, and it would have a narrow spectral bandwidth. Furthermore, it would be easy to control and flexible in format. Many other systems would benefit from such a device!

4.5.2 Design and Analysis

The SOA of analysis techniques is quite adequate for all forseeable design work. Considerable improvement in design techniques is expected, as more experience is gained with new design forms on complex systems. This experience will produce more efficient design techniques and better performance over a wider range of system parameters. In particular, as more is learned about the tradeoffs associated with aberrated construction beams for the HOEs, the final system will become simpler, lighter and cheaper.

4.5.3 Fabrication Techniques

Continued development in HOE fabrication technology will produce improved apparatus and techniques. In particular, we can expect contact-printing techniques for HOE production, computer generated hologram to warp the HOE construction beams, and lamination techniques for large aperture systems. These advances will permit larger apertures and improved integration in the final system.

4.5.4 Materials

Hoe recording materials provide the biggest challenge for advancing the SOA, and substantial gains can and will be made. Very little work has been invested in the development of photopolymers for high spatial frequency

hologram recording. There is clearly a tradeoff between this resolution and exposure sensitivity. With improved resolution and larger index modulation, which also appears to be very feasible, we will have rigid recording materials that can be exposed with dye laser sources directly at the operating wavelength. This will result in high yields, faster turn around, simpler fabrication procedures, and excellent environmental stability.

Continued development of DCG will provide larger index modulations with smaller exposure requirements. Improved process control and understanding of the basic DCG processes will provide increased production efficiency and better yield and uniformity. For the canopy display system, however, performance will not be substantially altered. This is because the limitations on the system performance are due to fundamental HOE properties and the fundamental tradeoff between see-through coloration and the extent of the field of view and system pupil. For other designs, including, perhaps, a better canopy display system design, these material improvements will allow HOEs to be used as field lenses, beam diverters, and high-efficiency dispersion and aberration correctors.

4.6 IMAGE SOURCE TECHNOLOGY

4.6.1 Introduction

The subject of this section is to discuss potential diffraction optics image sources. In order to be considered suitable in a diffraction optics application, an image source must exhibit certain characteristic qualities. One of the most demanding conditions for a see-through display occurs when viewing must be accomplished against an intensely bright background such as a sunlit cloud. Under these conditions the contrast of the display must be sufficient to permit rapid recognition of the symbology. The minimum contrast ratio for a see-through display is generally accepted to be 1.15 to 1.2. This translates into a symbol brightness of about 1800 foot-lamberts to the eye. Considering the light losses associated with see-through optical systems, most image sources are not capable of fulfilling this requirement.

Another consideration is lifetime. Most displays, when driven to high luminosity levels, exhibit abnormally shortened lifetimes. Replacement of sources generally entails a boresighting operation. In order to minimize the associated inconveniences, source lifetimes need to be in excess of a thousand hours.

Physical constraints, namely volume, power and form factor, are highly significant relative to the suitability of sources for this application. Water-cooled lasers and bulky drive systems represent types of items which are less desirable in light of this application. An additional constraint on the source is that its emission must be narrow in bandwidth to control chromatic dispersion and avoid degrading the inherent resolution of the display as it is relayed by the optical system.

Forthcoming in this section are discussions of various candidate sources as to their suitability for the system in view of the requirements mentioned above. In summary, the qualities sought after are the following:

1. Brightness in excess of 3000 foot-lamberts.
2. Bandwidth as narrow as possible (less than 10 nm is desirable).
3. Low weight, volume, size and power.
4. Lifetime in excess of 1000 hours at operating conditions.

The sources considered for this application are discussed in the forthcoming subsections. Candidate systems are the following: 1) Liquid Crystal; 2) Laser Scanner Display; 3) CRT, 4) Light Emitting Diodes and 5) incandescent lamps. Each of these sources is discussed in detail and a summary and tradeoff is presented at the end of the section.

4.6.2 General

Cathode Ray Tubes have for many years been the standard cockpit device for displaying information in a variety of formats from a variety of sources. They are utilized in small, medium and large display applications. They have the capability of presenting video imagery such as TV, radar and FLIR; stroke written or in-raster tactical symbology and alphanumeric character displays. Recent usages include helmet mounted displays and Head-up-displays, utilizing both conventional and reflective diffraction optical systems.

Some of the characteristics which give CRTs an advantage over other display image sources are: high brightness, large dynamic range and high resolution. The high resolution is important as it permits a reasonable density of information over a small area. Not all of the above characteristics are achievable simultaneously. For displays using line symbols rather than gray shade information, brightnesses as high as 15,000 foot-lamberts are achievable. CRTs are available in ruggedized packages designed to withstand 40 g shocks.

Some of the disadvantages of the CRT are listed below. The length of the envelope for a given display size is quite high. Several tens of kilovolts are required to achieve adequate brightness. Because of the high reflectance of phosphor material, CRTs tend to lose contrast under high ambient illumination when directly viewed. Power consumption is relatively high to achieve high brightness at moderate writing speeds. Life expectancies are in the few thousand hour category and the device is subject to drift and non-linearities.

In spite of these limitations, CRTs presently hold a position of dominance in electronic displays. The enormous variety of available CRTs provides a broad base for solving most display engineering requirements. CRTs are categorized as follows: Conventional CRT, Multi-beam CRT,

storage CRT and various types of Color CRT.* Inasmuch as color is not a requirement, the subject of color CRTs will not be addressed in this section.

Conventional CRT. The conventional CRT has been the object of the major development effort in the electronic display technology. For a diffraction optics application, the significant parameters in the Table are: brightness, contrast capability, resolution, power and ruggedness. Dynamic range and number of lines are not critical items. Some of the items which are not in the table, but which are critical are life, size, and reliability. The line widths cited in the previous table are greater than one would expect, however, this reflects the driving of the tube to high brightness levels as required with head-up type displays.

Conventional CRTs are normally operated in one of two modes, video raster scan or random write, although a single display may provide dual capability.

Raster Scan. In the raster scan mode, the beam sequentially scans the entire display area in a line-by-line fashion. Display brightness is determined by beam power, phosphor efficiency and duty cycle (beam dwell time on a resolution element per frame time). The video-type CRT is a mature technology, such that only marginal improvements in performance, life and reliability can be expected. No significant cost reductions are anticipated.

Random Write. The random address mode is used for computer-generated, non-video signals such as alphanumeric or vector-graphic information. The electron beam is rapidly deflected to specific areas on the screen where the information is typically generated with a stroke-written symbol, as utilized in head-up displays for example. Stroke written symbols are much brighter than raster-generated symbols due to the increased dwell time per character. Future effort will probably involve 1) attempts at reducing the higher power requirements associated with random-write operation, 2) continued work on combining the random-write technique with penetration-phosphor color tubes and 3) the reduction of size, particularly depth, associated with this display device.

*Table 10 lists characteristics of these various types of CRT.

TABLE 10. CHARACTERISTICS OF SEVERAL CRT TYPES

	STANDARD CRT MILITARY QUALITY	MULTIBEAM CRT	STORAGE CRT	COLOR CRT SHADOWMASK	PENETRATED PHOSPHOR
BRIGHTNESS, AREA AVERAGE	500 - 2000 fL	6000 fL	1000 fL	10 fL	20 - 100 fL 200 - 2000 fL
DYNAMIC RANGE, SHADES OF GRAY	12 (8 TO 10 TYP)	12	7	8	8
CONTRAST CAPABILITY (CONTROLLED AMBIENT)	> 50:1	>50:1	> 50:1	> 25:1	> 25:1
COLOR	1; GREEN TYP	1; GREEN TYP	1; GREEN TYP	RED, BLUE, GREEN AND COMBINATION	MINIMUM OF RED, GREEN AND COMBINATION
USABLE VIEWING AREA	4" x 4", 5" x 5", 5" x 7" TYPICAL	5" - 17" DIAMETER; EXPERIMENTAL	4" DIAMETER TYPICAL UP TO 8.5" DIAMETER	UP TO 25" DIAMETER	4" x 5", 7" x 7" UP TO 22"
RESOLUTION	100 LINES/IN. TYPICAL (40 - 100)	100 LINES/IN.	80 LINES/IN.	20 LINES/IN.	100 LINES/IN.
NUMBER OF LINES	2000		300 TO 700	300 TO 400 TYPICAL	1500
INHERENT MEMORY	NO	NO	YES (~ 2 MIN) STORAGE MESH INCORPORATED	NO	NO
SWITCHING SPEED	NA	NA	150 MILLISEC ERASE	NA	50 MICROSEC SWITCH AND VOLTAGES
EMITTER SIZE	10 MILS TYPICAL	10 MILS EA BEAM	12 MILS	12 MILS	10 MILS
EMITTER SPACING	CONTINUOUS	CONTINUOUS	CONTINUOUS	50 MILS TRIAD-TO-TRIAD	CONTINUOUS
EMITTER SHAPE	CIRCULAR, ELLIPTICAL	CIRCULAR, ELLIPTICAL	CIRCULAR, ELLIPTICAL	CIRCULAR	CIRCULAR, ELLIPTICAL
SWITCHING VOLTAGE	NA	NA	NA	NA	7 KV
POWER (VIDEO EXCITATION, DRIVER/ DEFLECTION)	0.75 MA; 20 KV; 15W 4a; 30V; 120W	30 W/BEAM 120W	30W FLOOD 14W WRITE 75W 27W ERASE 80W (2 GUNS)	3 MA; 27 KV; 81W 80W (TUNED)	0.23 MA; 4a; 30V; 120W
RELATIVE RUGGEDNESS	MODERATE	FAIR	MODERATE	POOR	MODERATE

Multi-Gun or Multi-Beam CRT. This tube is similar to the conventional CRT except that it has an electron gun structure capable of simultaneously producing several independently modulated electron beams. In writing a raster, the plurality of beams is swept across the face of the CRT in "paint brush" fashion, drawing several lines in parallel with each sweep. Thus, bandwidth is reduced by the number of beams in parallel.

Multi-beam operation offers advantages in high data-rate display applications or can be used to significantly increase display brightness. The multi-beam sweep of the display, however, requires that sensor video be stored and accessed in a compatible format. Also, scan generation circuitry and electron-optics are considerably complex and adjustments quite critical.

Storage CRT. A variety of CRTs with image storage have been developed over the past 25 years. For example, the Memotron writes full white imagery on a dark background with extremely long (many minutes) stored display time but with no shades of gray.

The Tonotron writes information in shades of gray with a display brightness of 800 to 1000 fL. The display can be stored for several minutes and totally erased in milliseconds or caused to fade at some pre-set and adjustable rate. The variable persistence feature allows scan-to-scan integration of sensor data, such as search radar, by integrating on the storage surface and improving the signal-to-noise ratio essentially by a correlation process. However, moving targets smear by an amount proportional to their speed.

The Multi-Mode Tonotron performs the functions of the Tonotron but with two additional modes:

1. Selective erasure of any part of the stored imagery to eliminate moving target smear, and
2. Write-through capability to simultaneously write non-stored dynamic imagery. The latter is chiefly of value for symbol overlays.

Phosphors. The visible energy characteristics that a CRT exhibits are almost entirely dependent on the type of phosphor which is deposited on the faceplate. The choice of phosphors is usually dependent on the requirements of the specific application. Phosphors are characterized by several variables; persistence, peak wavelength, quantum efficiency and bandwidth. Of primary concern for a high brightness display application are quantum efficiency, luminous efficiency and bandwidth. Persistence should be medium to medium short for non-smearing display presentations. The wavelength should peak in the yellow-green to produce the greatest visible sensation per unit excitation. Several broadband phosphors (white) are available, but the present application demands very narrow spectral outputs.

Table 11 shows a comparison between some of the more efficient phosphors.

TABLE 11. SELECTED PHOSPHOR CHARACTERISTICS OF YELLOW-GREEN PHOSPHORS

PHOSPHOR	PEAK WAVELENGTH	BANDWIDTH (10% POINTS)	QUANTUM EFFICIENCY
P1	525 NM	83 NM	0.06
P20	560 NM	180 NM	0.14
P22G	525 NM	120 NM	0.06
P31	522 NM	180 NM	0.22

Notice that none of these phosphors exhibit a narrow bandwidth. Recently, phosphors with narrower emission spectra have been developed.

One of these line spectrum phosphors is P-43, a pale, unsaturated, yellowish green phosphor with a medium rise time and persistence. It has a relatively linear energy response and is highly stable under electron bombardment. Its linear response yields high dynamic range displays. A spectral response trace is shown in Figure 16. A phosphor with a very similar response is P-44 (see Figure 17). Only very subtle differences exist between these two phosphors. Both are suitable for direct view applications utilizing optical filtering; however, the narrow band output also makes them most suitable for holographic applications. These phosphors show a high resistance to burning, thus allowing them to be driven to high

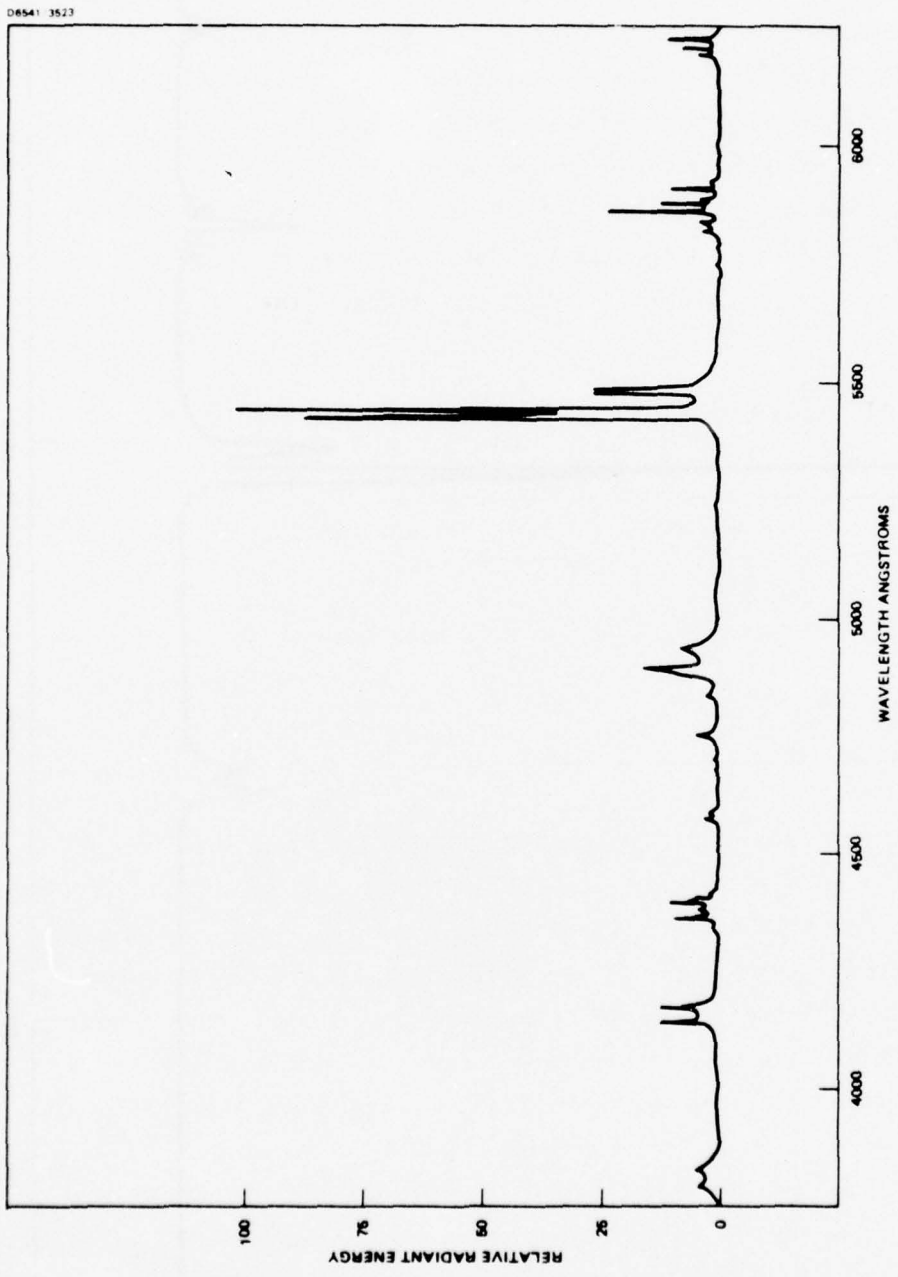


Figure 16. Spectral distribution of P43 phosphor.

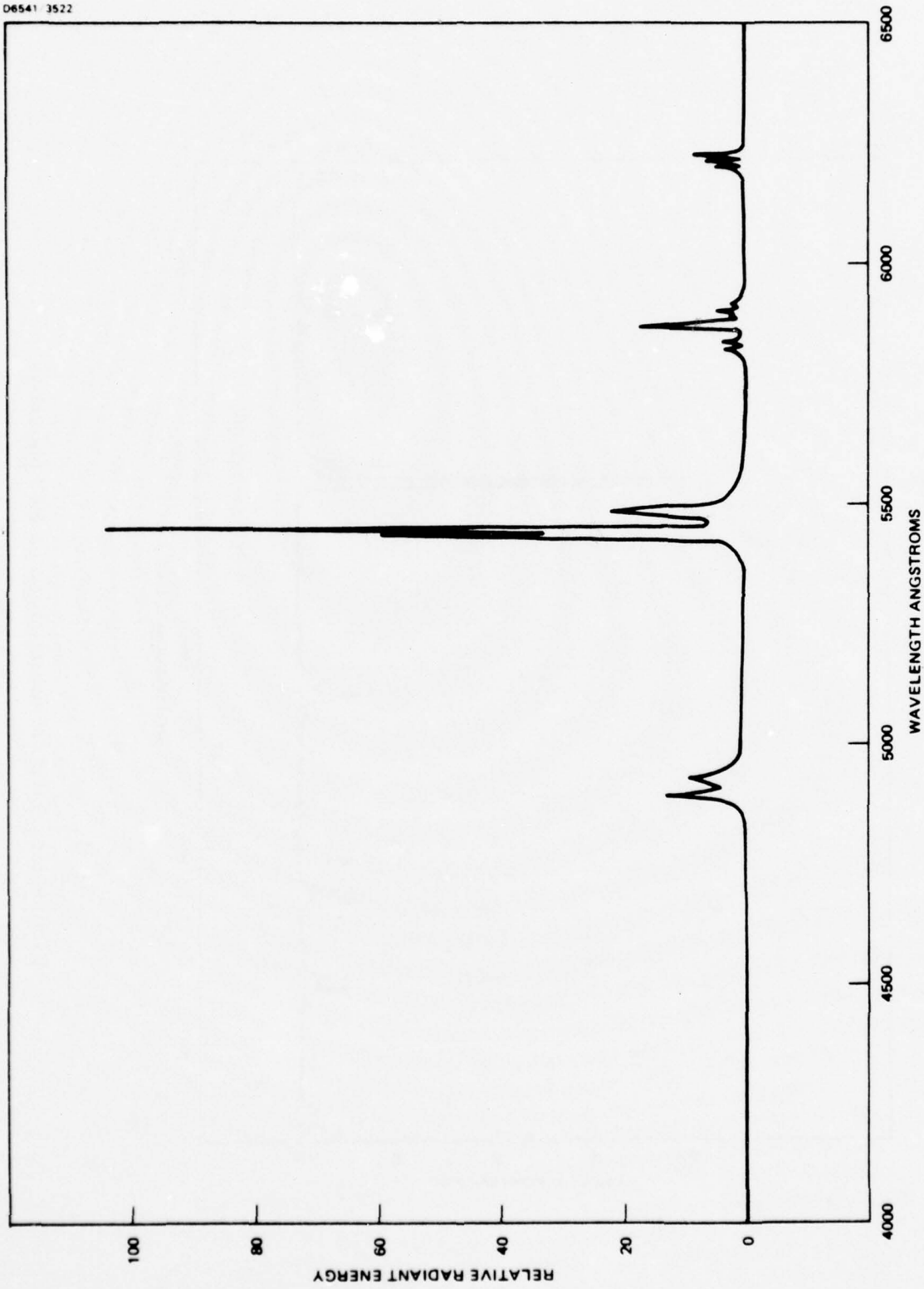


Figure 17. Spectral distribution of P44 phosphor

brightness levels. In choosing between the two phosphors it may be noted that both have a double peak with a 2.5 nm spacing. The P-44 phosphor smaller peak is 60 percent of the magnitude of the primary peak; whereas with P-43 the smaller peak is about 80 percent of the larger. A slight advantage in dispersion reduction may be realized with the P-44 for this reason.

Brightness Requirements. In a holographic visor, helmet-mounted display (HVHMD) which Hughes built for the U.S.A.F. Aerospace Medical Research Laboratory (AMRL), a one-inch CRT with a P-44 phosphor was utilized which produced approximately 350 foot-lamberts. This brightness was adequate for the HVHMD because the see-through transmittance of the visor was only 4 percent. In the canopy-mounted holographic system, the see-through transmittance will be around 95 percent. For a comfortable contrast of the required image, the brightness required is then 0.2 times 9500 or 1900 foot-lamberts to the eye. Considering a maximum overall system efficiency of 50 percent, a value readily achievable within the current SOA, the required source brightness is 3800 foot-lamberts. This brightness level is achievable with relatively high anode voltages as evidenced by the specifications listed in Table 12. This table compares available candidate image sources which were considered for use in the holographic Head-up-display. The table shows that 7000 foot lamberts is achievable with the narrow band P-43 phosphor. To extend the useful life of the CRTs, lower brightness levels should be used inasmuch as the required brightness for comfortable viewing is about half of the table value.

The high reflectance of CRT phosphor screens presents a serious problem when it comes to direct-view contrast of the display. The acceptance/rejection criterion for ease of viewing applied to a display is that it have a minimum contrast $[(B_H + B_B)/B_B]$ of 1.15; more specifically, that the highlight brightness be 15 percent greater than the background brightness. This rule-of-thumb assumes no surrounding eye adaptation mismatch. A typical reflectance value for phosphor screens is 70 percent in all directions (lambertian). Thus, it is extremely difficult to maintain the minimum contrast under high ambient illumination. Filtering for contrast enhancement has a limited degree of success. For broadband CRTs — a neutral density filter is best, while for more narrow band phosphors like P43 and P44,

TABLE 12. SELECTED CRT CHARACTERISTICS

	KC 3053 (DU MONT)	ICC 2980 (DU MONT)	3M27 (THOMAS)	3M41 (THOMAS)	4M59 (THOMAS)	4M58 (THOMAS)	5M252 (THOMAS)
SCREEN SIZE, INCHES	3.0	4.25	2.65	2.5	3.50	3.75	4.25
LINE WIDTH, INCHES	0.006	0.009	0.012	0.007	0.006	0.006	0.006
LIGHT OUTPUT, fL	10,000	10,000	14,000	4500	7000	7000	7000
WRITING SPEED, IN/SEC	2000	3500	2170	1600	20,000	20,000	20,000
FINAL ANODE, KV	15	15	14	12.5	16	16	16
FOCUS METHOD	E (1 KV)	2 (1 KV)	E (0.4 KV)	E (2 KV)	E (3 KV)	E (3 KV)	E (3 KV)
PHOSPHOR	P-1	P-1	P-1	P-1	P-43	P-43	P-43
DEFLECTION ANGLE, DEGREES	45	45	70	70	40	40	50
LENGTH, INCHES	6.7	7.9	6.1	7	9.5	9.5	9

the most efficient filtering technique is a narrow bandpass absorption filter with a circular polarizer to defeat intrasurface reflections.

In the see-through mode, the reflected, collimated CRT image will be viewed against a variety of outside world objects, the brightest of which will be sunlit clouds having a brightness of 10, 000 foot-lamberts. In this situation filtering has no beneficial effect. Stray light striking the CRT face will normally add to the background and reduce contrast.* The CRT image source should nevertheless be shielded from stray light or placed "down a hole" to provide the darkest possible background.

An illustration of the relationship between source brightness and display contrast for different illumination levels is shown in Figure 18. For this plot, the CRT is unfiltered, is receiving no stray light and the hologram system efficiency is 40 percent. The significance of the plot is the identification of the worst case required CRT brightness which turns out to be

*This effect is minimized with a diffraction optics system since the hologram reflects only the chosen wavelength efficiently and rejects the broadband background.

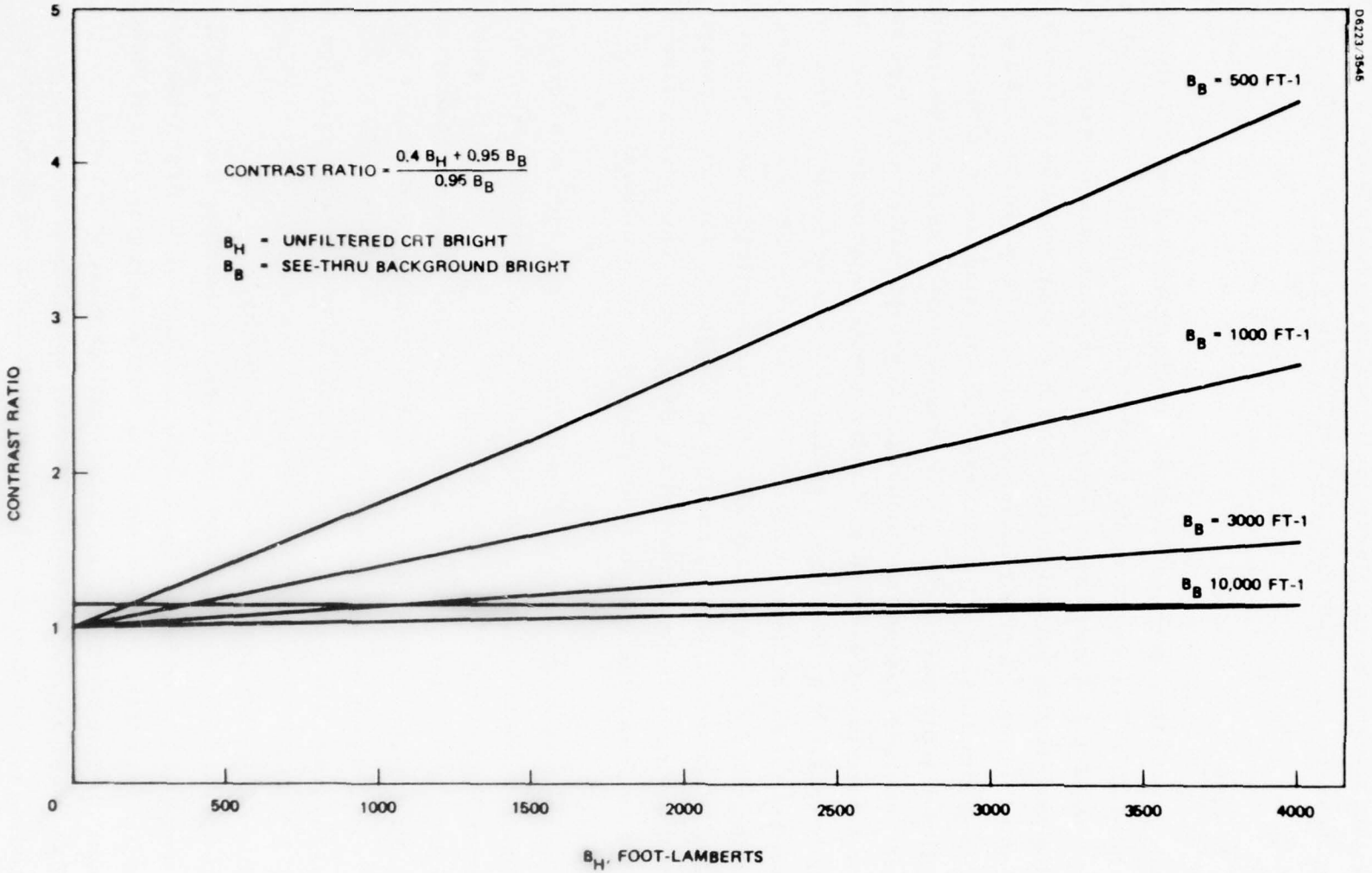


Figure 18. Achievable contrast ratio versus source brightness for various background brightness levels.

almost 4000 foot-lamberts. Under conditions less severe than a 10,000 foot-lambert background, a 4000 foot-lambert CRT gives excellent contrast and recognition.

4.6.2 Lasers

General. Laser light sources have been emphatically and enthusiastically promoted as ideal light sources for general display applications as well as displays requiring narrow band illumination. Lasers have been popular for scanning and printing operations involving hard copy recoding materials. Their output is high and their output bandwidth is very narrow, down to tenths of nanometers. What is the feasibility of using lasers in the diffraction optics cockpit application? It is assumed that in such an application the laser would be scanned and modulated to provide either a TV type raster scan or a random, stroke written display format. Approaches using a laser to simply backlight or frontlight a stationary, passive display seems an impractical use of the laser, although it is certainly feasible. Scanning can be accomplished either mechanically or acousto-optically. Mechanical scanning is accomplished with rotating or oscillating mirrors. Acousto-optical scanning is accomplished with a Bragg cell. The incorporation of a scanning laser into the system as an image source is illustrated in Figure 19.

The scanned laser beam is optically directed to a high gain screen with the impinging beam incident in the direction of the holographic element for maximum light output. The screen would require baffling or light shielding to maintain good contrast at the display. The ultimate size requirement of the display determines the laser path length. Beam modulation usually requires a pockels cell. To preserve a true system redundancy for display backup purposes would demand an individual laser scanned display for each HOE. It does not seem likely that a single laser might be able to supply multiple HOEs without a great degree of difficulty.

In order to be consistent with the recording wavelength of the HOE, the wavelength of the display scanning laser should be of the Argon-ion type. Size will, of course, be a consideration from a packaging point of view. In addition, certain other physical considerations must be made:

The power and/or cooling required for operation of the laser and its modulating system must be within reasonable limits and be suitable for

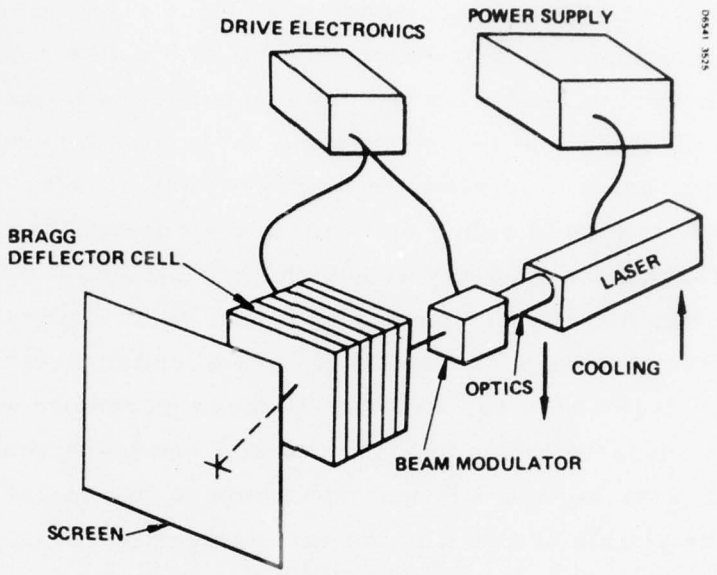


Figure 19. Components of a scanned laser display system.

airborne use. The resistance to environmental extremes, both in temperature and vibration, will be important for stability of a ruggedized laser. Safety considerations, including possible harm to the operator's eyes, high voltage and high temperature are also of prime concern. Radiated interference may also be a consideration. Based on the number of operational considerations associated with the use of such a system, the current appeal of this technique is substantially less than with other approaches.

Employing lasers in airborne displays is a newly emerging technology. As such, it contains many areas which require development before the practicality of such systems are realized. Included in this section are subsections devoted to the state-of-the-art of laser sources and laser scanning devices. The development status as well as directions for further improvement are also indicated.

Visible Laser Sources. There are several visible laser sources which could fill the optical needs of the display system under consideration. Several of these lasers are commercially available for immediate use; other systems

have been demonstrated in laboratory conditions only, but show near-term promise of development for commercial needs. In this study we have confined our interest to sources with output wavelengths in the range 490 nm to 640 nm. In the middle of this wavelength range, the laser power required to fill the system brightness needs is approximately 10 mW. The required power increases toward either extreme in the wavelength range, finally reaching approximately 50 mW at 490 nm and 640 nm.

All the candidate laser sources with near term applicability use a gaseous active medium. The specifications of commercial models of each of these are given in Table 13. For the purposes of comparison we also have included the characteristics of a commercial semiconductor diode laser. This type of laser is very efficient and compact, but materials which provide outputs in the visible are still in the early stages of development. Each of the systems included in the table are discussed in more detail below.

TABLE 13. LASER SOURCES AVAILABLE

LASER TYPE	WAVELENGTH	OUTPUT POWER (FUNDAMENTAL MODE)	ELECTRICAL POWER REQUIREMENT	LIFETIME	WEIGHT		COMMENTS
					LASER HEAD	POWER SUPPLY	
HELIUM-NEON [1]	633 NM	50 MW	450 WATTS	1 YEAR	90 LBS	35 LBS	1.6 METER LASER HEAD FORCED AIR COOLING
HELIUM-SELENIUM[2]	518 NM 523 NM 531 NM	1 MW 1.5 MW 2 MW	300 WATTS	1000 HOURS	9 LBS	12 LBS	10 MINUTE WARMUP FORCED AIR COOLING
ARGON[3]	488 NM 515 NM	10 MW 8 MW	1150 WATTS	1 YEAR	10 LBS	29 LBS	FORCED AIR COOLING
ARGON[4]	488 NM 515 NM	100 MW 120 MW	2600 WATTS	1000 HOURS	36 LBS	34 LBS	WATER COOLING, 1.5 GAL/
INJECTION (GaAs) [5]	850 NM	10 MW	25 WATTS	1000 HOURS	9 LBS		FORCED AIR COOLING

1. SPECTRA-PHYSICS MODEL 125
2. LICONIX MODEL 501
3. SPECTRA PHYSICS MODEL 162
4. LEXEL MODEL 65
5. POWER TECHNOLOGY MODEL ILCW

Helium-Neon. The helium-neon laser was the first gas laser discovered and is the most commonly used laser at this time. The laser transition at

633 nm occurs between excited states of the neon atom. The active medium is a low current (10-20 mA) DC discharge in a glass tube of 2-4 mm diameter containing a mixture of helium and neon. The upper laser level in neon is populated by resonant collisions between helium metastables and neon ground state atoms.

In terms of immediate applicability to the needs of the proposed scanning system, the helium-neon laser appears to be the best choice. The technology for this system is highly developed, and a commercial model producing the required output power is readily available (see Table 13). The disadvantages of this laser are its relatively large size and weight. Due to the advanced stage of development of this laser, it is unlikely that significant further improvements in packaging or efficiency can be expected.

Helium-Selenium. The helium-selenium laser is a relatively new addition to the list of visible gas lasers, having been discovered in 1970, and commercially developed in 1974. A total of 46 laser transitions have been observed in this system, including 22 between 490 nm and 640 nm.

The helium-selenium laser operates in a similar fashion to the helium-neon laser. A DC discharge is operated in a mixture of helium and selenium vapor. The selenium is introduced into the discharge by evaporation from selenium metal in a separately heated sidearm, or from selenium which is heated directly by the discharge. The upper laser level (in the selenium ion) is pumped by resonant charge transfer collisions between helium ions and selenium ground state atoms. The tube bores used are again in the range 2-4 nm, but the required current is on the order of 50-100 mA in order to provide adequate laser pumping, and to heat the tube walls above the condensation temperature of the selenium.

Presently available versions of the helium-selenium laser (see Table 13) are relatively low power devices, due to their short active length (≈40 cm). However, in laboratory experiments on longer tubes an output power of 50 mW has been observed for each of the transitions listed in the table, with somewhat smaller values for several transitions in the yellow and red portions of the spectrum. The discharge length for these experiments was 2 meters, but it is reasonable to expect 15 mW per transition from a one-meter tube.

Thus, the helium selenium laser is expected to satisfy the system power requirements from a relatively small device with modest prime power requirements. The only major disadvantage to this laser are its relatively short lifetime, determined primarily by consumption of selenium from the vapor source, and optical degradation from condensed metal on the laser optics.

Argon. The argon ion laser is the most powerful laser in the blue-green region of the spectrum, and has reached a high level of commercial development. The laser transitions occur between excited states of singly ionized argon. These states are populated by electron collisions with ground state ions in a high current DC discharge. Typical current levels are 5-50 amperes in 2 mm-5 mm bore tubes. Due to the high electrical power input into the discharge tube, either high flow forced air cooling (at low currents) or water cooling (at higher currents) is required. The argon laser operates most efficiently at higher discharge currents, because the laser output power varies quadratically (while the input power varies linearly) with current.

Table 13 presents typical specifications of presently available forced air cooled and water cooled argon lasers. The forced air devices are relatively light and small, but are inefficient since they run at low current. It is possible to produce larger output power by increasing the current or active discharge length, but in both cases the cooling requirements increase proportionately. Water cooled argon lasers are in more common usage and are rated as high as 20 watts. The specifications shown in Table 13 are for the smallest commercial version. This device is relatively heavy, but modest in size (60 cm laser head). The biggest disadvantage is its large power consumption, due to the high currents involved. The tube lifetime is also limited, due to deterioration at the high currents. However, if this device is operated at a current level just sufficient to supply the output power required for the scanning system, then tube life is prolonged, and electrical power consumption is reduced.

Injection Lasers. Injection lasers are still in the early stages of commercial development, but show great promise for providing efficient outputs from devices in small, lightweight packages. These lasers operate

by the electrical injection of carriers into a p-n junction in a semiconductor. The carriers then recombine across the bandgap producing a laser output whose wavelength corresponds to the bandgap energy. The laser process in most junction lasers is very efficient, with values commonly observed in the range 5-10 percent.

The most highly developed junction laser devices use GaAs as the active material. As shown in Table 13, typical devices produce 10 mW of power at 850 nm, with very low required input power. In order to produce devices with visible outputs, materials with larger bandgaps must be used. The two materials which show the most promise are the alloys $GaAs_{1-x}P_x$ and $Al_{1-x}Ga_xAs$. Injection laser action in both these materials has been achieved in laboratory experiments. The bandgap in these materials (and thus the laser wavelength) is determined by the composition factor x. In both cases the bandgap increases with x up to a point where the bandgap becomes indirect and nonradiative processes compete with radiative recombination. At the highest x values which allow laser action, the laser wavelength in $GaAs_{1-x}P_x$ is 6350 Å, while in $Al_{1-x}Ga_xAs$ the wavelength is 6450 Å. Other well known semiconductors with larger bandgaps cannot be produced with p-n junctions or have indirect bandgaps so that laser action is not possible. In the former case, optical or electron beam pumping is still possible, but probably not useful for the application of interest here.

As mentioned above, lasers using the alloys $GaAs_{1-x}P_x$ and $Al_{1-x}Ga_xAs$ have been operated successfully at the edge of the acceptable range of wavelengths, where average powers on the order of 50 mW are required. Unfortunately, at the compositions which produce the required wavelengths, the devices are lowest in efficiency so that most of the pump power is dissipated in the junction. This leads to a severe cooling problem, which is shared (to one degree or another) by all diode lasers. The best solution is very efficient heat sinking, but it is unlikely that sufficient improvements can be made to meet the program requirements. The junctions also operate more efficiently at liquid nitrogen temperatures, but this added complexity removes some of the advantages of the diode laser over other choices.

Laser Beam Scanning

Techniques. There are several techniques for deflecting a laser beam; however, they all fall into two general categories; inertial and non-inertial. The inertial category encompasses mechanically rotating mirrors and mirrors driven by both galvanometric and piezoelectric action. Rotating mirrors produce a rapid, line-scan capability while the other deflection systems provide random access, but are typified by a slow response time.

Non-inertial techniques encompass both acousto-optical and electro-optical deflection. The absence of moving masses permits rapid response characteristics in a random access mode. The electro-optic technique uses special optical materials which exhibit changes in refractive index as a function of electrical field modulation. These refractive index changes produce deflection in a light beam. The other, major, non-inertial deflection technique employs the interaction of sound waves with optical beams using diffraction in an acousto-optical medium. Beam deflection is achieved by varying the frequency of the acoustic wave.

Table 14 summarizes the above techniques and their characteristics which relate to performance in a display systems utilization. The acousto-optical technique is the choice for the random access application while the rotating mirror has a definite advantage in a raster scan application, especially in terms of efficiency.

TABLE 14. LASER SCANNING TECHNIQUES

TECHNIQUE		OPERATING MODE	RESOLUTION	WRITING SPEED	EFFICIENCY
INERTIAL	GALVANOMETER DRIVEN MIRRORS	RANDOM ACCESS	LOW	LOW	90%
	PIEZOELECTRIC DRIVEN MIRRORS	RANDOM ACCESS	LOW	LOW	90%
	SCANNED MIRRORS	RASTER SCAN	HIGH	HIGH	90%
NON-INERTIAL	ELECTRO-OPTIC	RANDOM ACCESS	LOW	HIGH	90%
	ACOUSTO-OPTIC	RANDOM ACCESS	HIGH	HIGH	10-30%

It works out that, for this application either the random access or the raster scan would be suitable from a performance standpoint; however, from a packaging viewpoint, the raster scan system with a rotating mirror might pose problems and might be susceptible to on-board aircraft vibration. Use of the less efficient, random access/acousto-optical technique has the advantage of solid state construction; however, the system is also subject to thermal drifts, etc.

Requirements. A set of representative requirements which might be imposed on such a display source/system uses lines, scales and alpha-numerics as symbols. An assumption is that 6200 resolution elements are used for the lines and scales while another 1100 elements are used for the alphanumerics. With a 50-Hz update (refresh) rate the data rate is 365,000 elements/second which requires a 2.7 μsec response time. For the random access mode, only the acousto-optical implementation is feasible. A review of the state-of-the-art in acousto-optic scanners is presented in Table 15. The performance of a current system (1973 vintage) is compared with a 1980 state-of-the-art system. The major contributor to the SOA advancement will be the development of lead molybdate as the candidate acoustical material, having a higher optical transmission and a faster response time – that approximating the requirements of the system mentioned above. The current material, paratellurite, has greater deflection capabilities, but exhibits slower response and higher optical losses.

Conclusion. It has been pointed out in the preceding subsections that the complexity of a scanning laser display source not only lies in the system area, but with the components themselves. Of primary concern is the weight, power and ruggedness of such a system. Another possible drawback is the generation of EMI within the cockpit confines, possibly causing problems with other instruments. The size of such a system is determined by the choice of Laser source. The optical path could be folded on itself; however, the length of the package would almost certainly exceed 18 inches. For usage as a source behind the seat, the system might be folded such that the major length of the system ran vertically.

TABLE 15. ACOUSTO-OPTIC SCANNING STATE-OF-THE-ART

CHARACTERISTIC	CURRENT* SOA	FUTURE** SOA	
OPERATING WAVELENGTH, NM	672.8	514.5	632.8
MATERIAL	PARATELLURITE (TeO_2)	LEAD MOLYBDATE ($PbMoO_4$)	
DEFLECTION, DEGREES	3.8	1.4	1.7
TRANSIT TIME, μSEC	10.5	2.9	
OPTICAL INSERTION LOSS, dB	9	~6	
RESOLUTION SPOTS PER AXIS	500	500	
DRIVE POWER, W	5.2	4	6

*ISOMET SYSTEM (1973)
**ACHIEVABLE IN 1980

Generally speaking, the laser display image source is feasible, volumetric constraints disregarded. Future developments should result in a decrease of the volume and power required. From an optical viewpoint, it is the most promising source and should be so regarded.

4.6.3 Light Emitting Diodes

General. The applicability of the Light Emitting Diode (LED) as an image source for the diffraction optics application has received careful attention, particularly because it is a new technology and many of its characteristics seem to make it ideally suited for a holographic application in a military environment. Numerous studies have been conducted relative to the applicability of LEDs to cockpit readouts and matrix displays, the latter to provide a substitute for the well developed, well used, Cathode Ray Tube. Before making a judgment on their applicability, the characteristics and development status of LEDs will be reviewed.

The LED is a device which emits light by means of a forward biased p-n diode junction phenomenon. The junction is located on a small diode chip which is usually encapsulated singly or with a group in typical semiconductor sized packages. Visible LEDs commercially available emit light at a variety

of wavelengths as shown in Figure 20. LEDs which radiate in the near infrared (904 nm) are also available. The limitation of state-of-the-art in LED development is primarily in materials technology. Common, visible LEDs are made up of the following materials and combinations thereof: Gallium Phosphide (GaP), Gallium Arsenide Phosphide (GaAsP), Gallium Aluminum Arsenide (GaAlAs), Indium Gallium Phosphide (InGaP) and Silicon Carbide (SiC). A listing of the characteristics of these types is found in Table 16.

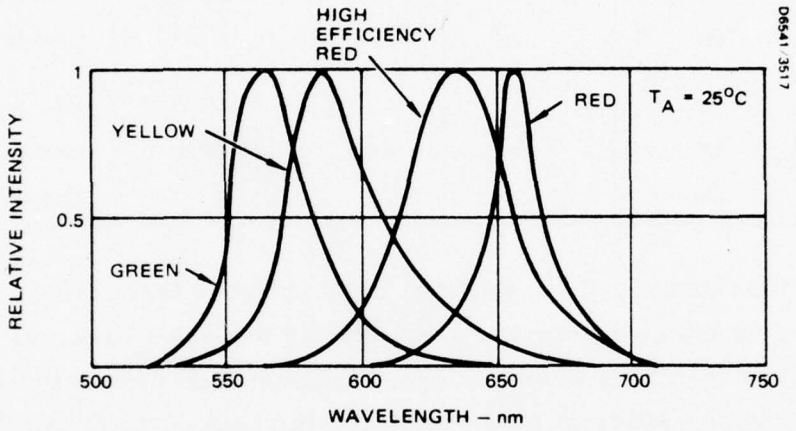


Figure 20. Relative intensity versus wavelength – LEDs.

Material Properties. Table 16 indicates quite a few materials which exhibit characteristics making them suitable for LED application. Disregarding the laboratory curiosities, however, leaves a relatively few wavelengths and materials for consideration: Gallium Arsenide Phosphide at 660 nm (red), Gallium Phosphide at 550 nm (green) and GaAsP on GaP at 583 nm (yellow). There is also a high efficiency red LED (GaAsP on GaP) available which emits at 635 nm peak wavelength. This high efficiency red LED has almost a 3 to 1 efficiency advantage by virtue of its increased bandwidth and lower peak wavelength. An important difference exists between GaAsP red LEDs and GaP red LEDs. This is the ability of GaAsP devices to be pulsed in order to achieve higher brightness.

TABLE 16. CHARACTERISTICS OF SEVERAL LED MATERIALS

MATERIAL	PEAK WAVELENGTH, NM	LUMINOUS EFFICIENCY, ℓ/W	OVERALL EFFICIENCY, ℓ/W	TYPICAL BRIGHTNESS, fL	STAGE OF DEVELOPMENT
GaP, GREEN	550	675	0.04	300	QUALITY NOT UP TO GaAsP
GaN, GREEN	520	–	VERY LOW	–	LAB USE ONLY
SiC, YELLOW	590	–	–	25-65	HARD TO FAB
GaAsP .5 AMBER .5	610	340	0.015	300-500	REASONABLY GOOD
GaAsP, RED	660	50	0.15	500-2000	ADVANCED
GaP, RED	690	20	0.14	–	GOOD CRYSTALS HARD TO GET
InGaP, YELLOW	570	–	–	600	POOR MAT'L QUALITY
GaAlAs, RED	670	40	0.024	GOOD	LOOKS PROMISING
GaN, BLUE	440	20			RESEARCH PHASE

In contrast to this, GaP material does not give increased light output with increasing current density. Instead, the material becomes saturated and light output remains constant. So, although GaP red material is significantly more efficient as an emitter, the GaAsP LED can be driven to much higher brightnesses by multiplex-pulsing with high current levels at frequencies above which the eye is able to detect flicker. Recently developed techniques of putting GaAsP on a GaP substrate yields the high efficiency red LED. This device exhibits the higher quantum efficiency of the GaP material, but does not exhibit the saturation effect at low current levels. As a result, GaP red LEDs are somewhat obsolete.

The ability to be pulsed using high current is essential for any type of matrix or character display which requires a continual refresh cycle. Even without pulsing, the current-carrying ability of GaAsP devices with proper heat sinking allows luminance levels of 2500-5000 foot-lamberts at drive currents up to one ampere. These high brightness levels are a must for any application where high contrast is required against a bright background.

Results of an experimental study produced evidence that greater visibility is achievable with red characters against a bright, neutral background than with green or yellow characters of the same luminance.* Even though

*The use of modern light emitting displays in the high illuminance conditions of aircraft cockpits, AGARD Conference Proceedings No. 167, Electronic Airborne Displays, April 1975.

the red LEDs provide the brightest available outputs, however, red colored displays are frequently not desirable. To get away from the red color, other materials and processes are introduced. Orange and amber devices are obtained by combining GaP with GaAsP. Unfortunately, the combinations yielding amber and orange have quite low quantum efficiencies and overall brightness is down to about 25 percent of an equivalent red LED. Commercial devices yielding 500 foot-lamberts in the orange region are available. The achievement of yellow emission is obtained from GaAsP diodes doped with nitrogen. A typical brightness of 300 foot-lamberts at 50 mA is available in commercial devices made by Monsanto.

Because of eye sensitivity considerations, much effort has been devoted to the development of green emitting, LED devices, the most promising being of GaP construction. The green GaP devices do not exhibit the saturation problems that the red GaP emitters do. Therefore, it is possible to use them in pulse-current applications. Green LEDs exhibit good brightness and high luminous efficiency. The limiting factor is the maximum current which they can take. Typical brightness values of 200 to 300 foot-lamberts are common in commercial devices.

An indirect technique for producing a more narrow band, green emission employs a green phosphor in conjunction with a GaAs infrared emitting LED. The phosphor is coated over the LED chip. When operational, the phosphor absorbs the IR and re-emits it at its own characteristic wavelength. Efficiencies are low, however, the luminous output is confined to the relatively narrow band of the phosphor.

Applicability. The above discussion essentially covers the state-of-the-art in LED development. The relative suitability of LEDs for this application will now be discussed. The LEDs advantages over other light sources are surely strongest in the areas of life, reliability and ruggedness. The necessity of having to replace LEDs in the field is practically non-existent. They also emit all of their energy in the visible spectrum and run significantly cooler than most sources because of their low power consumption. Switching speed, although not essential here, is extremely fast compared with other light sources. In spite of all these strong points of the LED, some careful considerations must be made concerning this application.

Size and Power. LED material is expensive and present techniques make it extremely difficult to fabricate large area light emitters. Monolithic arrays have been fabricated in patterns, such as reticles or bar graphs. Matrix displays have been fabricated as an X-Y grid to provide a TV-type area display. The limitation of these large area displays is required power. For instance, a one-half inch diameter reticle with quadrant lines would require about 160-8 mil square diodes. To generate this reticle with green LED chips at 20 mA/chip would require 3.2 amperes of continuous power. A reticle twice as big would require twice the power, etc. Area matrix displays have an even more severe problem. A one inch square display module containing 64 x 64 = 4, 096 elements was developed by Monsanto using 8 x 8 = 64 element monolithic chips. To drive all elements assuming 10 mA/element require 40 amperes. A utilization factor of 10 percent requires more modest current levels. The characteristics of the aforementioned array display which represents the state-of-the-art are listed in Table 17.

Alternate types of displays have been suggested using LEDs to edge light a stationary display such as a reticle on glass. The achievable brightness using this technique is probably adequate for application if designed properly. Either the edge lighted display or a display using discrete, heat sinkable, high power LEDs would minimize the power required to produce highly visible, useful displays.

Brightness/Contrast. Directly viewed LED indicators can have high brightness; however, they are essentially point sources and their very small size makes them reasonably hard to see in spite of their brightness. Human factors studies prove element viewability goes up with the angular subtense, i.e., element size, but the brightness goes down with the square of the element size. Techniques which use diffusers to spread out light from a point source tend, therefore, to cause the viewability to rapidly decrease.

For see-through applications, namely, displays viewed against high ambient backgrounds, contrast enhancement is not achievable by filtering. The significant consideration therefore becomes luminance rather than contrast. A 300 foot-lambert display would present a contrast ratio of

TABLE 17. MONOLITHIC GaP LED ARRAY PERFORMANCE CHARACTERISTIC

	PRESENT	PROJECTED
TOTAL SPATIAL ELEMENTS	64 x 64 = 4096/MODULE	64 x 64/MODULE (A/N)
VIEWABLE DISPLAY AREA	1" x 1" MODULE	8" x 8" (64 MODULES)
PERCENT ACTIVE AREA	21%	46%
PIXELS PER INCH	64	64 (A/N) 100 (VIDEO)
PIXEL SIZE	8 MIL DIA ON 15.6-MIL CENTERS	12 MIL DIA ON 15.6-MIL CENTERS
PIXEL SHAPE	SQUARE DIODE; CIRCULAR OUTPUT	SQUARE DIODE; CIRCULAR OUTPUT
PIXEL BRIGHTNESS (Pk) (Av)	200 fL 90 fL	300 fL
BRIGHTNESS UNIFORMITY	DIODE TO DIODE: GOOD MODULE TO MODULE: POOR	±15% MODULE-TO-MODULE DISTRIBUTED IN RANDOM FASHION WITHIN PANEL
CONTRAST RATIO	3:1	10:1
NUMBER OF GREY STEPS	10 DEMONSTRATED	2 TO 3 (A/N) 8 TO 10 (VIDEO)
HUE	GREEN: 5650Å	GREEN-5650Å
REFRESH RATE	200 Hz	500 Hz FOR VIBRATION ENVIRONMENT
RISE TIME	1 TO 10 NANOSEC	1 TO 10 NANOSEC
DECAY TIME	1 TO 10 NANOSEC	1 TO 10 NANOSEC
MEMORY	NONE	NONE
VOLTAGE	1.5 TO 5V	1.5 TO 5V
POWER	FEW MILLIWATTS/ELEMENT	FEW MILLIWATTS/ELEMENT

1.03 which is not adequate for comfortable viewing. In contrast, a modern Heads-up display exhibits a contrast of 1.2 to one. Conclusions are that a high power LED such as a 1500 foot-lambert red would be the minimum acceptable candidate.

Spectral Characteristics. Perhaps the most significant drawbacks of LEDs as a narrow bandwidth light source is that they are not narrow band. The bandwidth of a typical GaAsP LED is shown in Figure 21. It is 5 times as wide (20 nm) at the 50 percent amplitude points as good design dictates, considering dispersion at the holographic element. It is about 10 times wider than the spectral response of a CRT. In order to utilize the LED with the HOE, narrow bandpass filtering would have to be accomplished, further reducing the available brightness for viewing. It is doubtful, however, that

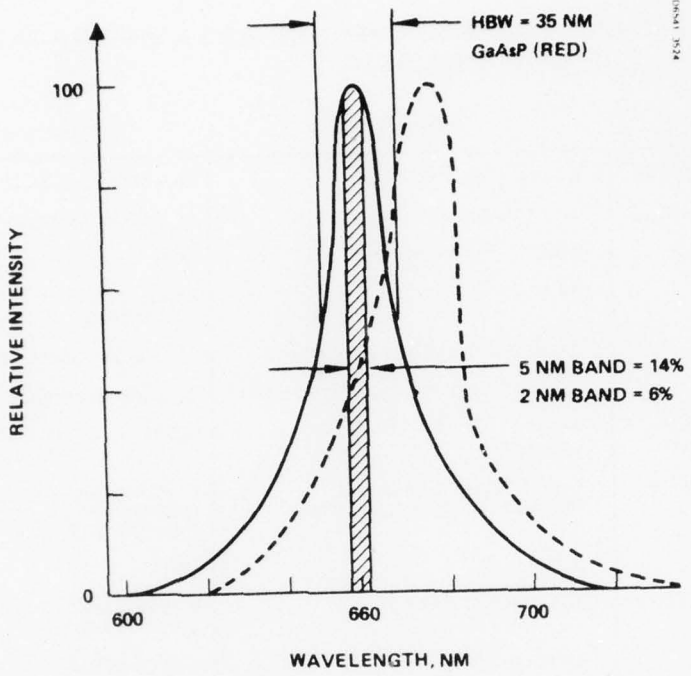


Figure 21. Spectral emission characteristics of a typical GaAsP LED.

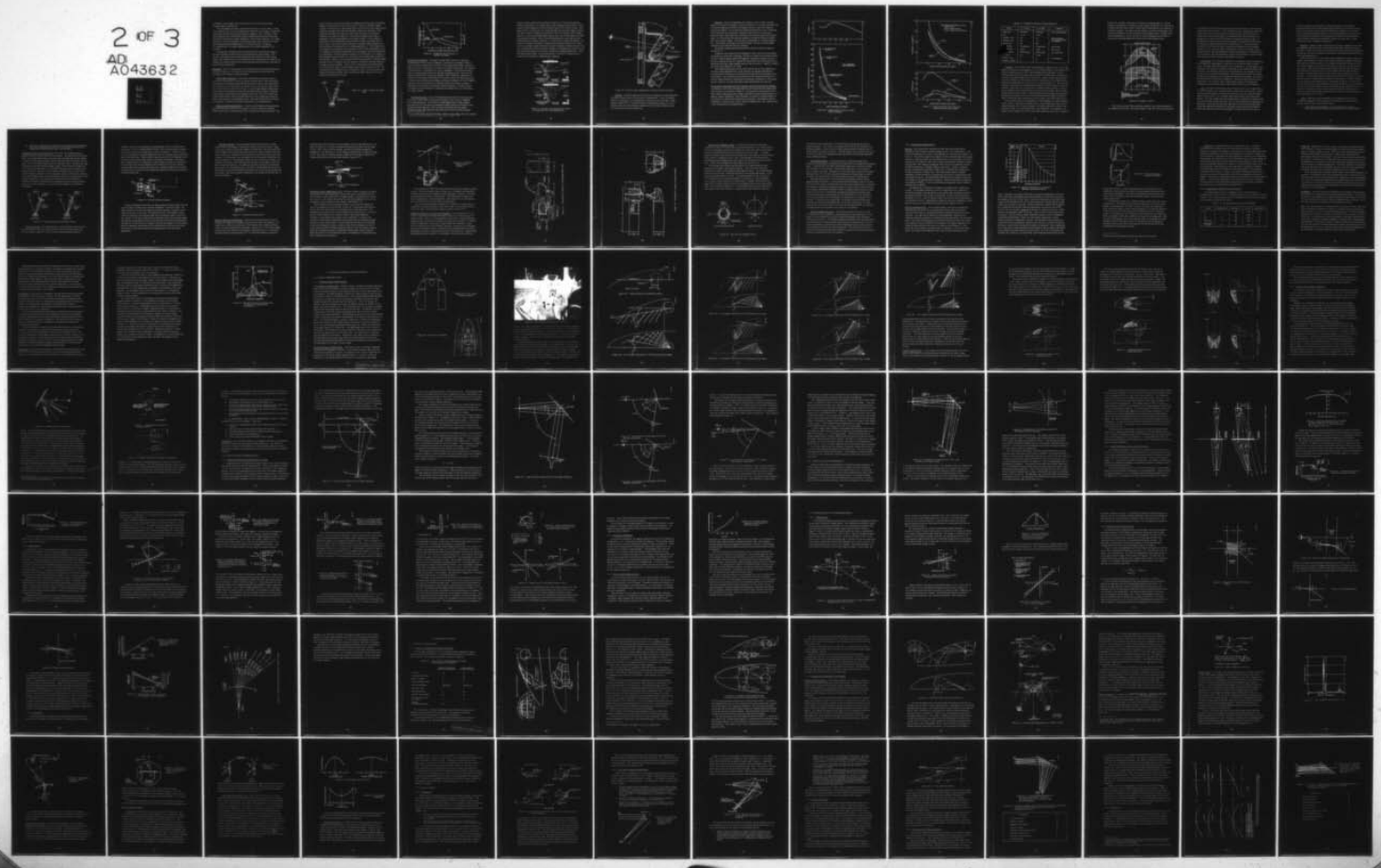
even this technique would be successful because of a characteristic, peak wavelength-temperature dependence. The peak wavelength experiences a shift of approximately 2.5 angstroms (0.25 nanometer) per degree Celsius. As a result, over a 20°C range, a matched LED/filter combination could experience a 5 nanometer mismatch. To make matters worse, variables encountered in manufacturing account for variations in peak wavelength of the final product. Because of the brightness limitations and unstable spectral characteristics discussed above, the LED cannot realistically be considered as a suitable candidate source for a diffraction optics system.

4.6.4 Liquid Crystals

General. The liquid crystal (LX) technology has recently become significant in the displays field. The phenomena which liquid crystals (LX) exhibit is a modulation of light as a function of applied voltage across the material. The characteristics of LX and the physical explanation of their operation has not been included in this section, but is explained in detail in Appendix B. The purpose of this section is to examine the LX technology relative to its

AD-A043 632 HUGHES AIRCRAFT CO CULVER CITY CA DISPLAY PRODUCTS DEPT F/G 20/6
DIFFRACTION OPTICS STUDY.(U)
JUN 77 W N LEWIS, D H CLOSE, L G COOK F33615-76-C-0508
UNCLASSIFIED AMRL-TR-76-119 NL

2 OF 3
AD
A043632



usefulness in the display field in general and to the diffraction optics implementation specifically.

The LX display has seen considerable attention in recent years. It has been developed for use as an alphanumeric indicator for watches, clocks and calculators as well as airborne character displays. Most recently, it has been employed in an addressable matrix display which produces real-time television with shades-of-gray capability. In this latter capacity, it is being hailed as a serious competitor to the Cathode Ray Tube in both direct view and optically projected applications for several reasons, including: decreased power, increased high ambient contrast and simplified drive circuitry.

Two specific examples will be discussed which illustrate the usage of the LX technology in both direct view and projective type systems. The specific considerations to be addressed will be presented for both system types. The requirements for an illumination and viewing system using an LX display are primarily determined by the optical characteristics of the type of liquid crystal being used.

Materials. There are many types of LX materials and associated phenomena utilized in displays. Two types are most commonly used, these are the field-effect and dynamic scattering types.

Field-Effect Materials. Field-effect materials are normally used in conjunction with polarizers and act in such a manner as to rotate the polarization plane of the light passing through the liquid crystal. Since polarizers are required for this material to be useful, there is an inherent light loss of over 50 percent due to the filters alone. In see-through display applications such as this it is necessary to have an extremely bright display to maintain contrast against the high ambient lighting conditions. The use of polarizers in the optical system reduces overall efficiency and increase the output and power requirements of the lighting system. The use of field effect materials is, therefore, considered generally undesirable for this application.

Dynamic Scattering Materials. A liquid crystal display utilizing dynamic scattering material consists of a reflective mirror electrode structure covered with liquid crystal material and a transparent counterelectrode. The

liquid crystal in its quiescent state is transparent and any light striking the display will specularly reflect off the mirror surface. When the liquid crystal is excited into its scattering mode, some of the incident light will be scattered at angles other than at the angle of specular reflection. This scattered light takes the form of a lobe centered around the specular reflection, as shown in Figure 22. The size and shape of this lobe is dependent on the voltage applied to the liquid crystal. As the voltage is increased, the lobe becomes broader and more light is scattered over a wider angle. The liquid crystal is therefore acting as light modulator by scattering light in proportion to the voltage applied to it. The brightness of the display is proportional to the intensity of the incident illumination, and its brightness is therefore expressed as a percentage, using the brightness of a lambertian surface (a perfect diffuser) as 100 percent, as in Figure 23. Both brightness and contrast are a function of the viewing angle relative to the specular reflection. The contrast reaches its maximum at viewing angles between 10 and 15 degrees from the specular reflection, and decreases as the angle becomes smaller. This is due to dispersion and scattering that occurs at narrow angles off the display surface and the liquid crystal. An illumination and viewing system is required in order to use as much of the scattered light as possible, while avoiding the light scattered at narrow angles from undesired sources.

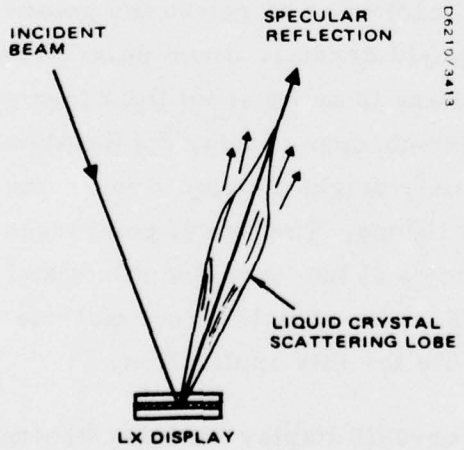


Figure 22. Liquid crystal scattering lobe.

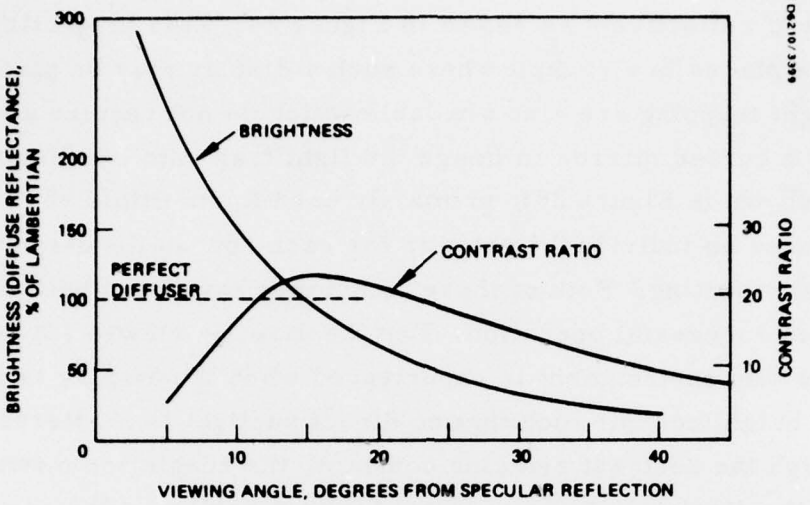


Figure 23. Brightness and contrast of a typical LX display.

Operational Properties. The liquid crystal offers some very significant advantages over other types of displays. The primary advantage is that of high achievable contrast under the most severe high ambient light conditions. Since LX emits no radiation, but rather, acts upon incident light, the required switching power is extremely low, almost negligible. LX fabrication entails the use of photographic masks for defining modulating areas. The sizes and shapes of patterns are completely flexible. Reticle patterns, alphanumeric readouts and complete, addressable X-Y matrix arrays have been fabricated. A direct-viewed LX television display, developed by Hughes Aircraft Company, represents the state-of-the-art in flexibly addressed miniature displays.* Depending on the display requirement format complexity, a similar type of TV display could conceivably be utilized as the image source for the diffraction optics system.

Viewing Geometry. One of the difficulties which must be overcome with a directly viewed dynamic scattering LX display is the control of lighting and viewing geometry. All possible viewing angles must be light trapped such that any ray from the eye striking the display surface terminates in the darkest possible light trap. This usually necessitates that the display surface be tilted from normal to the viewer and a hood or projecting light

* M. N. Ernstoff, Liquid Crystal Pictorial Display, Hughes Aircraft Company, Culver City, California. Presented at: SID Technical Meeting, Culver City, Calif., November 6, 1975.

trap be viewed reflectively as shown in Figure 24. This projecting hood restricts the places in a cockpit where such a display may be placed. Other means of light trapping are also available which do not require a hood. One means uses a curved mirror to image the light trap onto the display surface. The other (shown in Figure 25), primarily used for multiple rows of alpha-numerics, uses an individual light trap for each row so the display may have a flush panel mounting. Both of these techniques have been built and have demonstrated successful operation. For the directly viewed LX display, the severest viewing environment is experienced when the display is in a dark corner of a bright cockpit such that no direct sunlight is scattered back to the eye. Although the contrast remains constant, the adaptation mismatch of the eye causes the display to be hard to read with a sunlight adapted eye. Under low illumination levels, very modest power (1 watt for 22 characters) is required for satisfactory supplementary lighting.

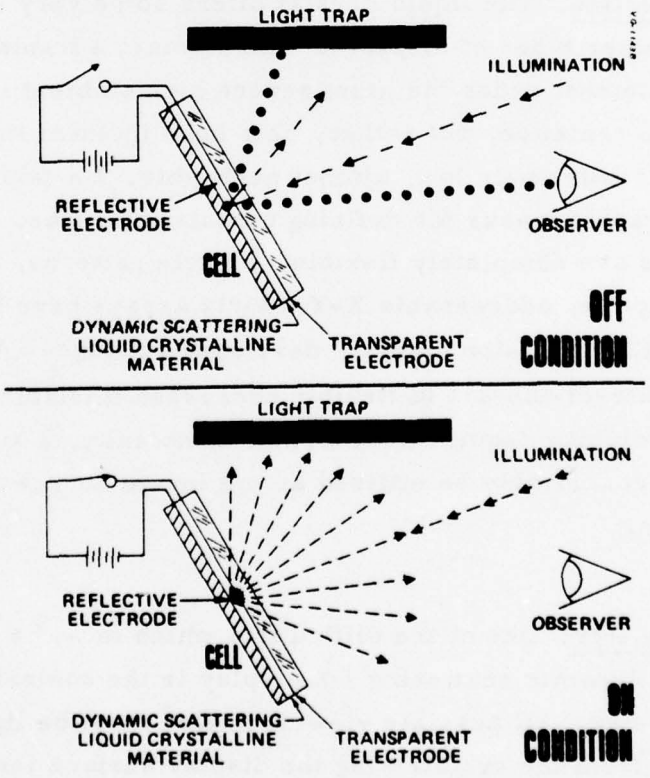


Figure 24. Dynamic scattering liquid crystal cell operation and viewing geometry.

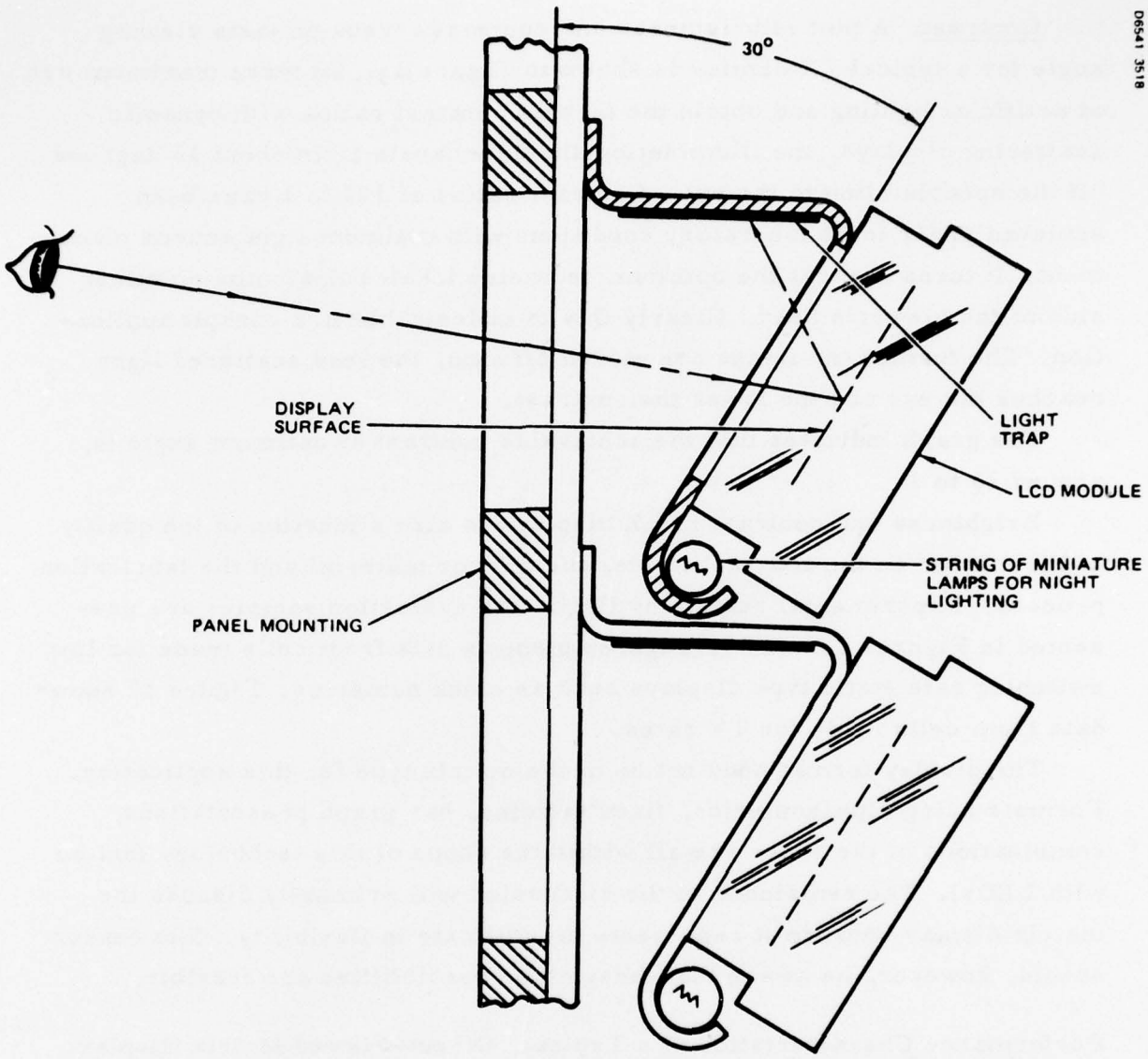


Figure 25. Liquid crystal alphanumeric display module mounting.

Lighting. Artificial lighting schemes for LX displays are determined by the size and form factor of the area to be illuminated. A very successful means for lighting rows of alphanumeric characters has been side or edge lighting (Figure 25). A string of miniature incandescent lamps or a line filament lamp provides adequate lighting which is largely confined to the row through total internal reflection.

Contrast. A plot of brightness and contrast versus off-axis viewing angle for a typical LX display is shown in Figure 23. To make maximum use of artificial lighting and obtain the highest contrast ratios with dynamic scattering displays, the illumination should emanate from about 15 degrees off the specular line to the eye. Contrast ratios of 100 to 1 have been achieved under ideal laboratory conditions with optimum light source placement. It turns out that the optimum geometry locates the lamps on either side of the viewer's head. Clearly this is undesirable in a cockpit application. The further the lamps are moved off axis, the less scattered light reaches the eye and the lower the contrast.

The graph indicates that the achievable contrast at optimum angle is around 25 to 1.

Brightness and contrast of LX displays is also a function of the quality of the mirror on the rear substrate, the mirror material and the fabrication process. Experimental results by Hughes on evaluation samples are presented in Figures 26 and 27. Figure 26 shows data from cells made for low switching rate static type displays such as clock numerics. Figure 27 shows data from cells made for TV rates.

The display format need not be of the matrix type for this application. Formats using alphanumerics, fixed reticles, bar graph presentations combinations of the above are all within the scope of this technology (not so with LEDs). The remainder of the discussion will primarily discuss the matrix display because it represents the ultimate in flexibility. The reader should, however, be aware that these other possibilities are feasible.

Performance Characteristics of a Typical, Direct-Viewed Matrix Display. A summary of performance characteristics for single-module displays and quad displays is presented in Table 18. Performance measurements were taken under illumination and viewing conditions considered appropriate for a typical cockpit installation, where the pilot is allowed a viewing window of ±15 degrees in azimuth and ±5 degrees in elevation. Parameters such as brightness, contrast, gray scale, viewing configurations, life, memory and color techniques are discussed below.

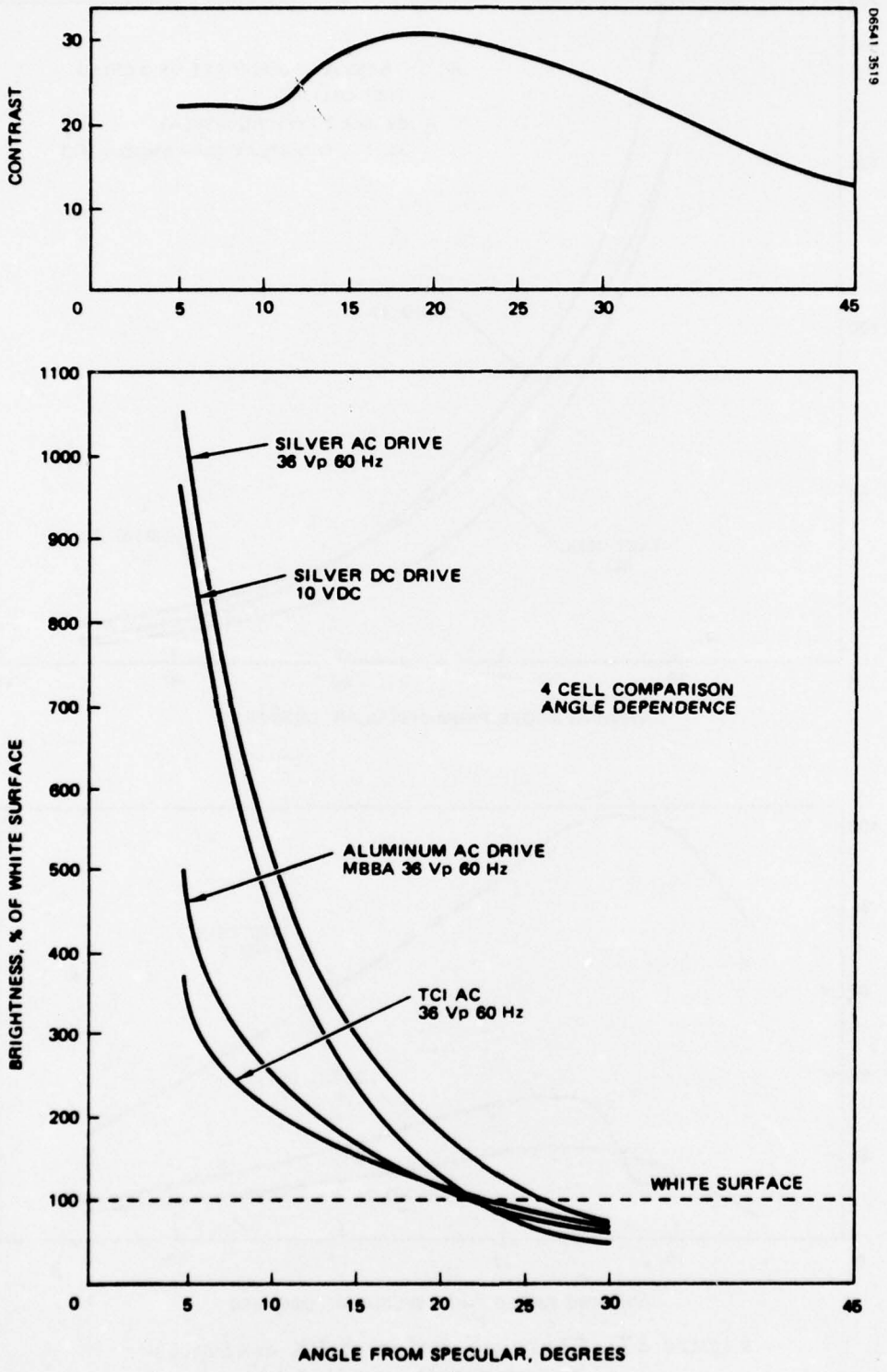
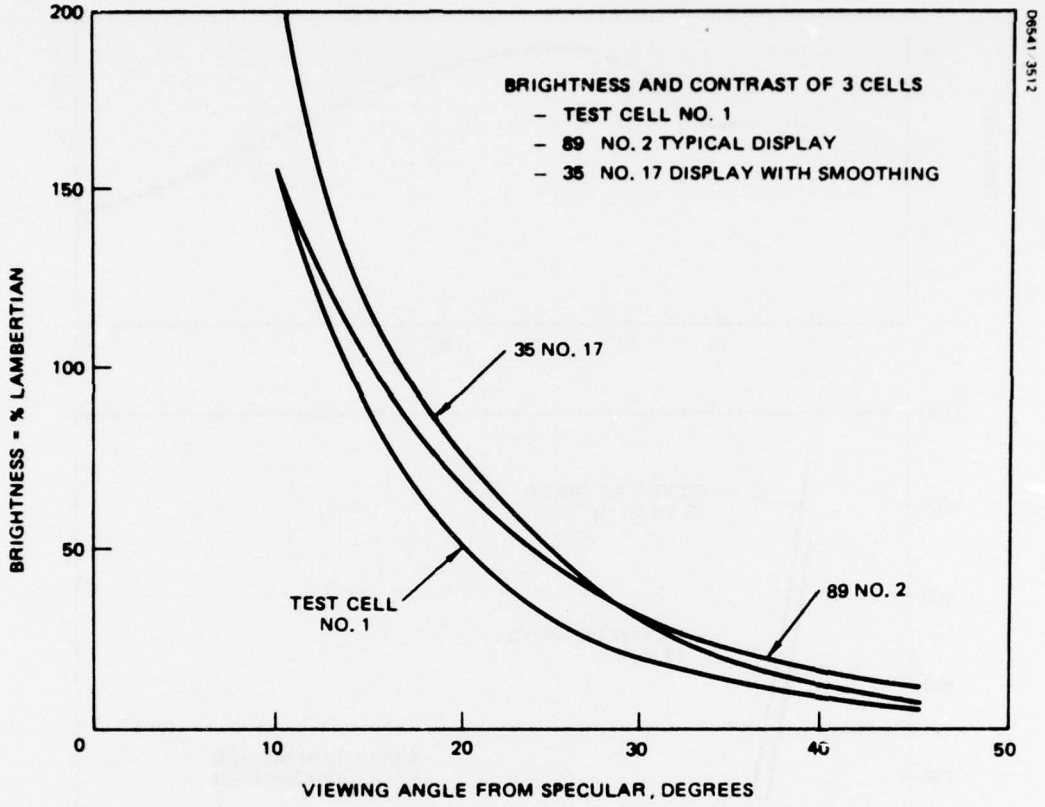


Figure 26. Experimental results on liquid crystal samples.



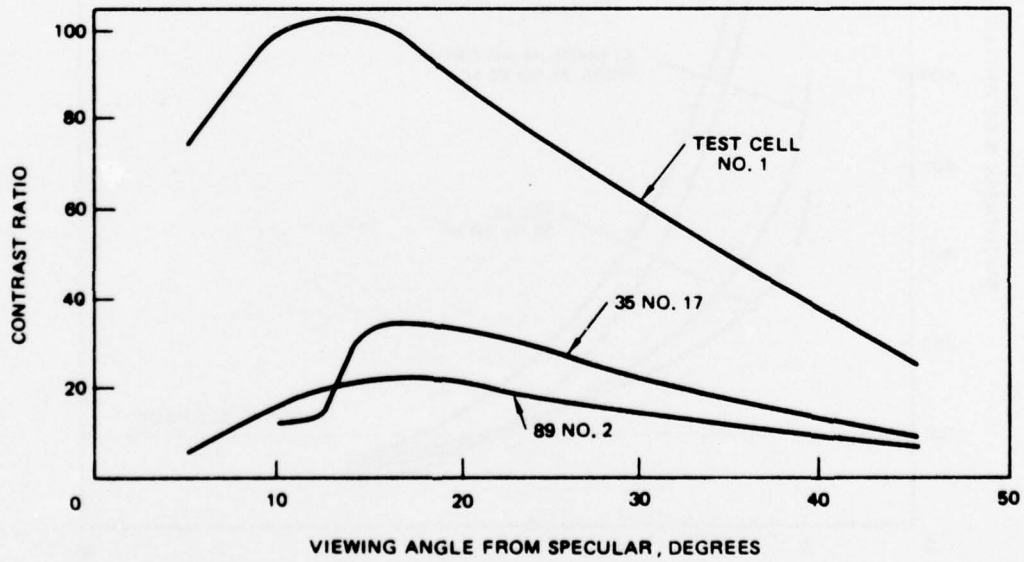


Figure 27. Characteristics of LX examples (experimentally determined).

TABLE 18. PRESENT DISPLAY PERFORMANCE

DISPLAY	1 X 1 IN. SINGLE	2 X 2 IN. QUAD	COMMENTS
RESOLUTION	100 ELEM/IN.	100 ELEM/IN.	EACH LINEAR DIMENSION
SIZE	1 X 1 IN.	2 X 2 IN.	
CONTRAST – MAX	24/1	19/1	IDEAL CONDITIONS WITHIN VIEWING WINDOW OF LAMBERTIAN
CONTRAST – MIN	2.5/1	1.2/1	
REFLECTIVITY	50%	50%	
WRITING SPEED	TV COMPATIBLE	TV COMPATIBLE	525 LINE RS170
RESPONSE TIME	120 MS	120 MS	DECAY TO 10%
DYNAMIC RANGE	8 GRAY SHADES	8 GRAY SHADES	IDEAL CONDITIONS
GAP WIDTH	N/A	<1.0 MIL	
DEFECTS – LINE	0	19	AFTER ASSEMBLY
DEFECTS – ELEMENT	3	17	

Contrast. The contrast ratio of the display is defined as the ratio of the diffuse reflectance of the display in its "ON" state (dynamic scattering) to its diffuse reflectance in its "OFF" state (background scattering). Curves showing brightness and contrast as a function of viewing angle are given for a typical chromium display cell in Figure 23. Under normal viewing conditions the brightness of the display is 40 to 100 percent of the brightness of a lambertian surface and the contrast ratio is greater than 15:1. The contrast reaches its maximum at viewing angles between 10 and 15 degrees from the specular reflection, and decreases as the angle becomes smaller. This is due to dispersion and scattering that occurs at narrow angles off the display surface and the liquid crystal. The illumination and viewing system should therefore be constructed to use as much of the scattered light as possible, while avoiding the light scattered at narrow angles from undesired sources.

The contrast values are independent of the magnitude of ambient illumination, and it is therefore possible to have a high brightness, high contrast demand display even in direct sunlight. At higher illumination levels – the contrast is less – so the display can be more readable. A comparison of a liquid crystal display and a CRT under high brightness conditions is shown in

Figure 28. Contrast is plotted as a function of viewing angle in a typical cockpit configuration. The liquid crystal display performance is equivalent to that of the best CRTs under 1000 ft-candles illumination, and superior at 10, 000 ft-candles. The liquid crystal display is the first technology to permit the presentation of real-time gray-scale imagery under viewing conditions comparable to, and as severe as, those frequently encountered in tactical aircraft operating above the clouds during daylight hours.

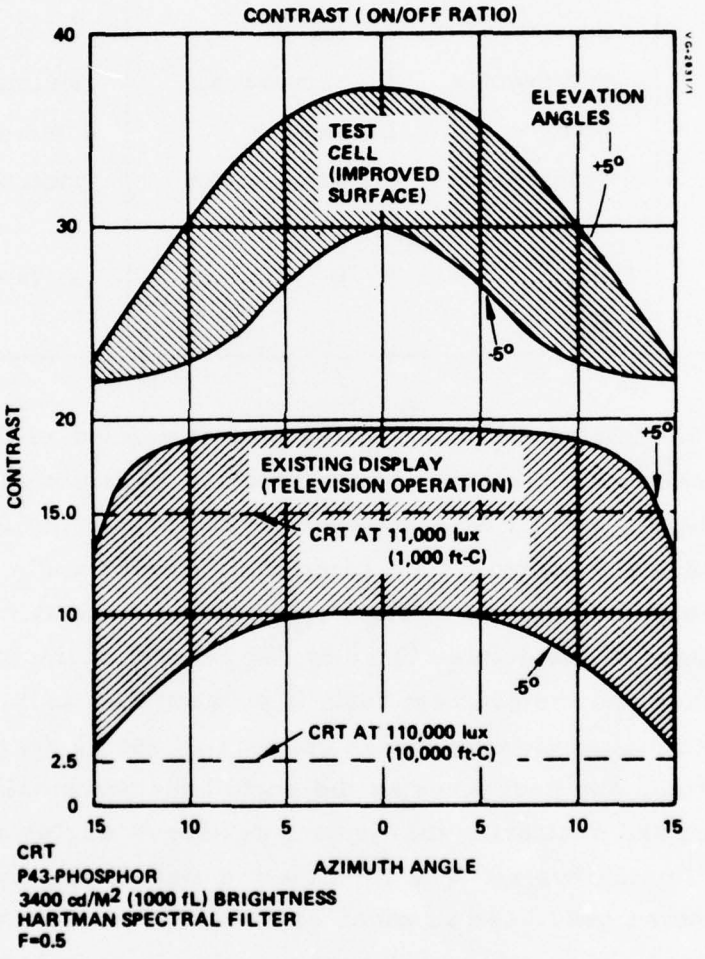


Figure 28. Display contrast.

The contrast of the display depends primarily upon the smoothness of the reflective electrode. In present display cells, the reflective electrodes

are deposited over the underlying circuit structure and hence the electrode follows this same structure. The resulting surface irregularities affect the optical performance of the display by creating unwanted reflections and dispersion of the incident light. The scattering that results elevates the background or black-level of the display limiting the dynamic range. A significant increase in contrast can be gained by improving the black-level by reducing or eliminating surface irregularities. To make the surface smoother or more mirror-like, a layer can be applied over the display surface to cover up underlying irregularities and thus provide a good optical surface. Several methods are being investigated for creating such a smoothing layer and measurements using smoothed wafers in liquid crystal test cells have shown contrast ratios greater than 40:1.

Gray Scale. The functional dependence of brightness upon the amplitude of the applied driving signal is referred to as the electro-optic transfer curve. Its shape and stability (with time, temperature, viewing angle, etc.) determines the number of shades of gray that can be reliably presented upon a display. The potential which must be applied before any significant scattering occurs is called the threshold. The potential above which no further increase in scattering occurs is called the saturation potential. The ratio of the saturated scattering level brightness to the background scattering level brightness is the contrast ratio. Eight shades of gray ($\sqrt{2}$ brightness levels) have been demonstrated by the Liquid Crystal Airborne Display.

Life. End life or total failure occurs when a device is no longer able to serve its intended role. This exact point is difficult to quantize for a Liquid Crystal Pictorial Display because all evidence points to a "graceful degradation" failure more, i.e., gradual rather than sudden total catastrophic failure. The only component of the display which is expected to degrade with time is the liquid crystal material. Some of the unneutralized components of the electro-chemical reactions that take place at the electrodes gradually reduce the degree of perfection of the liquid crystal molecular alignment, hence reducing the contrast of the display. Further action of this nature

causes the gradual accumulation of small gas bubbles in the display, preventing those areas of the display where bubbles occur from scattering. Tests are being run with 20 volts dc continuously applied to a set of test cells to obtain quantitative estimates of operational lifetime. To date, several of these test cells have run in excess of 15, 000 hours before failure. Actual displays should last considerably longer than test cells, as they operate at a lower voltage and duty factor.

Memory. Nematic liquid crystals have no memory capability other than the naturally long decay time, 100 to 200 milliseconds, which is the time required to reach 10 percent of the maximum scattering effect after the field is removed. (Various techniques can be used to shorten the turn-off time for video-type applications.)

Inherent memory in an LX device can be achieved by using a mixture of nematic and cholesteric crystal. The mixture exhibits a dynamic scattering effect similar to that produced in the nematic material alone when an electric field is applied. In the case of the mixture, however, the light scattering centers, which consist of interfaces between the two kinds of material, will remain for a period of hours or even weeks after the field has been removed. The molecules can be reordered by a given frequency voltage waveform. This type of storage display is possible if the "blinking" required between frames to update the presentation is permissible. Without blinking or bulk erasure, the display must be selectively erased on an element-by-element basis using large amplitude ac waveforms, thereby requiring different circuitry than the line-at-a-time addressing technique generally used. In addition, the response times of the nematic-cholesteric mixture may be much slower than the nematic material alone, thus preventing the display of pictorial imagery at TV rates.

Color. Although colored displays are not applicable to this study, proposed techniques to achieve multicolor presentations with the liquid crystal matrix display are presented below.

- Filtering the pixel elements on an assigned basis with dot or stripe patterns and illuminating the display with broadband light.

- Optically combining two or more matrix displays and illuminating each with an appropriate filtered or narrow-band source corresponding to the desired hue of the color primary.

Lighting and Optical Considerations. There are two imaging schemes possible with a projected liquid crystal display: the light field and the dark field. In the light field scheme the specularly reflected light off the display is used for producing the image, and the scattered light is blocked, and not used. In the dark field scheme, just the opposite occurs. The specular light is blocked out and the scattered light is used. This is shown in Figure 29. In the case of the light field, it is essential that the size of the aperture be kept quite small, since the contrast ratio will depend on how much of the scattered light is blocked. This is especially true since the liquid crystal is not an ideal diffuser and most of the scattered light is in the proximity of the specular reflection. This scheme is therefore much more difficult to implement within the normal optical constraints and performance requirements of a Head-Up Display, and the dark field approach is considered preferable.

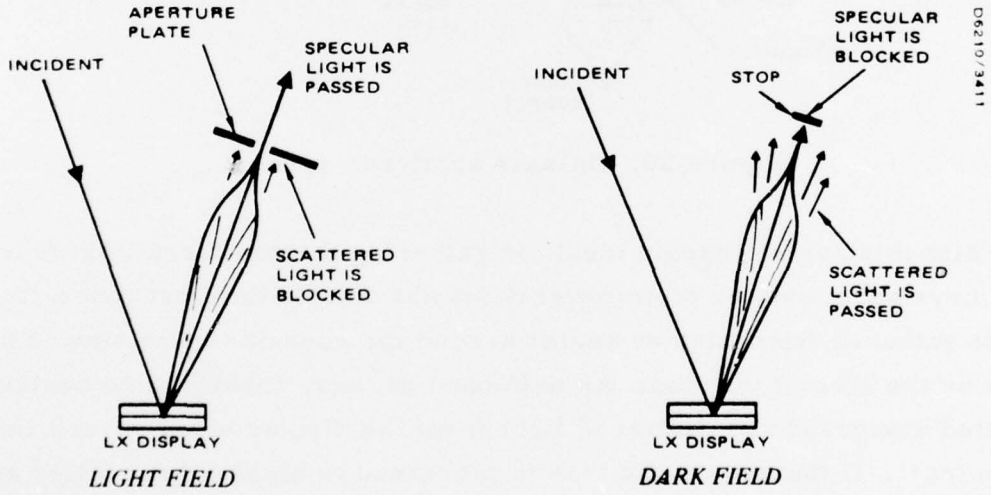


Figure 29. Imaging schemes using liquid crystal.

On-Axis Viewing. The implementation of a dark field system requires that the specular reflection off the display surface be blocked while the scattered light is gathered. There are two basic approaches that are

feasible, one for on-axis display viewing (display normal to optical axis), and one for off-axis viewing (display tilted). The on-axis approach consists of a Schlieren optical arrangement as shown in Figure 30. Light from the source is imaged onto a small diagonal mirror on the optical axis at the focal point of the field lens. This becomes a point source and is collimated by the field lens so that the incident rays are normal to the display. The specularly reflected rays are folded back on the incident rays and are focused by the field lens back onto the diagonal mirror which now acts as a stop and prevents them from entering the relay lens. Scattered light from the liquid crystal will not be normal to the display and therefore will miss the stop and reach the relay lens.

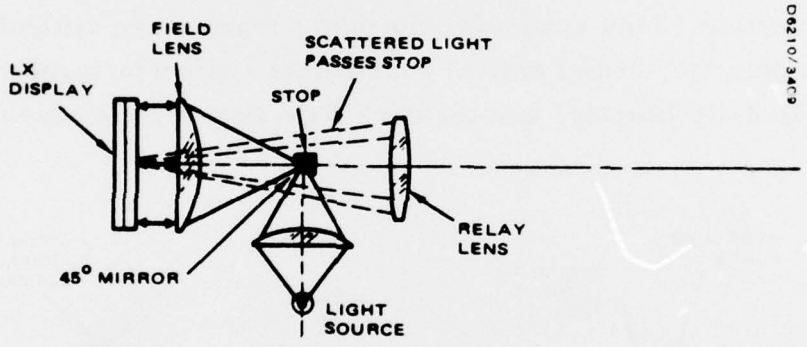


Figure 30. On-axis schlieren system.

While this system seems ideal for gathering the scattered light from the liquid crystal, it suffers from several drawbacks. In the first place, the light is gathered from narrow angles around the specular reflection, determined by the size of the stop. As menioned earlier, these angles contain unwanted dispersed and scattered light from the display surface, and limit the contrast. If the size of the stop is increased to block off a greater angle, the effective gathering area of the relay lens will be reduced and brightness will fall off. Furthermore, an image of the stop will appear at the exit pupil, thereby creating an undesirable "hole" proportional to the size of the stop. This system is therefore considered inappropriate for this particular application.

Off-Axis Viewing. A second approach utilizes an off-axis viewing system where the display is tilted with respect to the optical axis. Light sources are situated around the display such that their specular reflections off the display cannot reach the relay lens, but the light scattered from the liquid crystal can. Because of the non-uniform scattering lobe of the liquid crystal, it is advisable to use two light sources for greater uniformity, as shown in Figure 31. By placing the light sources at the proper angles, it is possible to maximize the brightness and contrast of the display to give the best overall performance. It is expected that this approach will yield the best results for a HUD application. The liquid crystal performance can be optimized, and the requirements on the light sources and optical system can be relaxed. This allows greater flexibility in the design and manufacture of these components.

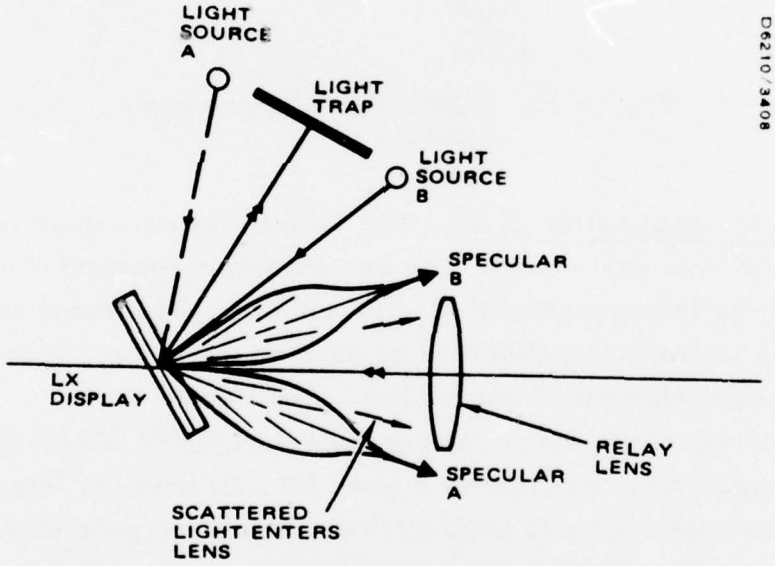


Figure 31. Off axis viewing system.

Special Lighting Considerations. Because of the wide dynamic range of background brightness normally encountered with Head Up Displays, it is desirable to control the brightness of the display over a similar dynamic range, thereby maintaining a reasonable contrast ratio. The types of light sources currently feasible in holographic applications have a controllable dimming range of approximately 10:1. An alternate method is therefore

proposed that uses two linear density wedges in front of the light source, as shown in Figure 32. As the two wedges slide past each other over the light source, their optical density changes, thereby controlling the apparent brightness of the light source. Such wedges frequently have a dynamic range of 10^3, and using two wedges sliding in opposite directions provides more uniform attenuation with a maximum dynamic range of 10^6.

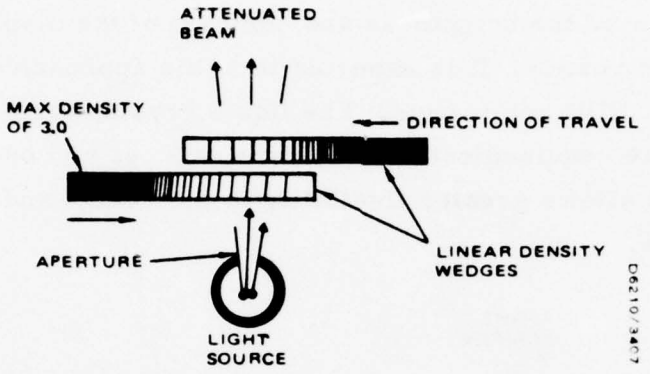


Figure 32. Light source brightness control.

Diffraction Optics Application of LX. The direct viewed display is not under consideration for this application. The system under consideration would use a dynamic scattering mode LX display surface, illuminated by a narrow band source. This surface would then be used as the display source for the holographic optical element on the canopy. (See Figure 33.)

This utilization of the indirectly viewed or projected LX display has several advantages over the directly viewed LX. Of primary importance is the fact that the illumination is controllable due to fixed geometry. The brightness and contrast may then be optimized for this geometry. Considerations of light baffling, etc., must be made so that under nighttime conditions, stray light in the cockpit is not a problem. Of course, the problem of choosing an illumination source which will be sufficiently bright remains a prime consideration. This problem has already been addressed as part of a proposal to utilize a liquid crystal matrix display as a source for an advanced HUD utilizing holographic optics. Since the display requirements are analogous between a holographic HUD and the canopy mounted HOE, the results of the illumination source investigation are applicable and will be included in this report.

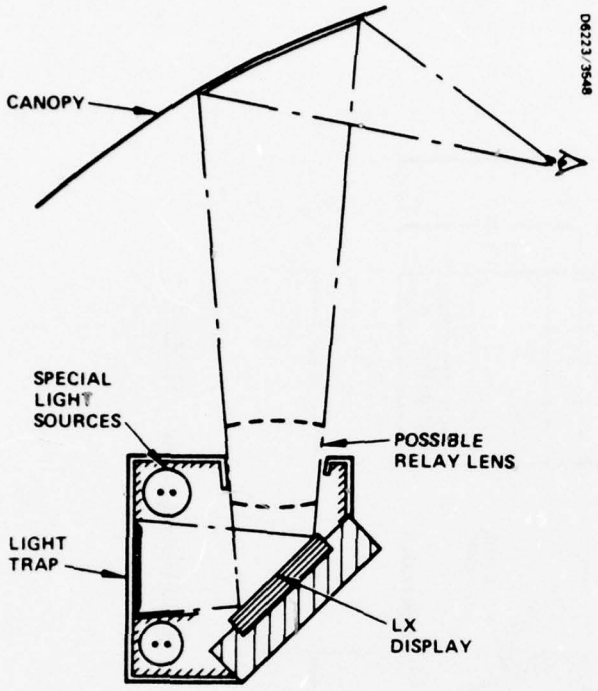


Figure 33. LX-HOE image source concept.

Two concepts of a HUD have been defined using the LX display as image source. The first concept, shown in Figure 34, is a flight test demonstration HUD utilizing the LX display and the holographic combiner. The internal arrangement concept is diagrammed. The illumination concept uses off-axis lighting and a special light trap. The relay optics are required to give a wide FOV and for geometrical considerations.

The second concept shown in Figure 35 is similar to a design which is being built on another program for use with a CRT. The internal construction is the same, but the larger combiner permits a wider FOV.

Illumination System for Projected LX Display. A tradeoff study was conducted to determine a suitable illumination source for a HUD using an LX matrix display. Based on the illumination requirements of high brightness, high efficiency and narrow bandwidth, the choice was narrowed to a thallium iodide arc lamp and a mercury arc lamp coated with a phosphor. Both sources exhibit narrow band radiation; however, the mercury arc-phosphor lamp is more efficient and was determined to be suitable within the system packaging constraints. Depending on the size and form factor a special lamp development may be required. A description of the chosen lamp follows.

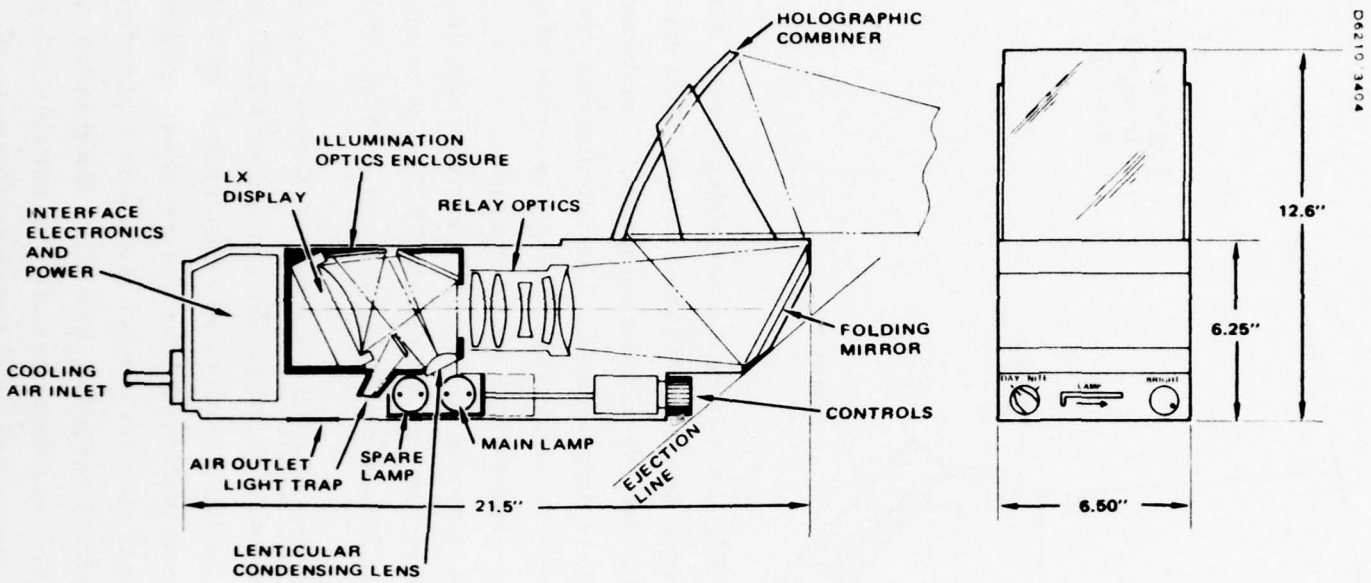


Figure 34. Illumination concept for LX/Holographic HUD.

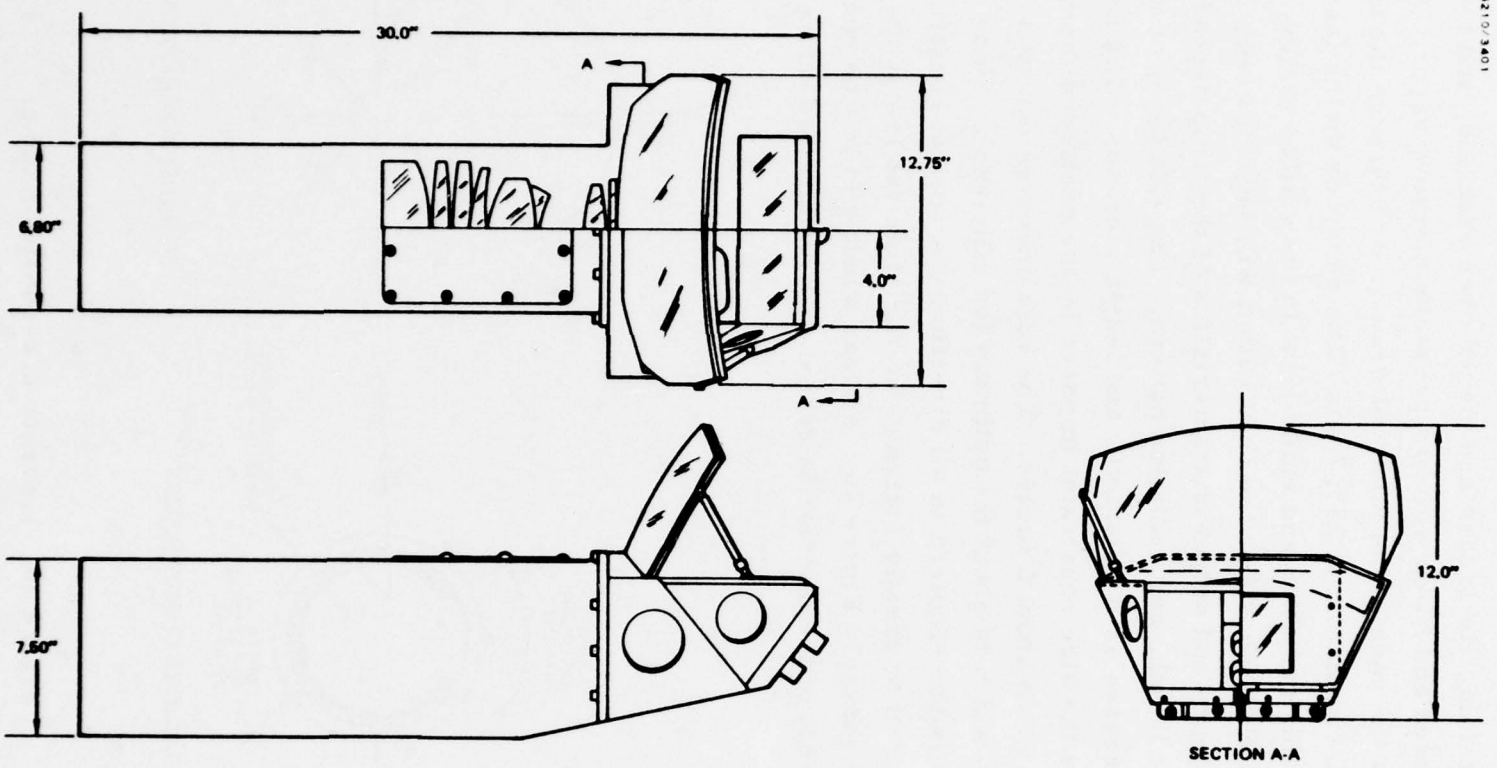
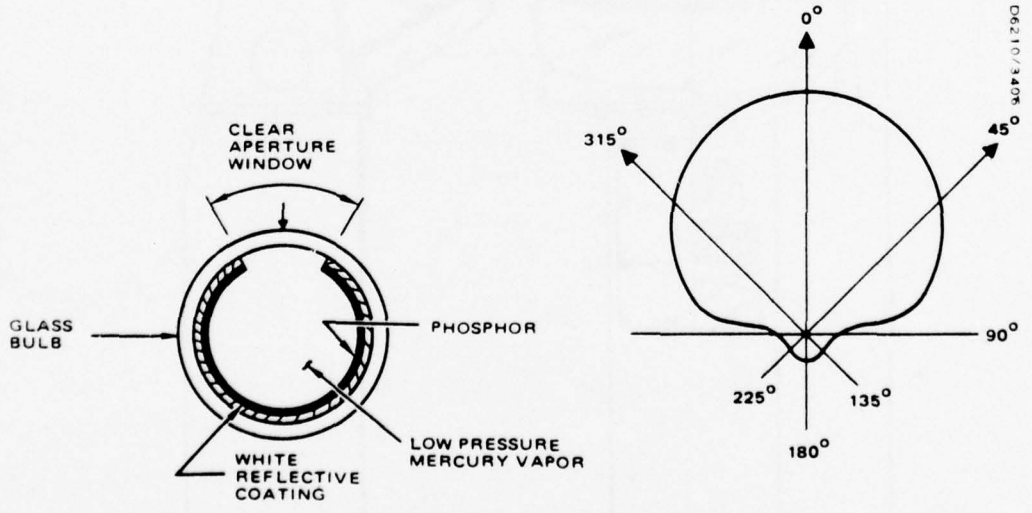


Figure 35. Preliminary outline of Advanced HUD.

Mercury Arc Phosphor Lamp. The basic construction of the lamp consists of a glass tube coated with the desired phosphor on its inside surface. End caps containing electrodes are placed over each end, and the entire tube is then evacuated and filled with low pressure mercury vapor. A voltage placed across the ends of the tube will draw an arc through the mercury vapor, which emits UV radiation at 253.7 nm. The phosphor on the inside of the tube absorbs this radiation and emits light in the visible portion of the spectrum. With a P-44 phosphor the light output will be 543.2 nm.

The efficiency and output characteristics of the lamp depend on bulb diameter, arc length, and radiation pattern. The efficiency of the bulb generally increases as its diameter and length increase. The limiting factor in this case is the size constraint imposed by the package dimensions, which limits the length to about 6 inches. The bulb diameter can be as large as 1-1/2 inches, which is about the optimum for efficiency. Since radiation from the bulb is not required in all directions, a special construction technique can be used to greatly increase its radiation pattern in the useful direction. This is shown in Figure 36. A clear window is left on one side of the bulb and the rest of the interior is coated with a white reflective material.



SPECIAL BULB CONSTRUCTION *RADIATION PATTERN*

Figure 36. Mercury arc-phosphor lamp.

The phosphor is then placed over this reflective material and the bulb is filled and sealed. As a result, the inside of the bulb acts somewhat like an integrating sphere, with most of the light being internally reflected until it exits through the aperture window. The light output of this lamp can be up to 10 times the output of a standard fluorescent lamp in the direction indicated by the radiation pattern.

Anticipated Results. The performance of a special purpose P-44 lamp can be estimated by scaling up the performance of a standard fluorescent lamp. A normal CW (cool white) fluorescent lamp with a 5 inch arc length puts out about 35 lumens/watt. The luminous efficiency of the CW phosphor is about 51 percent, compared to over 90 percent for the P-44 phosphor. Assuming that UV-to-visible conversion efficiency of the phosphor is about the same, the output of the P-44 bulb should be around 65 lumens/watt.

The gathering efficiency of the proposed illumination system will be approximately 20 percent. A typical advanced HUD display requires an incident flux of 800 lumens, and therefore the bulb output should be approximately 4000 lumens, assuming it radiates equally as a line source in all directions. If the special construction technique yields a radiation pattern that has a gain of only 2 to 3 times, it essentially increases the gathering efficiency and lowers the bulb output requirement to 1300-2000 lumens. At an efficiency of 65 lumens/watts, this corresponds to a bulb power in the range of 20 to 30 watts. A special power supply will be required to drive the bulb, and including its efficiency (ballast losses, etc.) in the calculations, the total power would remain less than 50 watts for the advanced HUD at 1.8 contrast and approximately 25 percent of this value at 1.2 contrast.

Thallium Iodide Arc Lamp. The Thallium Iodide Arc Lamp is a gas-discharge lamp which produces a strong emission at 546 nanometers. This lamp is not as efficient in the narrow spectral bandwidth as the phosphor coated mercury lamp. The Thallium Iodide lamp yields about 20 lumens/watt as compared with a P-44 phosphor coated lamp at 65 lumens/watt. The arc lamp is essentially a point source while the phosphor lamp is a line source - more difficult to control and collect light from. The tradeoff for a HUD is in favor of a point source and lower efficiency requires a concurrent increase in power requirement to drive the display.

4.6.5 Incandescent Image Source

General. The incandescent lamp has the dual nature of being both an illuminator and a directly viewable image source. As an illuminator it can provide broadband front, back or side lighting to a non-luminous display. As a source, it provides outputs far brighter and more intense than other image sources. A typical miniature lamp filament puts out an average of 150 millicandelas for a 40, 000 hour life – this is about 50 times the maximum output of a green LED. The filament brightness under these circumstances is about 50, 000 foot lamberts – a highly visible point source. Larger, tungsten-halogen incandescent lamps have outputs up to 30 million foot-lamberts at 150 watt rating and a 50 hour life. The relationship between voltages, brightness, power and life for incandescent sources are closely known with reasonable accuracy. The fundamental limitation on the output of incandescent lamps is the melting point of tungsten. The practical limit of operation of the lamp is 3800°K. A more reasonable operating point which results in extended life is 2800°K.

An application of incandescent lamps as an image source might be as follows: An extended stationary reticle is either back-lit or edge lit by incandescent lamps. Moving marks or bar-graph type information could be presented relative to the reticle via individual, directly viewed filaments switched on or off. Lines or figures made up of lines could be generated by line-filament sources. Alphanumeric characters are also available as incandescent sources in relatively small physical sizes (about 1/4 inch).

Spectral Characteristics. As one might expect, the major problem with incandescent sources is the incompatibility of their spectral emission characteristics with the acceptance spectral bandwidth of diffraction optic elements. For high source efficiency with holographic elements, the radiation should be confined to a relatively narrow bandwidth, say 10 nanometers. This requirement generates problems because not only is the blackbody emission curve at 2800°K very broadband, but highly weighted in the infrared region where 85 percent of its output is as in Figure 37. This spectrum must be highly attenuated with a notch filter to the desired bandwidth. This may be accomplished with a narrow band interference type

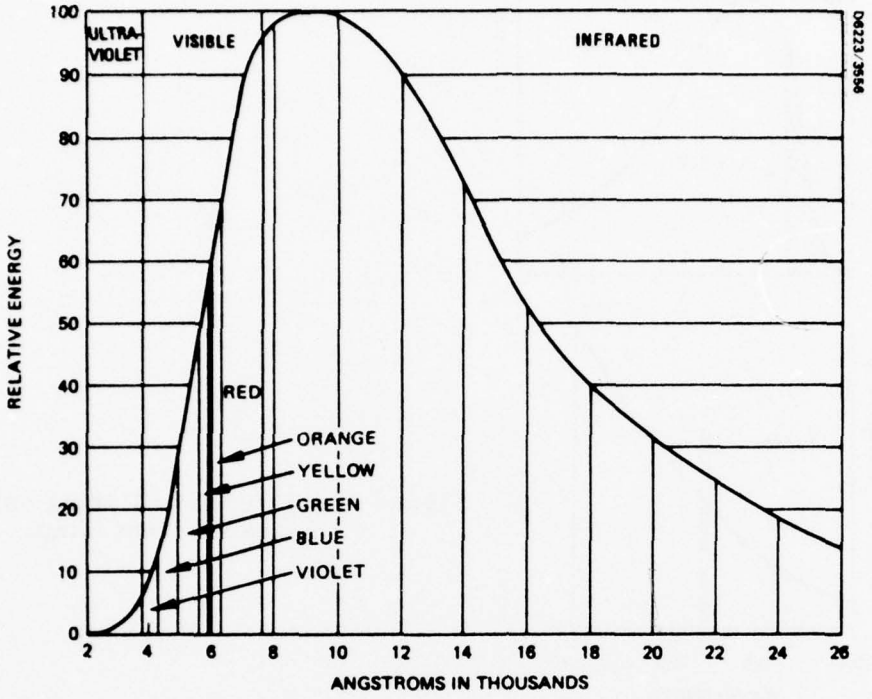


Figure 37. Spectral distribution of tungsten — Halogen incandescent lamp.

filter. Typically, this type of filter has an absolute transmission of 50 percent at its center wavelength and a half-bandwidth of ±1 percent of the peak wavelength at 550 nm) (11 nm total). Given the combination of this filter and a lamp at 2500°K (figure 38), the resultant efficiency considering the visible output only is about 1.4 percent. If the transmission losses of the hologram are considered (80 percent reflection efficiency), the overall source efficiency to the eye is about 1 percent if the peak is centered at 555 nm. Other dominant wavelengths would, of course, result in lower overall efficiencies to the eye. The use of such a filter would thus require a source brightness of 200, 000 foot-lamberts, which is a moderately bright lamp, to give 2000 foot-lamberts brightness to the eye. Increasing the color temperature of the source by increasing the voltage would result in a nominal increase in efficiency coupled with a moderate increase in brightness. The acceptability of a 10 nm source output bandwidth is predicated on the acceptance bandwidth of the hologram and the geometry of the system. In order to minimize see-through color distortion, the bandwidth of the hologram should be as narrow

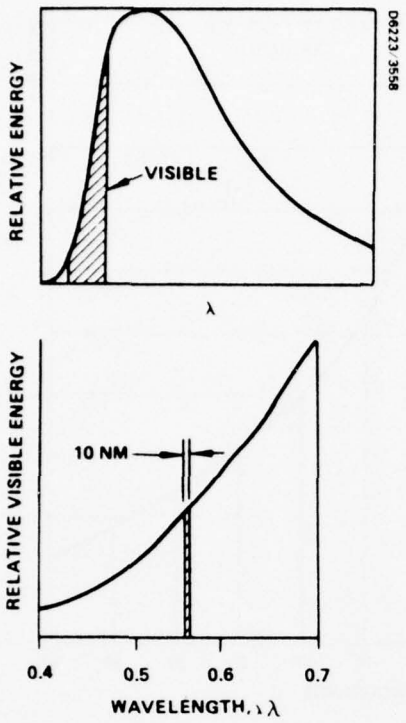


Figure 38. Effect of filtering on incandescent lamp.

as possible; however, a wider bandwidth source is desirable from the standpoint of matching the wavelength for peak hologram efficiency to the source peak wavelength. If the source and hologram have the same bandwidth, minor variations in the peak wavelength of either would result in drastic light losses.*

A demonstrator model of a collimated reticle system was built using a commercial 11 nm bandpass filter with an incandescent source and a holographic collimating lens. The bulb, rated at 150 watts, was operated at about 25 watts to yield a system overall brightness of 10, 000 foot-lamberts to the eye. The reticle was backlit by the filtered source and condenser optics. The brightness of the collimated reticle image was more than adequate to be highly visible when viewed with a bright cloud background. With a 10 nm wide hologram, the see-through coloration is noticeable as a light magenta tinting of the outside world. As the bandwidth of the hologram increases, more of the color is subtracted from the outside world, thus deepening the see-through coloration.

*A wider source bandwidth minimizes the loss due to mismatch.

Dispersion. Another factor must be considered here: The HUD demonstrator mentioned above was constructed to allow the reflection hologram to operate very nearly in a symmetrical reflection geometry; thus the grating component of the HOE was negligible and chromatic dispersion was minimized. If the canopy-mounted HOEs are operated in an asymmetric relationship, the dispersion of a 10 nm bandwidth source will most likely be excessive and that source would therefore be unacceptable. If this is the case, the filtering would have to result in a narrower band output, say 2 nm. The maximum visible efficiency of a lamp/filter combination yielding a 2 nm band light would be 0.2 percent, thus requiring 10^6 foot-lamberts (unfiltered) at the source. Clearly, this type of inefficiency makes incandescent sources out of the question for all but the simplest presentation display. This level of brightness foregoes the possibility of using "miniature lamps." If the output wavelength of the source can be 10 nm or greater, the practicality in the incandescent approach may be realistic; otherwise, they should not be considered for this application.

4.6.6 *Image Source Tradeoffs and Conclusions*

The tradeoff exercise for the display sources discussed may be summarized in Table 19 below. The performance of each of the sources with respect to the requirements listed at the beginning of this section are listed and comparisons may thus be made.

TABLE 19. IMAGE SOURCE CHARACTERISTICS

SOURCE	BANDWIDTH, NM	BRIGHTNESS, fL	LIFE, HRS	POWER, WATTS
CRT	2	4000	2,500	75
LX	2	2600	15,000	50
LED	45	2000	50,000	20
LASER 10 MW	0.5	5000	5,000	400
INCANDESCENT (FILTERED)	10.0	2000	5,000	75

Bandwidth. Bandwidth is a major concern in systems utilizing diffraction optic elements. There are two advantages of a narrow band source which apply to diffraction optic systems. The first is that optical systems which would normally suffer from chromatic dispersion do not exhibit this phenomenon with narrow band light. The second involves the argument that the relative contrast to the eye is greater for a narrow band source than a broadband source when both sources have the same luminance and both are viewed against a broadband background. The theory behind this argument is that at its characteristic wavelength, the source has far more energy than the background and, hence, appears sharper and more viewable.

In the canopy-based diffraction optics system, the narrow bandwidth is a necessity. The HOE acts as a narrow band filter; thus a broadband source will lose light because of the inefficiency of reflection at other wavelengths. All of the sources exhibit relatively narrow spectral emission characteristics; however, the 45 nm bandwidth of the LED is considered too wide for a diffraction optics application; the efficiency would fall off drastically after the first 8 to 10 nanometers.

Brightness. All of the sources in the table are reasonably bright; however, the LED and the incandescent seem barely adequate because: 1) 2000 foot-lamberts is not adequate for a conventional see-through display, and 2) they are too broadband for the more efficient, diffraction optics display. All of the other sources are adequate from a brightness criterion.

Life. The operating life of a display source is a function of the stress level and environmental conditions to which it is subjected and its inherent life characteristics. In terms of mission operating time, 1000 hours probably represents 250 missions, however, with checkout time considered, 2000 to 2500 hours to replacement is about the minimum reasonable specification. Using CRTs with burn-resistant phosphors is a great help in extending the life expectancy of this type of source. Liquid Crystal displays have generous life expectancies which undoubtedly far surpass the operating life of the illuminating source. For a mercury vapor lamp of the type suggested with the LX display, the typical operating life is about 10,000 hours.

Light Emitting Diodes possess the longest inherent life due to their solid state construction. Good heat sinking is necessary to maintain their thermal equilibrium at a reasonably low value to provide the life characteristics desired. A possible difficulty exists with a large matrix of 40, 000 chips if one or two chips fail prematurely. The entire device would be replaced and the defective chips repaired. Because of low yield of high density arrays and because of the high probability of failure associated with the large number of chips, the devices must be readily repairable. Laser sources according to manufacturer's data, exhibit very good life characteristics and should present no problem in that respect.

Power/Size. Of the sources considered, only the laser presents a problem with respect to size and power. Clearly, for this application, currently available sources do not meet the normal constraints on packaging. More modest sized laser heads are deficient from a brightness point of view due, in part, to the rapid scan rate required. Although state-of-the-art advances are expected to somewhat alleviate the problem, present thinking rejects the laser for this application.

From a bandwidth argument the LED and incandescent sources must be ruled out even through their inherent brightnesses seem nearly adequate. The laser display has the most desirable optical characteristics but is the most unwieldy from a physical standpoint. The LX and the CRT remain as the only reasonable choices, although their bandwidth is excessive for asymmetric geometries.

The narrow band, illuminated LX matrix display has very strong possibilities for this application provided the technology permits large area (4 x 4 in.) displays to be fabricated reliably and at reasonable costs. The size of an illuminated, light trapped source such as is shown in Figure 33 is probably too bulky to be considered for the F-16, particularly considering the need for multiple sources. The LX source has good potential for single displays with less stringent packaging constraints and is currently being incorporated into wide-field holographic HUD designs.

Conclusion. By process of elimination, the CRT has been determined as the only currently feasible display image source for the holographic optical element. It is well suited for this application as it has already been utilized

in similar applications – the Holographic Visor Helmet Mounted Display (HVHMD) and the Holographic Optical Unit (HOU). It is also to be used in an application for Holographic night vision goggles.

If the CRT were to be used in a near-symmetrical geometry, such as in a HUD, the magnitude of the dispersion would be minimal. The departure from symmetry initiates the image "smear" due to dispersion and the magnitude of the angular smear is a function of the asymmetry. Even though the CRT has a narrow band spectral emission-only 2 nm wide, the magnitude of the dispersion of a CRT display gets as high as 8 milliradians in the worst geometry. An acceptable value is about 2 milliradians for a cueing-type display. Thus, a source bandwidth of 0.5 nanometer as with a laser would be quite an improvement.

The chosen CRT utilizes P-43 phosphor and produces the emission spectrum shown in Figure 16. This phosphor has some very desirable characteristics. It has an energy peak at 543.2 nm which has a 97 percent visual sensitivity factor. The phosphor also has a high burn resistance which allows it to be driven at higher brightness levels. Its bandwidth is significantly narrower than is achievable with other types of emitters. The secondary emission peak at 547 nanometers appears as a ghost image displaced from the main image and having a relative intensity of 30 percent of the primary image. The efficiency rolloff of a reflection hologram as a function of wavelength acts in a manner to subdue the second lobe as shown in Figure 39. Thus the net spectral response of the system has a singular dominant wavelength and the ghost image should not be troublesome. A transmission hologram does not, however, exhibit this efficiency rolloff. Rather, the secondary peak is diffracted at a slightly different angle and appears as a displaced secondary image. The appearance of this image could only be filtered out and might then render the CRT unacceptable from a brightness standpoint.

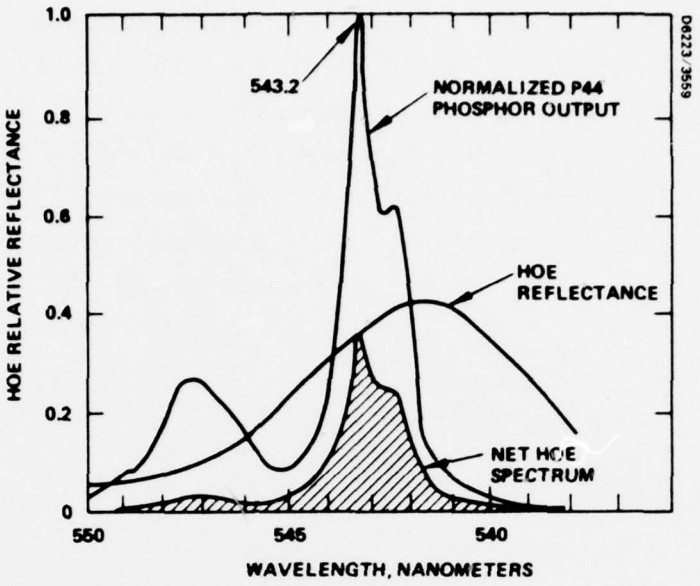


Figure 39. Spectral emission characteristics of reflective hologram/CRT combination.

5.0 SYSTEM FEASIBILITY AND TRADEOFFS

5.1 DESIGN CONSIDERATIONS

5.1.1 Physical Design Considerations

F-16 Cockpit Considerations. Without a doubt, the physical design constraints imposed by the requirements of a modern fighter aircraft like the F-16 present a tremendous obstacle to the design of the type of system associated with this program. With the exception of either the canopy substrate used as part of the optical system or the helmet visor, each component of the diffraction optic systems is a foreign body in the aircraft and its impact on the prime operating functions of the aircraft must be considered. The F-16 canopy, for instance, has been designed to provide the highest degree of visibility of any fighter aircraft previously built. The instrument and control clusters demand unobstructed visual and tactile access by the operator. In addition, the F-16 cockpit area is built like a glove around the pilot with a scarcity of space which is not already dedicated. Not defeating the purpose of this well-designed cockpit is and has been a prime consideration in the design of the baseline systems. The instrument panel is shown in Figure 40. A plan view showing the operator in relation to the canopy and the instruments is shown in Figure 41 while a forward looking photograph showing operator, canopy still and instrument panel location is in Figure 42. The photograph shows a YF-16 instrument panel. With respect to the pilot, shoulder clearance, head interference and arm and leg motion were all considered. The obscuration of visibility also presented a real problem. Placement of the image sources required a tradeoff between obscuring visual fields or causing physical interference. The baseline design has attempted to minimize encroachment of any kind into the man-space or see-space of the cockpit.

Canopy Geometry Considerations. The inside of the F-16 canopy, although not ideal as a holographic substrate, is the baseline surface upon which the HOEs will be mounted. As such, its properties will, in part, determine the properties of the various HOEs emplaced upon it. In order to study the properties of the canopy shape with respect to the design eye and image

PRECEDING PAGE BLANK-NOT FILMED

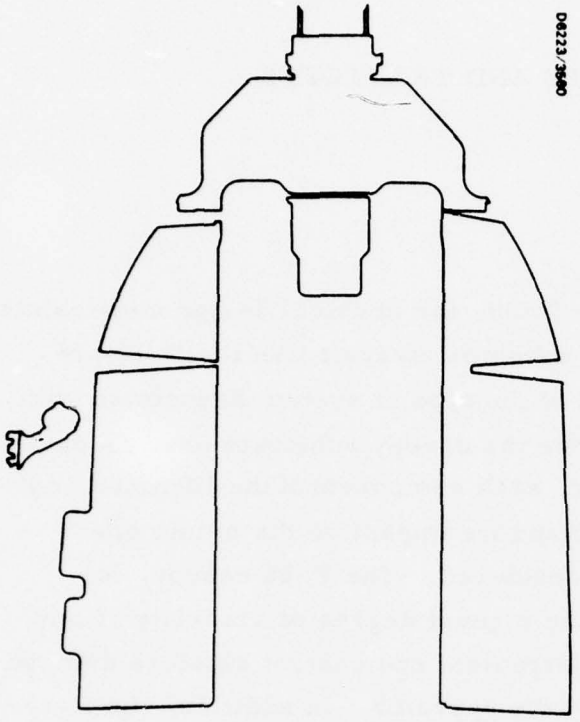


Figure 40. F-16 cockpit instrumentation.

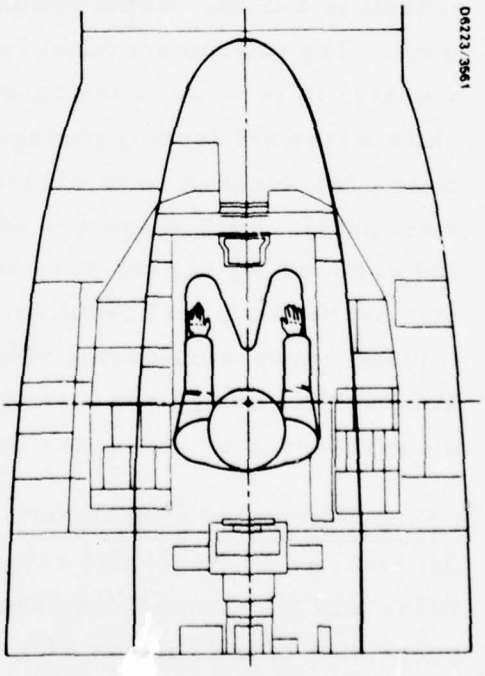


Figure 41. Pilot in F-16 cockpit.

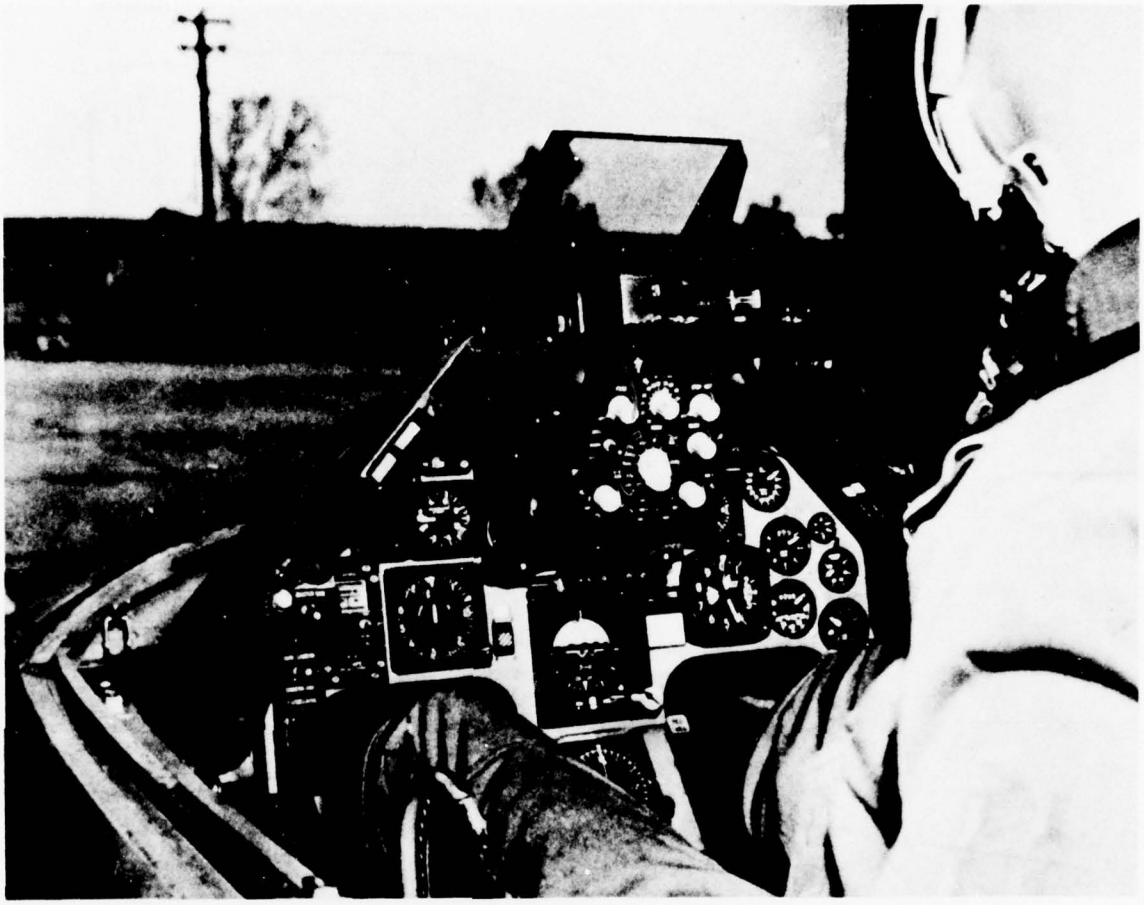


Figure 42. View looking forward in YF-16 cockpit.

sources, the shape coordinates were programmed into the Hughes computer, thereby permitting optical rays to be traced at its surface. The coordinate system shown in Figure 43 was used. The assumed center of rotation of the neck (Z=0) in azimuth and elevation was assumed to be six inches behind the design eye point. The zero point is arbitrary as long as the coordinates remain consistent.

This programming procedure allows a ray emanating from any point in any direction to be traced to the canopy. The strike point x, y and z coordinates are determined as well as the horizontal and vertical projected angles of the reflected ray off the canopy. A scan was made of azimuth angles between 0^{o} and 60^{o} for increments of elevation angles between -10^{o} and $+40^{o}$. The numerical results are found in Appendix C. The graphical significance of these results are shown in Figures 44 through 49. The significance of

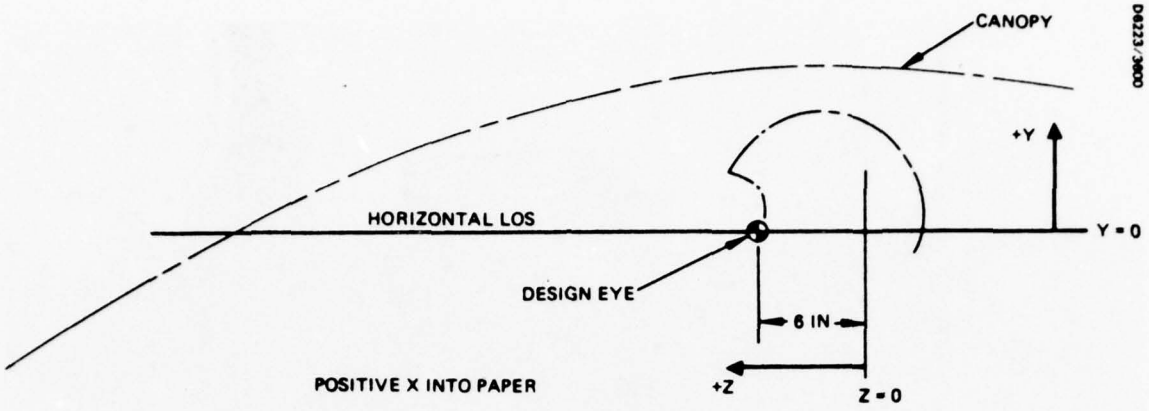


Figure 43. Canopy/design eye coordinate system.

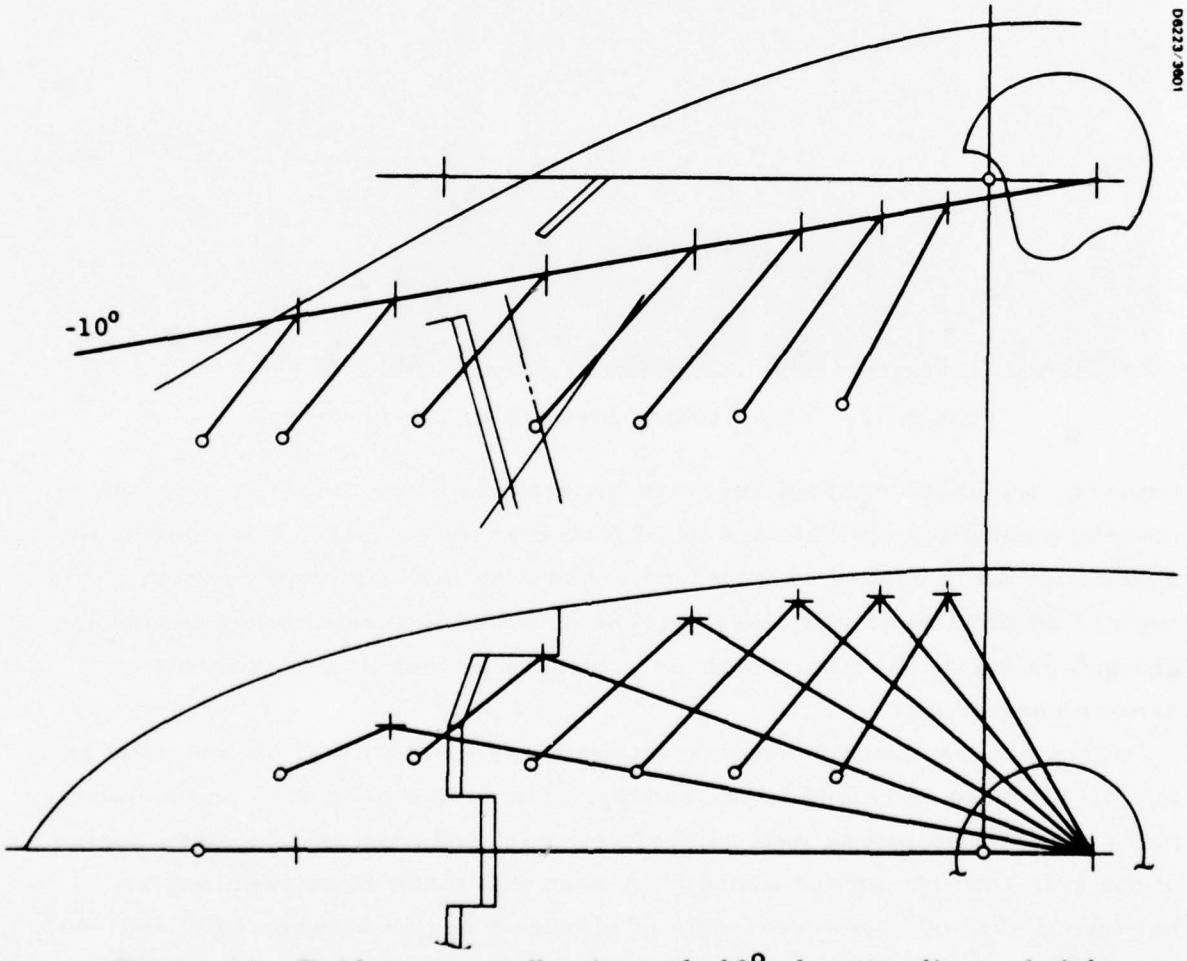


Figure 44. F-16 canopy reflections of -10° elevation lines of sight.

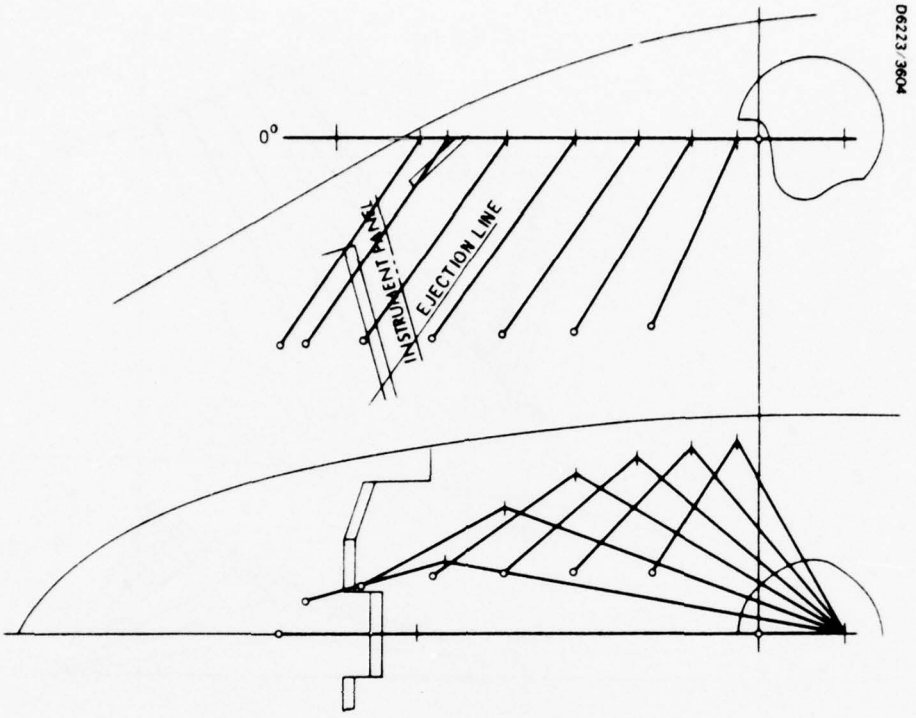


Figure 45. F-16 canopy reflections of 0° elevation lines of sight.

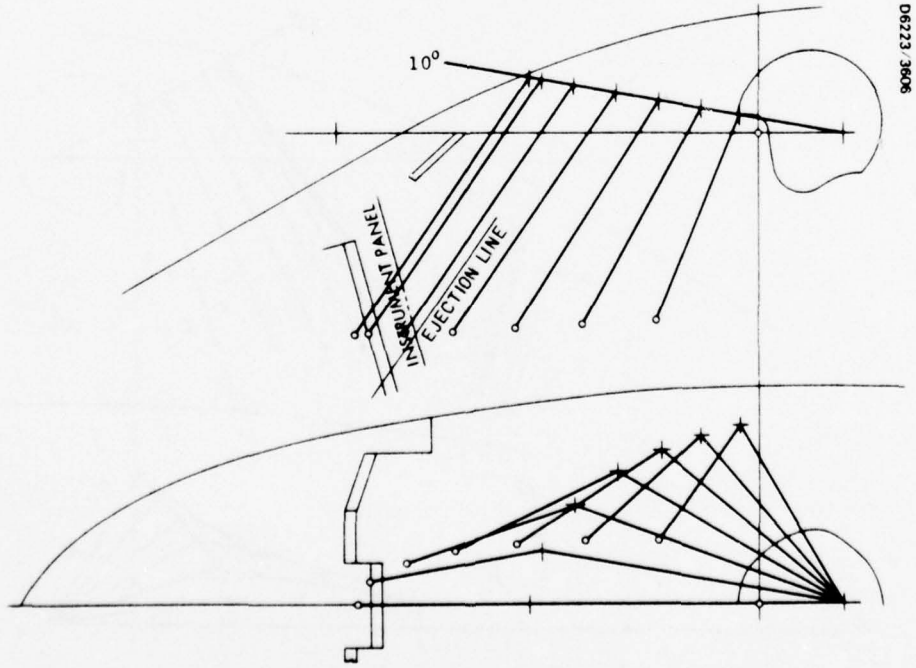


Figure 46. F-16 canopy reflections of 10° elevation lines of sight.

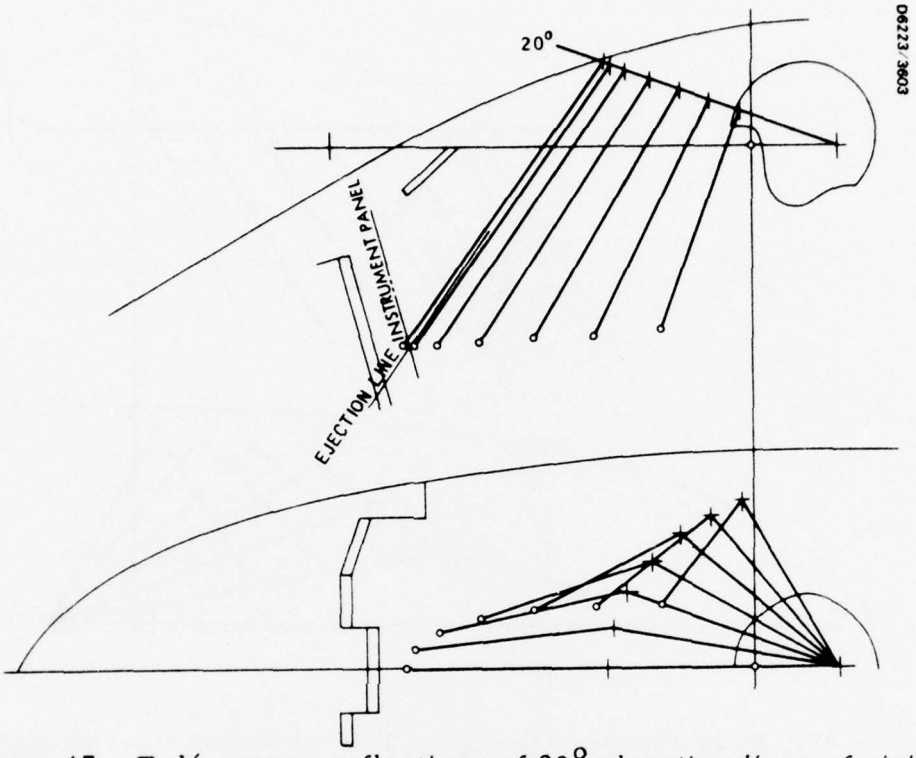


Figure 47. F-16 canopy reflections of 20° elevation lines of sight.

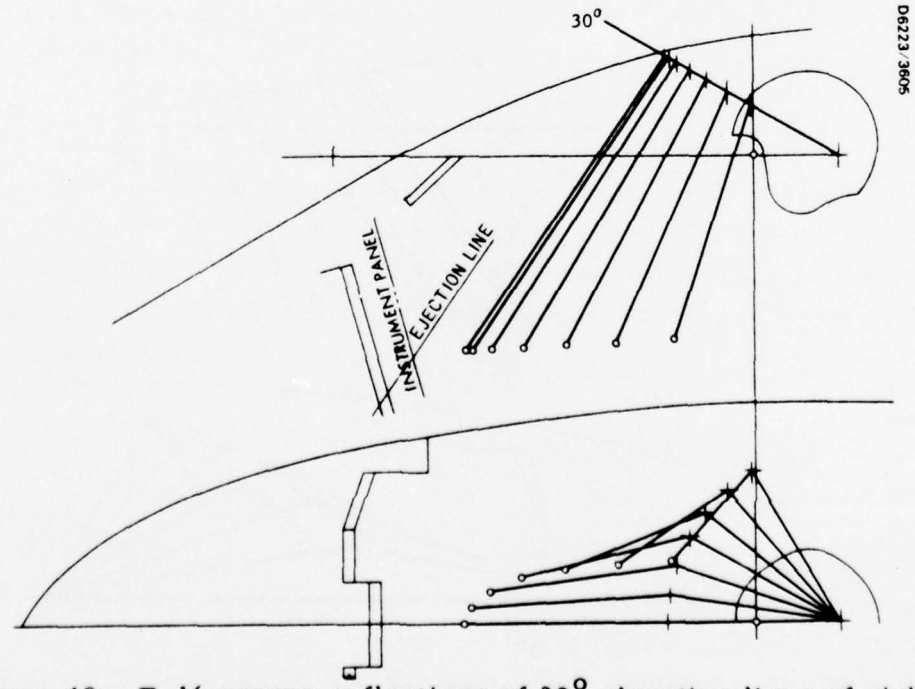


Figure 48. F-16 canopy reflections of 30° elevation lines of sight.

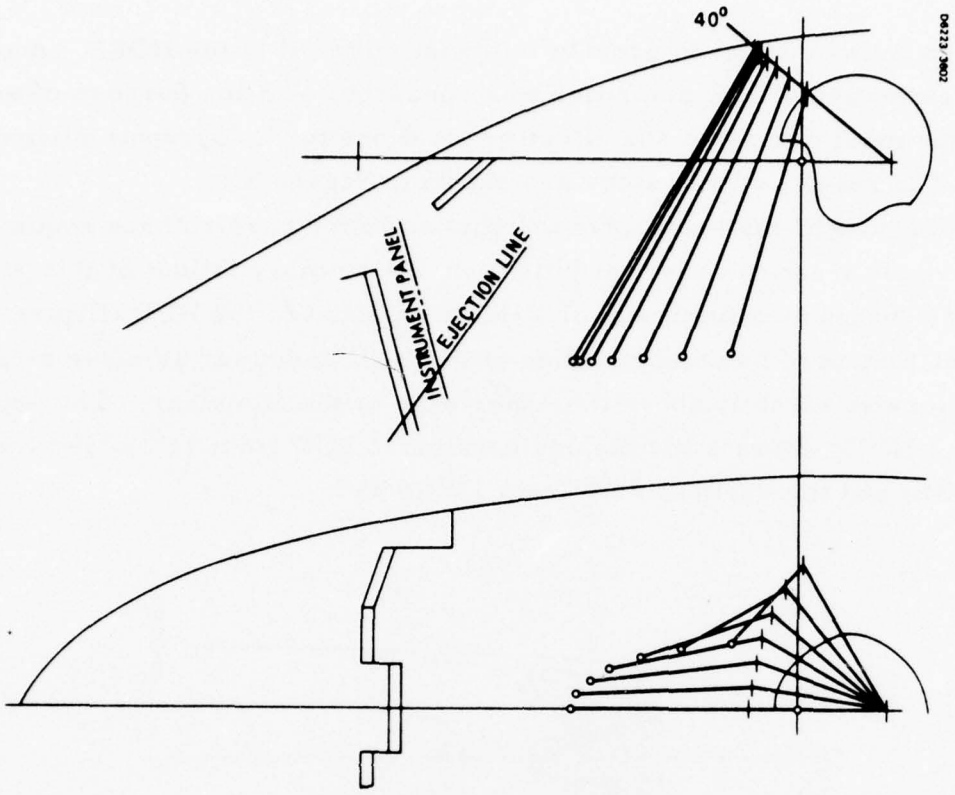


Figure 49. F-16 canopy reflections of 40° elevation lines of sight.

these graphical plots lies in the locus of end points of the symmetrically reflected rays. The end points were chosen to be the point where the reflected ray crosses the sill plane. A study of the plots reveals that symmetrically reflected rays off most portions of the canopy are directed towards the centerline of the fuselage and the nose of the aircraft. As the elevation angle is increased, the points in question move aft, but stay close to the fuselage centerline. The ideal positions for sources might be close to those end points, however, these points are not convenient locations for sources because they are in the middle of the operator. When the sources get displaced to the sill line, the angle between the symmetrical ray and the actual ray may be computed and the asymmetry evaluated for each choice of source location.

Canopy Considerations. It was evident early in the program that, due to the many cockpit physical constraints and optical problems, the entire canopy could not be considered as HOE placement territory, nor could enough sources

be located in the cockpit to provide information to all of the HOES. A study for determination of site priorities was conducted with the purpose of establishing the most desirable and effective locations for holographic element areas. The results of this study are shown in Figure 8.

The results of the study gave insights as to the performance requirements of the cockpit systems under investigation. A primary fallout of this study is that there should be a minimum of 3 HOEs adjacent to the HUD (Figure 50). One sight station to be on either side of the HUD combiner as close as possible and one located directly above the upper edge of the combiner. The application of these 3 HOEs expands the display horizontal FOV from 16° to 56° (assuming a 20° HOE) and the vertical FOV from 15° to 35°.

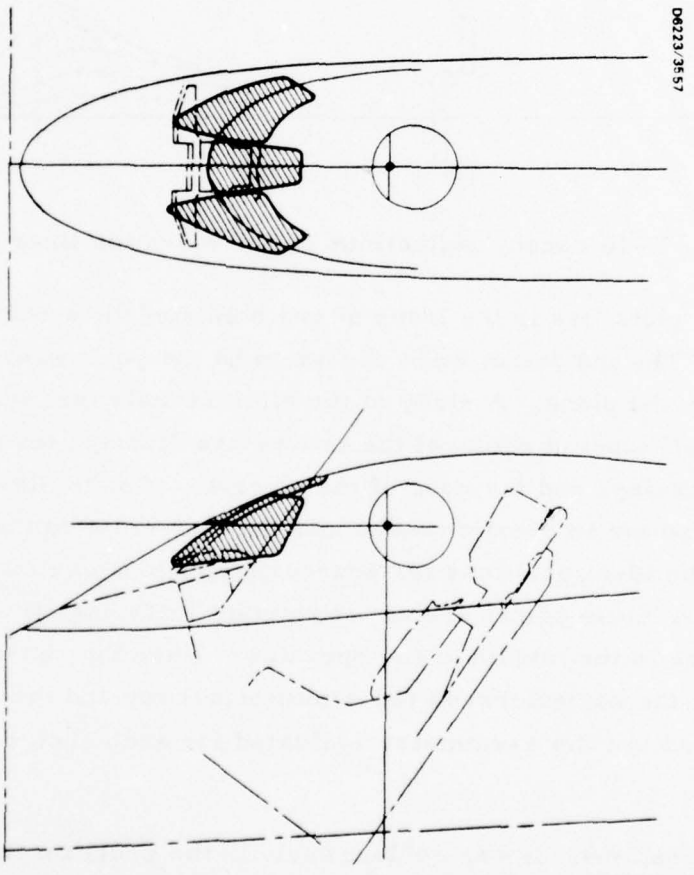


Figure 50. 3-hologram system in F-16 cockpit geometry.

For air-to-ground situations the wider the field of view, the better; hence, the logical expansion of the horizontally located HOEs around the periphery of the operator's visual field. Thus, a "bare bones" approach to the problem would require at least the three HOEs mentioned above. The next stage would be the additional 2 HOEs around the periphery (Figure 51). Expansion beyond the 5 would act to fill in the upper forward quadrant with 2 more HOEs (Figure 52). A final HOE could be placed directly above the central HOE (Figure 53). It is questionable if this last HOE would be practical in the light of probably requiring a special projection source all its own.

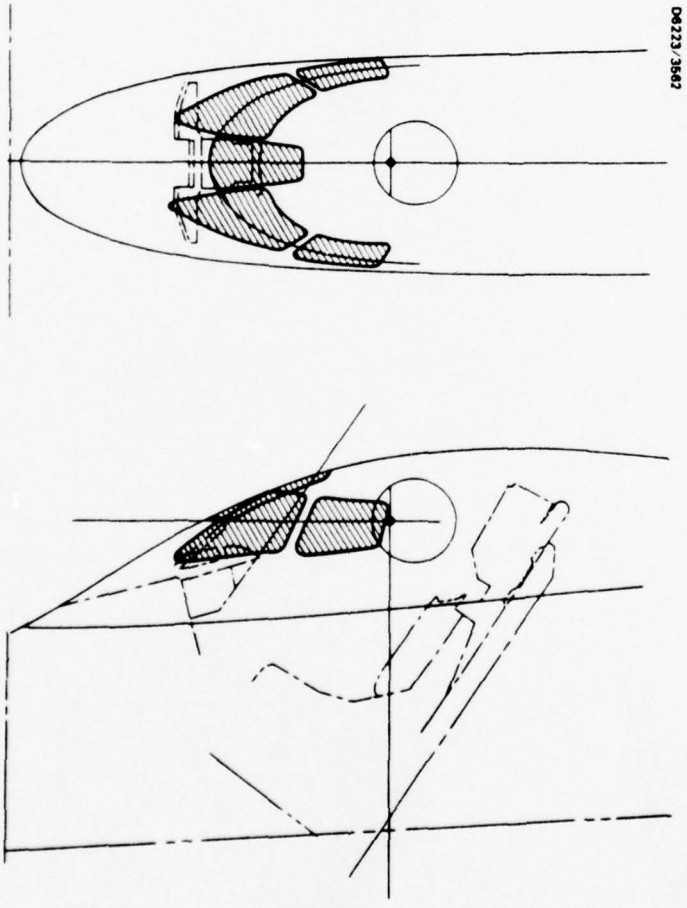


Figure 51. 5-hologram system in F-16 cockpit geometry.

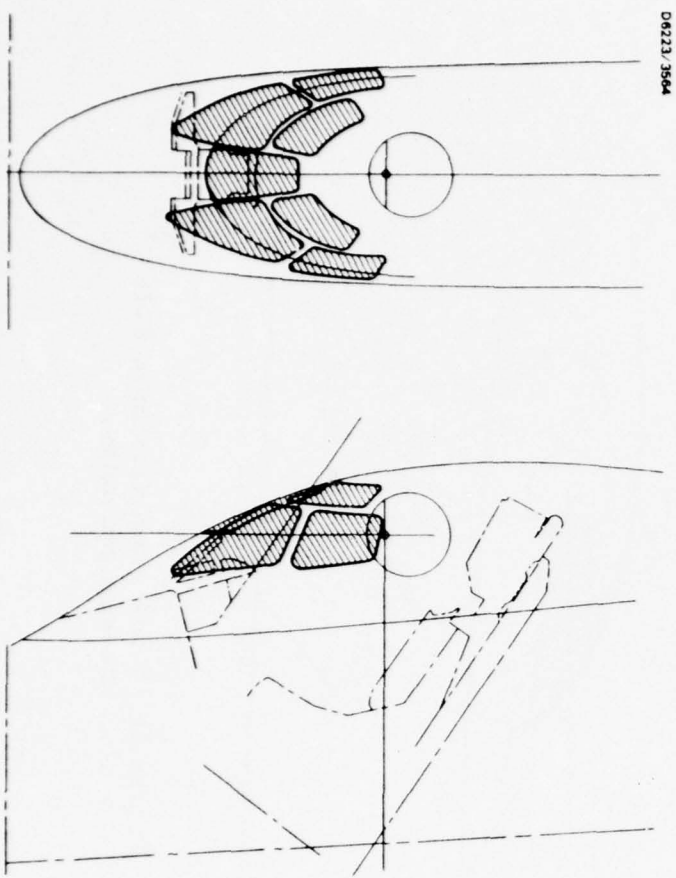


Figure 52. 7-hologram system in F-16 cockpit geometry.

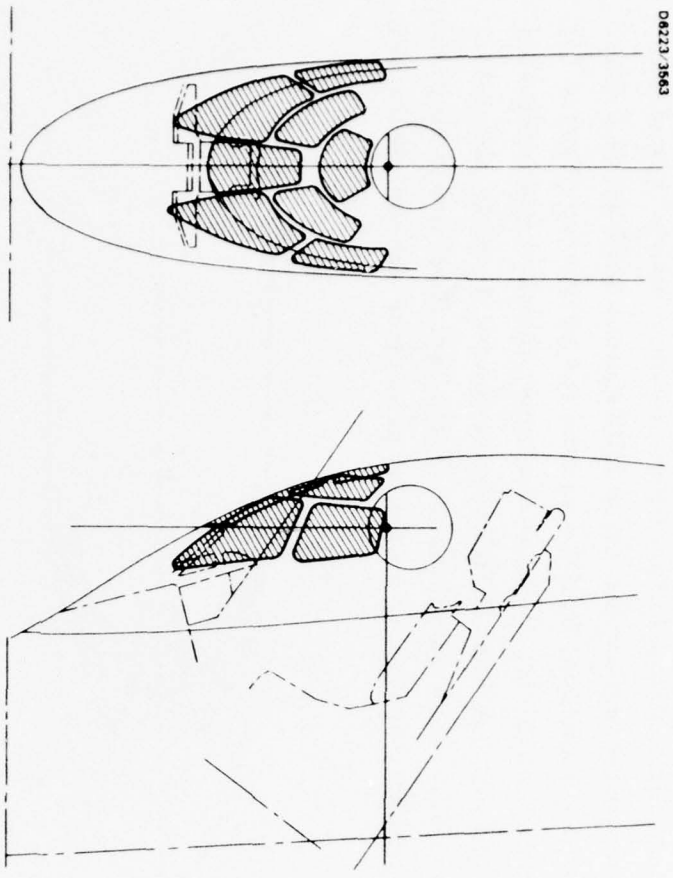


Figure 53. 8-hologram system in F-16 cockpit geometry.

An obvious question when regarding the illustrations showing the alternative HOE placements is why not provide another row under the horizontal group. Our human factors analysis indicated that from a first-pass target acquisition point of view, these additional HOE sites are not warranted.

The results of the study point out that employing more than 8 HOEs was in the area of rapidly diminishing returns and that, one could back off to as few as three HOEs and still effect a significantly improved operator capability.

5.1.2 Canopy versus Separate Substrate

The aircraft canopy has so far been the only considered surface for mounting the reflective holograms. In this subsection we will consider the suitability of the canopy as the substrate for holographic optic elements. The use of an alternate substrate will also be addressed and the tradeoffs between the two evaluated.

Initially, let us examine the function of a supersonic aircraft canopy. The design of such a canopy's shape is a result of minimizing aerodynamic drag, maximizing structural strength, operator protection and see-through visibility. No consideration has been given to optimizing optical performance in a reflective mode. In fact steps must usually be taken to avoid unwanted reflections off the canopy so that at night the pilot is not plagued by distorted reflections of his instruments in the canopy. A shroud is usually incorporated over the instrument panel to prevent this from occurring.

Two geometrical characteristics are of prime importance relative to reflection holograms. One is bend angle and the other is symmetry angle. For best optical performance, the total bend angle wants to be small — under 45 degrees — while the asymmetry wants to be minimal. The effect of excessive asymmetry is a high degree of chromatic dispersion, even with relatively narrow band sources. In order to achieve small bend angles and a low degree of asymmetry, the inclination of the holographic mounting surface to the eye must be nearly perpendicular (normal to surface is nearly parallel to line of sight). As the inclination of the surface normal to the line of sight exceeds about 30 degrees, a tradeoff must be made. In Figure 54 an off-axis situation is shown. A ray from A which is to be reflected to the eye at 0 has a small bend angle and a high degree of asymmetry. The ray from B which is to be reflected to 0 has reasonable symmetry but a larger bend

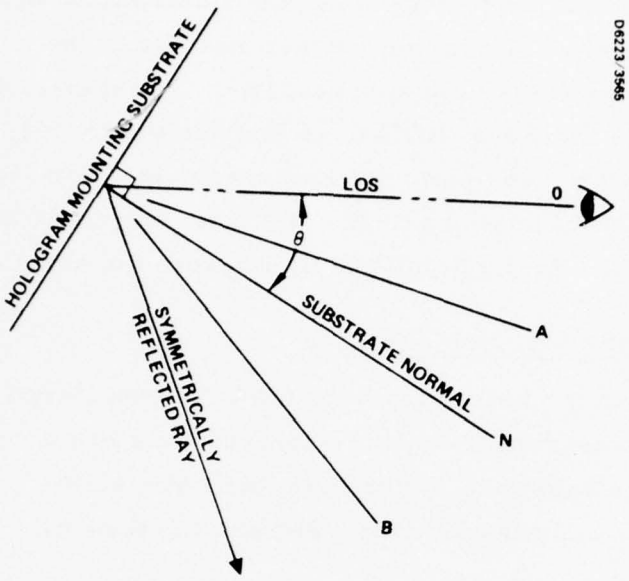


Figure 54. Canopy geometry consideration.

angle.* As the angle θ between the substrate normal and the LOS increases, the existence of an acceptable compromise location becomes less likely until an angle is reached where an acceptable solution cannot be achieved. The magnitude of this angle is a function of the system optical performance requirements. It is also possible that, even if the angle is not excessive, the placement of an image source at the optimum location may be anywhere from inconvenient to impossible. An examination of the canopy/design eye relationship for the F-16 aircraft yields the results which are presented in Figure 55. Azimuth line-of-sight directions between plus and minus 51° exceed 30° with the canopy normal. Angles less than $\pm 33^{\circ}$ in azimuth strike the surface at 45° or greater. In elevation the corresponding angles are 58° and 38°. On the basis of this information it may be concluded on a qualitative basis that the F-16 canopy is really not suitable for optimum application of HOEs in the forward areas of the canopy.

What type of surface, then, is suitable for this application in light of the above analysis? Figure 56 illustrates one proposed substrate surface geometry which might better lend itself to the application. The alternate surface

*For this geometry, there may be a compromise position which will satisfy the system's specific requirements.

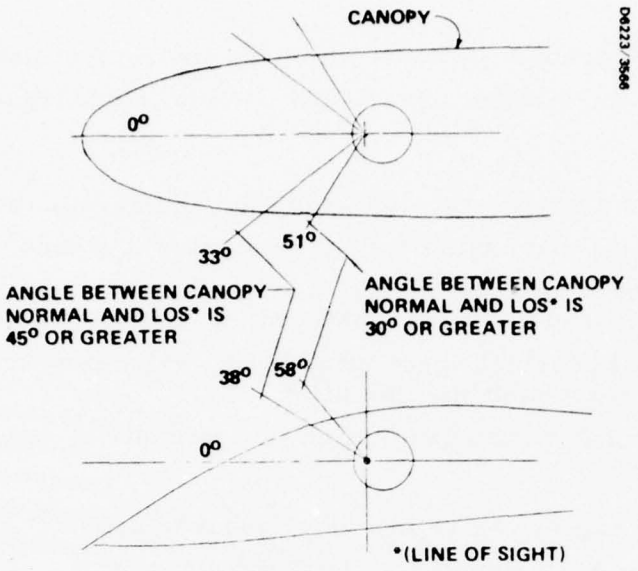


Figure 55. Examination of design eye/ canopy geometry.

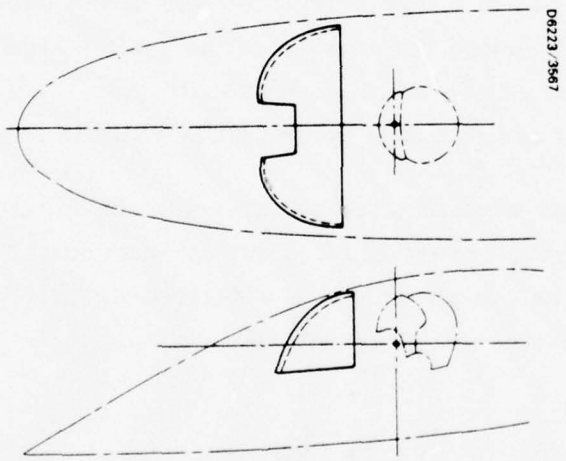


Figure 56. Example of alternate substrate installation.

geometry is a complex figure approximating a toric with a much stubbier profile than the original canopy. The alternate substrate has a cutout around the HUD combiner to prevent physical and optical interference with the instrument. The curvature is relatively flat in front of the operator and is faired into the regular canopy at the sides to move the edge line as far back as

possible. The substrate will mount off of the instrument panel hood and will not encroach over the ejection line. It has several advantages over the other surface:

a. Conjugate distances are shorter, thus holograms may be smaller.

b. Bend angles and asymmetry are considerably less.

c. The option of placing all image sources behind the head rather than on the sill leads to a more integrated, compact system.

d. Visual and physical obstruction by the various sources is minimized with the sources behind the pilot.

e. HOE fabrication and lamination to its substrate may be considerably simplified.

As one might expect, there are also disadvantages related to a separate substrate which must be weighed. These are:

a. Distortion or degradation of the see-through characteristics of the canopy.

b. The existence of a line along the edge of the substrate.

c. Possible unwanted reflections of the pilot's face and uniform.

d. Cost of fabrication and installation.

e. Loss of access to space behind HUD while in flight.

Conclusion. It is not evident whether the separate substrate is a reasonable alternate in light of the associated cockpit alterations. The study will, therefore, not pursue the alternate as a serious design baseline, but just address the existence of the alternate route should it develop into a realistic approach.

5.2 OPTICAL DESIGN CONSIDERATIONS

5.2.1 Summary of Reflection HOE Parametric Study

Cockpit geometry considerations strongly influence the type of holograms that can be considered for the canopy display. This strong influence arises for two reasons; first, the canopy itself is the substrate for the holograms. Second, very strong limitations exist on which part of the space inside the canopy can be utilized for lens systems and the image sources. Furthermore, the large bend angle associated with the canopy orientation tends to limit the vertical pupil height obtainable with the standard pupil hologram approach.

These considerations led us to a parametric study of image holograms, which are characterized by a large pupil size and a relatively small field of view. The construction geometry for an image hologram is shown in Figure 57, which shows a cross-section of a typical image hologram geometry. The nominal eye location for the user is at the origin of the $Y_p Z_p$ coordinate system, with the user's line of sight along the positive Z_p axis. A hologram is located a distance d away from the user's nominal eye location. The hologram tilt angle Ω is the angle between the hologram substrate normal and

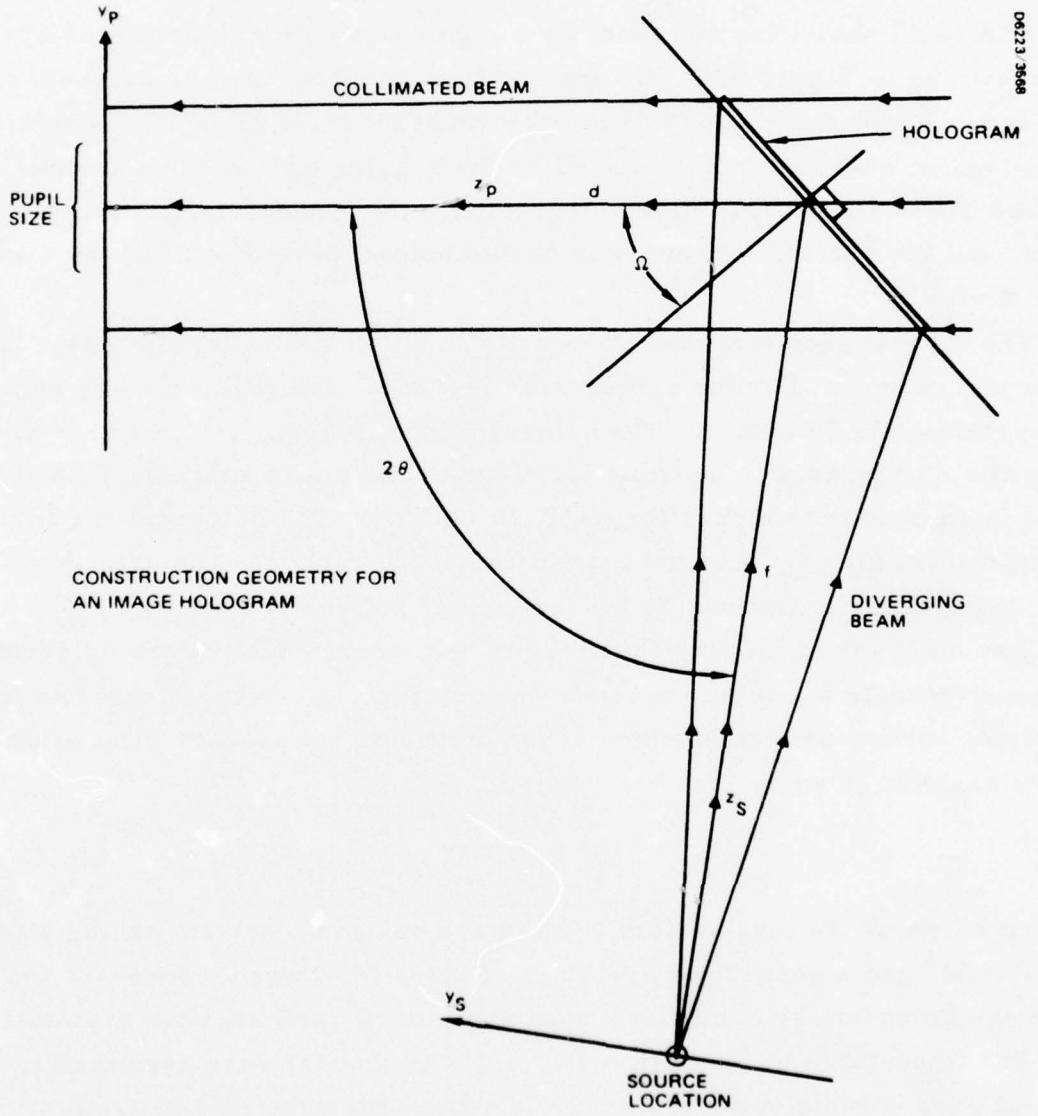


Figure 57. Construction geometry for an image hologram.

the user's line of sight at the center of the field of view. The hologram bend angle 2θ is the angle between the line of sight and the line connecting the center of the hologram substrate to the center of the image source at the origin of the $Y_s Z_s$ coordinate system. The image source is located at a distance f from the center of the hologram substrate.

The image hologram is a reflection hologram and is fabricated with one construction beam diverging from the center of the image source and the other construction beam coming from infinity along the line of sight direction. The distance f is therefore the nominal hologram focal length.

Figure 58 shows the typical system configuration for an image hologram fabricated as in Figure 57. The angular field of view, $2\theta_F$, is determined by the size of the image source and the hologram focal length f. The size of the hologram aperture is determined by the angular field of view and the desired useful pupil area. The hologram is a thick phase reflection hologram, and the efficiency properties of this hologram tend to limit the useful field of view.

The cockpit geometry determines the possible values for the image hologram parameters. For the canopy area just above the HUD, the eye relief d is approximately 20 inches. The hologram focal length, f, is the distance from this canopy area to possible locations of the image source. This distance is nominally 25 inches for the F-16 cockpit. The hologram tilt angle Ω is determined primarily by the orientation of the canopy. The hologram bend angle 2θ is determined by the location of the image source.

The interplay of these parameters is best represented by the hologram asymmetry angle Ψ, which we define here as the angle between the hologram substrate normal and the bisector of the hologram bend angle. The asymmetry angle is given by

$$\Psi = \theta - \Omega$$

Figure 59 shows a cross section of an image hologram system having a bend angle of 80° and a positive asymmetry. Figure 60 shows a cross-section of an image hologram system with a bend angle of 80° and negative asymmetry.

The importance of the asymmetry angle is that for zero asymmetry, the central rays of the display system reflect from the substrate as from a

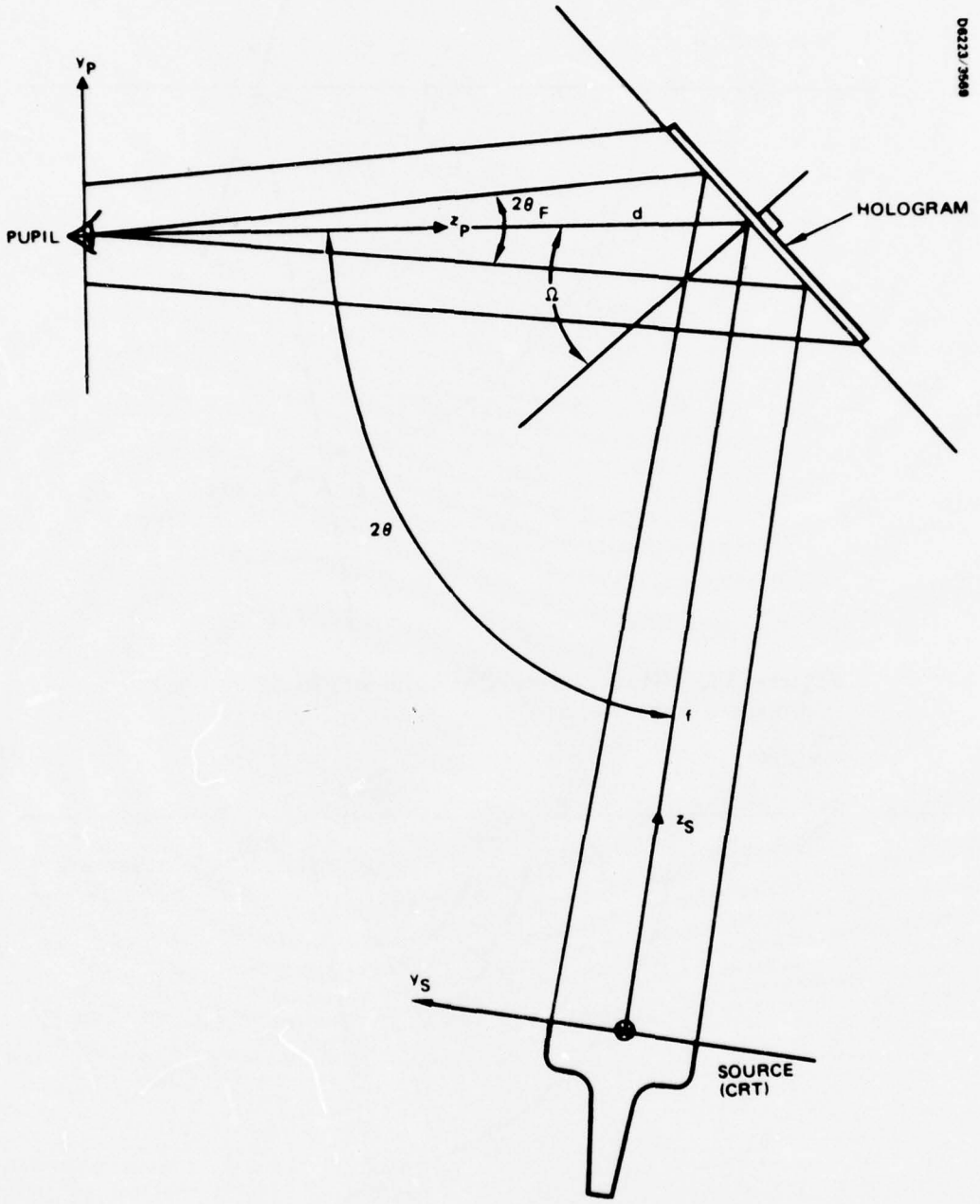


Figure 58. Typical system configuration for an image hologram.

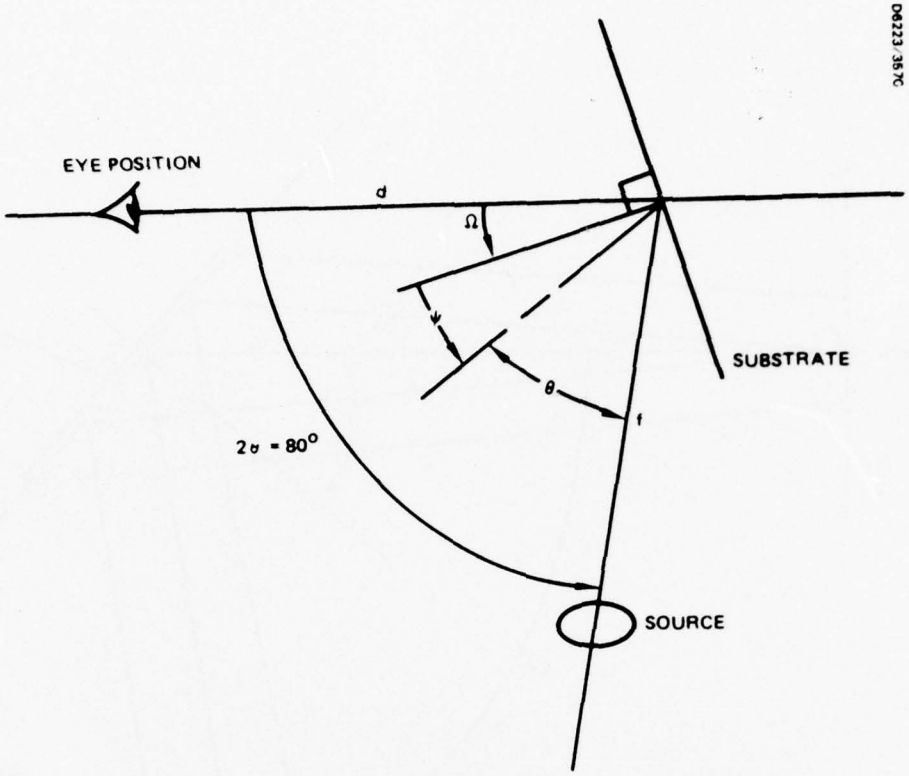


Figure 59. Illustration of a bend angle of 80° with positive asymmetry.

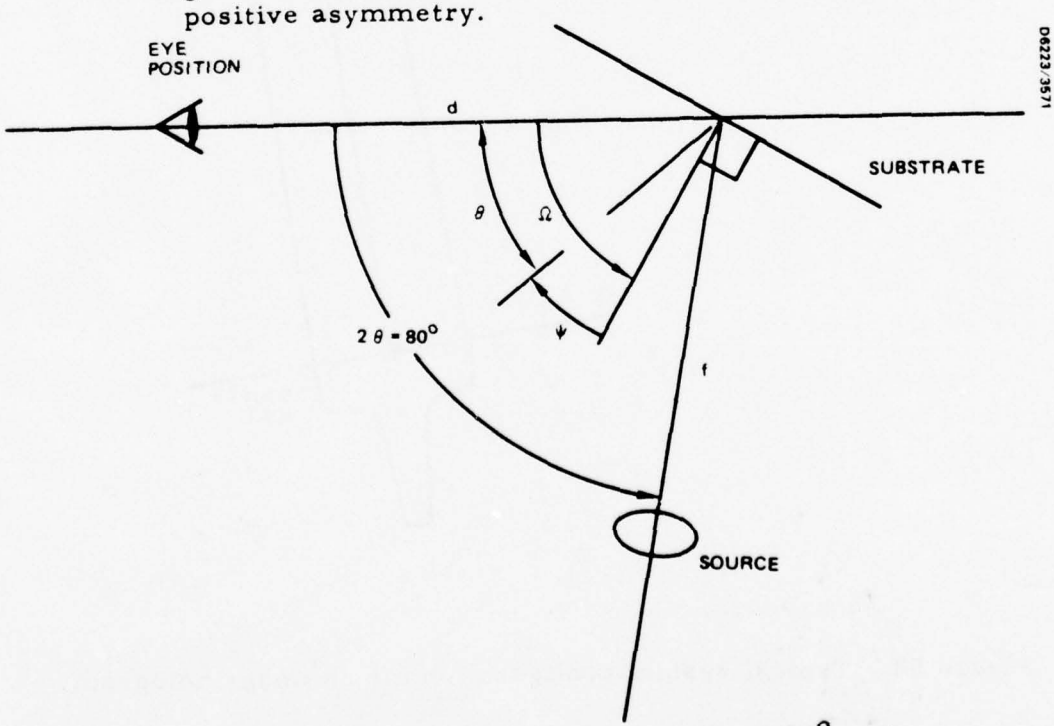


Figure 60. Illustration of a bend angle of 80° with negative asymmetry.

mirror. For zero asymmetry there is no surface grating component at the center of the hologram and therefore no angular dispersions.

The purpose of the image hologram parametric study was primarily to determine the image and efficiency characteristics of image holograms with varying asymmetry angles. The F-16 cockpit geometry produces holograms with negative asymmetry angle, such as that shown in Figure 60. In particular, for an image source located behind the pilot's backrest, the image hologram has a small bend angle and a large negative asymmetry. This situation is illustrated in Figure 61.

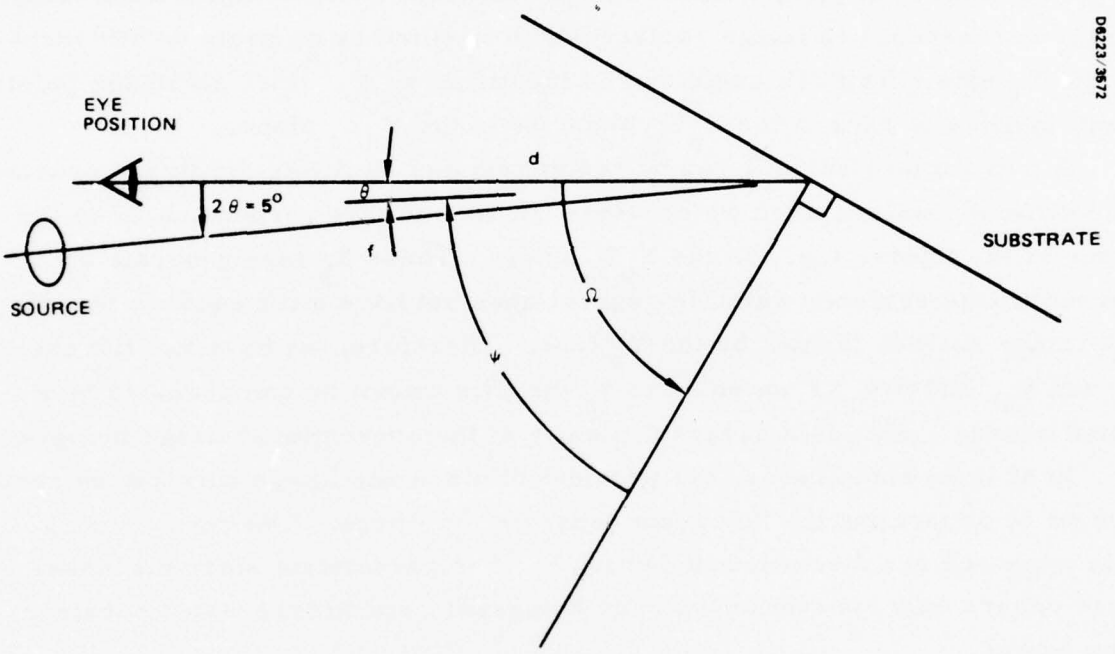


Figure 61. Illustration of a bend angle of 5°, giving large negative asymmetry.

There are two key features of the parametric study results discussed in the next section. The first is that for moderate to large asymmetry angles, the image hologram efficiency does not overly restrict the angular field of view. The field of view does tend to be limited by the size of the image source; for example, for a 4-inch diameter CRT, the typical image hologram provides a 6 to 7° full angular field of view. The second key result is that

image tilts are a rather severe problem for the conventional image hologram. The following discussion introduces the concept of image tilts.

The imaging characteristics of the hologram are such that a tilted image source is required in order to keep the image in focus at infinity. This situation is illustrated in Figure 62, which indicates the image characteristics for bundles of rays in the plane of the figure. Two such bundles of three rays each are shown coming through the pupil area in a reverse direction at the limits of the vertical field of view. Bundle 1, with single arrows on the rays, is focused at point 1 on the image surface. Bundle 2, with two arrows on the rays, is focused at point 2 on the image surface. A collection of such image points corresponds to image surface which is tilted by an angle ϕ with respect to the Y_s axis. This tilt angle can be identified as ϕ_y, since all image points from bundles of rays in the Y_pZ_p plane lie in the Y_sZ_s plane.

A tilted image surface can be accommodated by tilting the image source. The difficulty arises when we consider bundles of rays perpendicular to the plane of the figure, i.e., in the X_pZ_p plane. These X_p fans generate a second image surface, which in general does not have a tilt equal to that of the image surface formed by the Y_p fans. Therefore, we have two tilt angles, ϕ_y and ϕ_x, and if ϕ_u is not equal to ϕ_x the tilts cannot be compensated by a tilted source. This is a severe difficulty of the conventional image hologram.

In at least some cases, the problem of disparate image tilts can be corrected by aberrating the hologram construction waves. The results using this approach are discussed in Section 6. The parametric study discussed here covers only conventional image holograms without aberrated construction beams.

5.3 CANOPY DISPLAY PERFORMANCE

Before considering the performance of individual image holograms, we breifly consider here the characteristics of display systems that utilize multiple image holograms to cover an extended field of view. In general, varying distortion characteristics and variable magnifications make it difficult to provide accurately aligned imagery between two separate display components. To the extent that such alignment is not possible, we require that two different display elements do not provide imagery in the same part

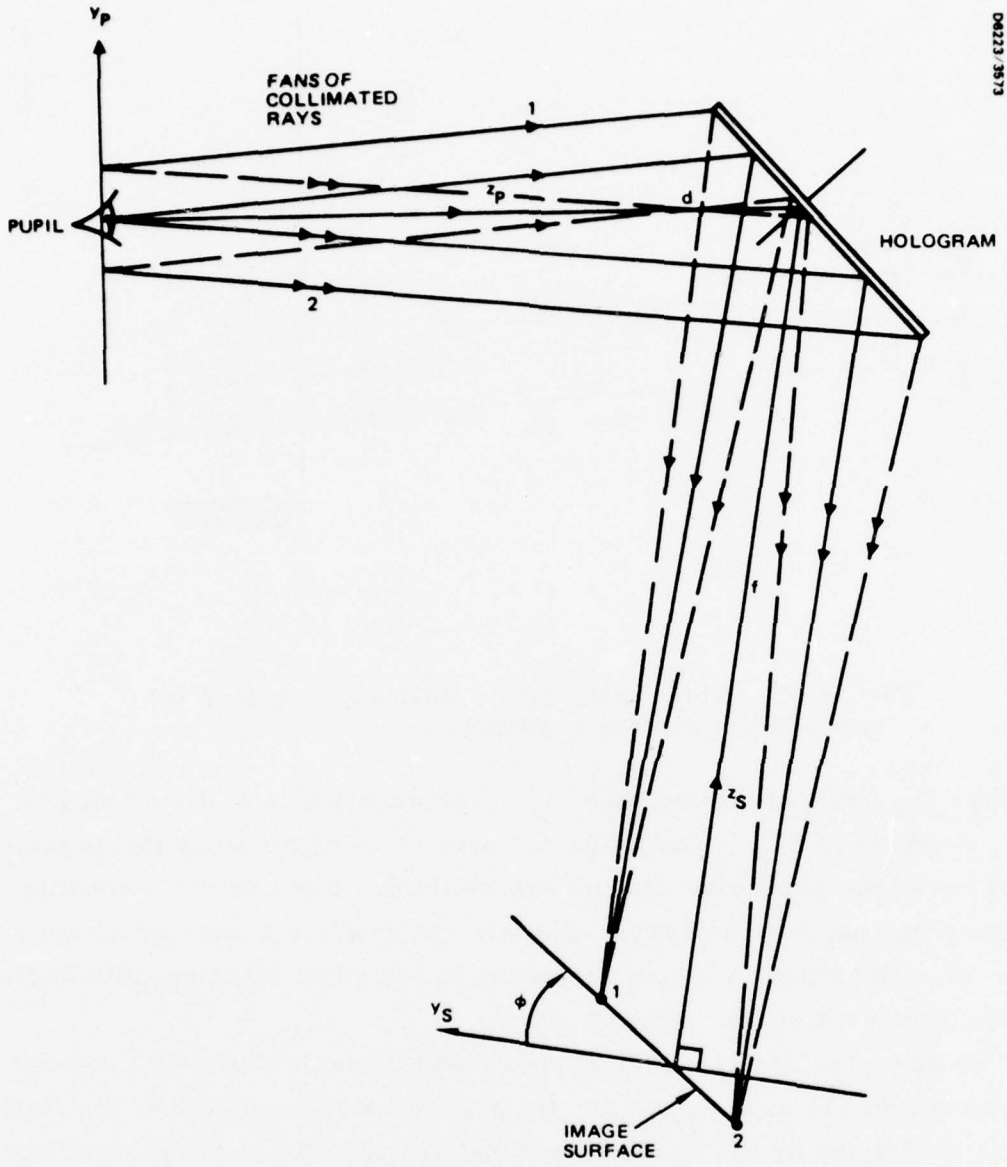


Figure 62. Illustration of a positive tilt of the y-fan, vertical field image surface.

of the angular field of view of the system. We show here that this requirement for independent display segments produces gaps in the angular field of view. Furthermore, there are minimum spacings required between independent sources in order to avoid overlapping of their angular fields of view.

Figure 63 illustrates the field gap required for independent display segments. This figure indicates a cross-section of a display segment with a

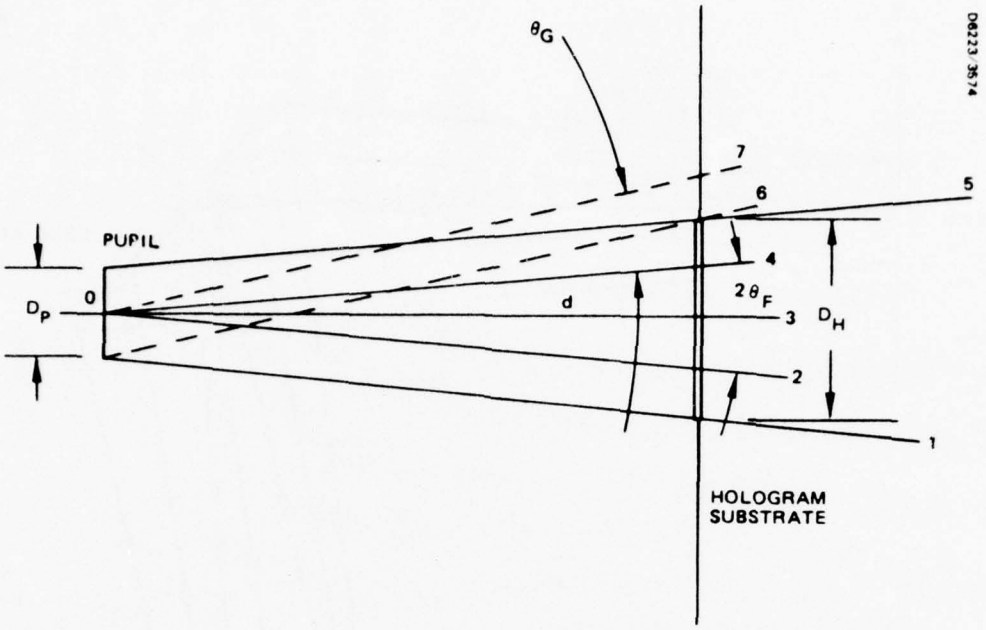


Figure 63. Illustration of the field gap required for independent display segments.

pupil size D_P and a hologram size D_H. The angular field of view of this display segment is $2\theta_F$. The hologram size is determined by the angular field of view, the pupil size and the eye relief d. The limiting rays that determine the required hologram size are ray number 1 and ray number 5 in Figure 63. The chief rays corresponding to the same limiting field angles are rays number 2 and 4, respectively.

If we now consider the field of view that can be provided by a second hologram above the area D_H on the same substrate, we note that the field angle is restricted by the requirement that the ray comes from above the first hologram area and still reaches the bottom of the desired pupil D_P. This ray is the dashed line number 6 in Figure 63. The corresponding chief ray is dashed line number 7. The angle between chief rays number 4 and number 7 is therefore a portion of the field of view that cannot be filled by these independent display segments. This is also the angle between rays 5 and 6, which is easily visualized as the angle, subtended by the pupil, at a distance equal to the eye relief d. The gap angle, θ_g is therefore given approximately in radians as D_P/d. This gap angle can be reduced if we permit vignetting of the pupil near the edges of the field of view.

Figure 64 illustrates the source gap required to prevent multiple images from the same hologram. The top of Figure 64 indicates the idealized geometry of hologram A with eye relief d_A in focal length f_A. This hologram covers a total field of view of $2\theta_A$, from an image source, source A. The lower part of Figure 64 indicates the geometry of the adjacent display segment provided by hologram B. This display segment has eye relief d_B, focal length f_B, and covers a full angular field of $2\theta_B$ separated from a field of view by the field gap angle θ_G. A source gap D_G is required to keep the B image source from being imaged to the user through hologram A. This gap can be determined approximately by drawing the line connecting the intersection between holograms A and B to the lowest part of the desired pupil. The chief ray parallel to this line is then drawn through the center of hologram A. In order to prevent multiple images source B must be entirely above this chief ray. Note that this chief ray is parallel to the lower limit of the B field of view.

This discussion is meant only to indicate the types of considerations necessary in using multiple display segments to cover an extended field of view. A specific configuration must be determined based on tracing of actual rays in the design process. Furthermore, it is quite possible to use the efficiency characteristics of the holograms to aid in eliminating interference between display segments.

5.3.1 Optical Efficiency Across the Field of View

The hologram diffraction efficiency as a function of the location in the field of view is determined by tracing chief rays at various parts of the field of view and calculating the diffraction efficiency based on Kogelnik's coupled wave theory for thick phase reflection holograms. Only the vertical field angle, i.e., rays in the $Y_p Z_p$ plane of Figure 64, are explicitly considered because the diffraction efficiency is relatively insensitive to angular offsets in the perpendicular direction.

Vertical field angles from -5° to $+5^\circ$ were considered. The hologram film was assumed to have a thickness t of 10 micrometers. Typical results are shown in Figure 65, for a vertical cylinder hologram substrate with a tilt angle of 50°, bend angle of 65° and a substrate radius of 13.8 inches.

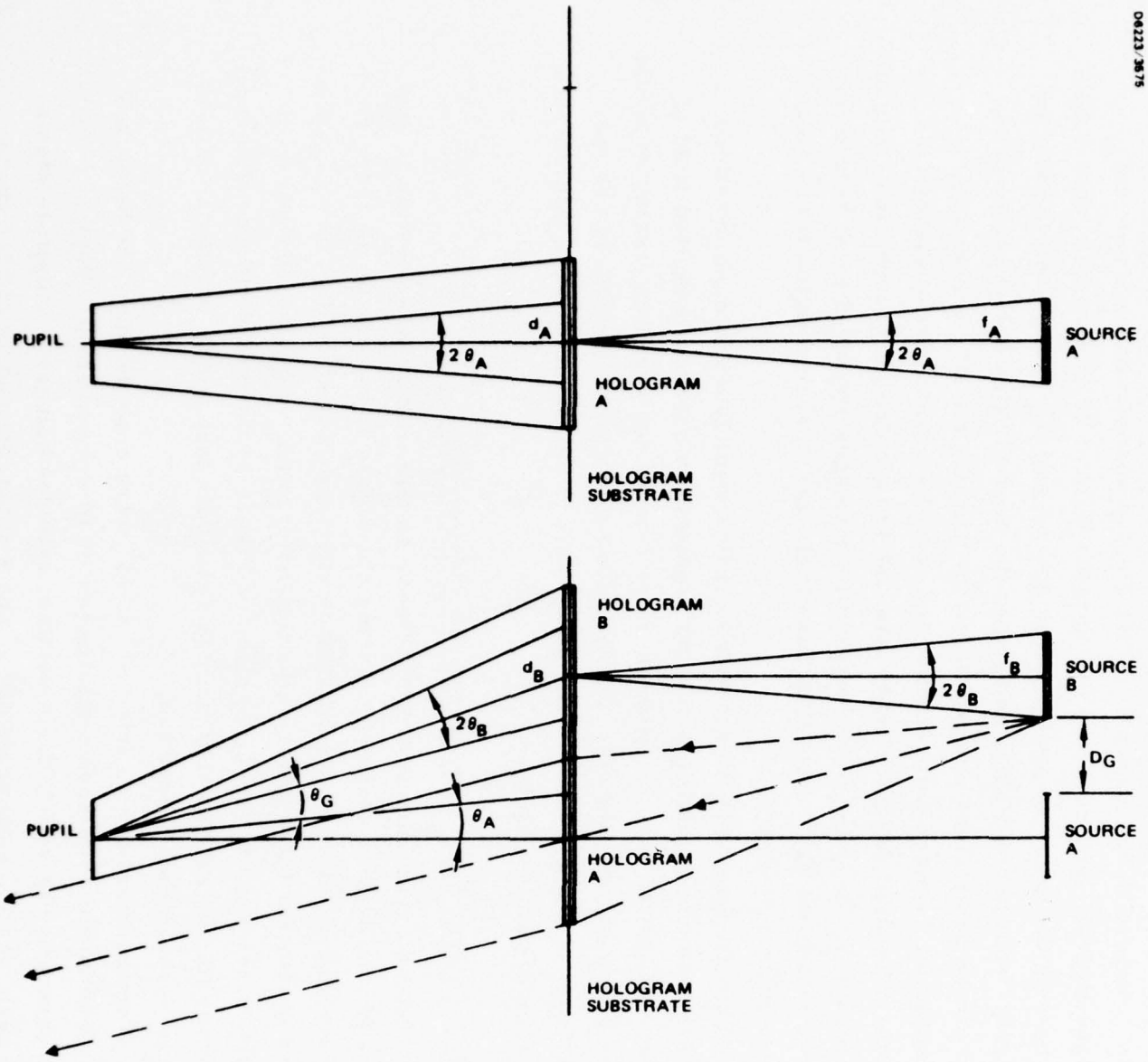


Figure 64. Illustration of the source gap required to prevent multiple images.

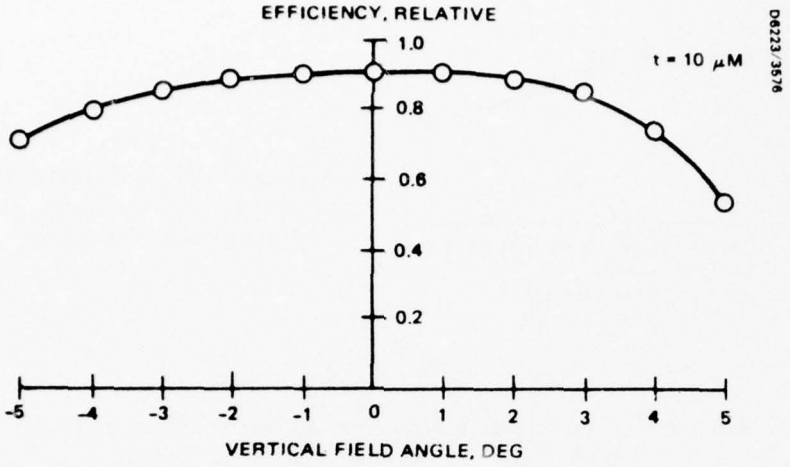


Figure 65. Chief ray efficiency for a vertical cylinder hologram substrate with $\Omega = 50^{o}$, $2\theta = 65^{o}$, d = 20 in., f = 25 in. and a substrate radius of 13.8 in.

Diffraction efficiency was also calculated for rays at various locations in the exit pupil. These results showed that the optical efficiency for desired pupil sizes of approximately 4 in. diameter, did not vary appreciably across the exit pupil, and were determined by the efficiency of the chief ray.

The results of the diffraction efficiency calculations are shown in Figures 66 and 67. We define a vertical field size as the total angular field of view between the points at which the diffraction efficiency drops to one half its peak value. In Figure 66 this full width at half maximum (FWHM) vertical field size is plotted as a function of asymmetry angle or several bend angles. These results show that for most negative asymmetry angles, the vertical field size exceeds 10 degrees.

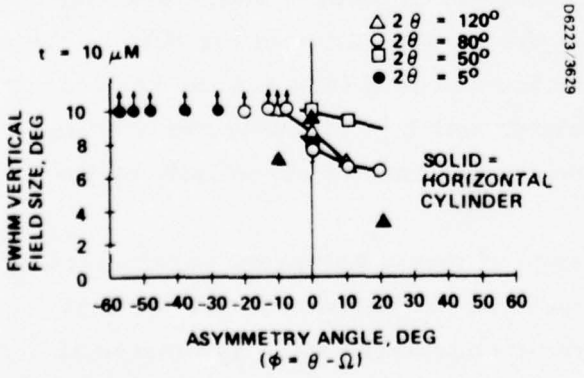


Figure 66. Vertical field size as a function of asymmetry angle.

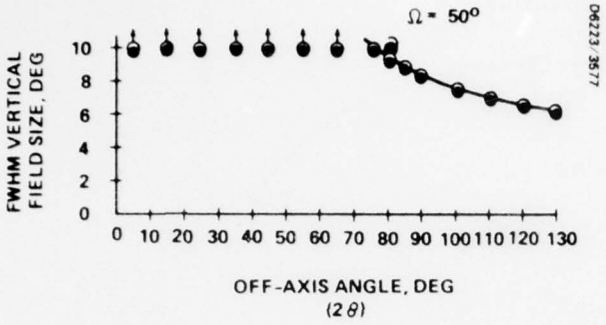


Figure 67. Vertical field size as a function of bend angle for hologram tilt of 50°.

Figure 67 shows the vertical field size as a function of hologram bend angle for a tilt angle of 50°. These results show that diffraction efficiency is not a substantial problem.

5.3.2 Image Quality

Image quality in the canopy display is specified in terms of resolution, distortion, collimation error, and binocular disparity. Since the user's eye pupil is so much smaller than the typical system pupil, the perceived resolution is limited only by chromatic dispersion and the image source spectral line width. The image hologram often has substantial distortion, which would be removed by a compensating distortion in the CRT scan characteristics. Collimation errors cause a wandering of image location as the user's eye scans the system exit pupil area. Horizontal collimation errors lead to binocular disparity, i.e., a difference in image location for the two eyes. Since the eyes are normally spaced in the horizontal or X direction, binocular disparity is determined primarily by the image errors of X fans in the pupil.

Image errors for image holograms are quite small, with the possible exception of distortion, as long as the image is in focus. Therefore, the consideration of image quality becomes the consideration of the tilts on the image surfaces corresponding to the horizontal or X fans and the vertical or Y fans. In particular, binocular disparity, which is probably the limiting factor in image hologram image quality, is determined essentially by the horizontal fans of rays.

Image quality was studied for a range of image hologram parameters by tracing fans of rays in the X and Y directions for horizontal and vertical field angles from -5° to +5°. All systems considered were symmetrical

about the Y, Z, plane, and therefore image surface tilts in the X, Z plane are inherently zero. Therefore, we are concerned only with the image surface tilts in the Y, Z plane section.

Figure 68 shows image points in the Y, Z plane determined by tracing vertical (or Y) fans of rays and horizontal (or X) fans of rays for vertical field angles from -5^{o} to $+5^{o}$. The results show the typical field curvature and distortion as well as the field tilts. This particular case, with a field tilt disparity of approximately 90^{o}, emphasizes the difficulty of achieving good collimation in both the vertical and horizontal directions. As shown in Figure 68 the vertical fan image surface tilt is about -30^{o}, while the horizontal fan image surface tilt is about +70 degrees.

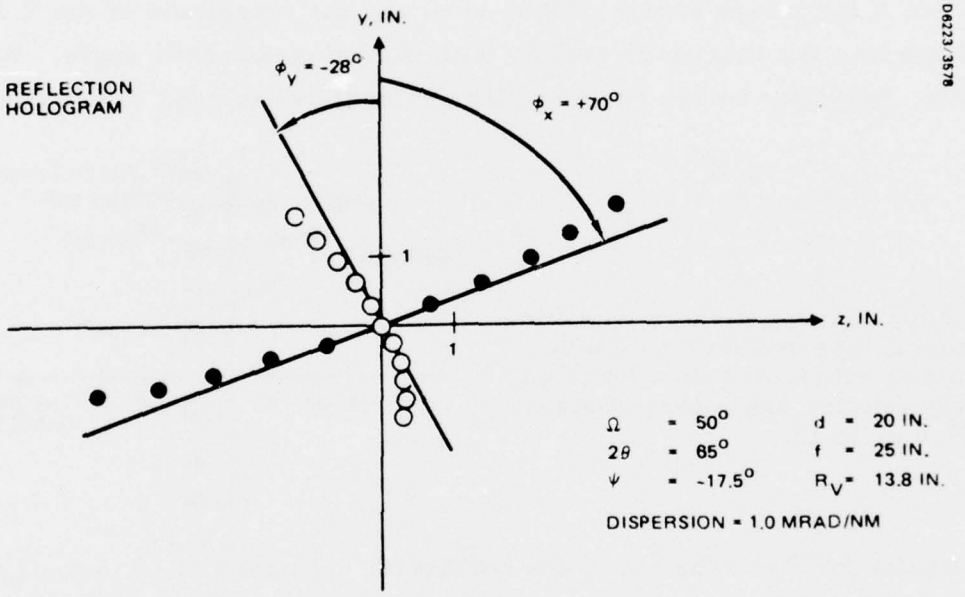


Figure 68. Image surfaces for a typical image hologram on vertical cylinder substrate.

In order to obtain a good understanding of the image surface tilt characteristics of image holograms, we considered image holograms on flat substrates and cylindrical substrates with the cylinder axis both horizontal and vertical. Figure 69 shows the image surface tilts for image holograms on flat substrates as a function of asymmetry angle. For flat substrates, the X fan image surface tilt is zero. The Y fan image surface tilts are

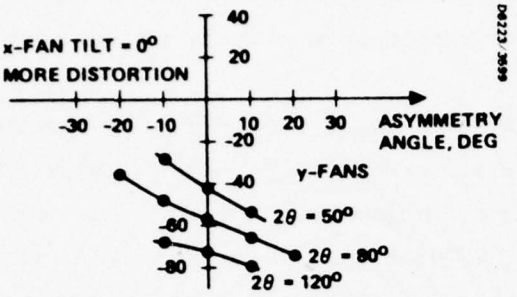


Figure 69. Image surface tests for image holograms on flat substrates as functions of asymmetry angle

positive and are larger for larger bend angles. Also the tilts are larger for positive asymmetry angles, and smaller for negative asymmetry angles.

Similar results are shown in Figure 70 for image holograms on horizontal cylinder substrates. In this case, the cylinder radius is 16 in. Again the X fan image surface tilt is zero and the magnitude of the Y fan image surface tilt increases rapidly with the hologram bend angle. Now, however, the Y fan image surface tilts are negative instead of positive.

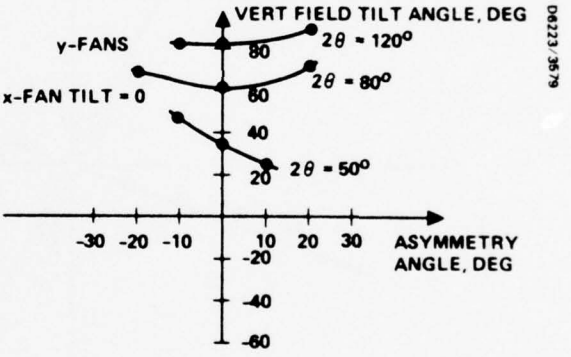


Figure 70. Image surface tilts for image holograms on horizontal cylinder substrates as a function of asymmetry angle for substrate radius of 16 in.

The results for flat substrates and horizontal cylinders of 16 in. radius indicate that for a somewhat larger horizontal cylinder radius the Y fan field tilts should also be zero, giving alignment of both X fan and Y fan image surfaces at zero field tilts. This is verified in Figure 71, which shows the vertical fan image surface tilt or image holograms on horizontal cylinder substrates of different radius. For a radius of approximately 30 in., the vertical fan image surface tilt angle is zero, so that there is no disparity in the image surface tilts. This particular case is not usable with the F-16 canopy geometry. However, if a separate substrate could be considered this would be a very promising approach.

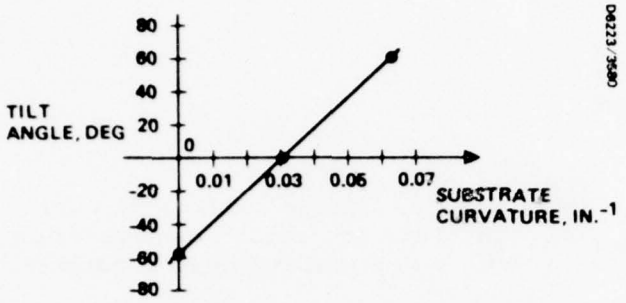
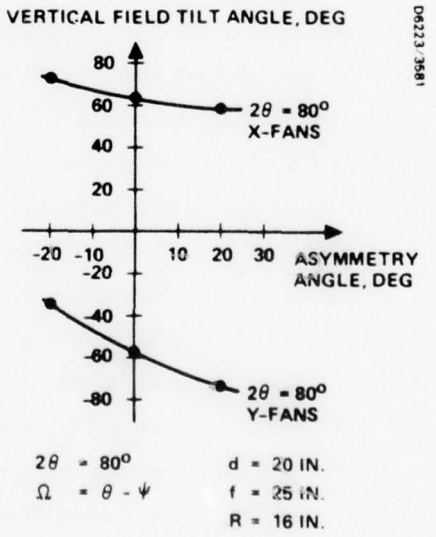


Figure 71. Vertical fan image surface tilt for image holograms on horizontal cylinder substrates of different radius.

The canopy areas of primary interest in the F-16 cockpit correspond closely to vertical cylinder substrates. Figure 72 shows the image surface tilts for image holograms on vertical cylinder substrates as a function asymmetry angle, for a hologram bend angle of 80°. This corresponds to source locations on the sill and forward in the cockpit area. In this case the cylinder radius is 16 in. With the vertical cylinder substrates the horizontal fan image surface tilt is no longer zero. Unfortunately, where the range of parameters covered by Figure 72 the horizontal fan surface tilt is in the positive direction while the vertical fan image surface tilt is in the negative direction, leading to very large disparities in the image surface tilt angles.

Figure 72. Image surface tilts for image holograms on vertical cylinder substrates as a function of asymmetry angle



A second promising configuration for image holograms in the F-16 cockpit places the image source to the side and behind the pilot's head. Figure 73 shows the image surface tilts for this "rear projector" configuration. In this case the vertical cylinder radius is 13.8 in., and the bend angle is 5°.

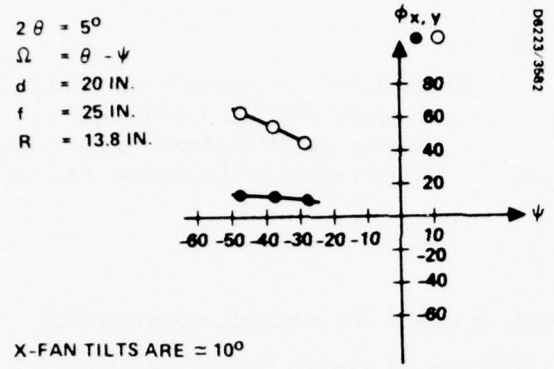
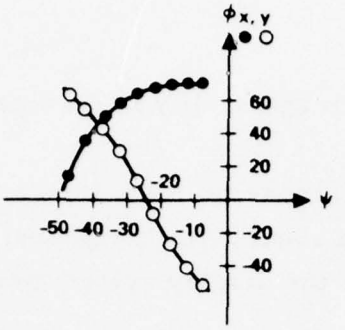


Figure 73. Image surface tilts for the "rear projector" configuration with a vertical cylinder substrate.

For this case, both image surface tilt angles are positive so that the disparity is substantially reduced. Furthermore, the X-fan image surface tilts are only about 10°, so that binocular disparity is minimized.

Since the most desirable canopy display areas in the F-16 cockpit correspond to a hologram tilt angle of 50° to 60°, we considered the case of varying bend angle and asymmetry angle holding the hologram tilt angle constant at 50°. The results are shown in Figure 74. The horizontal fan image surface tilt angle is zero for a bend angle of 0°, corresponding to a projector directly to the side of the pilot's head. The vertical fan image surface tilt angle is zero for a bend angle of approximately 50°, corresponding to an image source located on the substrate normal. For a bend angle of approximately 22°, the image surface tilt angles are equal. This forms a high image quality configuration without requiring aberration of the hologram construction beams. Unfortunately, this particular configuration is probably of limited utility in the F-16 cockpit geometry.

The image errors caused by the field tilts can be quantitatively studied by plotting ray intercept curves, giving in effect the variation of ray direction across the system exit pupil area. We performed this calculation for the image hologram for which image surface tilts were illustrated in Figure 68. This example had an image surface tilt disparity of about 90°. The ray intercept curves were calculated for an untilted source, for example, a CRT with a flat screen perpendicular to the image coordinate Z axis. The ray intercept curves were calculated for a positive vertical field angle of 3°. The results are shown in Figure 75, as angular errors as a function of location in the system exit pupil. The small deviations from the straight line

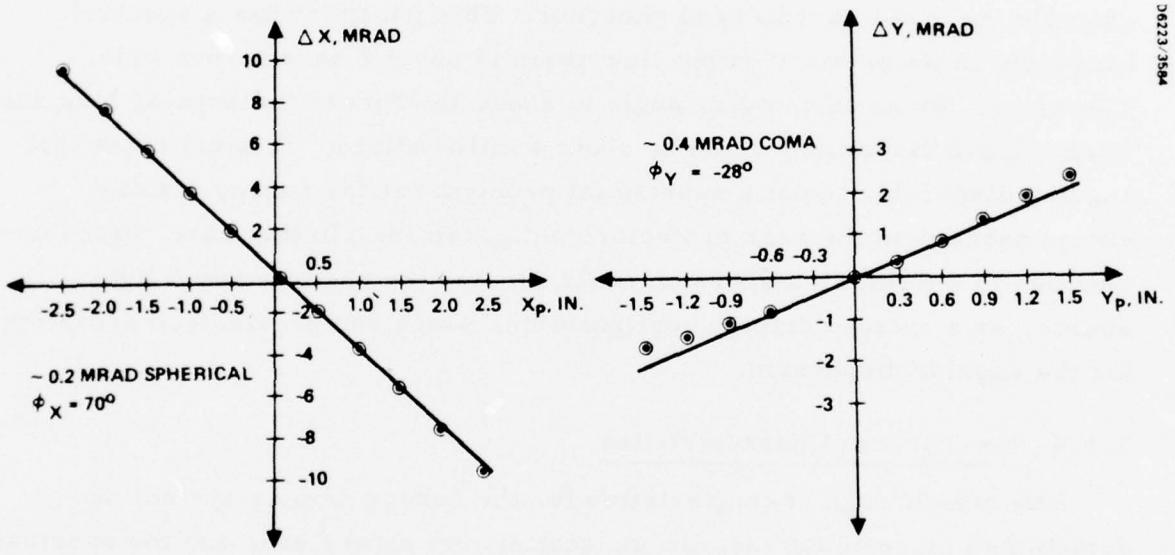


D6223-3583

Figure 74. Image surface tilts for a constant tilt angle of 50° with a vertical cylinder substrate.

- X-FAN TILT = 0 FOR $\theta \triangleq 0$
- Y-FAN TILT = 0 FOR $2\theta \triangleq 50^{\circ}$
- TILTS EQUAL (47°) FOR $2\theta \triangleq 22^{\circ}$ (THIS FORMS A "NATURAL" HIGH-IMAGE-QUALITY OPERATING POINT)

Ω = 50°
θ = $\Omega + \psi$
2θ = BEND ANGLE
R = 13.8 IN.
d = 20 IN.
f = 25 IN.



D6223-3584

Figure 75. Image errors for an untilted image source.

show that the aberration is essentially all due to the image surface tilt. The straight line slopes show opposite image surface tilts for the X and Y fans. The horizontal fan curvature of 70° causes binocular disparity of about 10 milliradians. The deviations from the straight lines indicate approximately 0.2 milliradian maximum spherical aberration in the horizontal direction and approximately 0.4 milliradian maximum coma aberration in the vertical

direction. This confirms the inherently high image quality in the image holograms for relatively small field angles.

We note that even with approximately 90° disparity in the image surface tilt angles, the image errors remain less than about 10 milliradians. The image errors remain relatively small because the display system has a relatively large f number.

5.3.3 Chromatic Dispersion

As previously indicated, the angular dispersion is zero for a symmetric configuration, i.e., an asymmetry angle of 0 degrees. The increase in angular dispersion for non-zero asymmetry angles is shown in Figure 76. These results can be interpreted by considering a particular image source, for example the P-43 narrow band phosphor. This phosphor has a spectral bandwidth in its primary output line which is about 2 nanometers wide. Therefore, for an asymmetry angle of about 35 degrees the angular blur due to chromatic dispersion would be about 4 milliradians. This indicates that angular dispersion is not a substantial problem for the canopy display, except perhaps in the rear projector configurations. In this case, excessive blur due to chromatic dispersion could require the use of a laser light source, or a relayed display configuration, which can provide compensation for the angular dispersion.

5.3.4 See-Through Characteristics

The see-through characteristics for the canopy display system are determined by residual absorption, scatter, spectral flare, and the spectral reflectivity bandwidth of the hologram. Residual absorption and scatter are functions of the hologram recording material. For the primary recording material, dichromated gelatin, residual absorption and scatter are minimal and quite acceptable.

Spectral flare is not an inherent problem with thick phase reflection holograms. However, through the recording of unwanted images caused by extraneous light existing in the exposure setup, spectral flare can be introduced. Elimination of spectral flare is therefore a matter of proper

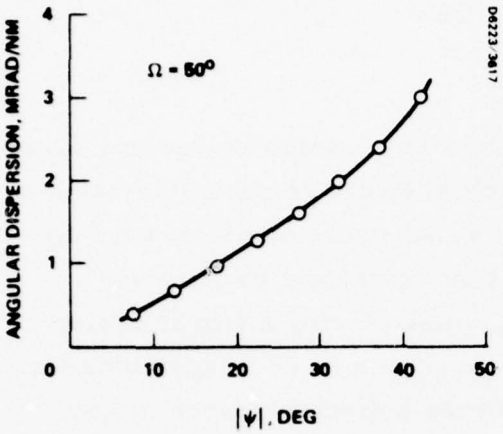


Figure 76. Chromatic angular dispersion as a function of asymmetry angle.

hologram recording techniques, which we have developed. We conclude that spectral flare should not be a substantial problem in the canopy display systems using reflection holograms on the canopy. However, the questions of spectral flare should be examined carefully as part of any further system development.

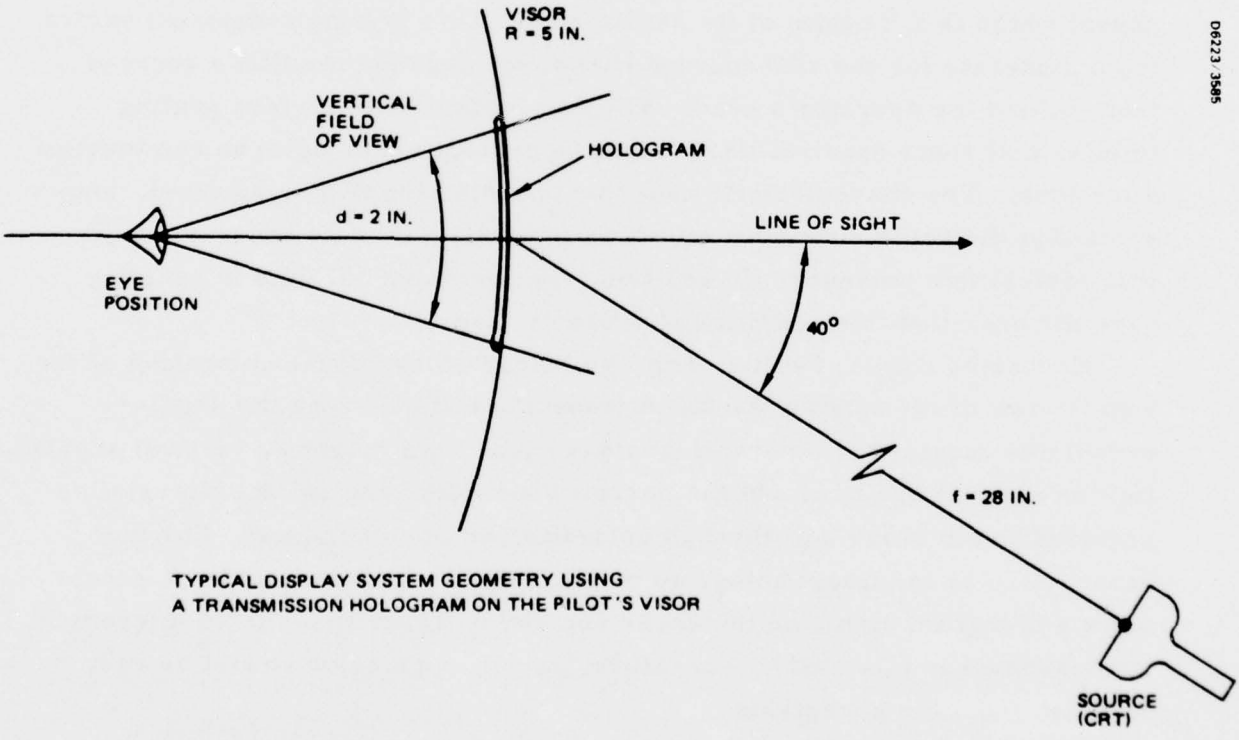
For the holograms described herein, there is a surface grating component which is a function of its asymmetry. This grating component varies from moderate for the sill-sourced HOEs, to large for the HOEs sourced from behind the operator's head. The existence of this surface grating implies that some spectral flare might be present under adverse sun location situations. The characteristic behavior of reflective HOEs, however, suggests that the rapid efficiency falloff as a function of angle and wavelength will combat this tendency. In addition, the operation of HOEs in practice have not exhibited this condition if properly made.

Excessive light reflection from the hologram can cause coloration of the user's view of the outside world. A tradeoff exists between the angular properties required to obtain adequate vertical pupil height or vertical angular field of view on one hand and the narrow bandwidth spectral characteristics required to minimize see-through coloration on the other hand. For the canopy display the image hologram optical efficiency characteristics should allow a hologram emulsion thickness somewhat larger than the 10 micrometers assumed in this study. Therefore, see-through color should be very minimal and quite acceptable.

5.4 SYSTEMS BASED ON TRANSMISSION HOEs

5.4.1 Configurations

We considered display systems based on transmission holograms located on the visor of the pilot's flight helmet. Such systems are possible using a transmission hologram with focal power or a transmission hologram that only introduces a deviation of angle rather than wavefront curvature. Figure 77 shows a typical display system geometry using a transmission hologram with focal power on the pilot's visor. This is an image hologram with a focal length of about 28 inches, assuming a display source on the sides of the F-16 cockpit instrument panel. No other optics are required in this system besides the transmission hologram on the visor; however, the collimation depends on the visor-CRT spacing. The wedge hologram system, which is not shown, has a focal length of infinity. In this case, the



TYPICAL DISPLAY SYSTEM GEOMETRY USING
A TRANSMISSION HOLOGRAM ON THE PILOT'S VISOR

Figure 77. Typical display system geometry using a transmission hologram on the pilot's visor.

system requires an auxiliary collimator lens. The collimation is independent of the visor-CRT spacing; however, the field of view and pupil are limited by the collimator aperture. Both of these systems have large angular dispersion and are especially troubled by strong spectral flare as will be discussed below.

The image quality for a typical transmission image hologram is indicated in Figure 78 which shows the cross-section of the image surfaces for a typical transmission image hologram. The image is characterized by large tilts of the image surfaces; however, the tilt disparity between the horizontal fan image surface and the vertical fan image surface is not large. This image surface tilt is so large that it would be difficult to accommodate it with conventional image sources.

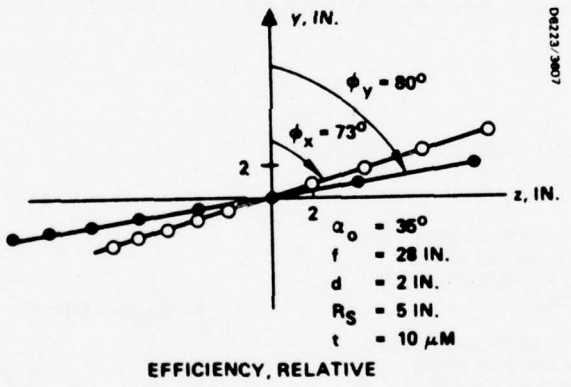


Figure 78. Image surfaces for a typical transmission image hologram.

Figure 79 shows the chief ray diffraction efficiency across the vertical field of view for the transmission hologram system shown in Figure 78. The FWHM vertical field size in this case is limited to about 5 degrees, so that the useful field size is small. This diffraction deficiency variation causes loss of image for visor movement of greater than ±5 degrees vertical.

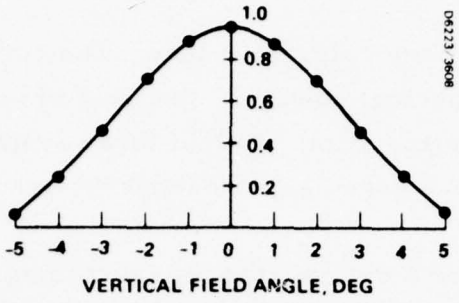


Figure 79. Chief ray diffraction efficiency across the vertical field of view for a typical transmission hologram.

Figure 80 shows the distortion characteristics of a wedge transmission hologram of similar configuration. This system shows good linearity, with about 20 percent image wobble caused by distortion for head movements of

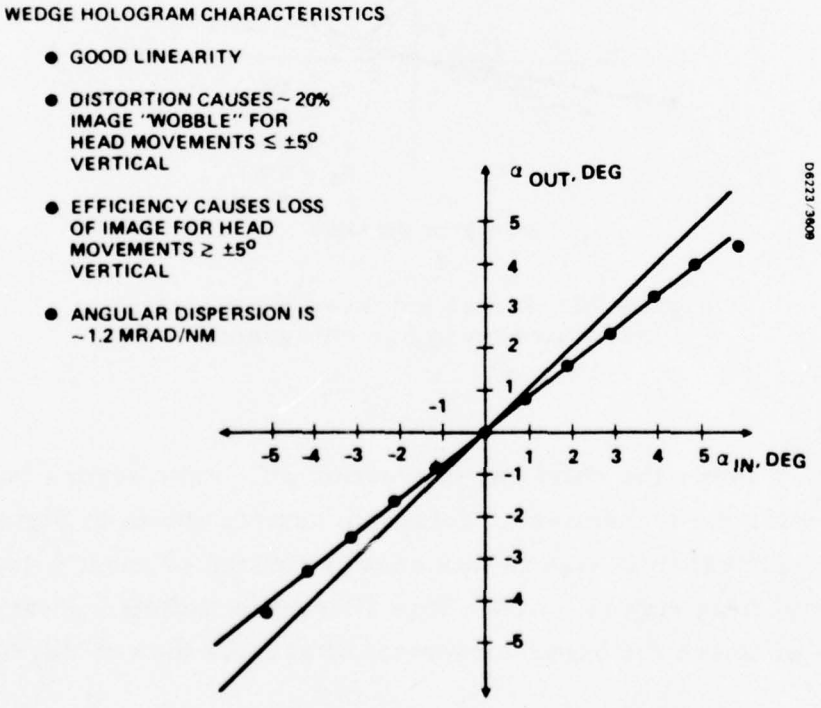


Figure 80. Distortion for a wedge transmission hologram.

less than ±5 degrees vertical. The diffraction efficiency characteristics are similar to those of the image hologram and again cause loss of the image for head movements of greater than ±5 degrees in the vertical direction. For both systems the angular dispersion is about 1.2 milliradians per nanometer.

5.4.2 Spectral Flare Characteristics

In contrast with the characteristics of thick phase reflection holograms, the fringe geometry of thick phase transmission holograms allows a high diffraction efficiency for a broad range of wavelengths. We show below how this efficiency characteristic produces very strong spectral flares that drastically limit the potential of transmission hologram systems. The approach to quantitatively calculate the geometry of the high efficiency configurations that exists when the Bragg condition is satisfied.

Figure 81 shows a magnified view of the hologram fringes at the central area of the transmission hologram on the visor. θ_e is the external chief ray angle, which is 40 degrees. θ_i is the corresponding internal angle which for an average refractive index 1.521 is about 25 degrees. For this case the fringe planes make an angle θF of 12.5 degrees with respect to the substrate normal. For a display operating wavelength of 543 nanometers the fringe spacing in the medium is given by

$$\Lambda = \frac{\lambda_o}{2n \sin \frac{\theta_i}{2}} = 0.825\ \mu m$$

The surface grating spacing d is given by $d = \Lambda / \cos \theta_F = 0.845\ \mu m$

Figure 82 shows the geometry of the high-efficiency flare calculation, again as a magnified view of the holographic medium on the visor. In general the high-efficiency chief ray is displaced from the center of the hologram and the external angle is different from the nominal 40 degrees for a wavelength of 543 nanometers. The general external angle is called θ_1, the corresponding internal angle is θ_2. The corresponding internal and external diffracted ray directions are θ_3 and θ_4 respectively. The fringe angle remains fixed at θ_f. In order to provide high diffraction efficiency, the external angles θ_1 and θ_4 must satisfy the grating geometry as shown in

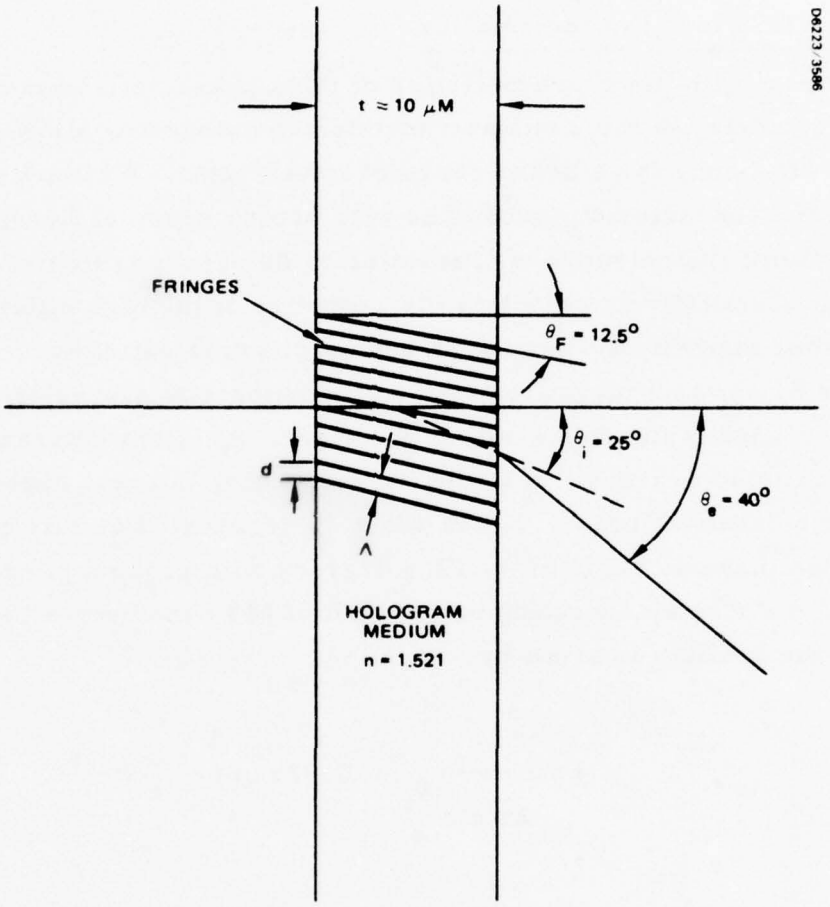


Figure 81. Magnified view of the hologram fringes.

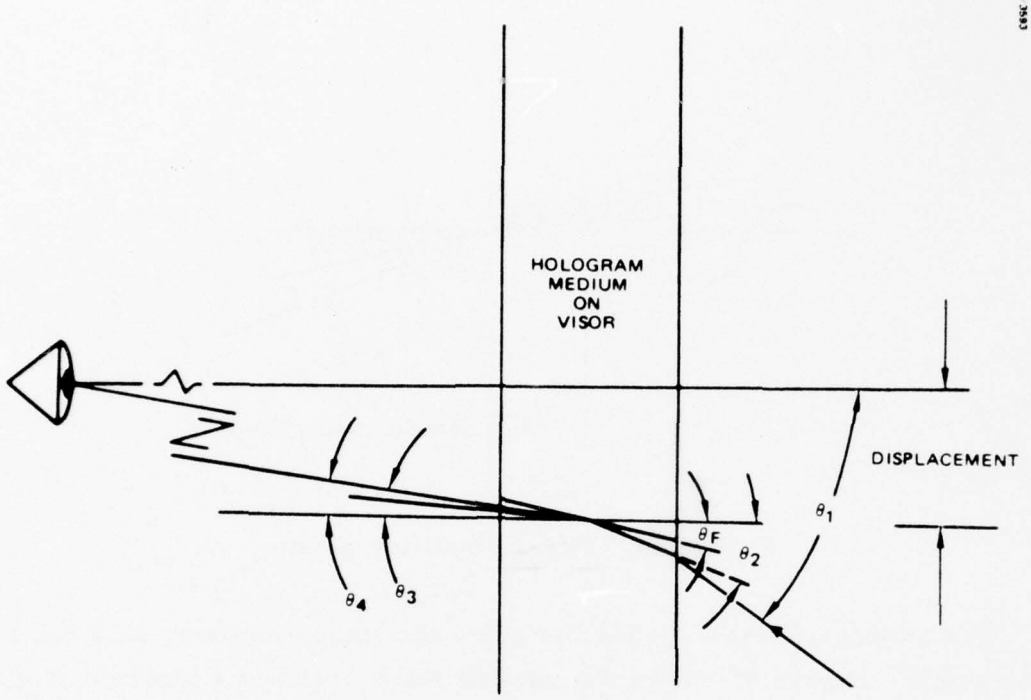


Figure 82. Geometry of high efficiency flare calculation.

Figure 83, and given by the grating equation $\sin \theta_1 + \sin \theta_4 = \lambda/d$. The internal rays must satisfy the Bragg condition geometry of reflection from the fringe planes as shown in Figure 84 and given by the equation $\theta_F - \theta_3 = \theta_2 - \theta_F$. Finally, the internal and external angles are related by Snell's law.

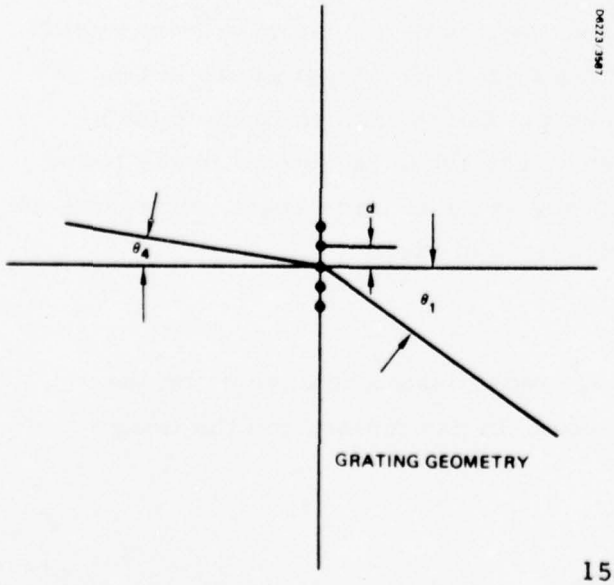


Figure 83. Grating geometry.

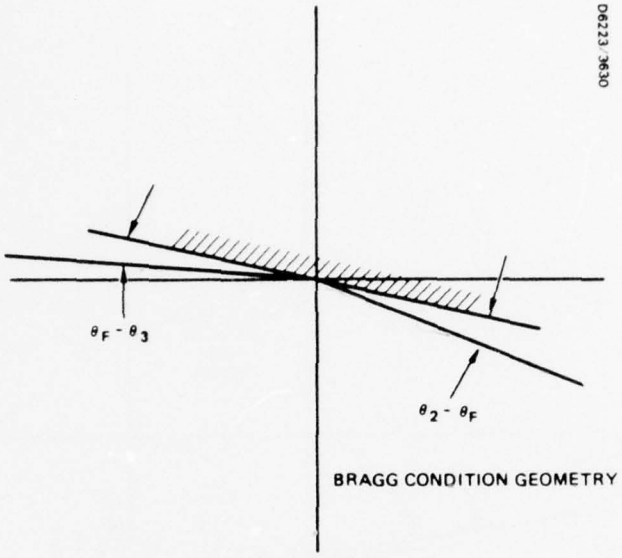


Figure 84. Bragg condition geometry.

The solution of these equations gives the flare geometry as a function of wavelength. Figure 85 shows the cockpit flare angle as a function of wavelength at peak efficiency. This angle is the angle of the incident chief ray relative to the display line of sight. The display operating point is 40 degrees at a wave length of 543 nanometers. Figure 86 shows the observed flare angle and displacement as functions of the wavelength at peak efficiency. The display operating point is an observed flare angle of 0 degrees and displacement at 543 nanometers. Finally, Figure 87 combines these data to show the high efficiency flare geometry drawn to scale for several wave lengths covering the extent of the visible spectrum. These results show that the high-efficiency flare geometry allows light from bright areas in the cockpit to produce bright, colored, spectral flares located in the pilot's forward visual area. The effect is that bright areas or objects in the lower cockpit will be imaged with high-efficiency at some wavelength, appearing as colored, defocused images in the pilot's field of view.

5.4.3 Conclusions

The image quality in displays using transmission holograms on the pilot's visor is limited but possibly useful. In particular, for the image

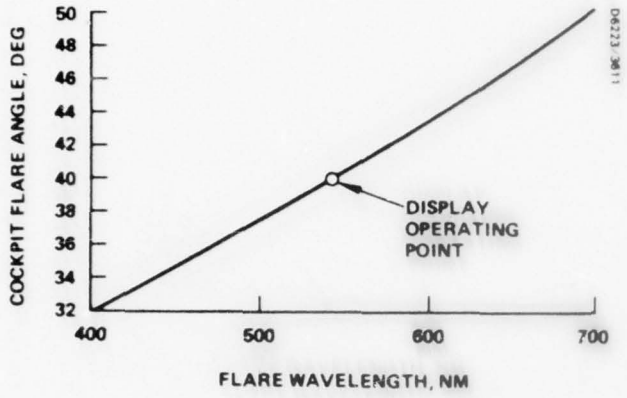


Figure 85. Cockpit flare angle as a function of wavelength of peak efficiency.

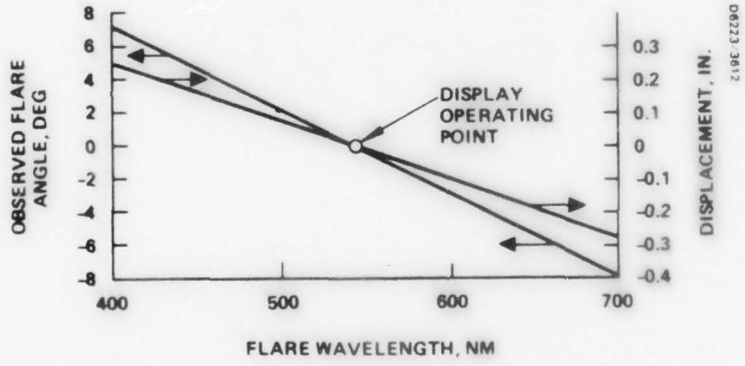


Figure 86. Observed flare angle as a function of wavelength of peak efficiency.

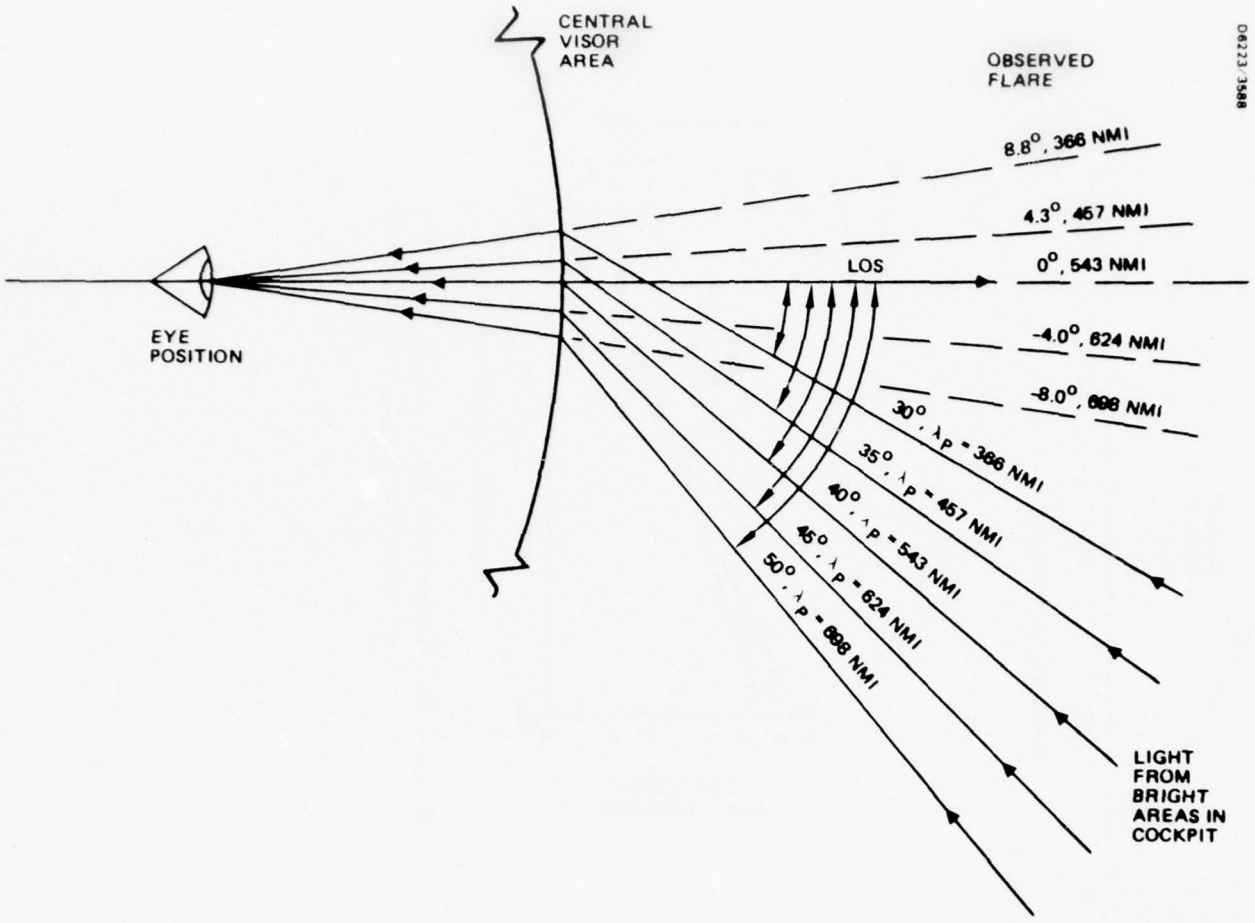


Figure 87. High efficiency flare geometry, drawn to scale.

hologram, the difficulty is that the collimation changes with visor-to-CRT spacing. With the wedge hologram the field of view and pupil are limited by the external collimator aperture. For both types of hologram there is a loss of image for vertical visor movement of greater than about ±5 degrees.

Spectral flare is a fatal and fundamental problem in these transmission hologram systems. It is a fatal problem because the bright, colored, spurious images in the forward field of view are extremely disruptive from a human factors point of view. It is a fundamental problem because there is no known solution to this problem through better technology. We must conclude, therefore, that the displays using transmission holograms on the visor are not viable systems.

6.0 BASELINE SYSTEMS

6.1 PHYSICAL DESCRIPTION

6.1.1 Reflective Holographic System Description

The summary description of the reflective baseline Diffraction Optics system was given in Section 2.0. A more detailed description is contained in this section. The system performance is given in Table 20.

TABLE 20. REFLECTIVE HOLOGRAPHIC SYSTEM PERFORMANCE SUMMARY

	CENTRALLY LOCATED HOE (OVER THE SHOULDER SOURCE)	SIDE HOE LOCATION (SILL-MOUNTED SOURCE)
EFL, INCHES	25	25
HOLOGRAM RADIUS, INCHES	15	15
IMAGE TILT, DEGREES	3	48
EXIT PUPIL DIAMETER, INCHES	3	3
FIELD OF VIEW, DEGREES	10(CIRCULAR)	10(CIRCULAR)
SOURCE SIZE, INCHES	4	4
BEND ANGLE, DEGREES	5	80
ASYMMETRY ANGLE, DEGREES	50	20
AXIAL COMA ACROSS PUPIL, MILLIRADIANS	4	6
DISPERSION, MILLIRADIANS/NANOMETER	4.4	1

The constraints, tradeoffs and design considerations leading up to the baseline configuration have been discussed. The baseline system has evolved as the best compromise of all the considerations.

Referring to Figure 88, the arrangement of HOEs and their relation to the pilot are shown. The spacing between the HOEs is that required to

PRECEDING PAGE BLANK-NOT FILMED

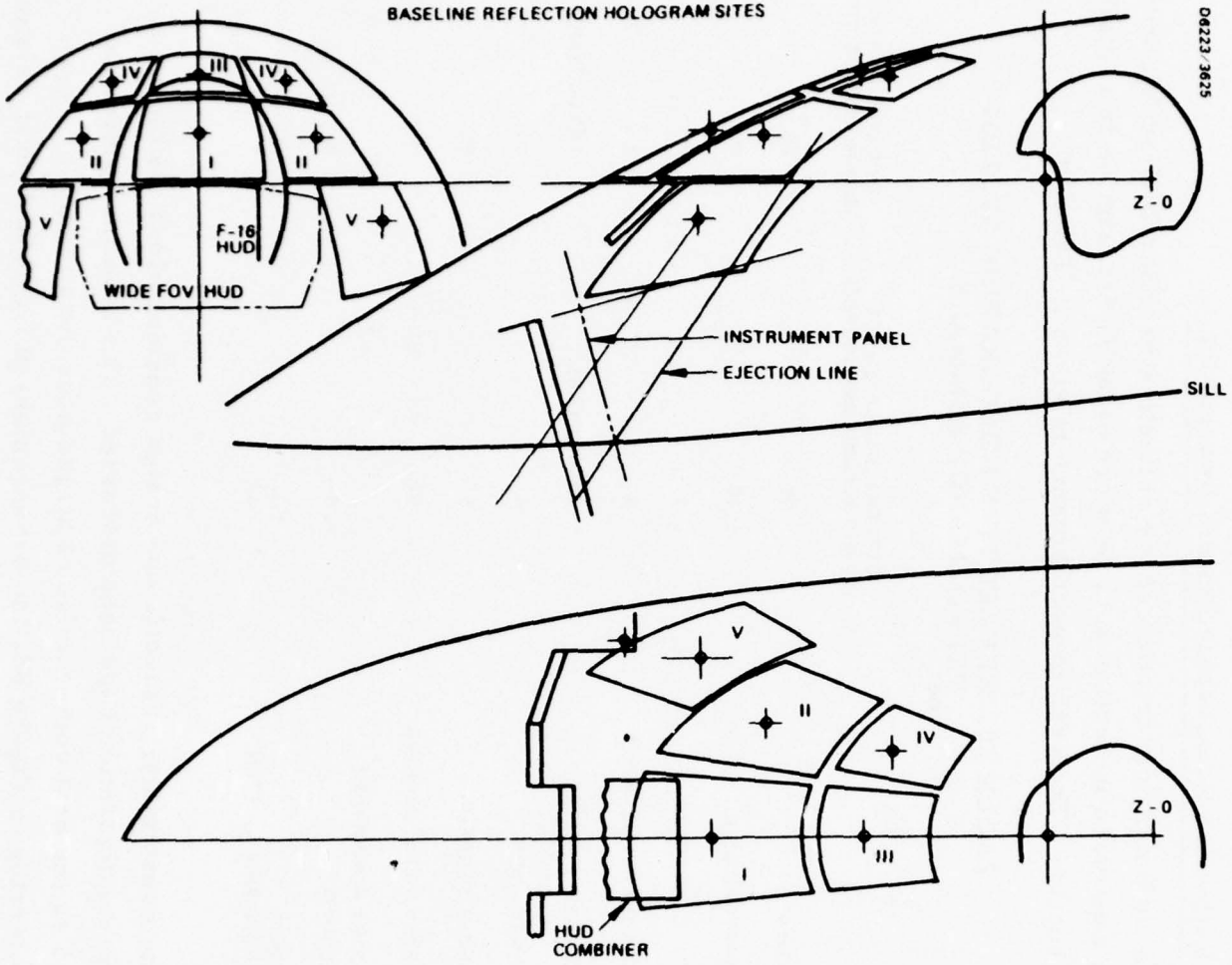


Figure 88. Hologram arrangement on canopy.

insure against crosstalk between unrelated HOE/Source pairs. The HOEs are clustered around the HUD and their purpose is to supplement it and declutter it by providing additional surface area for displaying information which is not critically registered with the outside world, as described in Section 3.0. The number of HOEs – eight, represents the maximum practical for this aircraft when considering the space available for image sources. The primary areas of importance around the HUD and above it are adequately covered by this arrangement.* The least important HOEs are those at either side of the HUD (V). If a wide FOV HUD is utilized, it is questionable whether they will be cost and space effective. With the narrower, existing F-16 HUD, their utility becomes more readily apparent.

The size of the HOEs is compatible with state-of-the-art fabrication techniques, although affixing them to a canopy has not been attempted before and may be more difficult than anticipated. A special effort must be made to de-emphasize any borderline of the HOEs so that operator vision is unaffected.

Figure 89 shows the location of the image sources for the eight HOEs. The sources consist of CRTs of various sizes mounted at either side of the instrument panel and on the canopy sill. Two additional image sources, either CRTs or lasers are mounted behind the operator at either side of his head. Due to the geometry of the canopy and the instrument panel – HOEs I and III can only be sourced from an over-the-shoulder location. As mentioned in Section 5.2, this condition produces a high dispersion geometry due to the large asymmetry, and the narrow bandwidth of a laser source is really desirable, if not necessary. A CRT has excessive dispersion and will render HOEs I and III essentially useless for all but very gross information. Because the HOE-to-source distance is the greatest for these sources – their display area size must be increased accordingly.

The remainder of the image source geometries do not suffer from dispersion problems so they can all be CRTs of 3- and 4-inch diameter.

The two 3-inch CRTs are the sources for the two number V HOEs. They are mounted at either side of the instrument panel. The two 4-inch

---

*The HOEs are designated I through V in order of importance.

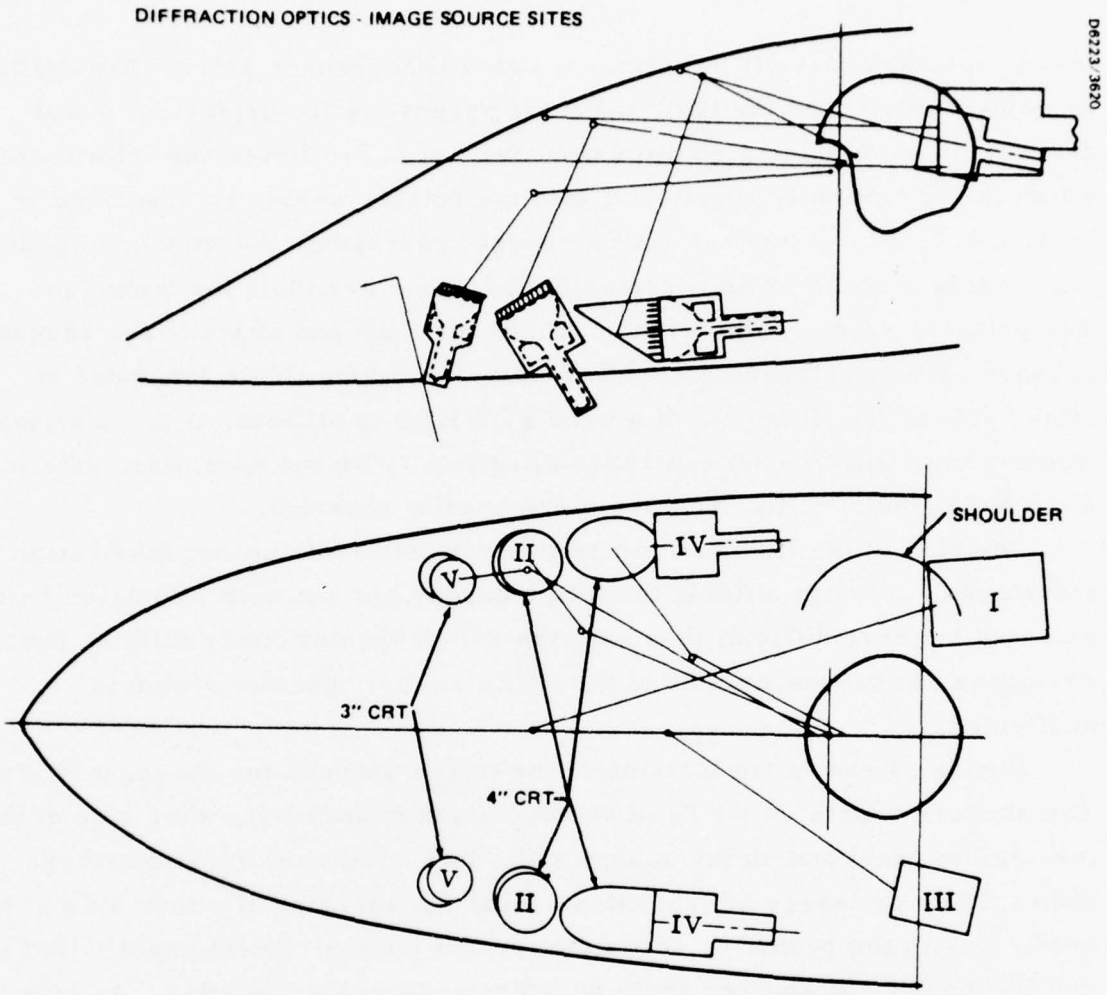


Figure 89. Location of HOE image sources.
(Numerals indicate which hologram they service.)

CRTs mounted along the sills are sources for HOEs II and IV. A special mounting provision for the sill-mounted sources must be devised to permit source disconnect if the canopy is jettisoned. The referenced mounting provisions can only be better defined when more detailed physical information on the aircraft is made available. All dimensional information on the cockpit was determined from scale drawings and photographs.

The sill mounting of the CRTs appears feasible; however, it is also the only space in the cockpit which appears to avoid physical interference with a prime flight function. If the sill cannot be made to serve as the source mounting area, then HOEs IV and V may be abandoned and a 4-HOE system made to suffice.

All of the CRTs have directional filter/baffles on their faceplates to prevent contrast washout by stray light. The aftmost CRTs on the sill have mirror folds in their optical paths to allow packaging above the sill line next to the other CRTs.

One of the considerations given to the final configuration is the control of stray light, both inside the canopy and, as viewed from outside the canopy, as from another aircraft.

Figure 90 is included to show the direction of the symmetrically reflected rays from the eye to the chosen hologram sites. Points A, B and C indicate the different eye and head positions used when viewing the different displays. Notice that, except for the on-axis HOE sites, the actual source locations do come quite close to the symmetrical positions except they have been moved outboard to put them out of the way. The bend angles are quite high, however, which contributes to the large field tilts, i.e., the necessity for tilting the CRTs in the object plane.

6.1.2 Transmission Holographic Visor System

Optical System Geometry. The prime purpose of the display is to provide the pilot with essential flight and combat information. The display must be visible close to the direction the pilot will be looking during the periods when such information is required to assist in the performance of his mission. The displayed information should not interfere with his vision but be available in the periphery of his line of sight where he can refer to it as necessary.

The display locations that should fulfill these requirements are slightly above and outboard on each side of the HUD. Looking directly forward, the display would not be visible to either eye but by pointing the LOS of the head to the right or left and up slightly the display becomes increasingly brighter as the LOS to the display is reached and decreasing as the optimum LOS is passed. The display will appear to the right eye on the right side of the HUD and to the left eye on the left side of the HUD, but never to both eyes simultaneously. In this manner, the target aircraft will never be obscured and can be tracked by one eye or the other even when the target is directly in line with the display.

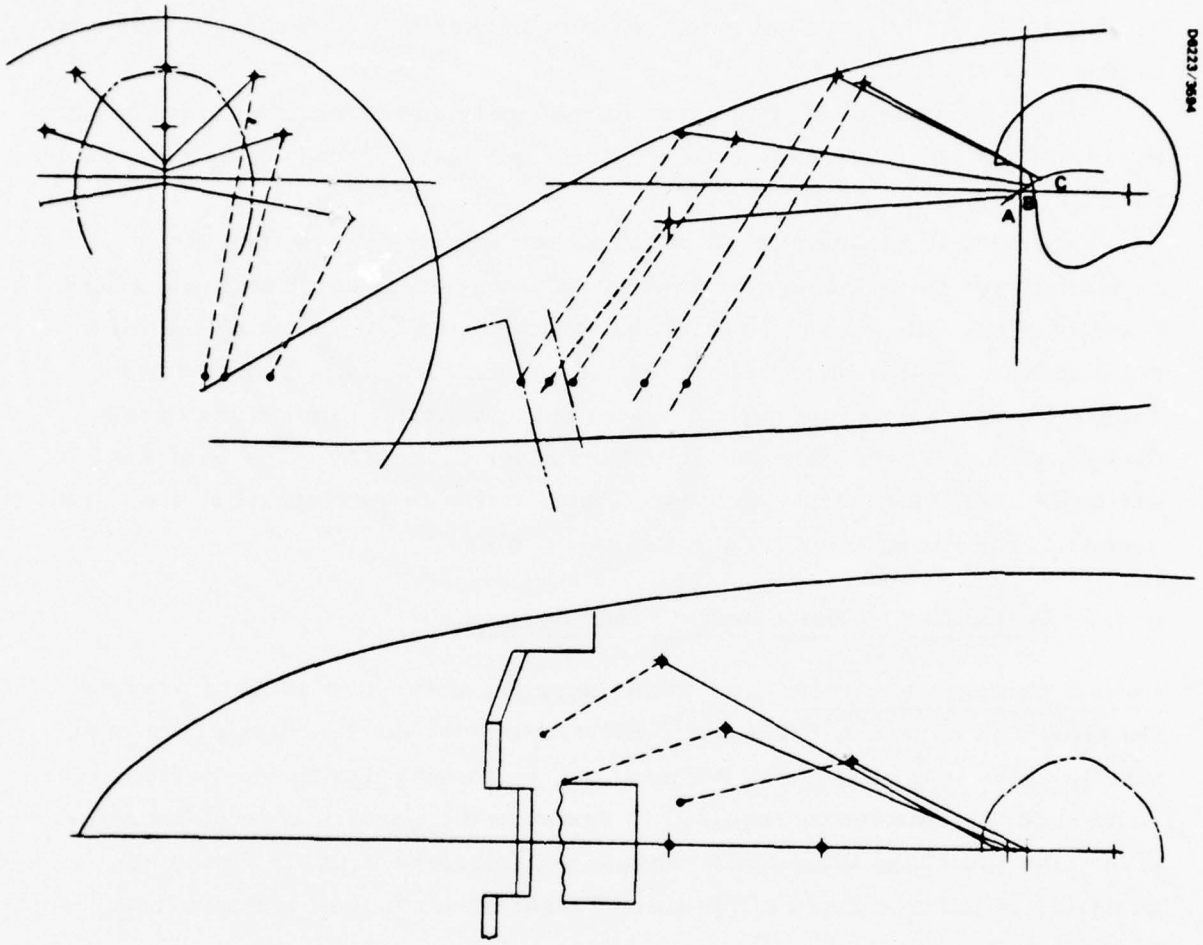


Figure 90. Reflection angles off chosen HOE sites.

The virtual image of the projected display will appear to the pilot at infinity and in the same location (approximately, depending on the exact head pointing LOS) in space. The image location in space and how it is observed can be better understood by referring to the optical system installation geometry shown by Figure 91. Figure 91 is an inboard profile and view looking forward of the F-16 cockpit. A display projection image source is located forward and on each side of the instrument panel just above the cockpit rail. The beams of each display are essentially projected at the pilot's helmet visor holographic lenses. Each visor lens is focused on a display and was constructed to produce a virtual image of the display,

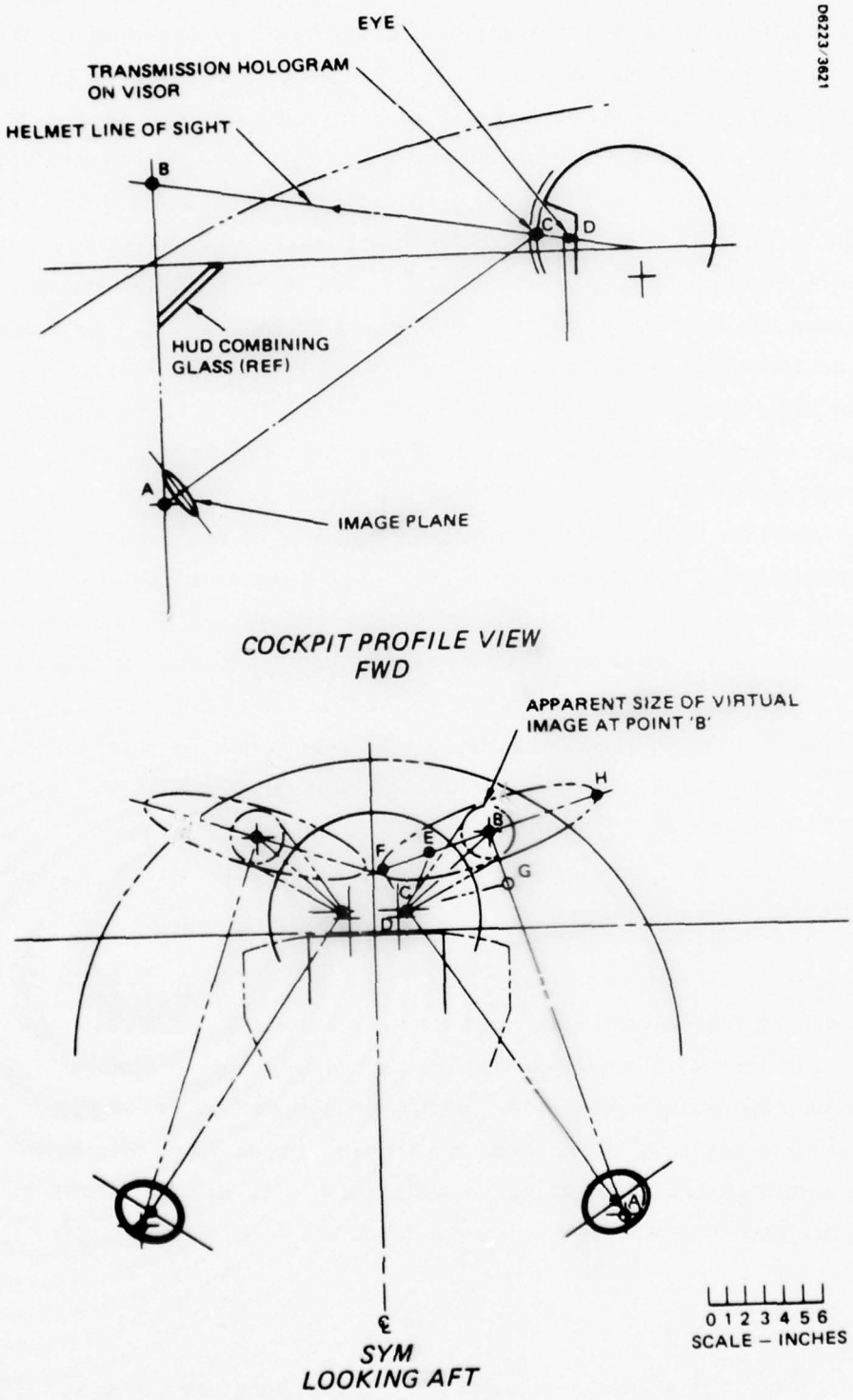


Figure 91. Transmission holographic visor optical system.

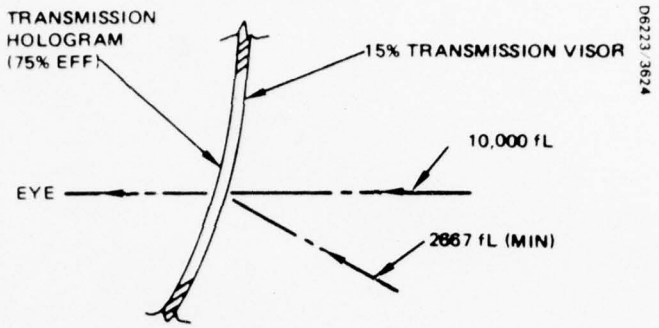
focused at infinity. The virtual image appears to the pilot's eye along the line C-B. An image source diameter of 3.25 inches was selected to produce a vertical image that subtends a conical FOV angle of 6.5 degrees to the eye. As the helmet LOS leaves this direction and moves (for instance) to be along line C-E, the virtual image can still be seen faintly by rotating the eye LOS to line C-D which in this case is approximately 9 degrees from the helmet LOS. As the helmet LOS is moved to be along line C-F, the image will have disappeared even if the eye is rotated to the D-C LOS. The same characteristics occur as the helmet is rotated downward to LOS C-G. The dimmer image can be observed by rotating the eye along C-D. The efficiency of the hologram is not equal vertically and horizontally. The ellipse around the virtual image representation at point B represents the approximate 50 percent efficiency locations.

Side-to-side or up-and-down movement limits of the helmet within the optical system "pupil" is a function of the visor hologram construction efficiency and the focal length of the hologram. It should be feasible to move the visor hologram within a 6 inch excursion circle without significant degradation of the image brightness. Outside of this limit the image vignetting will occur and the image brightness will decrease until the total image disappears.* The image will be increasingly out-of-focus as the visor is moved toward or away from the CRT image plane. As the helmet is moved the image will appear to move in space but it becomes stationary when the helmet motion is stopped.

Image Brightness. A contrast ratio $\left(\frac{\text{ambient light level + display brightness}}{\text{ambient light level}}\right)$ at the eye of 1.20 (minimum) has been accepted for transmission type symbol displays presented on head up display (HUD) combining glasses. The visor transmission holographic lens virtual image display is essentially the same as a HUD combining glass and, therefore, must meet this same criteria if the symbols are to be visible in the 10,000 fL cockpit ambient light level. The display brightness requirement (of 2667 fL) is calculated in Figure 92.

---

* The image plane will shift away from its infinity point as the visor HOE is displaced forward and rearward from its focal point geometrical relationship with the image source.



AMBIENT LIGHT LEVEL AT EYE = 10,000 x 0.15 = 1,500 fL

SYMBOL BRIGHTNESS REQUIRED = 1.2 x 1,500 - 1,500 = 300 fL

CRT DISPLAY BRIGHTNESS REQUIRED* = $\frac{300}{0.15 \times 0.75}$ = 2,667 fL

* INDEPENDENT OF VISOR TRANSMISSION

Figure 92. Display brightness rationale.

Image Source. A CRT was selected as the image source because of the need for the high display brightness and also the narrow spectral band width available using P-43 phosphor. The brightness of the CRT, using stroke written symbols, will approach 5000 fL without damage to the phosphor and therefore can exceed the display minimum brightness requirement of 2667 fL. The P-43 phosphor characteristics are illustrated by Figure 93. As shown, the predominant radiant energy is within a narrow bandwidth (approximately 2.5 NM wide) and centered at approximately 543 NM wavelength. Even though the radiant energy is distributed over a very narrow bandwidth it will still result in unwanted chromatic dispersion and degrade the symbol image quality. Also added to the dispersion problem is the small energy spike at 548 NM, which will contribute to the dispersion magnitude under most viewing conditions. The chromatic dispersion resulting from the CRT phosphor bandwidth and for this optical system geometry is calculated in Figure 94.

The use of a narrow band notch filter was considered as a possible means of reducing the radiant energy bandwidth at the holograms. The practical limit for such a filter is about 0.5 percent which results in a band pass of approximately 2.7 NM. The filter could help reduce the maximum dispersion caused by the spike at 548 NM; however, the use of the filter would decrease the display brightness to an unacceptable level.

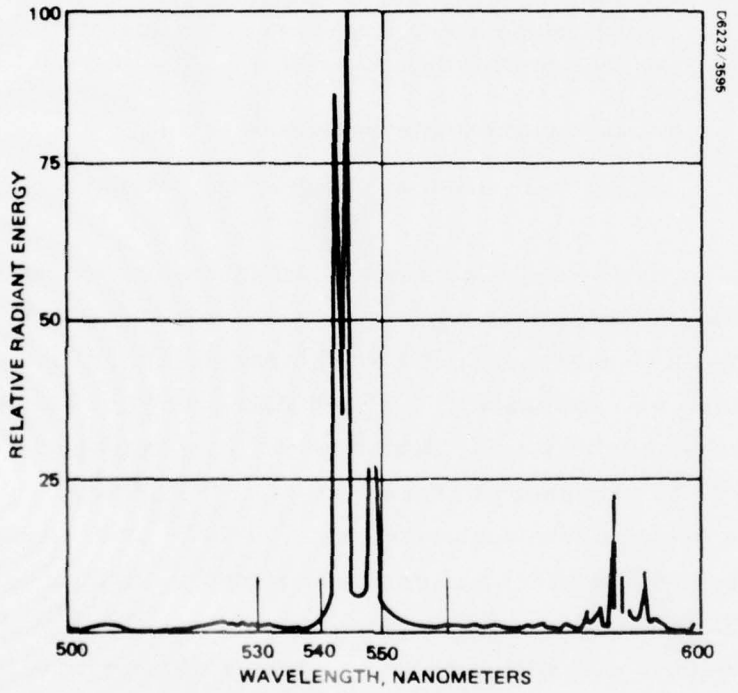


Figure 93. P-43 phosphor spectral distribution.

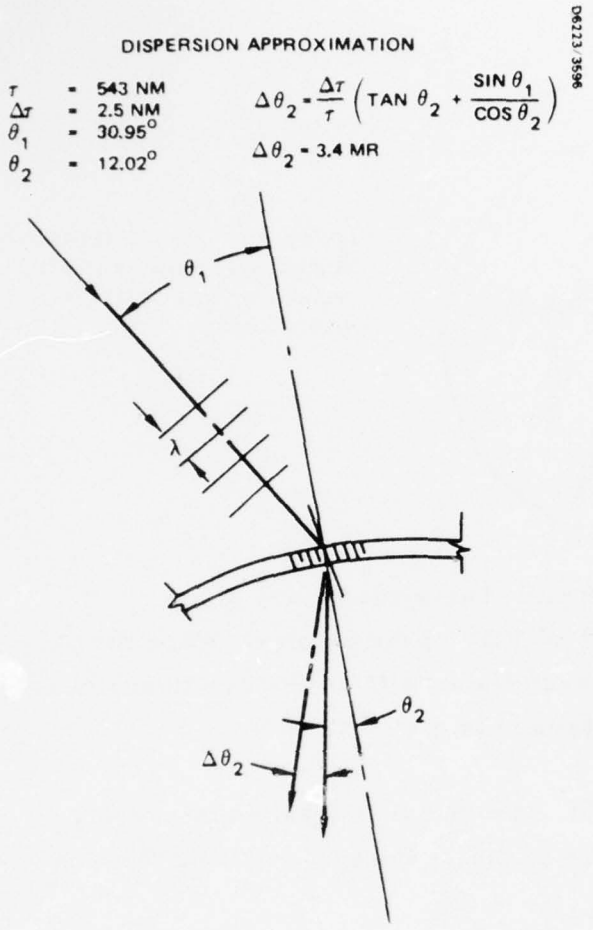


Figure 94. Transmission hologram optical geometry.

Light Emitting Diodes (LEDs) were also considered as an image source. They were immediately eliminated as a candidate because of their broad (comparative) spectral bandwidth (40 NM) and their insufficient radiant energy.

Display Chracteristics. A display of representative aircraft energy management symbology is used to illustrate the type of information (and symbols) that can be presented to the pilot. The display is shown in Figure 95. The major amount of chromatic dispersion occurs in the optical system bend plane. For the optical system geometry used for this study, the dispersion is dominant at approximately 17 degrees off of the vertical display axis. Figure 95 illustrates the variation in line width and symbol

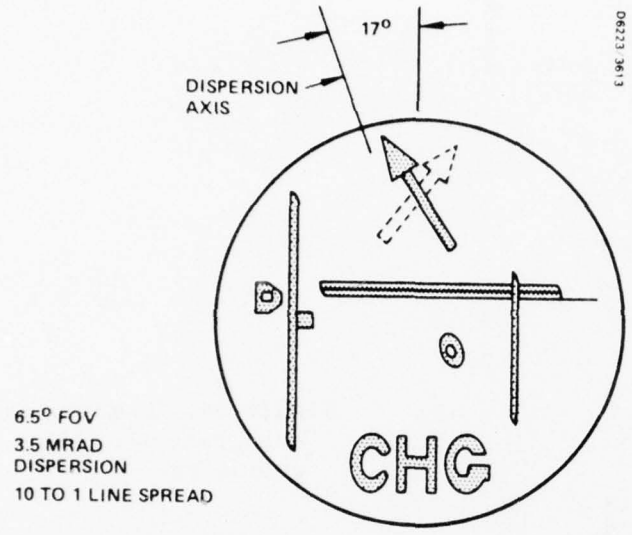


Figure 95. Representative display format showing effect of chromatic dispersion.

shapes caused by a dispersion of 3.5 mr. The symbols are sized proportionally to the 6.5 degree conical FOV of the display. When the display illustration is placed the correct distance from the eye to subtend a 6.5 degree FOV, the symbols will appear the size and shape to be viewed by the pilot.

The display illustration serves to show that it is feasible to present usable information to the pilot in spite of the resolution reducing dispersion.

Optical System Problems

Dispersion. As discussed in the previous sections, dispersion will increase line width and reduce image sharpness. The magnitude of image degradation will determine the amount of information or number, size and shape of symbols that can be displayed for a given display FOV. The chromatic aberrations can be eliminated (or reduced) by using a monochromatic image source. A laser could be used for this application; however, the state of development for such an image source precludes its consideration at this time. The dispersion is a direct function of the holographic lens optical path asymmetry relative to the substrate plane. As the optical path approaches symmetry the dispersion approaches zero. Two typical reflecting hologram geometries are shown in Figure 96. As shown, reflecting type holograms can be made with symmetrical reflecting optical paths and therefore without dispersion. Unfortunately, to construct a transmission type

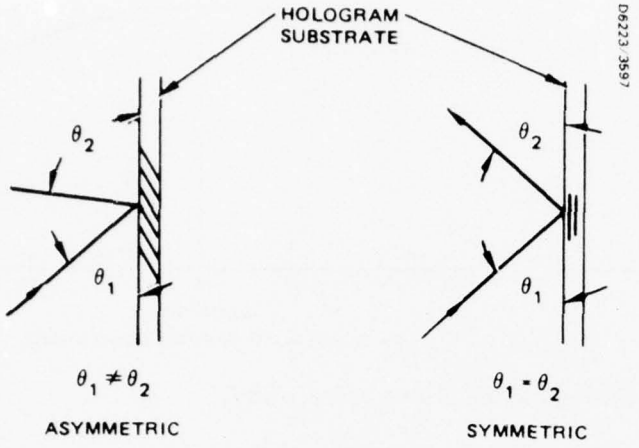


Figure 96. Optical geometry illustration.

hologram with a symmetrical optical path the image source would have to be directly in front of or directly behind the eye. This geometry is, of course, impossible; therefore, only asymmetric geometries are feasible making dispersion inherent in a transmission hologram.

Lens Efficiency Across Field. As described in Section 5.3.2, the efficiency varies greatly across the field in the optical system bend plane. In the optical plane normal to the bend plane the efficiency is very constant for the FOV selected for this design. This difference in efficiency and variation in brightness is illustrated in Figure 97. For this particular optical system geometry, the optical bend plane and the major brightness variation are essentially vertical to the CRT displayed image. Electronic compensation for the variation in hologram efficiency can be accomplished by programming the CRT display brightness to give the display a consistent brightness across the field. That is, the stroke written symbol brightness can be varied as a function of display vertical position as shown in Figure 98. The maximum CRT brightness that can be achieved is the only limit to the compensation. As discussed earlier, the minimum required brightness of the display is 2667 fL. It should be possible to obtain 5000 fL brightness at the display top and bottom thus giving a $\frac{5000}{2667}$ or 1.87 variation. This magnitude approaches the amount required to produce the consistent brightness across the vertical field.

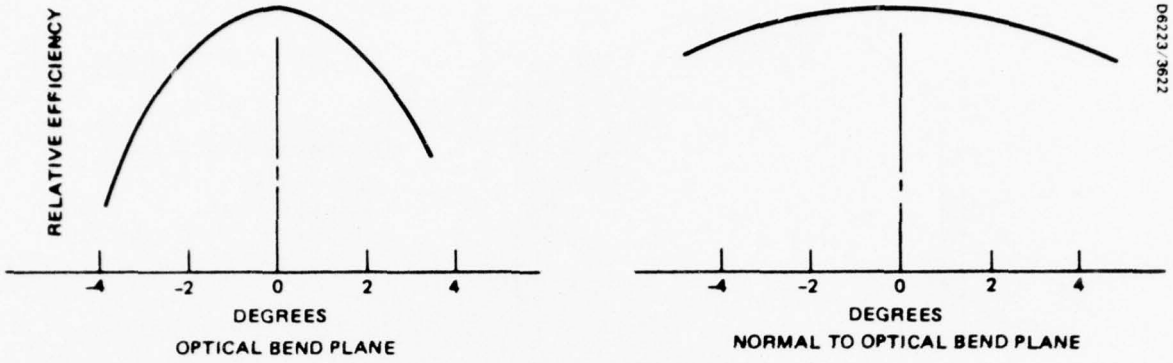


Figure 97. Holographic lens efficiency.

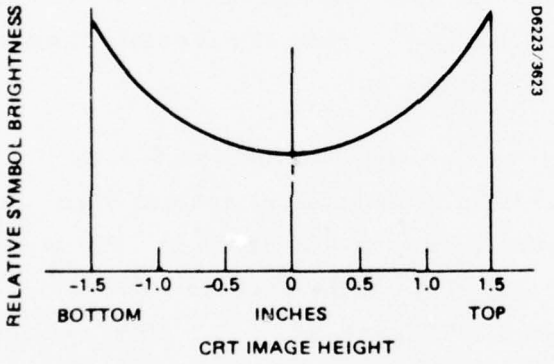


Figure 98. CRT symbol brightness.

For other optical geometries where the bend axis is not along the CRT vertical or horizontal deflection directions a more complex electronic compensation mechanization would be required.

Spurious Reflections. Perhaps the most serious problem inherent in transmision hologram lenses is caused by their high efficiency over a relatively large FOV normal to the optical bend plane. Because of this characteristic, bright (and distracting) virtual images of objects near either (right or left) CRT image source will appear horizontally along the line F-H and on each side of the CRT display virtual image and within the ellipse shown in Figure 91. To further compound the problem, the virtual image of any object that is near the focus location of either visor hologram

will appear before the eye or eyes of the pilot, no matter where he is pointing his head. Objects in focus will be clear and bright and objects out of focus will appear as blobs of light. Transmission holograms are also responsive to a relatively broader wavelength spectrum than the reflective type. This broader wavelength increases the range of reflection from objects and also causes an increase in chromatic dispersion which will grossly increase the size of the virtual image of the object's reflected light.

There does not appear to be a solution to the spurious reflection problem obtainable through optical design because of the holographic lens characteristics. However, one possible but not practical solution can be obtained by covering the cockpit switches, knobs, instruments, etc., with a non-reflective coating.

6.2 OPTICAL DESIGN

6.2.1 Introduction

This section is concerned with the optical design of display systems that utilize holographic optical elements operating in a reflective mode. The holographic element is most generally used as an eyepiece in the system; i.e., the display to be viewed is placed at (or relayed to) the focal surface of the holographic element, and the viewer sees a collimated image of that display. The unique properties that make a holographic lens so useful in this capacity are:

a. the narrow spectral and angular bandwidth diffraction sensitivity
b. the broadband transmission characteristics resulting in good see-through
c. the thin-film nature of holographic elements and the fact that their first order properties are independent of the hologram shape

The construction of a holographic element is a photographic process in which the interference pattern formed by two coherent beams is recorded in a suitable medium. The way in which a hologram is constructed directly affects its imaging properties, both in terms of image quality and diffraction efficiency. The two extremes of the many ways of constructing a hologram are shown in Figure 99. Part I illustrates the construction and reconstruction of an image hologram. This type of hologram is made with a beam

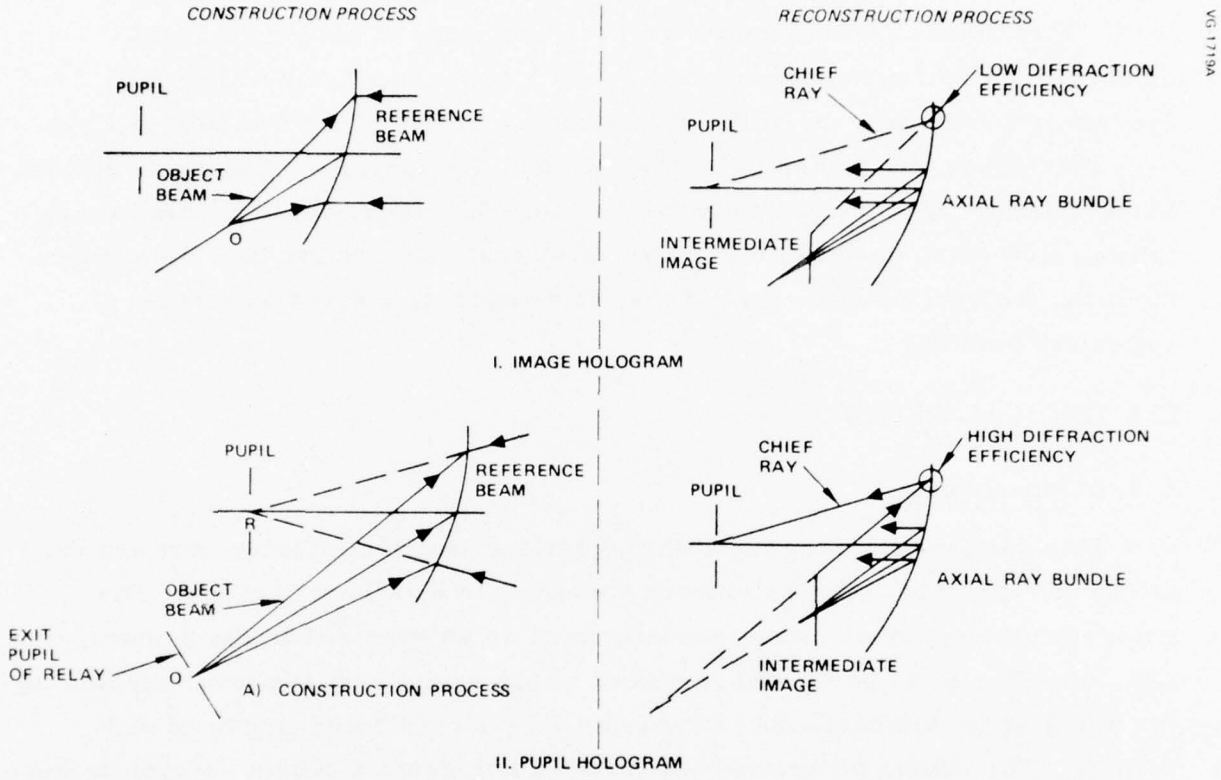


Figure 99. Construction and reconstruction of I) an image hologram and II) a pupil hologram.

diverging from a point source located at the image surface and a parallel beam entering from the right. This results in a hologram with good axial imagery and a large exit pupil. Away from the axis, however, the diffraction efficiency falls and limits the field of view (FOV) and a rapid increase in aberrations, particularly image surface tilts, makes this type of hologram unsuitable for wide FOV use. Part II of Figure 99 shows the construction and reconstruction of a pupil hologram. It is made using two spherical wavefronts; one diverging from the hologram entrance pupil and one converging on the hologram exit pupil. High diffraction efficiency is achieved for the chief rays thus insuring a wide FOV capability, but the diffraction efficiency decreases across the exit pupil and limits the pupil size; some axial aberrations are also introduced.

Both of the holographic elements described above have application to display systems and this will be discussed in Section 6.2.2. In Section 6.2.3 the F-16 cockpit and canopy will be examined and their impact on the optical design assessed. Two representative design geometries applicable to this study are presented in Section 6.2.4.

6.2.2 First Order Design Considerations

Figure 100 is a schematic of how an image hologram might be used in a relayless head up display (HUD). It is a simple system where the image source is placed at the hologram focal surface. The display will have good axial imagery and a large exit pupil. The display FOV will be limited by one of three things:

a. A large image surface tilt disparity – the tilt of the image surface formed by fans of rays traced in the plane of asymmetry (the plane containing the bend angle) can be very much different from the tilt of the image surface formed by fans of rays traced in the plane of symmetry. This aberration, if uncorrected, is severely limiting.

b. Hologram diffraction efficiency – The hologram has a limited FOV due to decreased efficiency for off axis rays.

c. Image source subtense – The image source subtends a certain angle at the hologram and this is a function of the image source size and the hologram focal length.

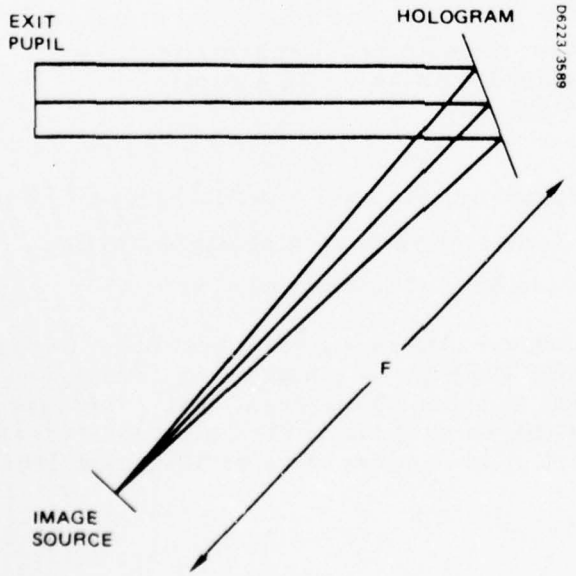


Figure 100. First order optical schematic of relayless display using an image hologram.

Figure 101 shows a schematic of a pupil hologram used in a relayed HUD. Due to its large FOV capability, this configuration is widely used. A relay lens located at the hologram entrance pupil transfers a magnified image of the source onto the focal surface of the holographic lens. The viewer then sees a collimated image at the exit pupil. The desired FOV and source size determine the system focal length, which, with the exit pupil size, determines the system f-number. Once the hologram focal length is chosen, the necessary relay lens optical characteristics can be calculated.

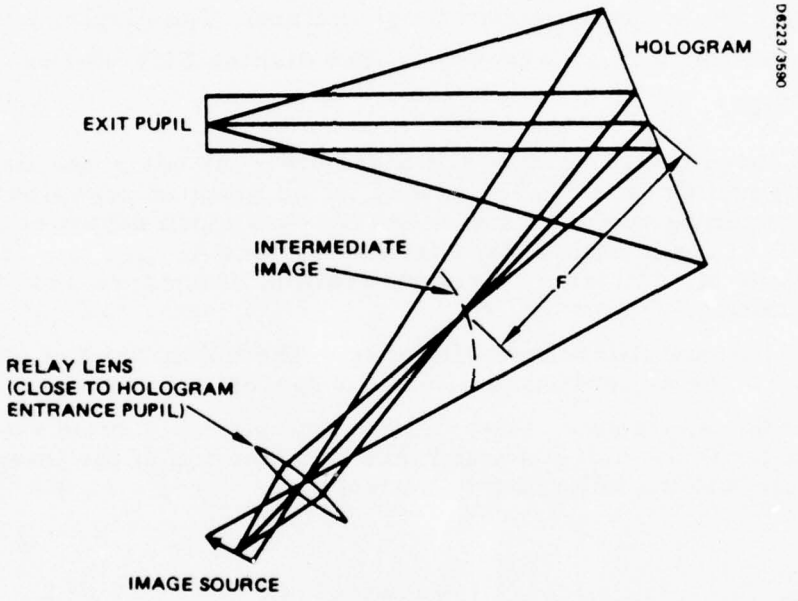


Figure 101. First order optical schematic of relayed display using a pupil hologram.

The aberrations that are present in the pupil type holographic lens can be compensated for in the relay lens to give good display performance. A typical pupil hologram will have the following aberrations.

a. Image surface tilt disparity – this is a problem similar to that found in image holograms although to a much smaller degree. The disparity is constant at about 20 degrees, while the tilts themselves increase as the bend angle of the hologram increases The tilts (and the disparity) are independent of hologram focal length.

b. Image surface curvatures – In addition to being tilted, the image surfaces are curved in a complex manner. Generally, each one is toric, i.e., with different mutually orthogonal curvatures. Compensating for four widely varying curvatures is often difficult.

c. Coma – This is the dominant aberration in the hologram image. It increases with increasing bend angle and decreases with increasing focal length.

d. Distortion – A complex distortion pattern is characteristic of this type of hologram. This distortion presents no real problem if the image source is programmable, as is usually the case.

e. Dispersion – For asymmetric holograms, where the hologram normal does not bisect the bend angle, there exists a surface grating component. This grating effect causes chromatic dispersion; it is a problem in both image and pupil holograms. For highly asymmetric holograms, this dispersion may dictate a narrow spectral bandwidth source.

As was mentioned earlier, some of these hologram aberrations can be corrected or compensated in the relay lens during the system optimization. The ability to vary the hologram curvature and to aberrate the construction wavefronts are valuable tools if they are available to the designer.

6.2.3 Cockpit and Canopy

The aircraft geometry has important implications and strong restrictions in light of this study's objectives. The F-16 cockpit is shown in Figure 102. Of special interest are the canopy profile, the location of the pilot's eyes, the ejection line, and the line of sight (LOS) over the cowl.

Consistent with the baseline concept presented earlier, it was assumed that the aircraft is equipped with a wide FOV HUD which occupies the central field of view and instrument panel space. This display is to be supplemented with a number of smaller FOV displays using holographic elements on the canopy. Since the holograms are to be directly on the canopy, the hologram curvature is not available as a variable to the designer during optimization. For a given LOS, the hologram curvature is exactly that of the canopy. For certain locations, the canopy can be closely approximated by a tilted vertical cylinder; for other locations it is more complex. The eye relief, i.e., the distance from the exit pupil to the hologram, is also not a variable.

The locations of relay lenses and/or image sources for the displays must be consistent with the ejection envelope of the aircraft. In order to keep this area clear, the focal lengths of the holographic lenses will have to

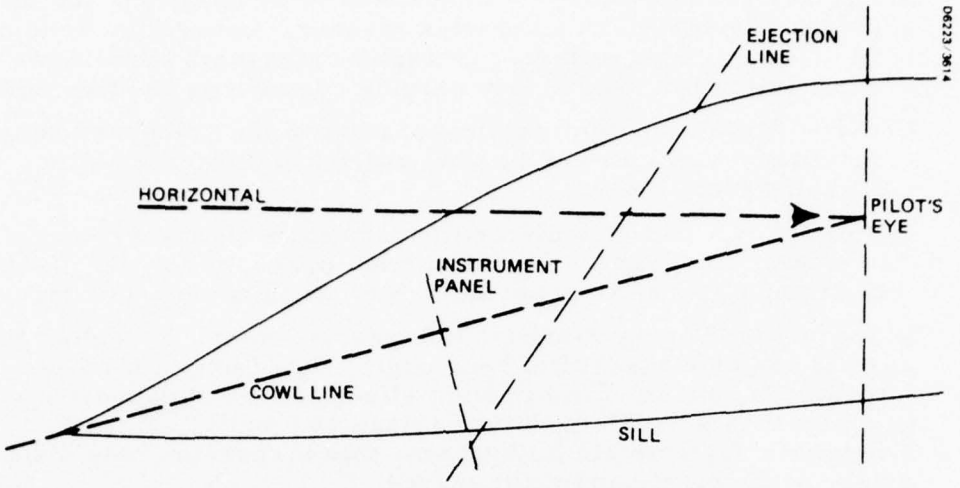


Figure 102. F-16 cockpit and canopy

be long. For a relayless display it means a smaller FOV for a given object source size. For a relayed display it means larger relay lens elements and higher magnifications. When one considers the desired positions for holograms and the available space for image sources, the resulting geometries fall into two groups, those with large bend angles and small asymmetry angles and those with small bend angles and large asymmetry angles. Those in the former group would result from placing the image source on the canopy sill, and those in the latter from having the source to one side of the pilot's head.

It is clear from the trade-off studies of image holograms and from the above discussion of the imaging properties of pupil holograms, that the disparity of image surface tilts is a problem which must be given some attention. If these tilts are not matched in a relayless display, it will have a prohibitively small FOV. In a relayed display, an extremely complex relay lens would have to be employed.

6.2.4 Representative Design Geometries

Even with the design restrictions outlined above, it is possible to match the image surface tilts in holograms throughout the broad range of geometries applicable to this study. Two examples are presented in detail here.

Figure 103 shows a holographic lens that has a large bend angle, moderate asymmetry angle, and a single image tilt of 48 degrees. Table 21 lists the characteristics of this lens. With the 25 inch focal length and a 4 inch diameter image source, a relayless display using this hologram would have

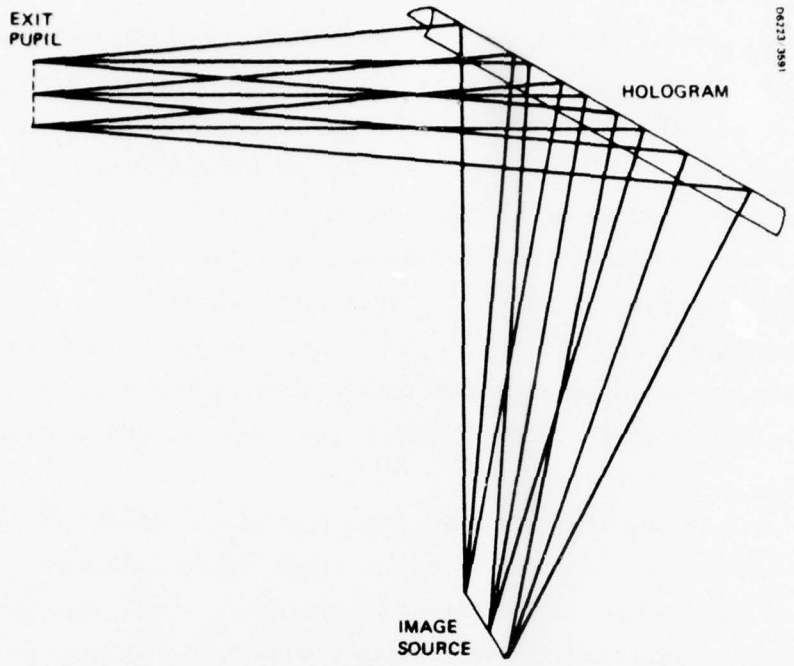


Figure 103. A holographic lens having an 80 degree bend angle, a 20 degree asymmetry angle, and a single image tilt of 48 degrees.

TABLE 21. OPTICAL CHARACTERISTICS OF HOLOGRAM HAVING AN 80 DEGREE BEND ANGLE AND A 20 DEGREE ASYMMETRY ANGLE

CHARACTERISTIC	VALUE
FOCAL LENGTH, INCHES	25
BEND ANGLE, DEGREES	80
ASYMMETRY ANGLE, DEGREES	20
IMAGE TILT, DEGREES	48
HOLOGRAM CYLINDRICAL RADIUS, INCHES	15
EXIT PUPIL DIAMETER, INCHES	3
AXIAL COMA (ACROSS PUPIL), MRAD	6
DISPERSION, MRAD/NM	1

a 10 degree circular FOV. A higher horizontal FOV could be obtained by using a relay lens (or larger source, of course), but the vertical FOV is limited by the diffraction efficiency. The amount of dispersion present might allow the use of a phosphor screen CRT as an image source in this example.

The geometrical aberration curves for this hologram are given in Figure 104. Fans of rays are traced vertically and horizontally across the 3 inch diameter exit pupil and their deviations from the chief ray at the image surface are plotted. These curves show about 6 mrad of coma across the pupil throughout the FOV. The resolution for each eye is much better than this because each eye only samples a small portion of the exit pupil at any one time. This coma results in accuracy errors and binocular disparity.

Figure 105 shows a holographic lens that has a small bend angle, a large asymmetry, and a single image surface tilt of 3 degrees. Table 22 lists its characteristics. FOV considerations are similar to those of the previous lens, except that the efficiency restrictions on the vertical FOV are not as severe. The amount of dispersion is very much larger in this hologram due to the increased asymmetry.* The geometrical aberration curves for this lens (Figure 106) are similar to the previous ones and result in the same kinds of collimation error and binocular disparity.

6.2.5 Conclusions

The requirement that the holographic elements be affixed directly to the canopy surface places strong restrictions on the optical designer, both in terms of resulting geometries and elimination of some important design variables.** Holograms such as the two described in Section 6.2.4 have application in simple relayless displays with moderate FOVs and moderate image quality and also in more complex relayed displays with wider FOVs and better image quality.

---

*A CRT would not be suitable as the display source because a 2 nm spectral bandwidth results in intolerable image smear. A laser source would be much more suitable for this example.

**Therefore, compromises in image quality or in field of view must be made.

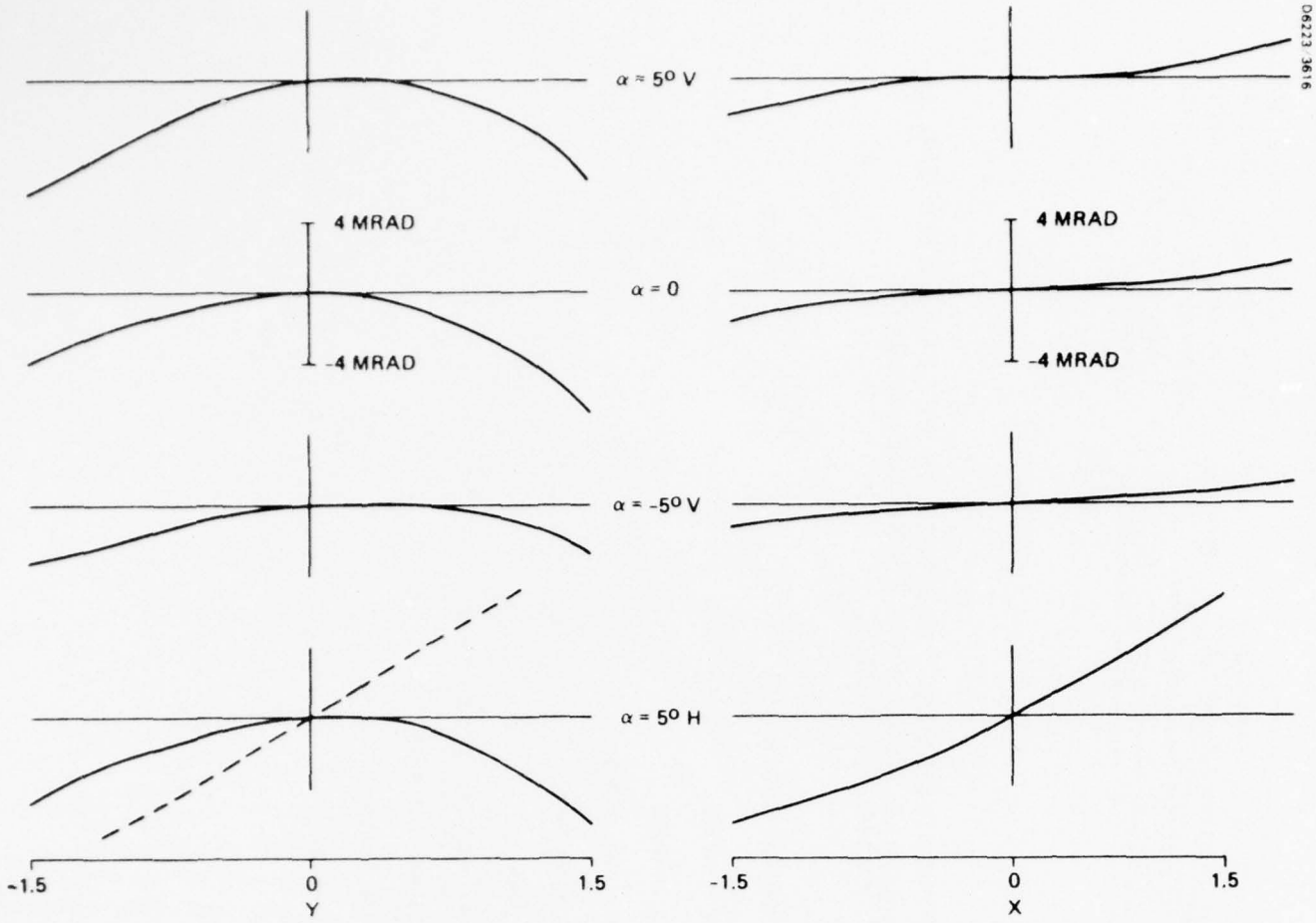


Figure 104. Geometrical aberration curves for the hologram with 80 degree bend angle and 20 degree asymmetry angle.

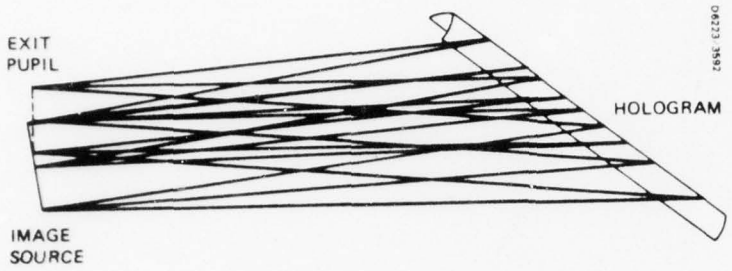


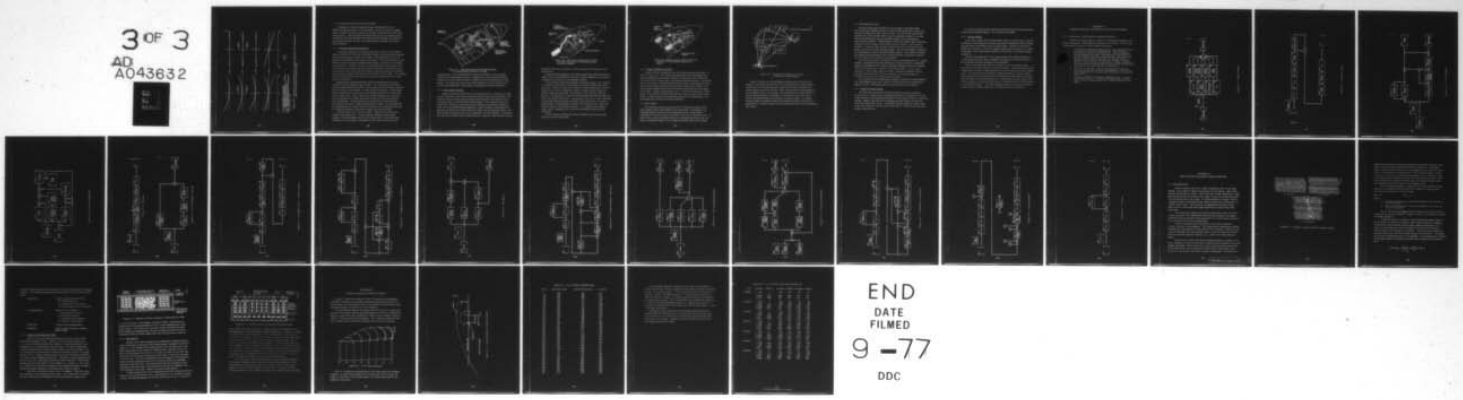
Figure 105. A holographic lens having a 5 degree bend angle, a 50 degree asymmetry angle, and a single image tilt of 3 degrees.

TABLE 22. OPTICAL CHARACTERISTICS OF HOLOGRAM HAVING A 5 DEGREE BEND ANGLE AND A 50 DEGREE ASSYMMETRY ANGLE

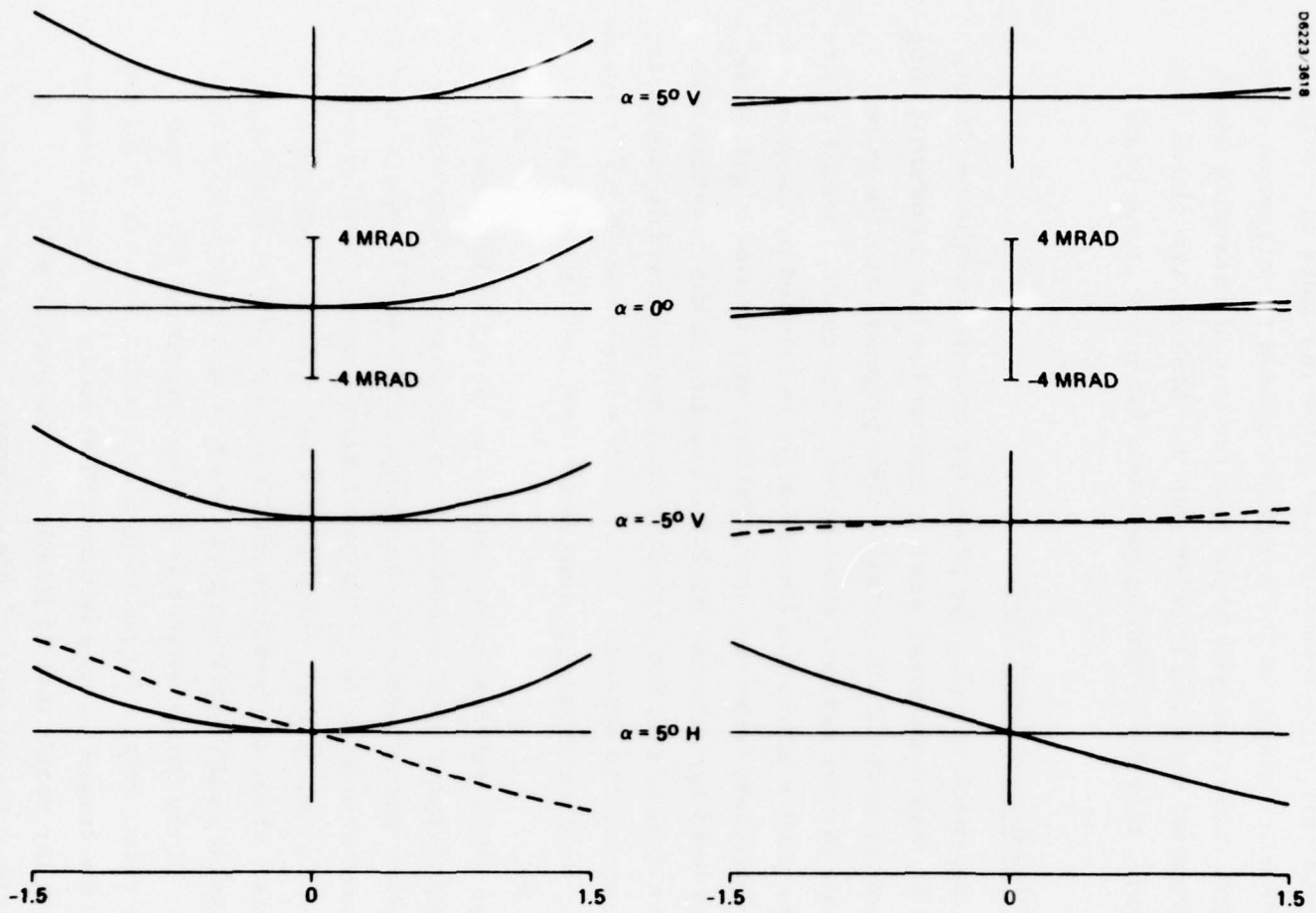
CHARACTERISTIC	VALUE
FOCAL LENGTH, INCHES	25
BEND ANGLE, DEGREES	5
ASYMMETRY ANGLE, DEGREES	50
IMAGE TILT, DEGREES	3
EYE RELIEF, INCHES	25
HOLOGRAM CYLINDRICAL RADIUS, INCHES	15
EXIT PUPIL DIAMETER, INCHES	3
AXIAL COMA (ACROSS PUPIL), MRAD	4
DISPERSION, MRAD/NM	4

AD-A043 632 HUGHES AIRCRAFT CO CULVER CITY CA DISPLAY PRODUCTS DEPT F/G 20/6
DIFFRACTION OPTICS STUDY.(U)
JUN 77 W N LEWIS, D H CLOSE, L G COOK F33615-76-C-0508
UNCLASSIFIED AMRL-TR-76-119 NL

3 OF 3
AD
A043632



END
DATE
FILMED
9 -77
DDC



X_1, Y_1 = ENTRANCE PUPIL COORDINATES
α_o = OBJECT ANGLE (H = HORIZONTAL, V = VERTICAL)
$\bar{x}_k, \bar{y}_k$ = IMAGE COORDINATES OF CHIEF RAY
x_k, y_k = LINEAR IMAGE COORDINATES OF GENERAL RAY
$\Delta x_k = x_k - \bar{x}_k, \Delta y_k = y_k - \bar{y}_k$

Figure 106. Geometrical aberration curves for the Hologram with 5 degree bend angle and 50 degree asymmetry angle.

6.3 ALTERNATE SYSTEM CONFIGURATIONS

In leading the reader through the design considerations for the diffraction optics systems, it is instructive to follow the lines of thought which, during the earlier stages of the program, guided the direction of the design efforts. This subsection will begin with the line of reasoning which prevailed at the proposal time and evolved into the thinking associated with the baseline systems, thereby revealing the basis for many of the basic study decisions.

6.3.1 Projector Mounted on Head Rest

The proposal approach of using the projector mounted on the headrest, shown in Figure 107, has been considered in light of the latest understanding of the optical geometry in the F-16 cockpit. The proposed system is not practical or feasible for the reasons cited below. The concept seems at first attractive since the pilot's azimuthal line-of-sight is tracked by the position of the headrest. Consider, however, the elevation axis line-of-sight; when the pilot moves his head forward and back the coupling to the headrest may be imprecise to the degree that the projector does not necessarily illuminate the area of the canopy in the direction of the pilot's line-of-sight. The coupling between the pilot's head and headrest does not accomplish this with a high degree of confidence.

Another factor which defeats the system as proposed is the lack of continuity of the holographic optic surface. It is not possible to provide a continuous diffraction optic surface on the canopy which will handle randomly directed image sourced beams. As with conventional optics, a holographic element must have an optical axis, focal length and optical curvature associated with the axis. Thus, a given area on the canopy will be associated with one specific point which represents the axes to which the projector must be directed. If the image source is directed at points other than the hologram axis point, image degradation may result. The exit pupil may be extinguished if the image source is directed at an off axis point between two holograms with the result that no image may be perceivable.

A third obstacle to the success of this approach is the continuously changing canopy geometry. As the hologram mounting surface shape changes, the single image source built-in distortions, scale factors and orientations must change to compensate for the characteristics of each

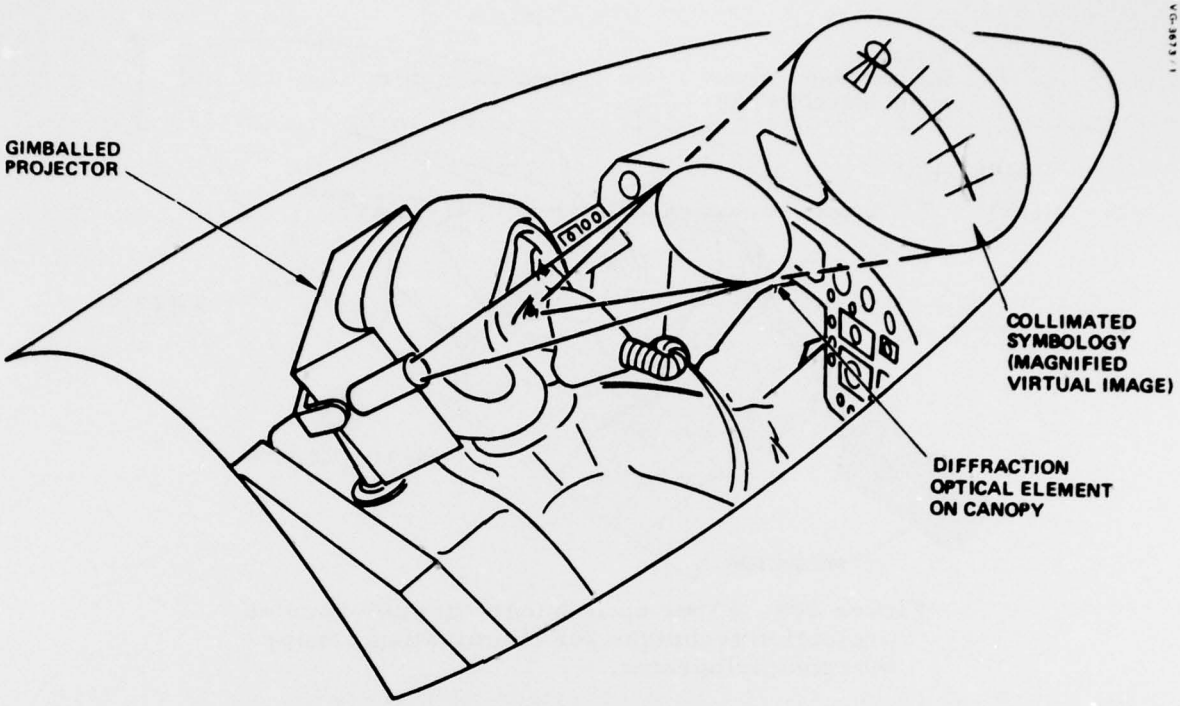


Figure 107. Headrest mounted projection technique for illuminating holograms on canopy.

separate HOE. The accomplishment of this would require a very complex geometrical compensation network. In addition, the area around the pilot's head may not be the ideal location for image sources serving all parts of the canopy. The image source has to be large enough to cover the field-of-view of the most distant HOE, which makes it upwards of 4 inches in diameter.

6.3.2 Fiber Optics Coupler

Another approach considered was the incorporation of a projector or image source which has its last optical element mounted on the top of the helmet, the balance of the projection system being mounted elsewhere and optical connection being made via a flexible fiber optics bundle. This concept is shown in Figure 108. Basically, the same optical drawbacks exist with this system as exist with the gimbaled headrest approach, namely variable compensation for geometrical distortion and the existence of fixed, discrete pointing angles. The extra weight on the pilot's helmet is considered a serious drawback. In addition, the fiber optics bundle and the requirement for a special, captive helmet creates

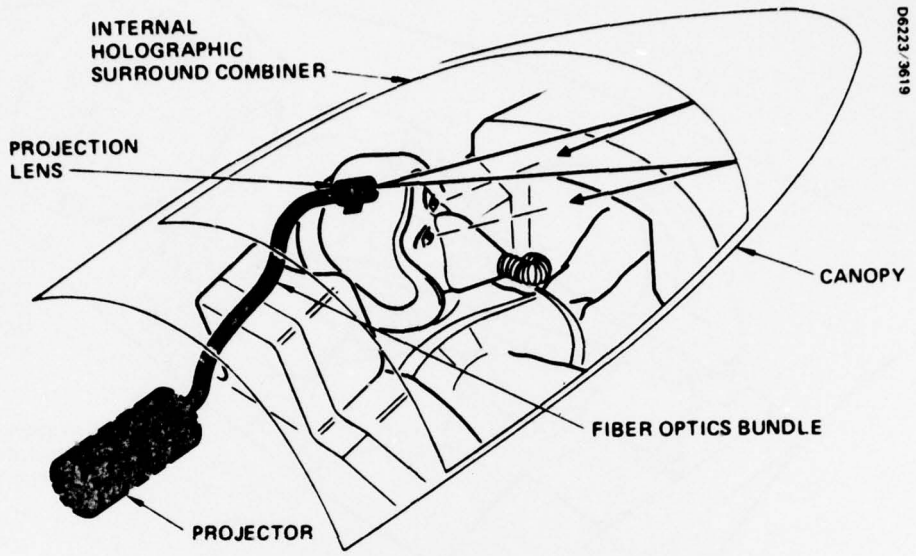


Figure 108. Fiber optic bundle-helmet-coupled projection technique for illuminating canopy mounted holograms.

additional problems pertaining to systems alignment and possible seat modifications.

It must be again pointed out that system approaches which incorporate a single source for multiple HOE, provide no backup capability in the event of a display source failure; an unacceptable situation.

A third system which was proposed, illustrated in figure 109, removed everything from the helmet except a battery operated infrared (IR) source projector. Instead of relying on a headrest-to-helmet coupling to orient the image source with the hologram, a pair of image sources (larger to achieve reasonable pupil size), with IR sensors are mounted to the seat backrest. These projectors follow the head locating beam and illuminate the HOE in the sensed field of view. Dual projectors are used to cover both sides of the cockpit and provide dual coverage in the forward area. If a source malfunctions, a backup display is present in the forward area. Again, the basic drawback to the headrest projector, i.e., alignment with selected areas, exists, although the fore-and-aft head motion problem has been eliminated.

An ever-present problem with these scanning systems is stray light, both in the aircraft and outside.

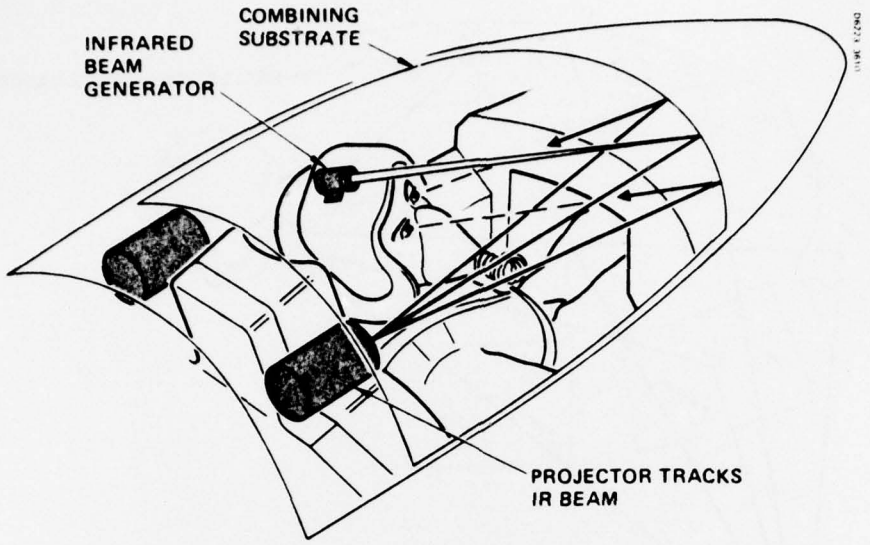


Figure 109. Infrared source-slaved projection technique for illuminating holograms on canopy.

6.3.3 *Single, Multistate Projector*

An early concept, perhaps the last of the single projector proposals, is shown in Figure 110. The underlying reasoning for this configuration was that of maintaining reasonable symmetry in the observer/source plane and, at the same time, using a single, centrally located image source. The source was to be located in a console between the pilot's legs. Information as to the pilot's visual angle was sensed and caused the image source to rotate, tilt and otherwise change state to provide displayed information from the appropriate HOE. Briefly, the drawbacks were: 1) excessive bend angle, 2) interference with the HUD (the HUD protrusion and combiner obscure the central HOE), 3) impracticality of the multistate projector (not impossibility), and 4) probable lack of space in the desired location.

6.4 CONCLUSION

The technical problems associated with the Diffractions Optics study have imposed major compromises on the end results. In retrospect, the canopy geometry coupled with the limited space in the cockpit almost precluded arrival at a compromise solution, much less a satisfactory one. In spite of this, it has been shown that there are isolated cases where one can achieve acceptable imagery with a canopy-based diffraction optics system.

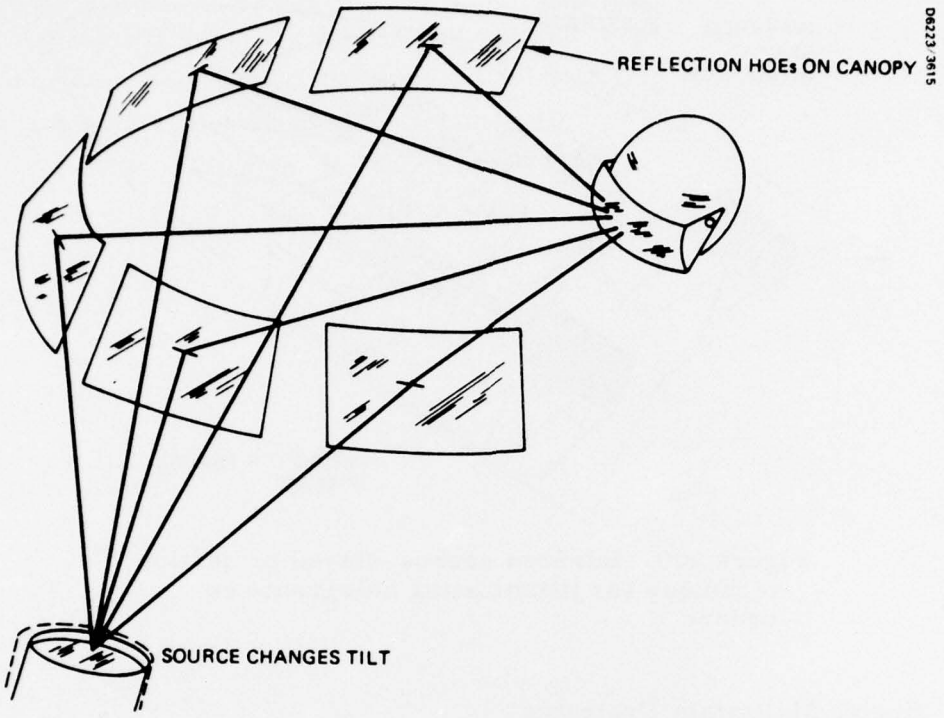


Figure 110. Concept for multiple line of sight coverage by a single source.

Section 3 pointed out the advantages of having such a system while Sections 5 and 6 point out that there are indeed solutions to the problem. Whether or not the technology can be married with the constraints of a modern fighter aircraft to produce viable results cannot be determined in this feasibility study. At this point, the tradeoff must be made whether to pursue this present line of thinking or revert back to the more viable, Helmet-Mounted Display as an operator-centered concept. If a canopy mounted Diffraction Optics system does provide the desired results, the guidelines for continued study may be extracted from the results contained in this report.

6.5 RECOMMENDATIONS

The information presented thus far has brought to light difficulties which limit the feasibility outlooks for both the diffraction optics canopy concept and the diffraction optics visor concept. It can be safely said that the baseline visor HOE concept suffers from a fundamental drawback - its high diffraction efficiency at many wavelengths leading to the objectionable spectral flare problems. Eliminating the rainbow of images without adversely affecting the see-through characteristics poses a difficult, if not insoluble problem. A second, major problem involves the shift in collimation of the image as the visor-to-CRT spacing changes. This second problem is inherent for conventional as well as diffraction optic systems. The concept of employing a helmet-mounted display with a variable display-to-hologram spacing is not a workable one if the head is moved about.

The reflection system's problems are more easily dispensed with. Optical designs are possible which will produce good imagery if there are sufficient degrees of flexibility in the system to permit adjustment of the more significant variables and permit "tuning" of the optical design. Given a fixed geometry, a fixed canopy shape and simple, relayless holographic optical systems which provide no correction capacity, the optical designer is literally at the mercy of first-order optical theory.

The usefulness of the supplementary display rationale has been identified. The need definitely exists for a system of this type in the next generation of fighter aircraft. Recommendations of follow-on effort are as follows.

6.5.1 Helmet Mounted Display

The difficulties encountered when the hologram-to-object spacing is allowed to vary, reinforces the argument that placing the display source back on the helmet and immobilizing the geometry of the optical system in a superior concept. Steps to be taken are in developing smaller, lighter sources and wider FOV holographic visors. An alternate concept could use a fiber bundle to relay the image of a one-inch CRT to the helmet. This idea also has some weight-saving features.

It is recommended that the next step be directed toward the improvement of the HMD in attaining lighter, more compact assemblies.

6.5.2 Canopy Display

In the early stages of the canopy display study, it was felt that a separate substrate for the holograms would permit greater flexibility in optical design and yield better performance than a canopy shape. The flavor of the feasibility study, however, was not to design a special optical system, but, rather to attempt to solve the problem within the restrictions of a baseline cockpit enclosure.

Now that the implication of the canopy shape on the optical performance of the HOE systems has been quantified, the departure from the canopy to a more suitable substrate geometry can be defended.

The recommended next step is the design of a wide coverage system allowing the substrate shape to be a design variable. The achievement of good image quality can have a high probability of success based on previous experience. The integration of the optimum substrate shape into various cockpits and the placement of display sources is addressable using definitive airframe data and specific display requirements. Work directly related to the solution of this problem is in process under various extended field of view HUD studies using diffraction optics. The canopy display problem is simply an expansion of those studies and the outlook for a workable solution is optimistic.

APPENDIX A
MISSION ANALYSIS FUNCTIONAL FLOW BLOCK DIAGRAMS

A. 1 FUNCTIONAL FLOW BLOCK DIAGRAMS (FFBD's)

FFBD's were generated as a means of subdividing the Missions into Mission Segments. These diagrams (Figures A-1 through A-15) follow the conventional format with a few exceptions as follows:

1. AND and OR "gates are always trailing. They require multiple or alternative completion, respectively, of the preceding functions to proceed to the next function. Thus, the diagram flow represents a time flow. Branches which terminate in an AND gate show functions which are required in the same time period. Branches which terminate in an OR gate indicate alternative functions for a given period. However, the alternatives (in time flow) are not alternatives in system capability. All of the functional alternatives (in time flow) are requirements, although they are never required simultaneously.
2. The first, or leftmost, block in each diagram indicates the function preceding the one which is diagrammed. The function being diagrammed is indicated by the "floating" block above the input arrow.
3. Small black squares in the upper righthand corner of a block indicate that the block is subdivided (diagrammed) on another sheet. Blocks without squares are not detailed below the level shown.

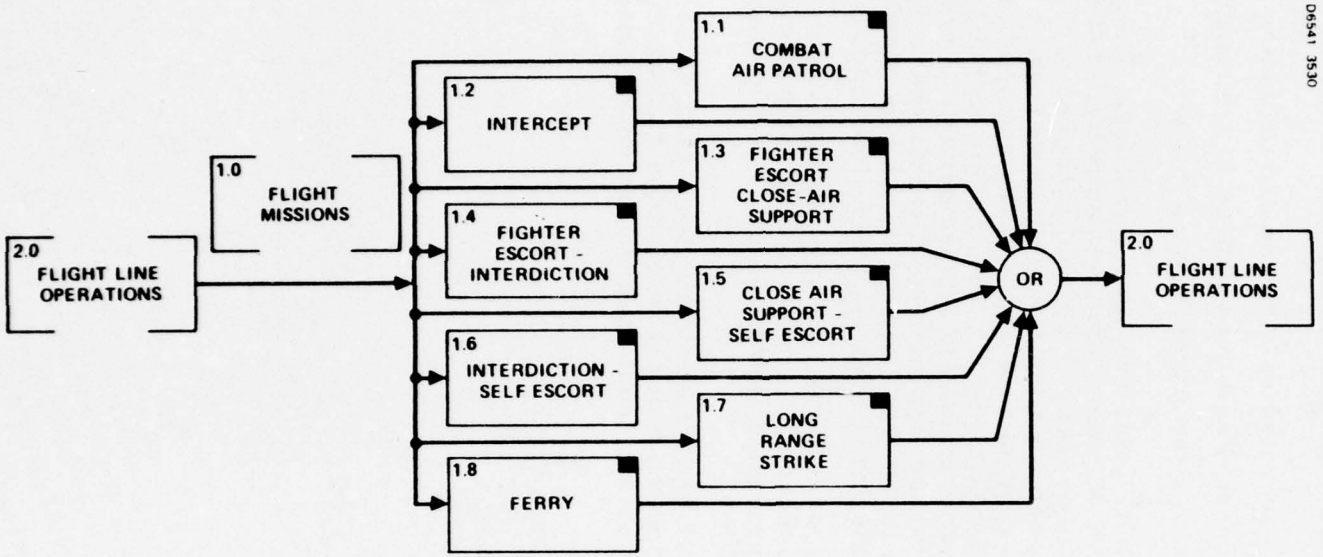


Figure A-1. Flight missions.

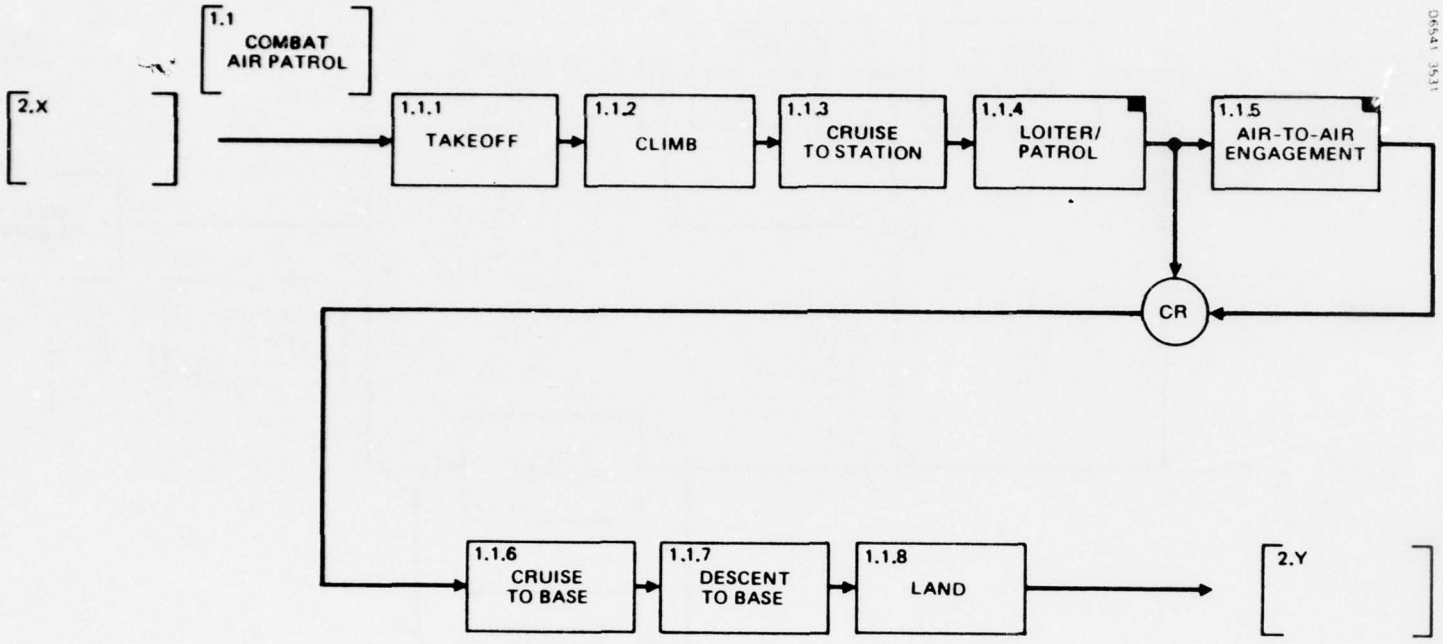


Figure A-2. Combat air patrol.

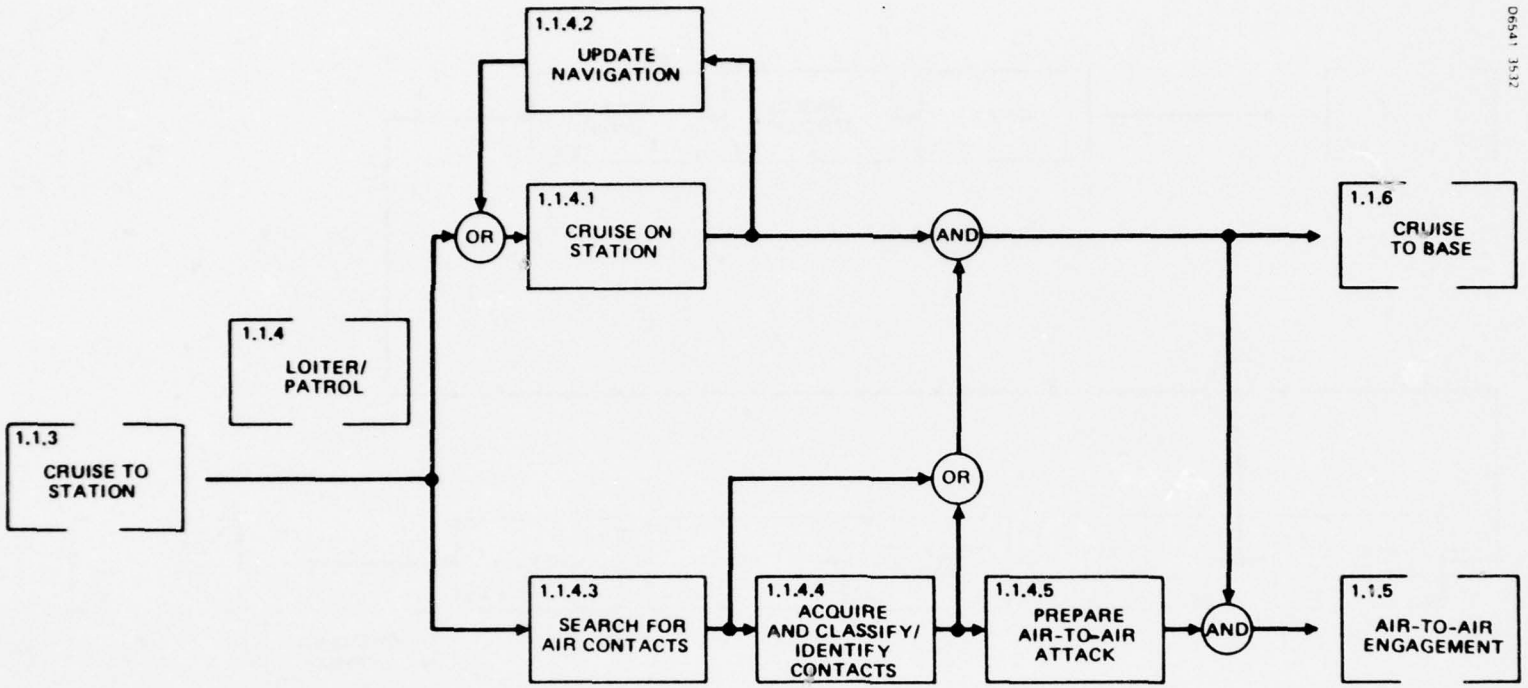


Figure A-3. 1.1.4 loiter/patrol.

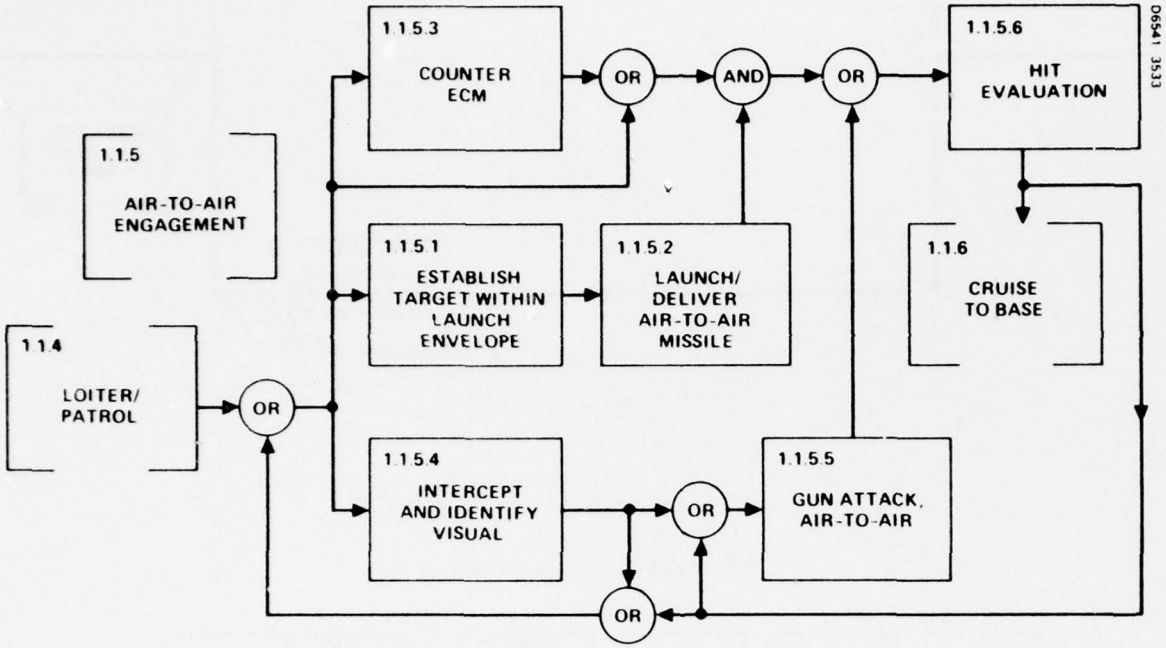


Figure A-4. Air-to-air engagement.

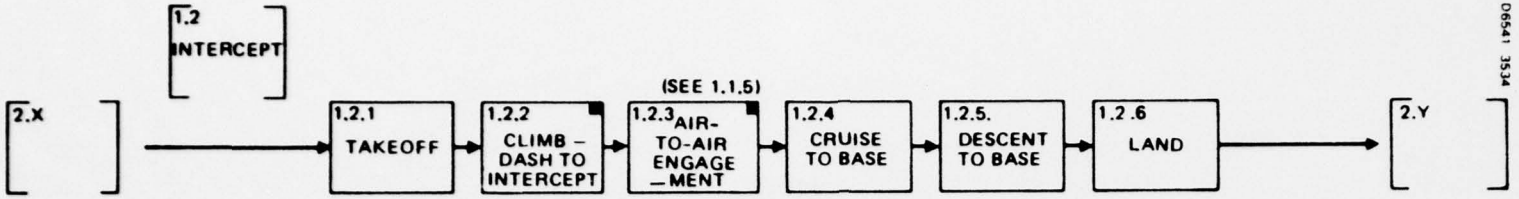


Figure A-5. Intercept.

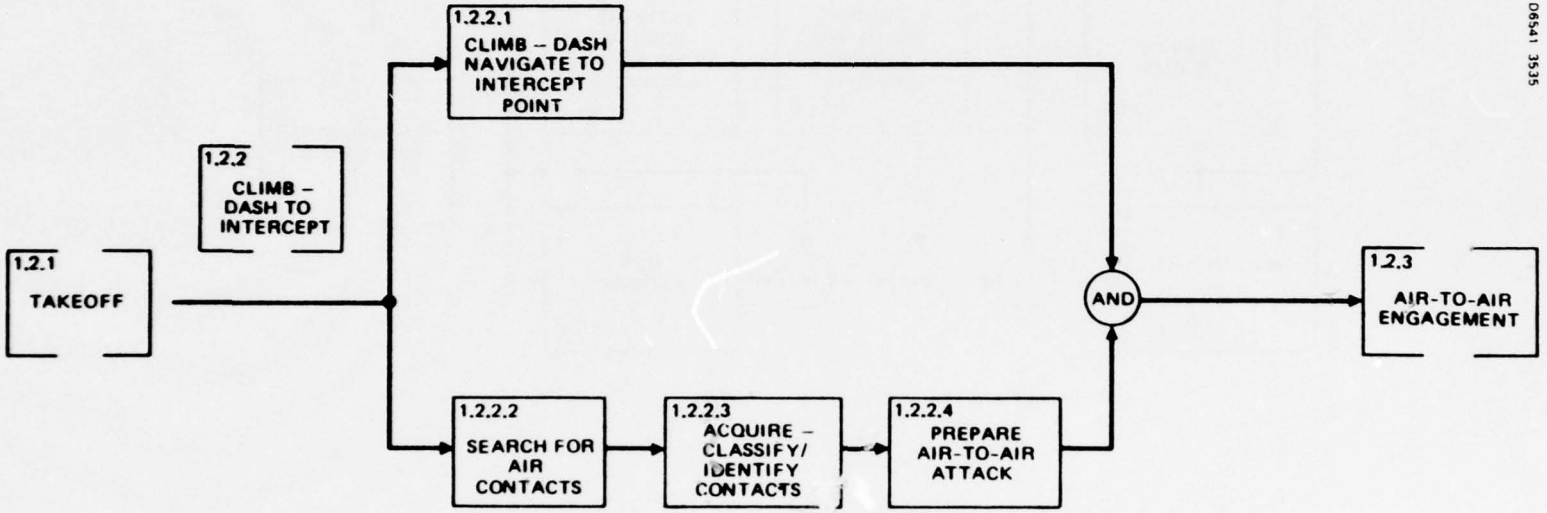


Figure A-6. TT climb-dash to intercept.

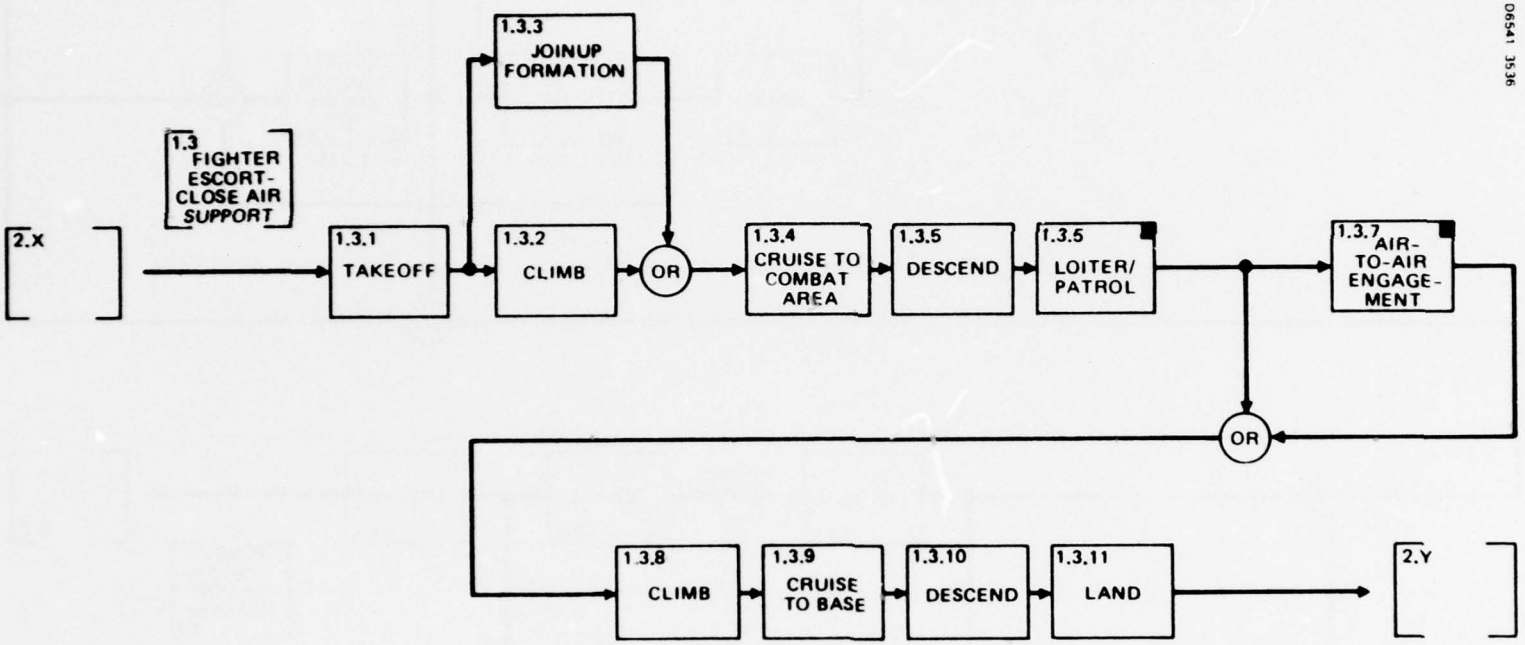


Figure A-7. UU fighter escort - close air support.

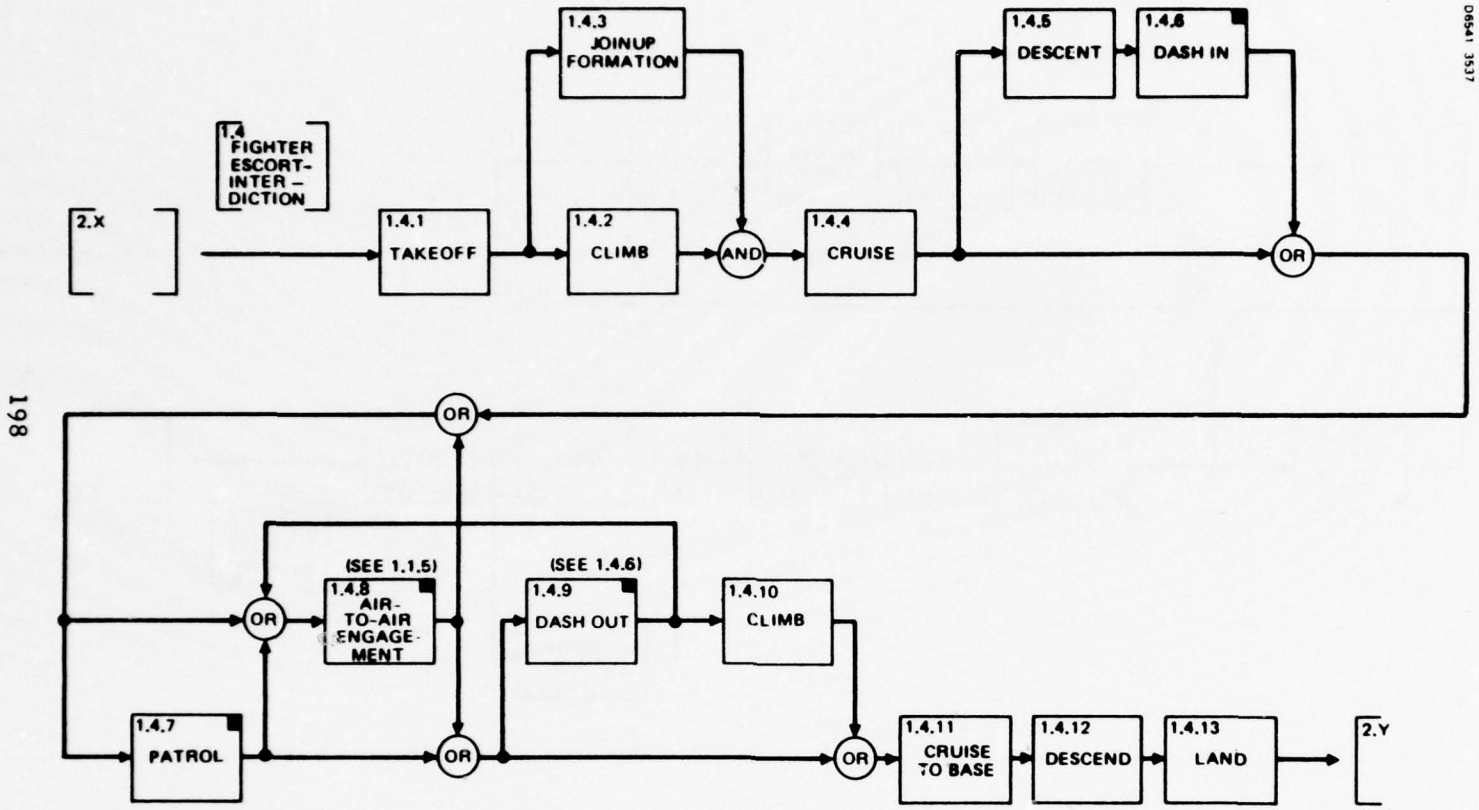


Figure A-8. VA fighter escort - interdiction.

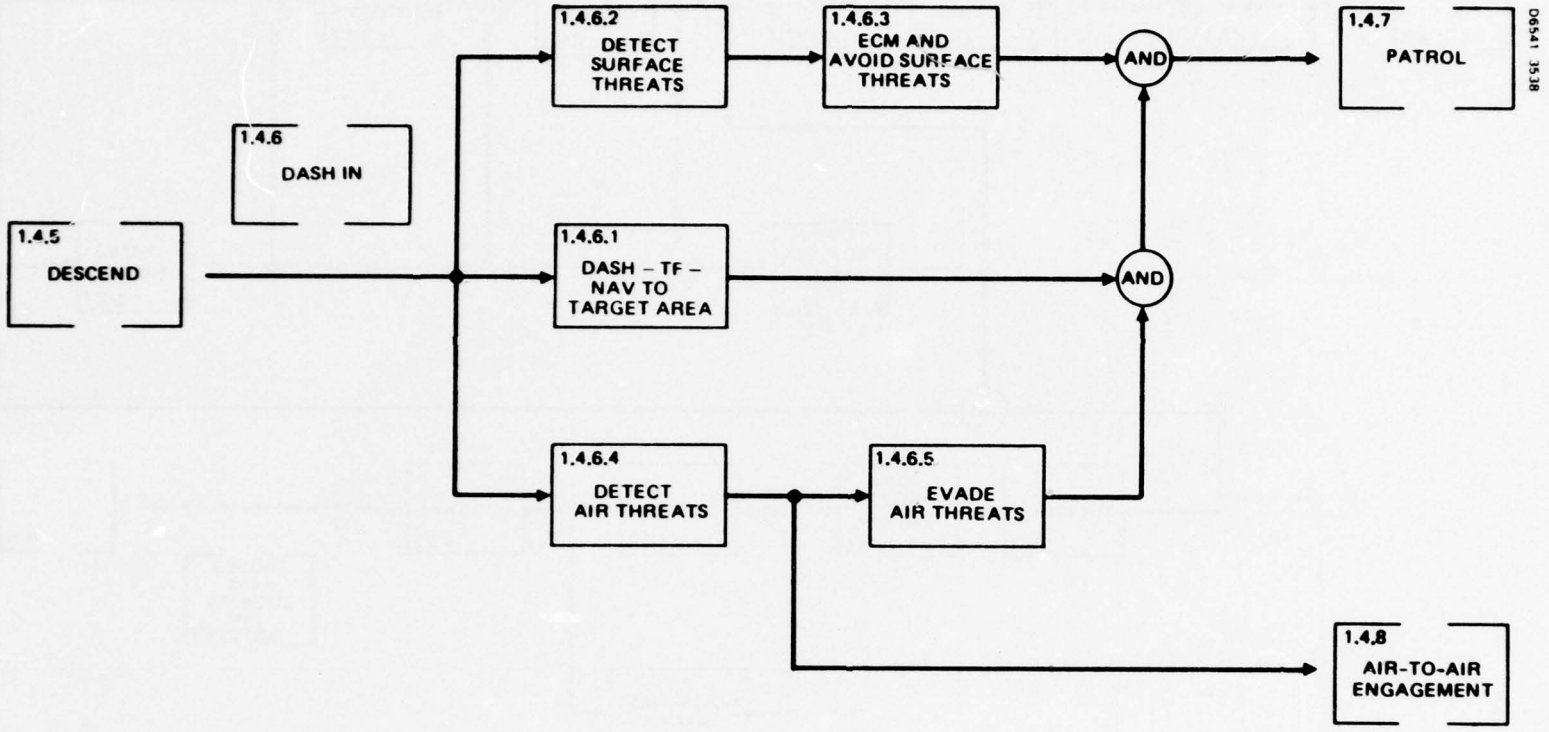


Figure A-9. WW dash in.

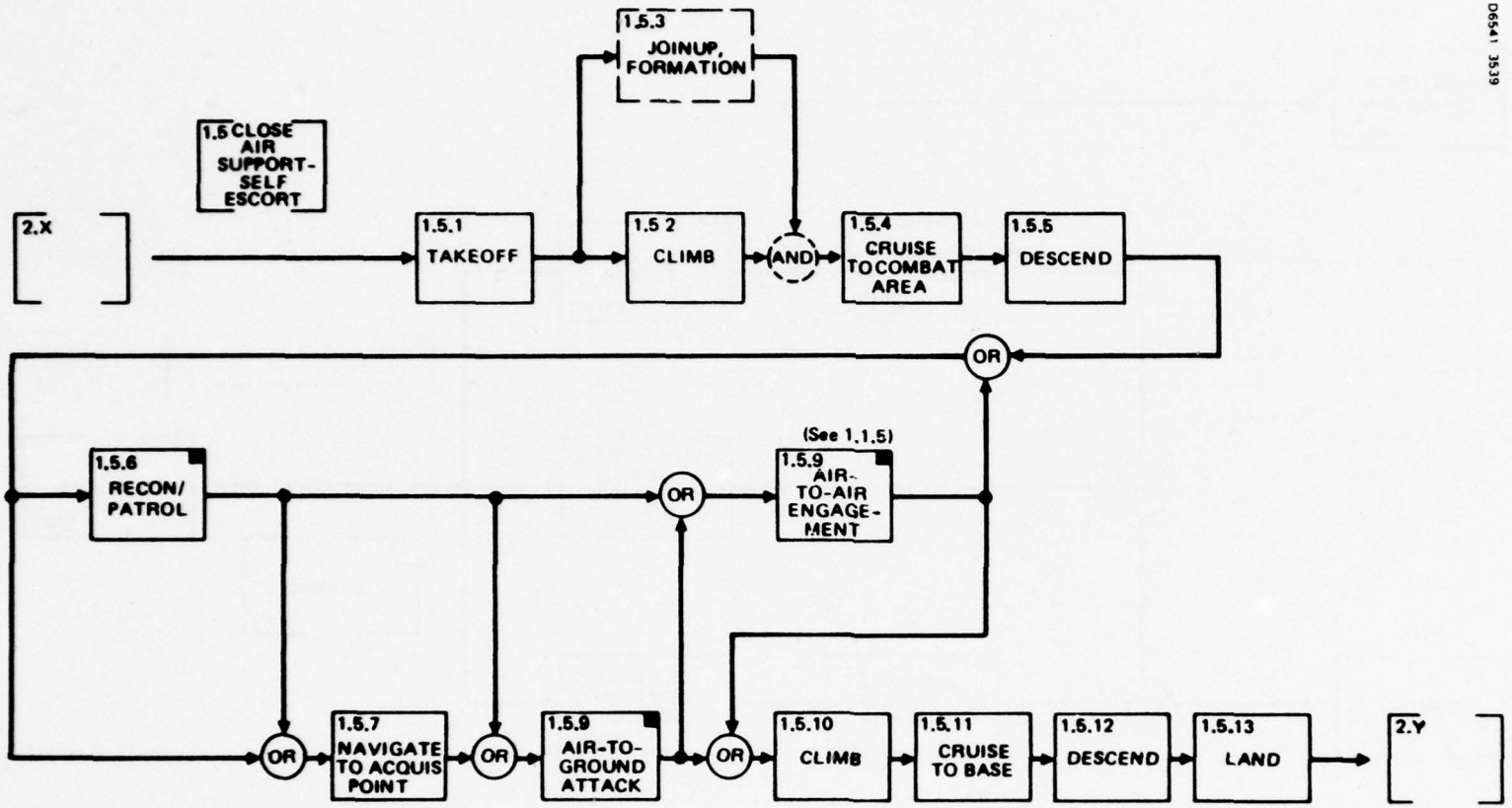


Figure A-10. XX close air support - self escort.

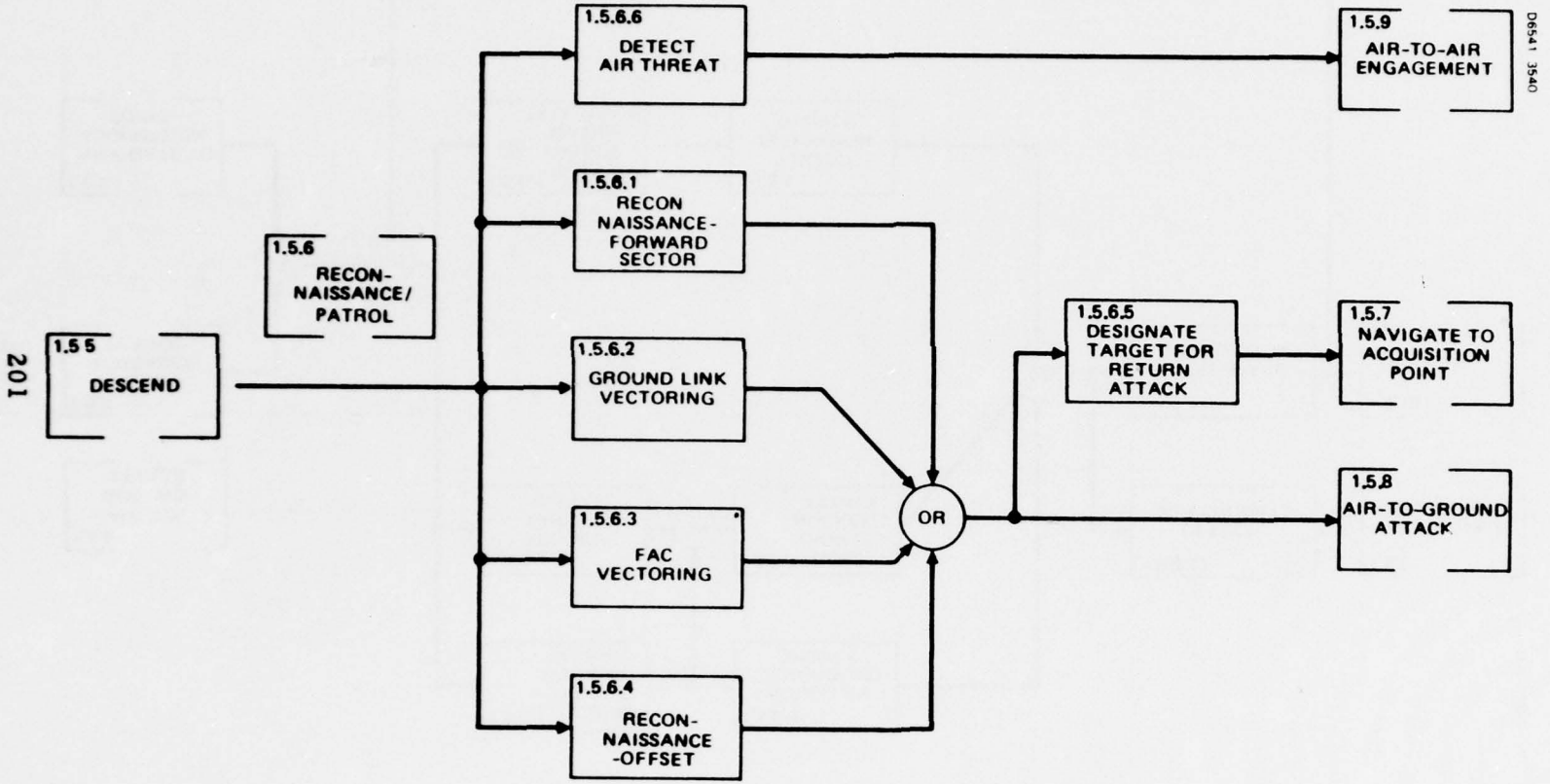


Figure A-11. YY reconnaissance/patrol.

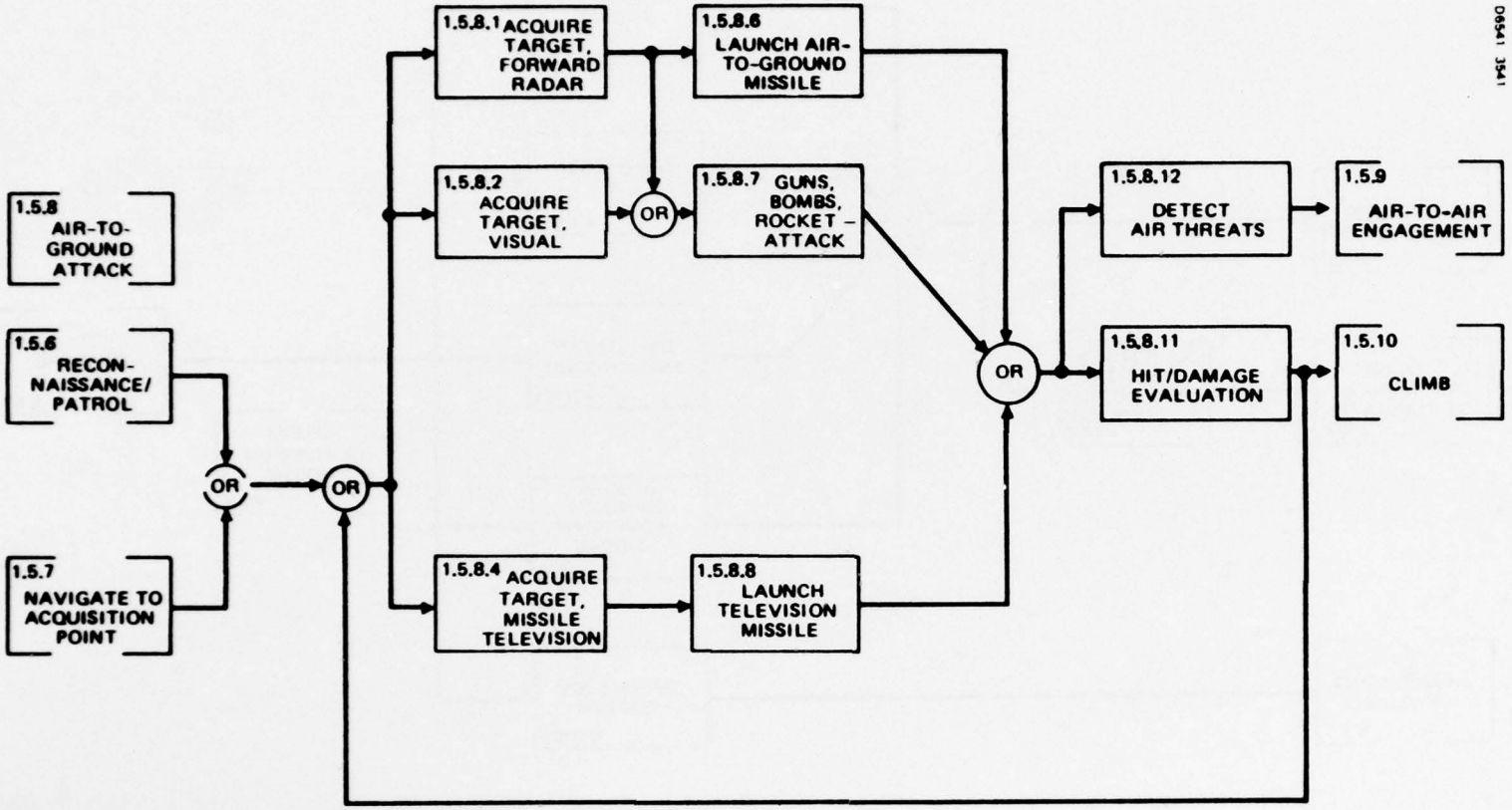


Figure A-12. ZZ air-to-ground attack.

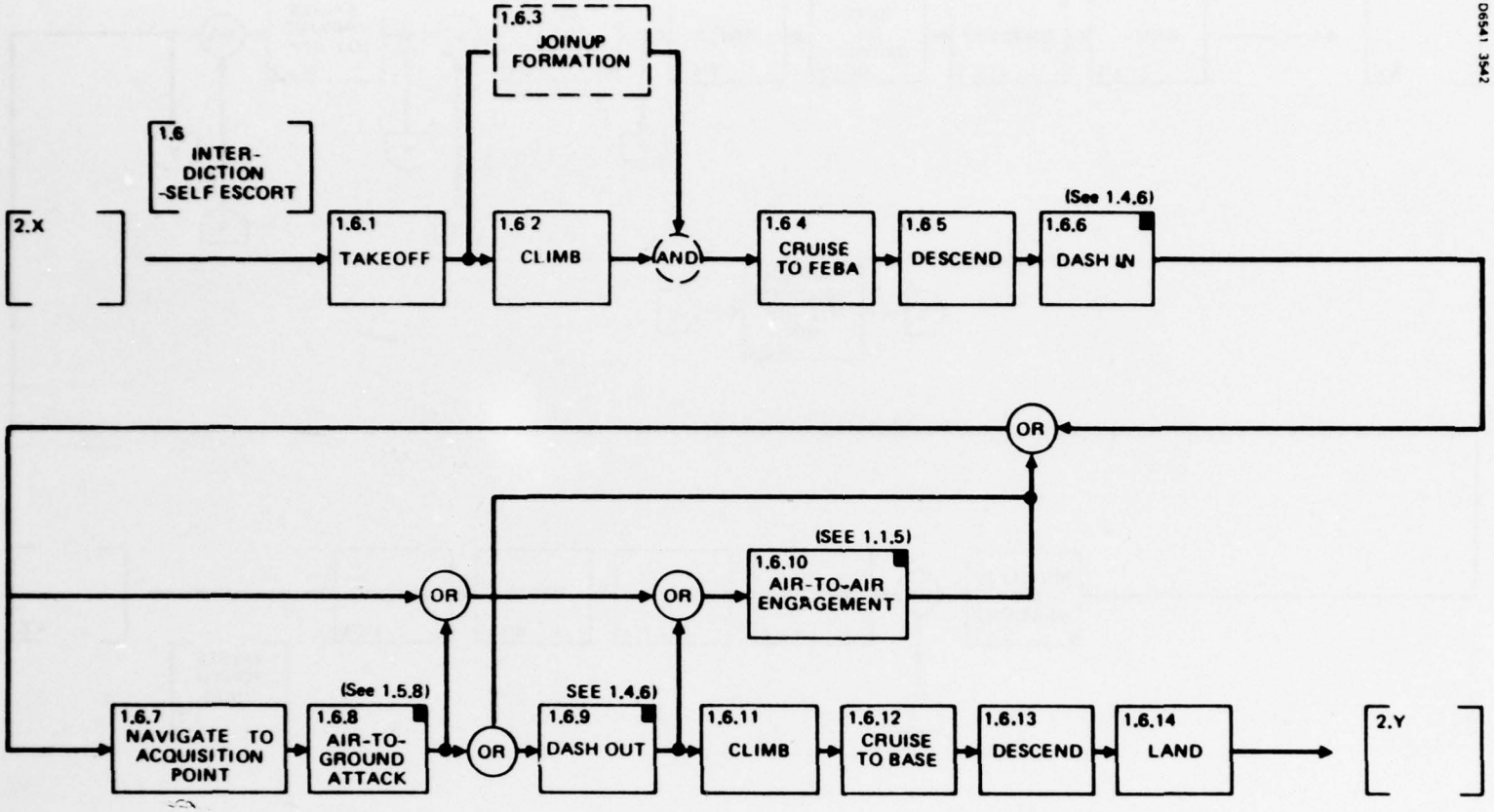


Figure A-13. ZA interdiction - self escort.

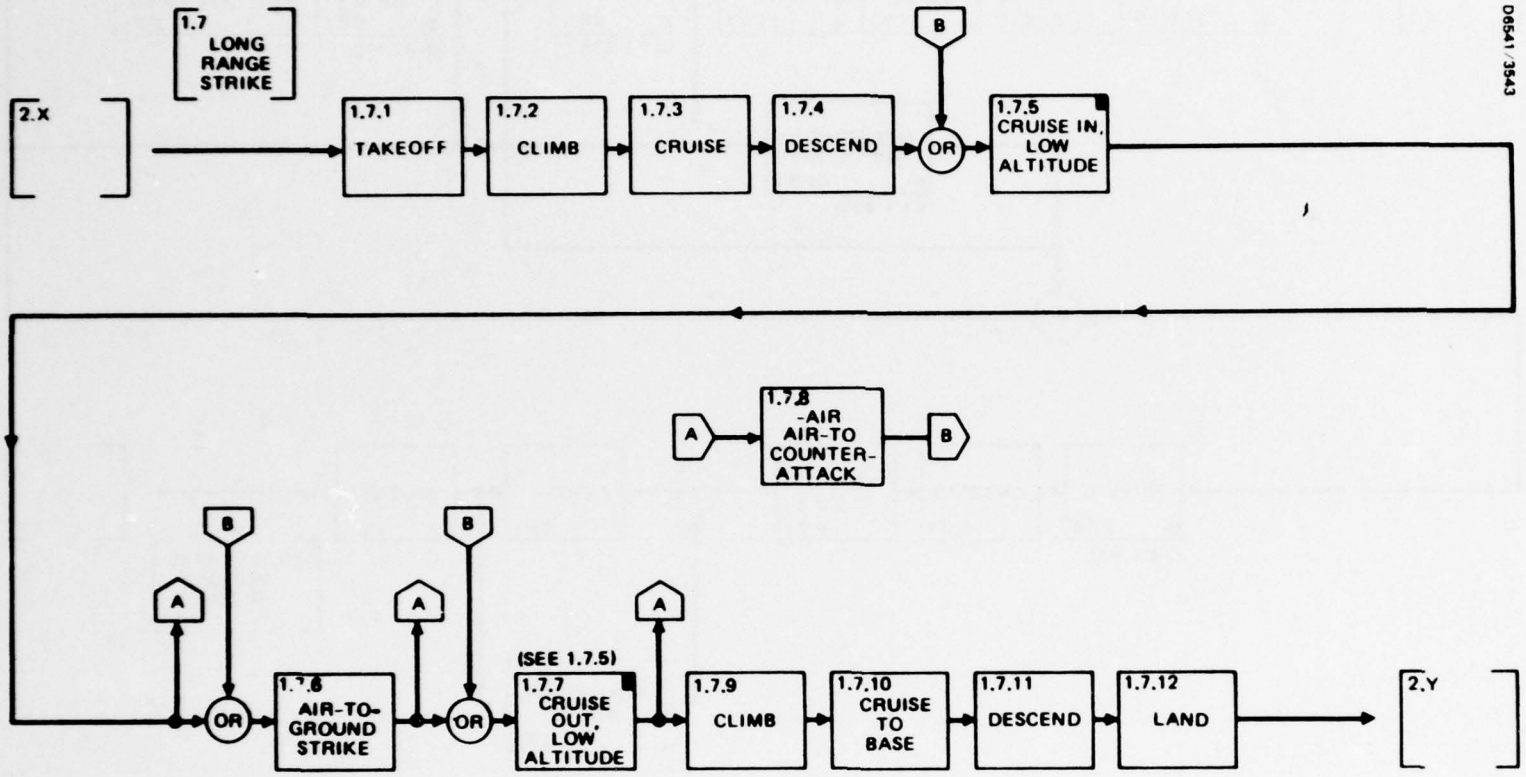


Figure A-14. Long range strike.

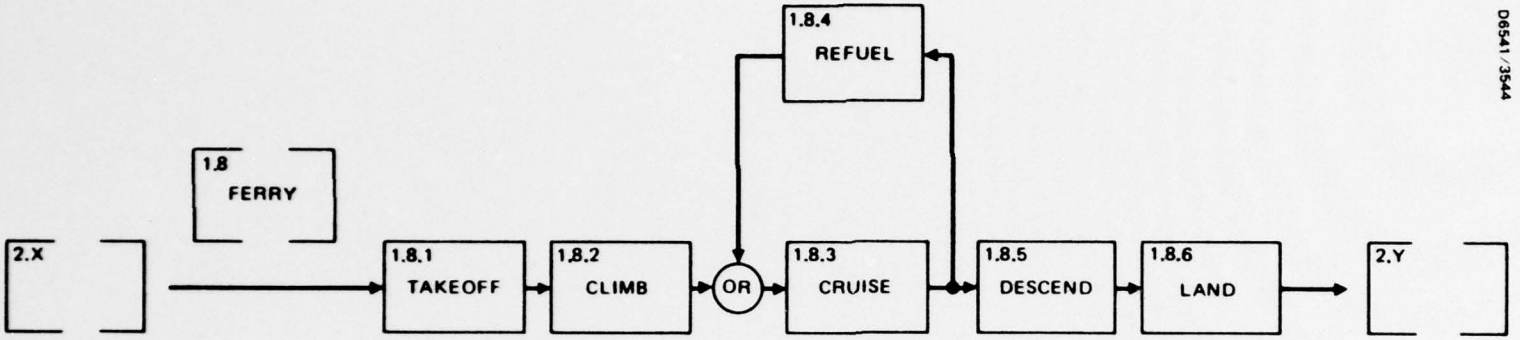


Figure A-15. 1.8 ferry.

APPENDIX B
LIQUID CRYSTAL MATERIAL CHARACTERISTICS

B.1 INTRODUCTION

Liquid crystals (LX's) are organic substances and, as the name implies, over a specific range of temperature act like liquids, while retaining some properties of crystals. Below the liquid crystal temperature range, the material becomes solid; above this range, it loses its crystalline properties and behaves like a true liquid. In the intermediate LX range, however, it passes through a turbid liquid state, which is termed the mesomorphic or "liquid crystal" state. The molecular arrangement in the liquid crystal state is more orderly than in the liquid state but less orderly than in the solid state.

The temperature range for the liquid crystal state varies with liquid crystal materials, and considerable effort has been devoted to developing materials which have liquid crystal properties over a wide range of temperatures, including normal room temperature.

Liquid crystals have been classified in three basic categories: nematic, smectic, and cholesteric. The terms denote characteristic spatial configurations assumed by the molecules of these materials. While the molecules of cholesteric LX's are optically active, those of nematic and smectic LX's are generally optically inactive, (i.e., they do not rotate polarized light).

Nematic LX's consist of rod-like molecules aligned in parallel, similar to matches in a box; it is this type of material that is presently used in the Hughes LX display. Each molecule can rotate only around its long axis and has limited freedom of movement from side to side or up and down (Figure B-1a). The smectic LX's have a layered arrangement. The layers can

PRECEDING PAGE BLANK-NOT FILMED

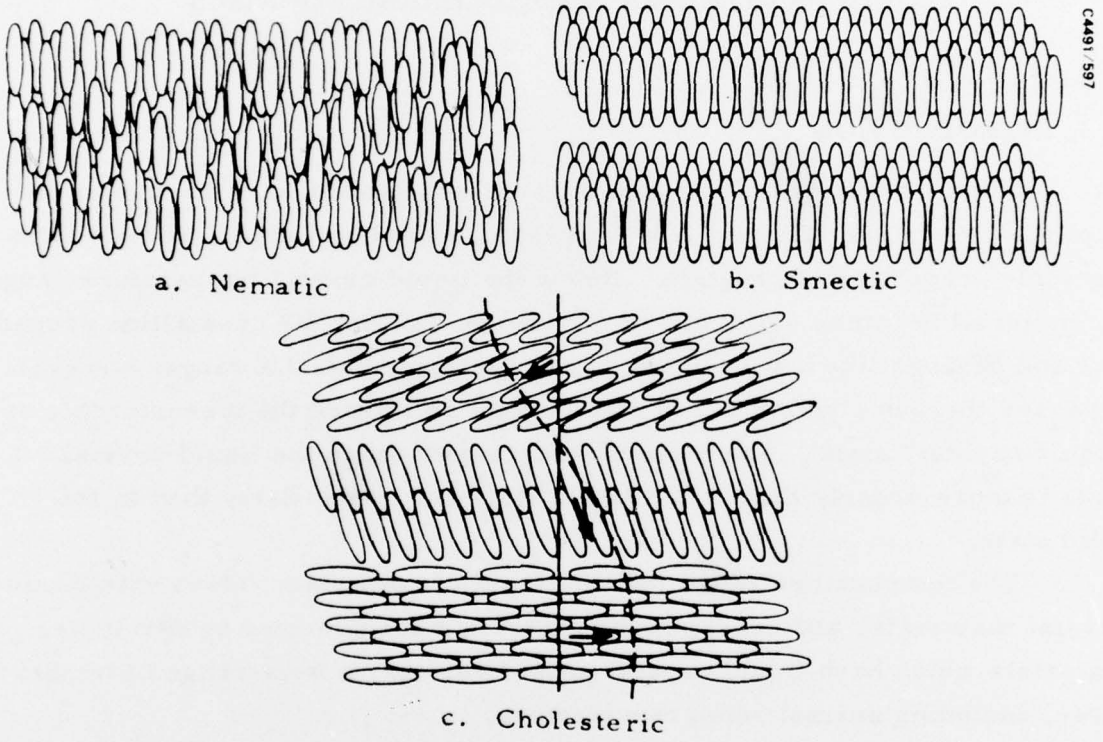


Figure B-1. Diagrams of packing effects in liquid crystals.

slide over one another, because the molecules in each layer can move from side to side or forward and backward but not up and down. Within each layer, molecules may be ordered in ranks (Figure B-1b) or randomly distributed. The cholesteric, like the smectic, LX's consist of layers. Within each layer, however, the molecules are parallel, as are the nematic molecules. Molecules in one layer influence the layers above and below, so that the long axes of the molecules in these layers are displaced slightly and a helical pattern forms from layer to layer (Figure B-1c).

A very important property of liquid crystals is the dielectric anisotropy eq. B-1, a quantity used to describe the orientation of liquid crystal molecules in the presence of electric fields.

eq. B-1 $$\Delta\epsilon = \epsilon_{\parallel} - \epsilon_{\perp}$$

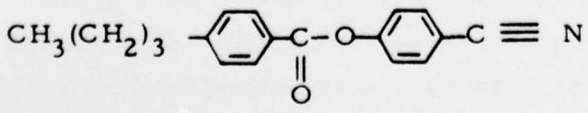
where:

$\epsilon_{\parallel}$ = dielectric permittivity in a direction parallel to the long axis of the LX molecule

$\epsilon_{\perp}$ = dielectric permittivity in a direction perpendicular to the long axis of the molecule

Eq. B-1 describes the <u>static</u> dielectric behavior and is most useful in evaluating the molecular behavior or figure of merit for LX materials utilized for display purposes.

In general, when $\Delta\epsilon$ is positive, the molecular axis aligns roughly in the direction of an electric or magnetic field, whereas when $\Delta\epsilon$ is negative, the molecules orient themselves at an angle roughly perpendicular to the field. For the molecules of the LX substances used for airborne display, only the electric field strength is of interest. The dielectric anisotropy is a function of the vector sum of the dipolar groups in the molecule. To prepare an LX with a strongly positive $\Delta\epsilon$, for example, it is conventional to introduce the strongly dipolar nitrile group at the end of the long axis of the molecule, as in



Individual properties of each of the types of LX's have been utilized in making displays. The properties associated with each type of LX material are listed below.

NEMATICS:	Dynamic scattering Field effects (1) Twisted Nematic (2) Birefringent color switch (3) Nematic dichroic dye interaction
CHOLESTERICS:	Reflective color displays (1) Temperature sensitive (2) Pressure sensitive (3) Chemical vapor sensitive (4) Electric field sensitive
SMECTICS:	Thermo-optic storage display
HYBRIDS:	Thermo-optic Cholesteric-nematic phase change

B. 1. 1 Dynamic Scattering Mode (DSM)

Briefly, DSM may be characterized by electrical current – field induced hydrodynamic motion. Nematic LX's are optically anisotropic (i. e., they have different refractive indices for directions parallel to and perpendicular to the long axes of the molecules.) The effect of applying a voltage to and passing a current through a typical LX cell (see Figure B-2) is to disrupt the normally uniform molecular orientation in favor of a large number of small regions (domains) whose molecular orientation is different from those of their neighboring domains. The effect on light passing through the cell is that of closely spaced refractive index boundaries. These index boundaries refract the light at various angles (i. e., scatter it). The result is a system that is optically homogeneous and transparent when no voltage is applied and highly diffusing or scattering when voltage is applied.

DSM can be activated by either AC or DC signals. When AC is used, the frequencies are typically less than 1 KHz. The voltage value is dependent upon the material constituency and classification and ranges from

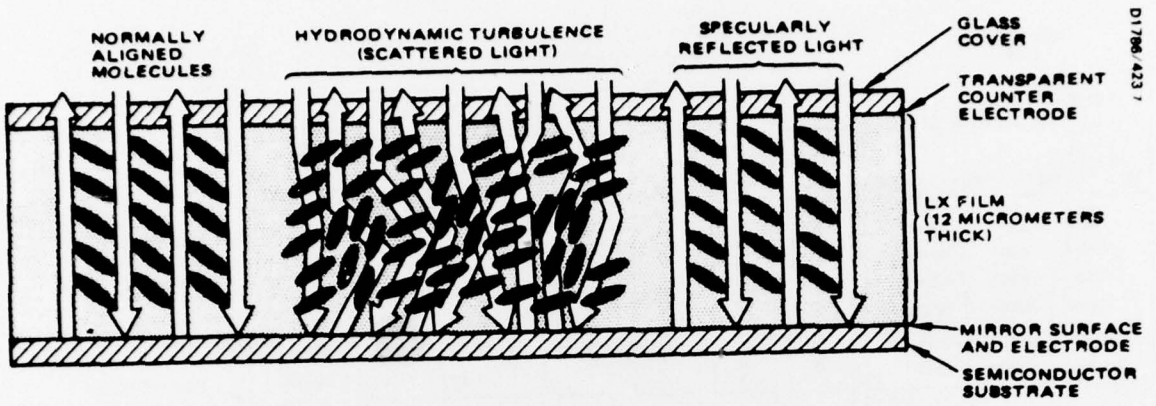


Figure B-2. Nematic LX shown in dynamic scattering mode (DSM)

0.5 volt to 60 volts. In the Hughes LX matrix display, the excitation is unipolar and of varying amplitude (22 volts or less) depending upon video scene content. An AC bias of 60 volts peak to peak amplitude and appropriate frequency (depending upon material constituency) helps return the molecules to their normally aligned state after the excitation is removed.

B.1.2 Field Effects

Another way to take advantage of the sympathetic alignment and the optical anisotropy of nematics is the twisted nematic configuration shown in Figure B-3. The design of the twisted nematic cell is the same as for the DSM, except that the cell walls are treated to make long axes of the LX's parallel to the plane of the cell wall. As result, on each cell wall the long axes of the LX molecules are parallel to each other as well as to the plane of the cell wall. The cell is assembled to form an angle of 90° between the direction of the long axes of the LX's on one wall and the corresponding direction on the other wall. Calculations show that the orientation of the long axes of the molecules varies smoothly across the cell thickness from one orientation to the other. Hence, the name twisted nematic.

If light incident on the cell is plane polarized either along the direction parallel to the long molecular axis or perpendicular to it, the plane of polarization of the light emerging from the other side of the LX cell is rotated 90°.

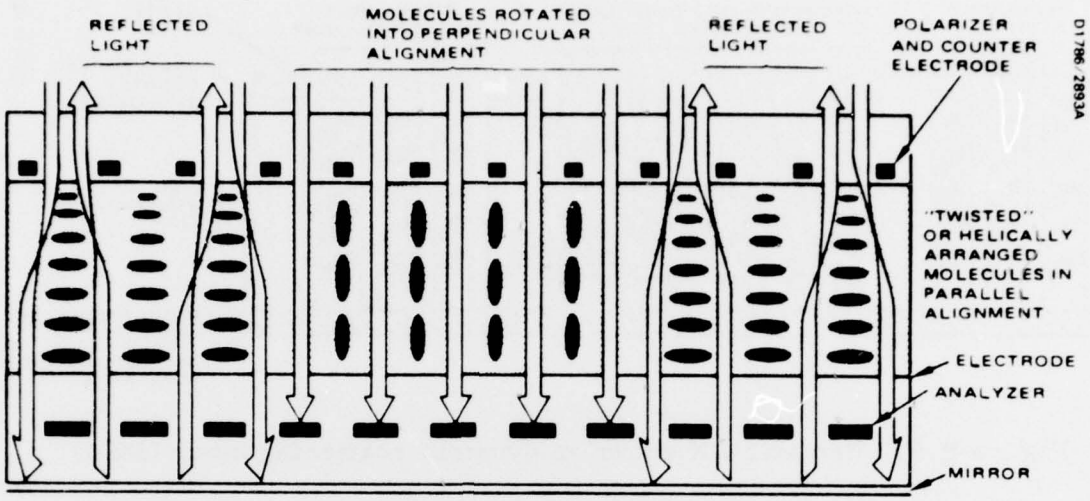


Figure B-3. Twisted Nematic LX shown in field effect mode.

When viewed through a polarizer oriented normal to the analyzer, this emerging light is observed to pass through the polarizer. However, if a field of sufficient strength (typically a few volts) is applied to the cell, light is blocked by the analyzer. The reason is that the molecules in the bulk change their alignment with the cell wall from parallel to perpendicular. As a result, no rotation of the plane of polarization of the light occurs when the field is applied. Since the analyzer is aligned normal to the polarizer, light is now blocked. Thus, by using a linear polarizer and analyzer in conjunction with a twisted nematic configuration, the intensity of the transmitted (polarized) light can be modulated with an electric field; hence the term "field effect," as opposed to DSM which is a current induced effect.

In their present state of development, nematic materials operated in the dynamic scattering mode, offer the most promising application to the matrix display technique described in this report. However field effect operation would be equally desirable if there were a practical method of applying a polarizer to the reflective surface of the matrix display substrate.

APPENDIX C

CANOPY GEOMETRY CHARACTERISTICS

In order to study the suitability of the F-16 canopy as a holographic substrate, the shape of the canopy required mathematical description. A computerized ray trace program was then employed to determine the strike point and the angle of reflection for any incident ray.

The mathematical shape of the canopy was derived from a scaled drawing which was supplied with the program statement of Work (see Figure C-1). Numbers scaled from this drawing were related to the coordinate system in Figure C-2 and injected into the computer. The computer mapped the data into a surface which was used as the basis for the ray trace program.

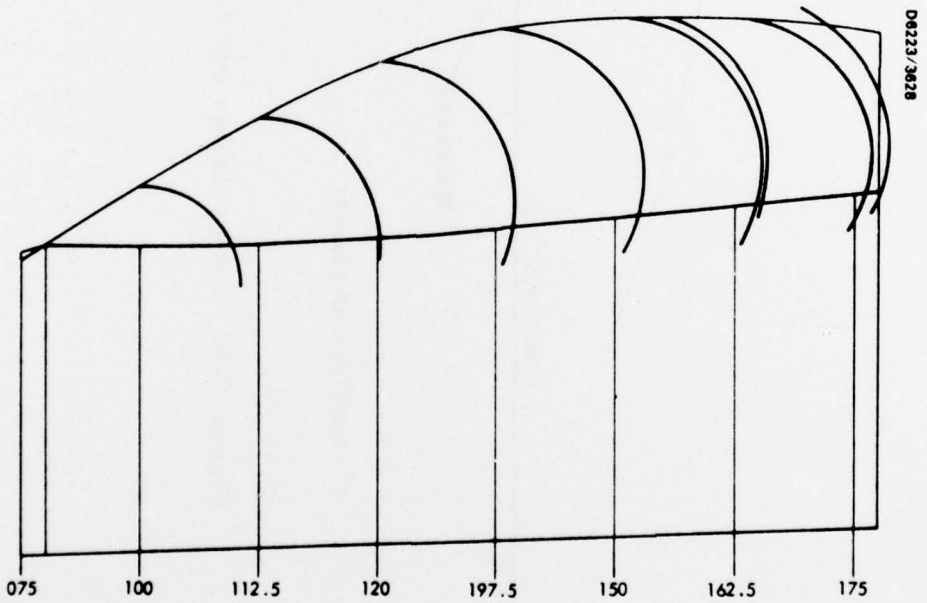


Figure C-1. F-16 canopy geometry.

Table C-1 contains the scaled data as it was inserted into the mapping program. At each z point along the fore and aft axes of the aircraft, the height y of the center of the canopy radius, the canopy radius and the sill height were specified.

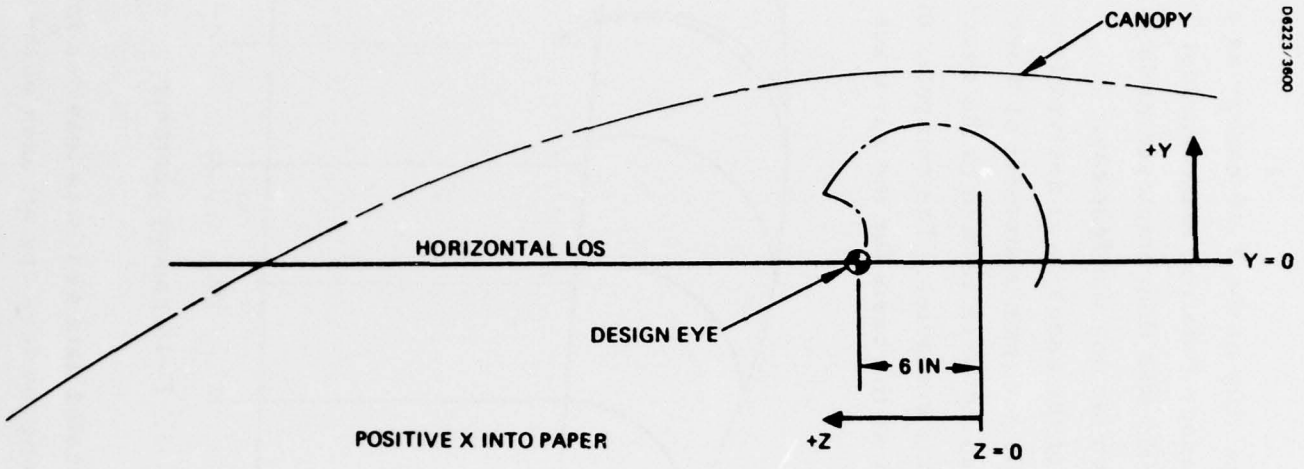


Figure C-2. Canopy design eye coordinate system.

TABLE C-1. F-16 CANOPY GENERATIONS

Z, INCHES	CANOPY RADIUS, INCHES	Y, CENTER OF RADIUS, INCHES	Y, SILL, INCHES
0	15.88	-6.76	+11.87
1.25	15.88	-6.88	-12.0
2.50	15.75	-6.88	-12.12
3.75	15.75	-7.75	-12.25
5.00	15.75	-7.12	-12.37
6.25	15.75	-7.25	-12.5
7.50	15.75	-7.5	-12.56
8.75	15.75	-7.75	-12.63
10.0	15.63	-7.88	-12.75
11.25	15.5	-7.87	-12.87
12.5	15.38	-8.00	-13.00
13.75	15.38	-8.26	-13.12
15.0	15.25	-8.62	-13.25
16.25	15.13	-8.88	-13.37
17.5	15.13	-9.25	-13.5
18.75	15.0	-9.62	-13.5
20.0	14.88	-9.88	-13.62
21.25	14.75	-10.12	-13.62
22.5	14.5	-10.37	-13.75
23.75	14.25	-10.62	-13.75
25.0	14.0	-11.12	-13.87
26.25	13.88	-11.5	-13.87
27.5	13.75	-11.87	-13.94
28.75	13.62	-12.37	-14.0
30.0	13.38	-12.88	-14.06
31.25	13.0	-13.25	-14.12
32.5	12.75	-13.75	-14.12
33.75	12.62	-14.12	-14.25
35.0	12.5	-14.75	-14.4
36.25	12.38	-15.38	-14.4
37.5	12.12	-15.87	-14.4
38.75	11.88	-16.38	-14.5
40.0	11.5	-16.75	-14.5
41.25	11.25	-17.25	-14.5
42.5	11.0	-17.75	-14.62
43.75	10.75	-18.25	-14.62
45.0	10.62	-18.87	-14.62
46.25	10.6	-19.6	-14.62
47.5	10.5	-20.25	-14.62
48.75	10.44	-20.94	-14.62
50.0	10.38	-21.63	-14.62
51.25	10.31	-22.31	-14.62
52.5	10.25	-23.00	-14.62
53.75	10.18	-23.68	-14.62
55.0	10.12	-24.37	-14.62

In the following tabulation (Table C-2), the results of the canopy ray trace are presented. All rays originated at the center of rotation of the head (0, 0, 0). The elevation angle, α, is the projection of the line-of-sight ray onto the y-z plane. The azimuth angle, β, is the projection of the line of sight ray onto the x-z plane. X, y and z are the strike point coordinates at the canopy inside surface. The elevation angle after symmetrical reflection is γ and the corresponding azimuth angle is δ. Angle β was scanned in 10 degree increments from 0 to 80 degrees for each elevation angle, α, from -10 through +40 degrees.

The purpose of this exercise was to determine the direction of the symmetrically reflected rays to see if a convenient area was close to the reflected ray loci. As it turned out, the reflected rays all terminate near the center of the fuselage – probably to avoid reflections to the eye from other lighted areas in the cockpit.

TABLE C-2. F-16 CANOPY RAY TRACE RESULTS

β \ α		-10 DEGREES	0 DEGREES	10 DEGREES	20 DEGREES	30 DEGREES	40 DEGREES
0 DEGREES	Y	-7.836	0	3.991	6.127	7.269	7.91
	X	0	0	0	0	0	0
	Z	44.439	30.912	22.636	16.835	12.59	9.43
	γ	-53.205	-55.906	-55.82	-54.54	-55.79	-60.42
	δ	0	0	0	0	0	0
10 DEGREES	Y	-6.904	0	3.838	5.976	7.158	7.840
	X	-6.904	5.11	3.838	2.895	2.186	1.648
	Z	39.158	28.984	21.765	16.419	12.398	9.344
	γ	-51.888	-55.59	-55.67	-54.725	-56.149	-60.733
	δ	-23.63	-15.97	-10.114	-5.977	-3.886	-3.062
20 DEGREES	Y	-5.305	0	3.434	5.551	6.829	7.620
	X	10.950	8.927	7.089	5.551	4.305	3.305
	Z	30.085	24.526	19.478	15.252	11.829	9.082
	γ	-49.71	-54.688	-55.411	-55.39	-57.258	-61.682
	δ	-35.957	-27.727	-18.852	-12.099	-8.350	-6.683
30 DEGREES	Y	-3.958	0	2.902	4.92	6.299	7.239
	X	12.959	11.291	9.502	7.81	6.299	4.981
	Z	22.446	19.556	16.458	13.526	10.909	8.627
	γ	-49.23	-54.06	-55.69	-56.85	-59.204	-63.34
	δ	-42.328	-34.83	-26.078	-18.814	-14.116	-11.594
40 DEGREES	Y	-2.924	0	2.343	4.175	5.588	6.672
	X	13.915	12.62	11.150	9.625	8.122	6.672
	Z	16.583	15.045	13.288	11.471	9.679	7.952
	γ	-50.933	-55.024	-57.409	-59.483	-62.118	-65.797
	δ	-46.22	-40.045	-33.234	-27.023	-22.179	-18.901
50 DEGREES	Y	-2.117	0	1.812	3.372	4.723	5.89
	X	14.306	13.348	12.247	11.042	9.749	8.369
	Y	12.005	11.200	10.276	9.266	8.180	7.022
	γ	-55.09	-58.599	-61.235	-63.611	-66.154	-69.211
	δ	-50.73	-46.673	-42.292	-37.888	-33.761	-30.216
60 DEGREES	Y	-1.468	0	1.32	2.553	3.73	4.865
	X	14.426	13.75	12.999	12.148	11.175	10.042
	Z	8.328	7.941	7.505	7.013	6.452	5.798
	γ	-62.52	-65.203	-67.418	-69.44	-71.487	-73.75
	δ	-58.699	-56.663	-54.46	-52.093	-49.55	-46.89

*U.S.Government Printing Office: 1977 — 757-001/08